

PHD

Activation of Carbon-Fluorine Bonds using Ruthenium Dihydride Complexes

Kirkham, Matthew Samuel

Award date:
2001

Awarding institution:
University of Bath

[Link to publication](#)

General rights

Copyright and moral rights for the publications made accessible in the public portal are retained by the authors and/or other copyright owners and it is a condition of accessing publications that users recognise and abide by the legal requirements associated with these rights.

- Users may download and print one copy of any publication from the public portal for the purpose of private study or research.
- You may not further distribute the material or use it for any profit-making activity or commercial gain
- You may freely distribute the URL identifying the publication in the public portal ?

Take down policy

If you believe that this document breaches copyright please contact us providing details, and we will remove access to the work immediately and investigate your claim.

Activation of Carbon-Fluorine Bonds using Ruthenium Dihydride Complexes

Submitted by Matthew Samuel Kirkham

For the degree of PhD

of the University of Bath

2001

COPYRIGHT

Attention is drawn to the fact that copyright of this thesis rests with its author. This copy of the thesis has been supplied on condition that anyone who consults it is understood to recognise that its copyright rests with its author and that no quotation from the thesis and no information derived from it may be published without the prior written consent of the author.

This thesis may be made available for consultation within the University Library and may be photocopied or lent to other libraries for the purposes of consultation

Signed



UMI Number: U484961

All rights reserved

INFORMATION TO ALL USERS

The quality of this reproduction is dependent upon the quality of the copy submitted.

In the unlikely event that the author did not send a complete manuscript and there are missing pages, these will be noted. Also, if material had to be removed, a note will indicate the deletion.



UMI U484961

Published by ProQuest LLC 2013. Copyright in the Dissertation held by the Author.
Microform Edition © ProQuest LLC.

All rights reserved. This work is protected against
unauthorized copying under Title 17, United States Code.



ProQuest LLC
789 East Eisenhower Parkway
P.O. Box 1346
Ann Arbor, MI 48106-1346

DATE OF DATA	
ENTRY	
30	14 JUN 2001
P.L.S.	

Acknowledgements

I would like to thank my supervisor at the University of Bath, Dr. Michael K. Whittlesey for his help and support throughout my PhD, and to EPSRC for the funding of this project. I would also like to thank Johnson Matthey Plc. for their kind loan of ruthenium starting materials, Dr. Sigrid Wocaldo of the University of East Anglia, Norwich, for collecting X-ray data on compound **9**, Dr. Mary Mahon of the University of Bath for collecting X-ray data on compounds **12** and **15**, Dr. Michael R  f of Bruker AXS GmbH Analyticals X-ray Systems for collecting data on compound **14**, Dr. Chris Pickett and Dr. Saad Ibrahim at the Nitrogen Fixation Laboratory, John Innes Research Park, Norwich, for their assistance in obtaining electrochemical measurements on the ruthenium dihydride species (chapter 3), Dr. Trevor Dransfield at the University of York for GC-MS measurements (chapter 4), Dr. Jason Lynam at the University of Bristol for the kind donation of the phosphine ligand, dcpe, and Dr. Paul Watson at the Universit  t Bremen, Germany, for coupling constant data for the iridium difluoride species (chapter 4).

Special thanks also to Dr. Lee Higham, Rodolphe Jazzar, Matt Hargreaves and Jose Goicochea for help and support in the laboratory.

Most of all I would like to Mum, Dad and Jo for all their support and Harriet for being there when I needed her.

Activation of Carbon-Fluorine Bonds using Ruthenium Dihydride Complexes

Matthew Samuel Kirkham

Abstract

The reactivity of a series of ruthenium phosphine dihydride complexes toward carbon-fluorine bonds has been studied. *cis*-Ru(dmpe)₂H₂ and *cis*-Ru(depe)₂H₂ were found to react with perfluoroalkanes containing two vicinal tertiary C-F bonds at 85 °C, to yield the bifluoride hydride complexes *trans*-Ru(dmpe)₂(FHF)H and *trans*-Ru(depe)₂(FHF)H. In the presence of pyridine as a base the former is trapped to give the pyridine hydride complex *trans*-[Ru(dmpe)₂(C₅H₅N)H][FHF]. The bifluoride hydride species were found to be effective fluorinating agents for small organic and early transition metal halides under mild conditions.

The dihydrides compounds, *cis*-Ru(depe)₂H₂ and *cis*-Ru(dmpm)₂H₂ were found to react with hexafluorobenzene at room temperature, yielding the *trans*-fluoroaryl hydride complexes *trans*-Ru(depe)₂(C₆F₅)H and *trans*-Ru(dmpm)₂(C₆F₅)H. The latter has been structurally characterised. The related dihydrides *cis*-Ru(PP)₂H₂ (PP = dcpe, dppe, (PMe₃)₂) showed no activity towards aromatic or aliphatic C-F bonds. Electrochemical studies have been used to determine the first oxidation potentials for all six dihydride complexes.

cis-Ru(dmpe)₂H₂ reacted with the vinylic C-F bonds in both perfluoropropene and perfluoro-2-methyl-2-pentene to give the bifluoride fluoride complex, *cis*-Ru(dmpe)₂F(F..HF), and partially hydrogen substituted fluoroalkenes. In contrast *cis*-Ru(dcpe)₂H₂ reacted with the same perfluoroalkenes to give the five coordinate ruthenium monohydride cation [Ru(dcpe)₂H]⁺ with the perfluoroenolate [(CF₃)₂C=C(O)CF₂CF₃]⁻ as the counterion. The structures of both these compounds have been determined by X-ray crystallography.

Abbreviations

dmpe	1,2-bis(dimethylphosphino)ethane
depe	1,2-bis(diethylphosphino)ethane
dmpm	1,2-bis(dimethylphosphino)methane
dcpe	1,2-bis(dicyclohexylphosphino)ethane
dppe	1,2-bis(diphenylphosphino)ethane
PFD	Perfluorodecalin
PFMCH	Perfluoromethylcyclohexane
PFPHPA	Perfluoroperhydrophenanthrene
PF1MD	Perfluoro-1-methyldecalin
PF2MP	Perfluoro-2-methylpentane
PFP	Perfluoropropene
PF2M2P	Perfluoro-2-methyl-2-pentene
Cp	Cyclopentadienyl
Cp*	Pentamethylcyclopentadienyl
DMSO	Dimethylsulfoxide
COD	1,5-cyclooctadiene
NMR	Nuclear Magnetic Resonance
δ	Chemical Shift
ppm	Parts per million
J	Coupling constant
Hz	Hertz
IR	Infra-Red
ν	Frequency
cm^{-1}	Wavenumbers
FABMS	Fast Atom Bombardment Mass Spectrometry
CV	Cyclic Voltammetry
SCE	Standard Calomel electrode
h	hours
min	minutes
Å	Angstroms
mol	moles
mmol	millimoles
g	grams
mg	milligrams
mL	Millilitres

NB: Field strengths on $^{31}\text{P}\{^1\text{H}\}$ and ^{19}F NMR spectra refer to ^1H frequencies e.g. for

$^{31}\text{P}\{^1\text{H}\}$, 400MHz corresponds to 162.9 MHz, ^{19}F to 376.1 MHz.

Table of Contents

1 Introduction	1
1.1 Approaches to C-F bond activation	4
1.2 Aromatic C-F bond activation	5
1.2.1 Non-transition metal aromatic C-F activations	5
1.2.2 Transition metal aromatic C-F activations	6
1.3 Aliphatic C-F bond activation	15
1.3.1 Non transition metal aliphatic C-F activations	16
1.3.2 Transition metal aliphatic C-F activations	20
1.4 Transition metal fluorides	30
1.4.1 Group 8 transition metal fluorides	31
1.4.2 Group 9 transition metal fluorides	34
1.4.3 Group 10 transition metal fluorides	36
1.5 Transition metal bifluoride complexes	38
1.6 An outline of the work in this thesis	43
References	45
 2 Activation of saturated C-F bonds by <i>cis</i>-Ru(dmpe)₂H₂ (1)	 52
2.1 Introduction	53
2.2 Preparation of <i>cis</i>-Ru(dmpe)₂H₂ (1)	56
2.3 Results	57
2.3.1 Reaction of 1 with perfluorodecalin (PFD)	57
2.3.2 Reactions with other perfluoroalkanes	62
2.3.3 Effect of base on the reaction of 1 with PFD	64
2.3.4 Other modifications to reaction of 1 and PFD	72
2.4 Bifluoride hydride (8) as a fluorinating agent	73
2.4.1 Reaction of <i>trans</i> -Ru(dmpe) ₂ (FHF)H, 8 , and CH ₃ C(O)Cl	75
2.4.2 Reaction of <i>trans</i> -Ru(dmpe) ₂ (FHF)H, 8 , and CH ₃ I	76
2.4.3 Reaction of <i>trans</i> -Ru(dmpe) ₂ (FHF)H, 8 , and Cp ₂ TiCl ₂	77
2.4.4 Reaction of <i>trans</i> -Ru(dmpe) ₂ (FHF)H, 8 , and CH ₂ Cl ₂	79
2.5 Discussion	80
2.6 Conclusions	83

References	84
3 Activation of C-F bonds with other ruthenium dihydrides	86
3.1 Introduction	87
3.2 Reactivity of <i>cis</i>-Ru(depe)₂H₂ (2)	88
3.2.1 Preparation of <i>cis</i> -Ru(depe) ₂ H ₂ , 2	88
3.2.2 Reaction with hexafluorobenzene	88
3.2.3 Reaction with perfluorodecalin	91
3.3 Reactivity with <i>cis</i>-Ru(dmpm)₂H₂ (3)	95
3.3.1 Preparation of <i>cis</i> -Ru(dmpm) ₂ H ₂ , 3	95
3.3.2 Reaction with hexafluorobenzene	95
3.3.3 Reaction with pentafluorobenzene	101
3.3.4 Reaction with perfluorodecalin (PFD)	103
3.4 Reactivity of <i>cis</i>-Ru(dcpe)₂H₂ (4), <i>cis</i>-Ru(dppe)₂H₂ (5), and <i>cis</i>-Ru(PMe₃)₄H₂ (6)	103
3.4.1 Preparation of dihydrides 4, 5 and 6	103
3.4.2 Reaction with hexafluorobenzene	104
3.4.3 Reaction with perfluorodecalin	104
3.5 Cyclic voltammetry of the series of dihydrides	105
3.6 Fluorinations using <i>trans</i>-Ru(depe)₂(FHF)H (11)	112
3.6.1 Reaction of <i>trans</i> -Ru(depe) ₂ (FHF)H, 11, and CH ₃ C(O)Cl	112
3.6.2 Reaction of <i>trans</i> -Ru(depe) ₂ (FHF)H, 11, and CH ₃ F	112
3.7 Discussion	115
3.8 Conclusions	117
References	118
4 Reactions of RuH₂(PP)₂ with perfluoroalkenes	120
4.1 Introduction	121
4.1.1 Nucleophilic attack on perfluoroalkenes	122
4.1.2 Electrophilic attack on perfluoroalkenes.	126

4.1.3 Free radical chemistry of perfluoroalkenes	127
4.1.4 Reaction by rearrangement	129
4.1.5 Reaction with metal complexes	129
4.2 Results	140
4.2.1 Reaction of <i>cis</i>-Ru(dmpe)₂H₂ (1) and perfluoroalkenes	140
4.2.1.1 Reaction with perfluoro-2-methyl-2-pentene	140
4.2.1.2 Reaction with perfluoropropene	159
4.2.2 Reaction of <i>cis</i>-Ru(dcpe)₂H₂ (4) and perfluoroalkenes	163
4.2.2.1 Reaction with perfluoro-2-methyl-2-pentene	163
4.2.2.2 Reaction with perfluoropropene	176
4.3 Discussion	178
4.4 Conclusions	182
References	183
 5 Experimental	 187
5.1 General Methods	188
5.2 Preparation of the ruthenium bis(diphosphine) dihydrides	189
5.2.1 <i>cis</i> -Ru(dmpe) ₂ H ₂ , 1	189
5.2.2 <i>cis</i> -Ru(depe) ₂ H ₂ , 2	190
5.2.3 <i>cis</i> -Ru(dmpm) ₂ H ₂ , 3	191
5.2.4 <i>cis</i> -Ru(dcpe) ₂ H ₂ , 4	192
5.2.5 <i>cis</i> -Ru(dppe) ₂ H ₂ , 5	192
5.2.6 <i>cis</i> -Ru(PMe ₃) ₄ H ₂ , 6	193
5.3 Reactions of ruthenium dihydride complexes with perfluorocarbons	194
5.3.1 Reactions of <i>cis</i> -Ru(dmpe) ₂ H ₂ , 1, with perfluoroalkanes	194
5.3.2 Reactions of <i>cis</i> -Ru(depe) ₂ H ₂ , 2, with perfluoroalkanes	198
5.3.3 Reactions of <i>cis</i> -Ru(dmpm) ₂ H ₂ , 3, with perfluoroalkanes	201
5.3.4 Reactions of other dihydrides with perfluoroalkanes	202
5.4 Fluorination reactions using ruthenium bifluoride hydride complexes	202
5.4.1 Fluorinations with <i>trans</i> -Ru(dmpe) ₂ (FHF)H, 8	202
5.4.2 Fluorinations with <i>trans</i> -Ru(depe) ₂ (FHF)H, 11	204

5.5 Reactions of ruthenium dihydride complexes with perfluoroalkenes	205
5.5.1 Reactions of <i>cis</i> -Ru(dmpe) ₂ H ₂ , 1 , with perfluoroalkenes	205
5.5.2 Reactions of <i>cis</i> -Ru(dcpe) ₂ H ₂ , 4 , with perfluoroalkanes	208
5.6 Cyclic Voltammetry	210
References	211

Chapter 1

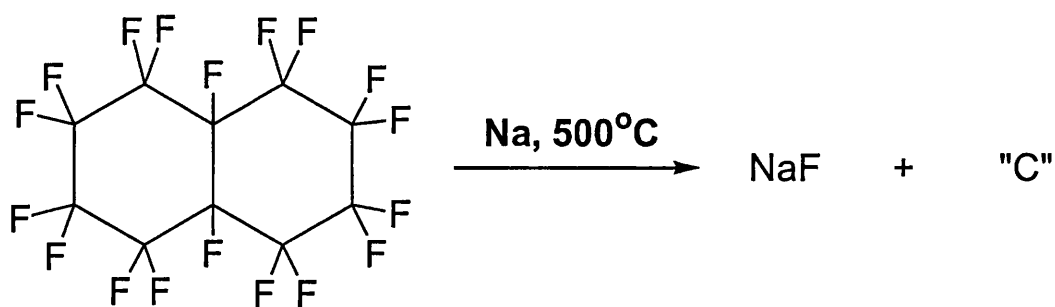
Introduction

1 Introduction

The activation of saturated perfluorocarbons is a challenging task. The large electronegativity of the fluorine atom combined with the high C-F bond dissociation energy (B.D.E of $\text{CF}_4 = 456 \text{ kJ mol}^{-1}$) imparts a stability towards chemical attack, which has led to these compounds being regarded as among the most inert of chemicals. This ‘inertness’ has led to this group of compounds being used for many industrial, medical and commercial applications, such as blood substitutes (perfluoro-tri-*n*-butylamine), non-stick coatings (PTFE), and fire extinguishers (perfluorobutane).¹ However, the longevity of these compounds, which do not occur naturally, is of environmental concern. Fluorocarbons and the related chlorofluorocarbons (CFCs) of low molecular weight, used as propellants, have been found to be effective as greenhouse gases.¹

The early chemistry of saturated perfluorocarbons was restricted to reactions that required extreme conditions. For example, the reaction of perfluorodecalin (PFD) with sodium metal requires heating to 500°C , yielding NaF and elemental carbon (fig 1.1).

Fig 1.1 Reaction of PFD and Na metal



Although this reaction is useful for fluorine analysis, the products from these reactions are obviously not of any great use. The activation or cleavage of saturated C-F bonds under milder conditions, and with a degree of selectivity, has only recently

become accessible. A mild and selective reduction of perfluorodecalin can be obtained using organic electron donors such as benzophenone ketyl.²

The low reactivity of perfluoroalkanes is in marked contrast to that of perfluoroarenes. There are many examples of aromatic C-F bond activation by both organic and transition metal complexes.³ The aim of this project is to extend the reactivity of transition metal complexes for the activation, and ultimately the functionalisation, of saturated C-F bonds. C-F bond activation and subsequent use of the fluorine has the potential for making perfluoroalkanes a chemical feedstock for the production of high value fluoroorganic compounds and in developing new applications for chemically modified fluoropolymers.

In the first part of this introduction, an outline of the strategies used for C-F activation will be described followed by examples of both aromatic and aliphatic C-F bond activation. An introduction to the chemistry of perfluoroalkenes will be described in its own section at the beginning of chapter 4. The second part of this introduction will concentrate on the synthesis and reactivity of transition metal fluoride, and bifluoride complexes.

1.1 Approaches to C-F bond activation

There have been several different strategies used to try and facilitate the cleavage of the strongest single bond to carbon. They include:-

- *Electrophilic attack:* The use of a strong Lewis base can remove a fluoride ion from perfluoroalkanes. This fluoride abstraction is mainly seen in coordinated perfluoroalkyl ligands.
- *Nucleophilic attack:* The polarity of the C-F bond makes the carbon electrophilic and susceptible to attack by nucleophiles especially in perfluoroarenes. Perfluoroarenes preferentially undergo nucleophilic attack, unlike analogous perhydroarenes, which are subject to electrophilic attack. This is a prime example of the inversion of reactivity than can be seen between fluorocarbons and hydrocarbons.
- *Homolytic pathways:* Extraction of a fluorine atom from a perfluorocarbon is very slow. Even when the process is exothermic this reaction does not occur easily.
- *Metal induced C-F bond activation:* Metal induced C-F bond cleavage of perfluoroarenes, in many cases, leads to oxidative addition products. However, the metal fragments capable of reacting in this manner are all highly reducing, so an initial electron transfer cannot be ruled out. Coordination of the π -system of the arene is also a plausible initial step, a mechanism often seen with hydrocarbon analogues.⁴ C-F bonds can be activated via an electron transfer from an electron rich metal complex. The C-F bond is cleaved to give a carbon radical and a fluoride anion. The process is assisted by using a polar solvent and

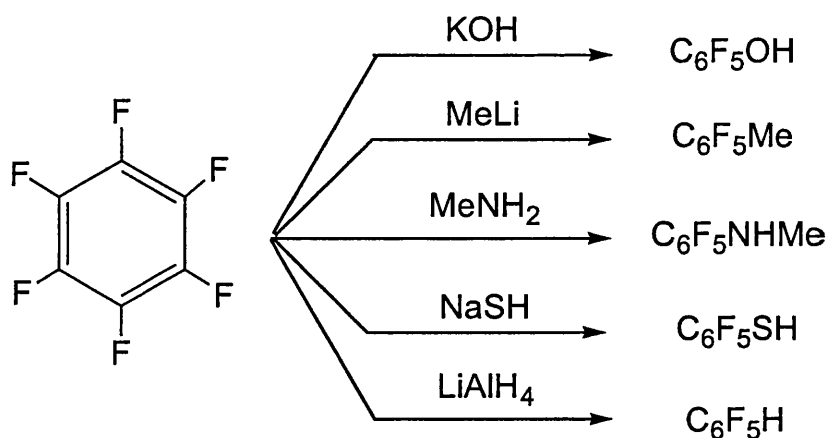
a electrophile to accept the fluoride ion. Photochemical methods provide another way of delivering the energy necessary for C-F cleavage to occur. The use of a suitable photosensitiser (either organic or transition metal species) can provide a source of electrons, which can be transferred to the C-F bond.

1.2 Aromatic C-F bond activation

1.2.1 Non-transition metal aromatic C-F activations

As mentioned previously, perfluoroarenes are very susceptible to nucleophilic attack. The use of suitable nucleophiles with hexafluorobenzene has led to a variety of substituted perfluoroarenes (fig 1.2). The fluorine is removed in a two-step mechanism where the initial nucleophilic attack is the rate-determining step.⁵ Charge transfer complexes may also be formed but they do not have any effect on the rate of reaction. The high reactivity of C_6F_6 makes it the most popular substrate for scouting possible reagents for C-F bond activation.

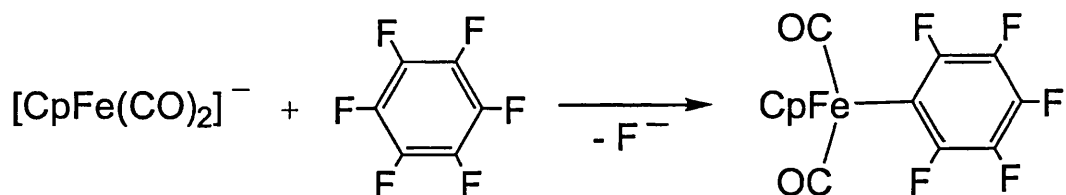
Fig 1.2 Reactions of C_6F_6 with nucleophiles



1.2.2 Transition metal C-F activations

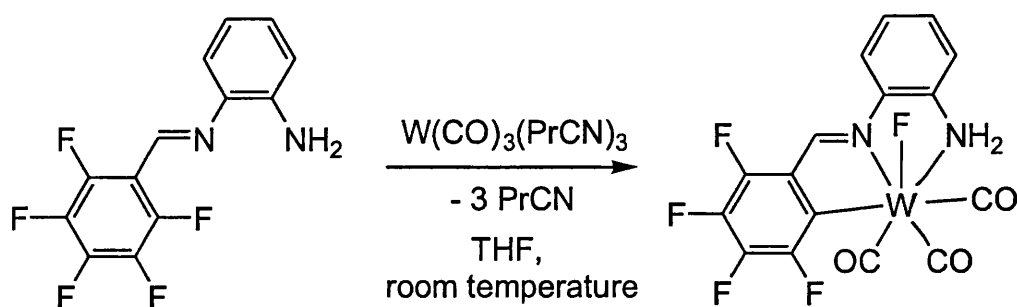
It has been shown that perfluoroarenes are susceptible to attack by nucleophiles. The first report of transition metal induced aromatic C-F cleavage showed that organometallic nucleophiles react in the same manner as their organic counterparts. Hexafluorobenzene was found to react with $[\text{CpFe}(\text{CO})_2]^-$ (fig 1.3).⁶

Fig 1.3 Reaction of C_6F_6 with an organometallic nucleophile



Since then, Richmond et al.⁷ showed that aromatic C-F bonds can undergo oxidative addition to a transition metal centre. Treatment of a Schiff base that incorporated a pentafluorophenyl ring with $\text{W}(\text{CO})_3(\text{PrCN})_3$ led to an insertion into an aromatic C-F bond and oxidation of the metal to yield a tungsten (II) fluoride complex in high yield under mild conditions (fig 1.4).

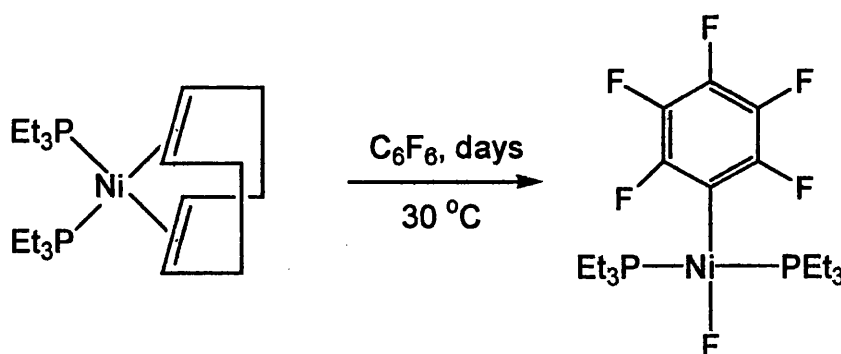
Fig 1.4 Intramolecular oxidative addition of a C-F bond



This chemistry has also been repeated using Mo(0)/Mo(II), Ni(0)/Ni(II) and Pt(II)/Pt(IV) redox systems, although the rate of reaction decreases with decreasing fluorination of the ring.⁸

Intermolecular aromatic C-F bond activation has also been reported. One of the earliest examples involved the reaction between C₆F₆ and the low-valent nickel complex Ni(PEt₃)₂(COD).^{9,10} The reaction proceeds slowly, independent of temperature, to yield the square planar complex, *trans*-Ni(PEt₃)₂(C₆F₅)F (fig 1.5), which decomposes at 30 °C.

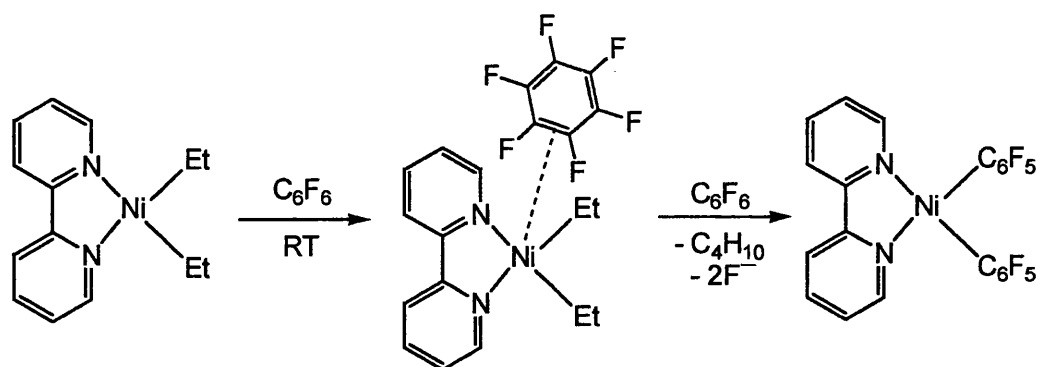
Fig 1.5 Aromatic C-F bond activation by Ni(0)



In the reaction of Ni(PEt₃)₃ with pentafluoropyridine, the C-F bonds *ortho* to the pyridyl nitrogen are cleaved in preference to the other C-F bonds and with 2,3,5,6-tetrafluoropyridine, the *ortho* C-F bond is cleaved in preference to the other C-F bonds and the *ortho* C-H bond. It is thought that an initial coordination of the pyridyl nitrogen may direct the C-F activation regioselectivity to the *ortho* position. Also in the reaction of Ni(PEt₃)₃ with pentafluorobenzene, only C-F activation occurs.¹⁰ Two other C-F activation reactions of hexafluorobenzene with nickel complexes containing chelating ligands have been recently reported. An η^2 -C₆F₆ intermediate is implicated in the formation of (tBu₂PCH₂CH₂PtBu₂)Ni(C₆F₅)F,¹¹ whereas low temperature experiments

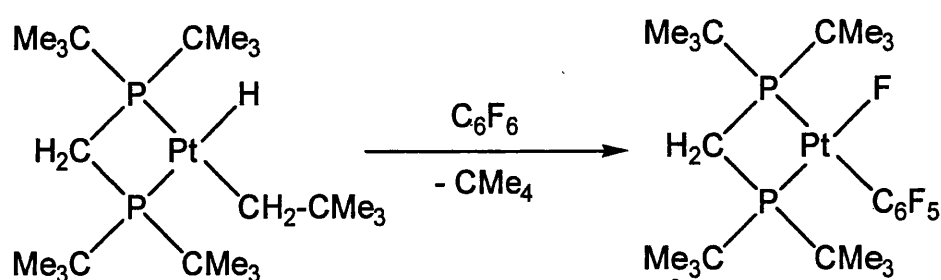
on the reaction of $\text{Ni}(\text{bipy})\text{Et}_2$ and C_6F_6 provide evidence for the precoordination of the perfluoroarene, before formation of $\text{Ni}(\text{bipy})(\text{C}_6\text{F}_5)_2$ (fig. 1.6).¹²

Fig 1.6 Aromatic C-F bond activation by $\text{Ni}(\text{bipy})\text{Et}_2$



Intermolecular oxidative addition of an aromatic C-F bond was reported by Hofmann¹³ using a $\text{Pt}(\text{II})$ complex with a bulky chelating phosphine. The complex reductively eliminates neopentane, leaving a 14-electron $\text{Pt}(0)$ intermediate which oxidatively adds an aromatic C-F bond of hexafluorobenzene (fig 1.7).

Fig 1.7 Intermolecular oxidative addition of a C-F bond

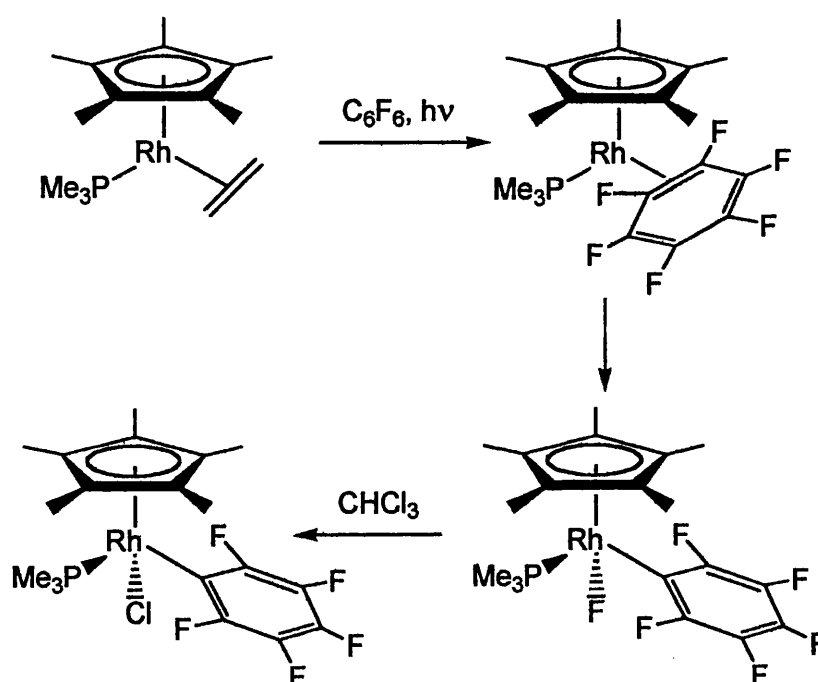


Photolytic C-F activation was displayed by a rhodium complex that is known to photochemically activate C-H bonds in benzene. Near UV photolysis ($\lambda > 285 \text{ nm}$) of $\text{Cp}^*\text{Rh}(\text{PMe}_3)(\text{C}_2\text{H}_4)$ in the presence of C_6F_6 yields $\text{Cp}^*\text{Rh}(\text{PMe}_3)(\eta^2\text{-C}_6\text{F}_6)$.¹⁴ The coordination of the hexafluorobenzene has the effect of lowering the C-F activation

energy barrier, and with continued photolysis, the oxidative addition product

$\text{Cp}^*\text{Rh}(\text{PMe}_3)(\text{C}_6\text{F}_5)\text{F}$ is formed. Subsequent halide exchange with CHCl_3 led to the isolable chloride complex, $\text{Cp}^*\text{Rh}(\text{PMe}_3)(\text{C}_6\text{F}_5)\text{Cl}$. The reaction only proceeds under photochemical conditions; thermal activation of C_6F_6 with $\text{Cp}^*\text{Rh}(\text{PMe}_3)(\text{C}_2\text{H}_4)$ is not seen, even on heating to 110 °C. These reactions are summarised in fig 1.8.

Fig 1.8 Photolytic C-F activation by $\text{Cp}^*\text{Rh}(\text{PMe}_3)(\text{C}_2\text{H}_4)$

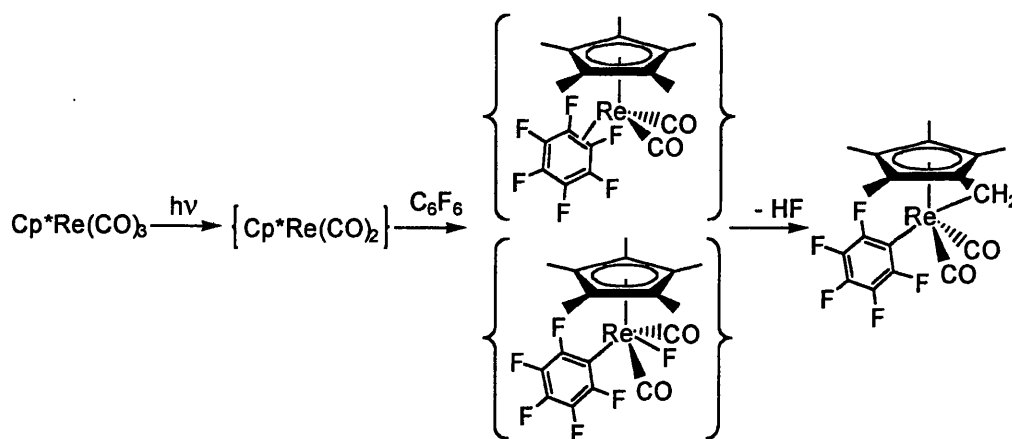


The less basic cyclopentadienyl analogue does form $\text{CpRh}(\text{PMe}_3)(\eta^2\text{-C}_6\text{F}_6)$ but C-F cleavage does not occur on further photolysis or heating in solution. It should be noted though that in lesser fluorinated arenes, both $\text{Cp}^*\text{Rh}(\text{PMe}_3)(\text{C}_2\text{H}_4)$ and $\text{CpRh}(\text{PMe}_3)(\text{C}_2\text{H}_4)$ effect C-H activations and not C-F activations under photolytic conditions.¹⁵ Density functional calculations¹⁶ on the reaction of 1,4-difluorobenzene with the reactive intermediate $[\text{CpRh}(\text{PH}_3)]$ show that the oxidative addition of the C-F is thermodynamically preferred over the oxidative addition of C-H. However, the

activation energies for C-F activation are considerably higher than those for C-H activation. This implies that the inertness of the C-F bond has a kinetic origin.

A rare example of C-F activation at a rhenium centre is seen upon photolysis of $\text{Cp}^*\text{Re}(\text{CO})_3$ and hexafluorobenzene.¹⁷ This reaction is unique, as not only does the rhenium complex cleave the aromatic C-F bond of hexafluorobenzene, but also leads to intramolecular C-H bond activation of the C_5Me_5 ligand yielding $\text{Re}(\eta^6\text{-C}_5\text{Me}_4\text{CH}_2)(\text{CO})_2(\text{C}_6\text{F}_5)$. It is uncertain whether, after initial photochemical displacement of a carbonyl ligand, $\text{Cp}^*\text{Re}(\text{CO})_2(\eta^2\text{-C}_6\text{F}_6)$ is formed or whether C_6F_6 oxidatively adds to the unsaturated rhenium centre in $[\text{Cp}^*\text{Re}(\text{CO})_2]$ to give $\text{Cp}^*\text{Re}(\text{CO})_2(\text{C}_6\text{F}_5)\text{F}$. It is certain that subsequent loss of HF is responsible for the final product (fig. 1.9).

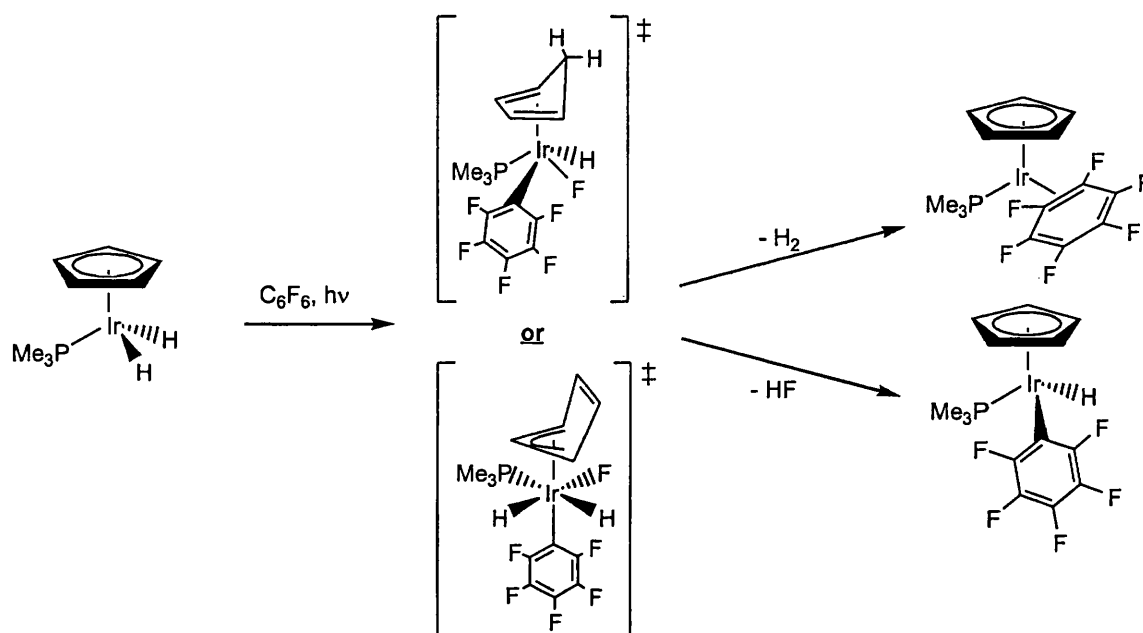
Fig 1.9 Reaction of $\text{Cp}^*\text{Re}(\text{CO})_3$ with C_6F_6



Another example of photochemical C-F bond activation has been described using $\text{CpIr}(\text{PMe}_3)\text{H}_2$.¹⁸ Upon photolysis in C_6F_6 both $\text{CpIr}(\text{PMe}_3)(\eta^2\text{-C}_6\text{F}_6)$ and $\text{CpIr}(\text{PMe}_3)(\text{C}_6\text{F}_5)\text{H}$ are formed concurrently. Deuterium labelling studies reveal that the hydride in the second complex originates from the starting material. The mechanism is proposed to proceed via a hydride transfer to the cyclopentadienyl ring or a ring slip to

allow coordination of C_6F_5 and fluoride. Subsequent loss of dihydrogen or HF leads to $\text{CpIr}(\text{PMe}_3)(\eta^2\text{-C}_6\text{F}_6)$ and $\text{CpIr}(\text{PMe}_3)(\text{C}_6\text{F}_5)\text{H}$ respectively (fig 1.10).

Fig 1.10 Photolytic reaction between $\text{CpIr}(\text{PMe}_3)(\text{C}_6\text{F}_5)\text{H}$ and C_6F_6 .

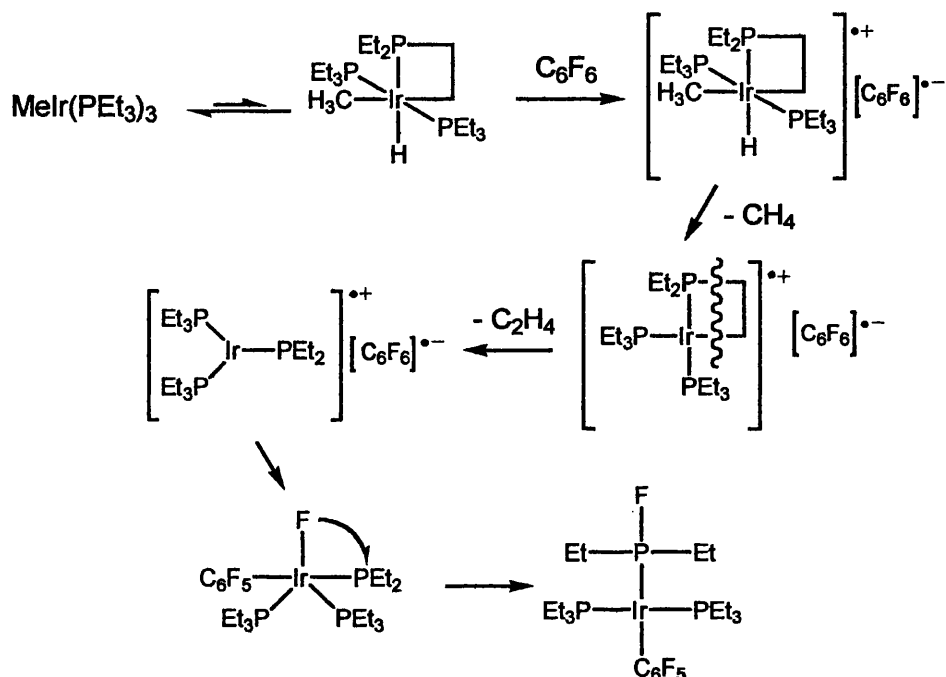


Thermal C-F bond activation of perfluoroaromatics has also been reported. The reaction of $\text{MeIr}(\text{PEt}_3)_3$ with hexafluorobenzene at 60°C involves not only C-F bond cleavage, but also P-C bond cleavage and P-F bond formation to give $\text{Ir}(\text{PEt}_3)_2(\text{PEt}_2\text{F})(\text{C}_6\text{F}_5)$.¹⁹ Elimination of methane and ethane, detected by GC-MS, has led to a mechanistic hypothesis in which a PEt_3 ligand cyclometallates prior to an electron transfer to C_6F_6 . Subsequent reductive elimination of methane and the metathetical elimination of C_2H_4 leads to two radical species which recombine to give $\text{Ir}(\text{PEt}_3)_2(\text{PEt}_2)(\text{C}_6\text{F}_5)\text{F}$. This rearranges by fluoride transfer to give the final product, as summarised in fig. 1.11.

There are several examples of electron rich transition metal hydrides that react with fluoroaromatics under thermal conditions. The dihydride *trans*- $\text{Pt}(\text{PCy}_3)_2\text{H}_2$ reacts with pentafluorobenzonitrile to yield *trans*- $\text{Pt}(\text{PCy}_3)_2(p\text{-C}_6\text{F}_4\text{CN})\text{H}$ and 2,3,5,6-

tetrafluorobenzonitrile.²⁰ ESR studies detected a radical when the reaction was performed in the presence of a spin trapping agent, leading to the suggestion that an electron transfer process was involved in this reaction.

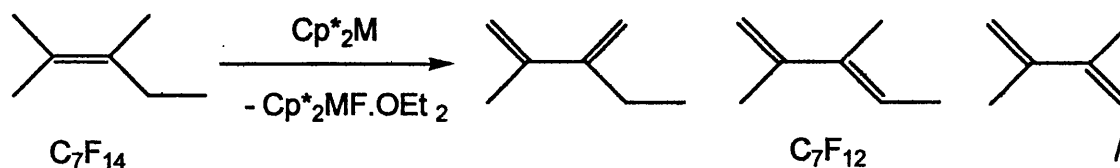
Fig 1.11 Proposed mechanism for reaction of $\text{MeIr}(\text{PEt}_3)_3$ and C_6F_6 .



Divalent lanthanide metallocenes also activate C-F bonds in perfluoroarenes via an electron transfer. Burns and Andersen²¹ reported that Cp^*_2Yb can cleave the C-F bonds in C_6F_6 , $\text{C}_6\text{H}_5\text{F}$, $\text{C}_6\text{H}_5\text{CF}_3$ and CFHCH_2 but not in C_2F_6 to form, in all cases, the mixed valence dimer $[\text{Cp}^*_2\text{Yb}]_2\text{F}$. Watson²² also showed that Cp^*_2M ($\text{M} = \text{Yb}, \text{Eu}, \text{Sm}$) complexes can convert perfluoroalkenes to perfluorodienes (fig 1.12) via a similar mechanism (the use of visible light photolysis, which provides energy for the electron transfer, is seen to accelerate the reactions). The highly reducing nature of these complexes and the strength of the resulting metal fluoride bond provides an excellent driving force for these reactions. It was also seen that the reactions are more facile in

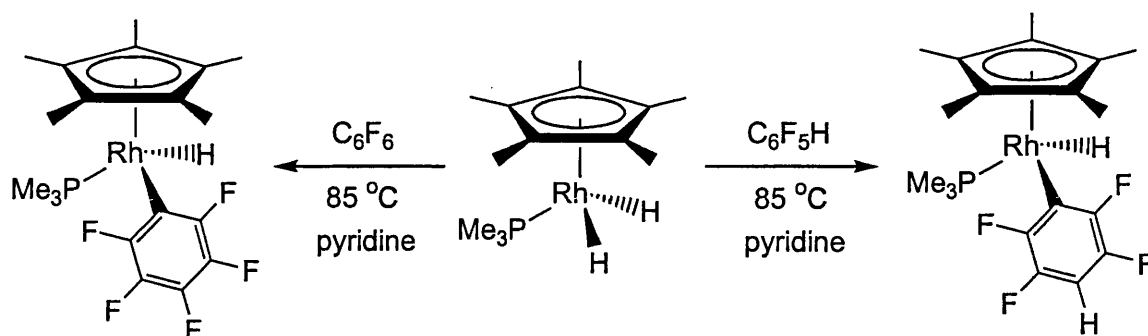
non-coordinating solvents, which has led to the postulation of a transient fluorocarbon complex, $\text{Cp}^*_2\text{M}\cdots\text{F-R}$, being formed prior to the C-F bond cleavage.

Fig 1.12 Defluorination of perfluoroalkenes



More remarkably, the reaction of *cis*- $\text{Ru}(\text{dmpe})_2\text{H}_2$ and C_6F_6 occurs at -78°C to yield *trans*- $\text{Ru}(\text{dmpe})_2(\text{C}_6\text{F}_5)\text{H}$.²³ In contrast to $\text{Cp}^*\text{Rh}(\text{PMe}_3)(\text{C}_2\text{H}_4)$, less heavily fluorinated aromatics undergo C-F rather than C-H activation. The reactions are proposed to proceed via an electron transfer mechanism and will be discussed in more detail in chapter 2. Loss of HF, which is the thermodynamic driving force, also leads to the formation of the bifluoride hydride complex, *trans*- $\text{Ru}(\text{dmpe})_2(\text{FHF})\text{H}$.²⁴

A mechanistic study of the reaction of an electron rich transition metal hydride with perfluoroaromatics was reported by Edelbach and Jones.²⁵ In the reaction of $\text{Cp}^*\text{Rh}(\text{PMe}_3)\text{H}_2$ with C_6F_6 at 85°C , the presence of pyridine was shown to increase the yield of $\text{Cp}^*\text{Rh}(\text{PMe}_3)(\text{C}_6\text{F}_5)\text{H}$, as well as accelerate the rate of its formation. As with *cis*- $\text{Ru}(\text{dmpe})_2\text{H}_2$, the reaction with pentafluorobenzene results in C-F (not C-H) bond activation exclusively at the *para*-position (fig. 1.13)

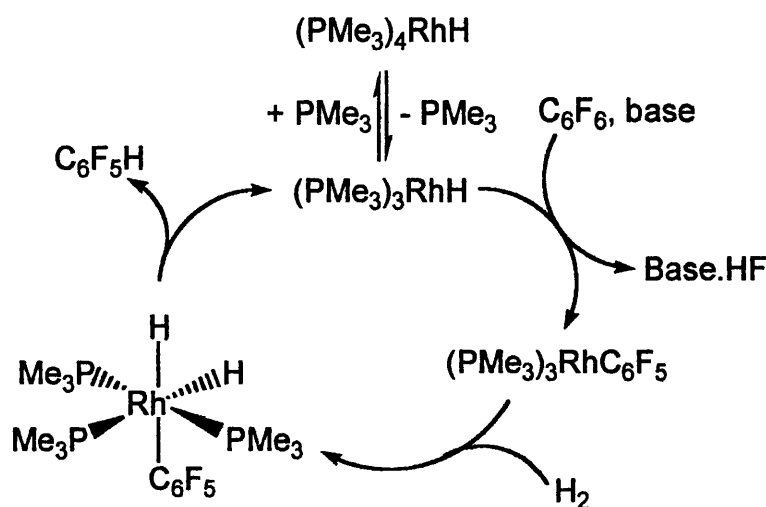
Fig 1.13 Thermal reaction of $\text{Cp}^*\text{Rh}(\text{PMe}_3)\text{H}_2$ with fluorinated aromatics

Kinetic studies implied that reaction of $\text{Cp}^*\text{Rh}(\text{PMe}_3)\text{H}_2$ and C_6F_6 was autocatalytic in nature. It was also seen that the rate of reaction increased on addition of a source of fluoride, such as Bu_4NF . This has led to a proposed mechanism involving the deprotonation of the starting dihydride followed by nucleophilic attack on the perfluoroarene and cleavage of the C-F bond. Independent generation of $[\text{Cp}^*\text{Rh}(\text{PMe}_3)\text{H}]^-$ and reaction with C_6F_6 showed similar rates of reaction and products. Jones proposes that related transition metal hydride systems (including *cis*- $\text{Ru}(\text{dmpe})_2\text{H}_2$) may proceed by the same mechanism. This proposal is considered in more detail in chapter 3.

The study into C-F bond activation by transition metal complexes is driven by the possibility of development of catalytic C-F bond functionalisations. This idea was first realised by Aizenberg and Milstein²⁶ who used $\text{Rh}(\text{PMe}_3)_4\text{H}$ to catalyse the selective hydrogenolysis of hexafluorobenzene to pentafluorobenzene at 95 °C. The homogeneous catalytic cycle requires the presence of an H_2 atmosphere and a base to sequester the HF by-product. In the catalytic cycle, the active species is $[\text{Rh}(\text{PMe}_3)_3\text{H}]$, which reacts with C_6F_6 to give $[\text{Rh}(\text{PMe}_3)_3(\text{C}_6\text{F}_5)]$ and eliminating HF. Subsequent oxidative addition of dihydrogen gave the six-coordinate dihydride complex $[\text{Rh}(\text{PMe}_3)_3(\text{C}_6\text{F}_5)\text{H}_2]$, which undergoes facile reductive elimination of pentafluorobenzene, regenerating $[\text{Rh}(\text{PMe}_3)_3\text{H}]$ (fig. 1.14). The reaction, performed in

neat hexafluorobenzene, is reported to have a turnover number as high as 114 for a 36 hour reaction and the catalyst precursor can be recovered in 52 % yield. Some PMe_3 is consumed due to a reaction with fluoride to form F_2PMe_3 . It is also reported that 2,3,5,6- $\text{C}_6\text{F}_4\text{H}_2$ is also formed at a slower rate.

Fig 1.14 Catalytic hydrogenolysis of hexafluorobenzene



1.3 Aliphatic C-F bond activation

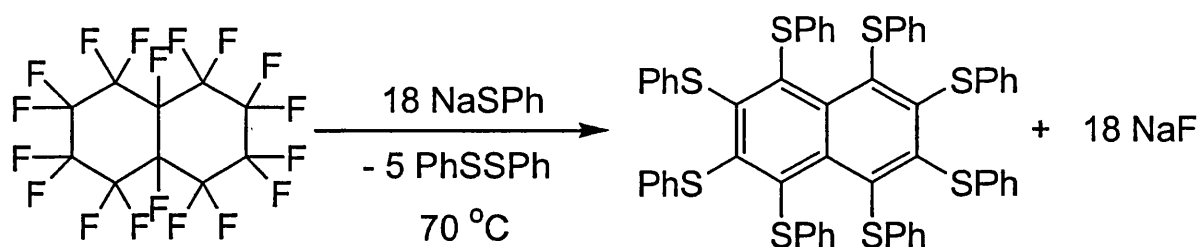
Although saturated perfluorocarbons generally have weaker C-F bond strengths than perfluoroaromatic compounds (sp^3 C-F^{3a}, 480-500 kJ mol^{-1} , aryl-F¹⁹, 644 kJ mol^{-1}) they tend to have a higher stability towards chemical attack. Perfluoroarenes undergo nucleophilic attack and electron transfer much more easily than perfluoroalkanes due to the repulsion between the lone pairs on fluorines bound to the sp^2 carbon and the π -electrons of the aromatic ring,²⁷ whereas the unreactivity of perfluoroalkanes is thought to be connected to the steric effects and shielding offered by the non-bonding electron pairs on fluorine.⁵ The high electron affinities of perfluoroalkanes mean that, with a

suitable reducing agent, electron transfer is possible. Poor Lewis basicity, however, implies that protonation or binding to a transition metal centre is unlikely.²⁸

1.3.1 Non transition metal aliphatic C-F activations

There are few examples of aliphatic C-F bond activations that do not involve transition metal complexes. The energy required to activate the C-F bond is very high, but photochemical methods provide another way of supplying the energy. ArF (193 nm) laser photolysis of liquid hexafluorobenzene leads to many organic products that include decafluorobiphenyl and perfluoronaphthalene. The nature of the products suggests that a homolytic C-F cleavage pathway is in operation with the formation of pentafluorophenyl radicals.^{36,29} In contrast to the destructive removal of fluorine by sodium (fig 1.1), systems that enable the selective removal of fluorine have only very recently been discovered. MacNicol and Robertson³⁰ reported that the treatment of perfluorodecalin with sodium phenylthiolate for 10 days at 70 °C in DMF led to complete defluorination to yield hexakis(thiophenoxy)naphthalene (fig. 1.15)

Fig. 1.15 Defluorination of perfluorodecalin

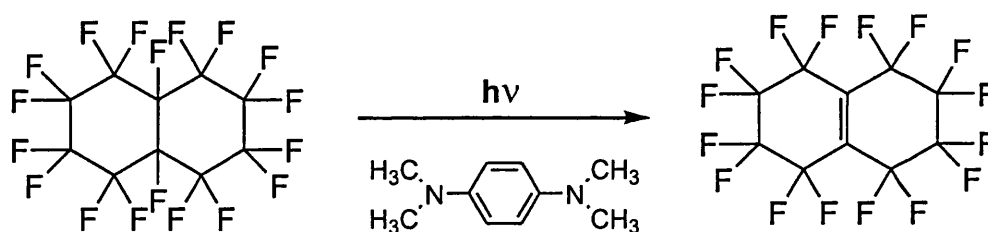


The reaction proceeds due to the ability of the thiolate to act as a nucleophile and a reducing agent. Pez et al.² has also shown that careful addition of the sodium

benzophenone radical anion to perfluorodecalin also performs a defluorination to yield perfluoronaphthalene. Perfluoronaphthalene and perfluorophenanthrene can be obtained by treating their respective saturated analogues with the radical anion in thf in yields of 62 % and 22 %, respectively. With perfluorocarbons lacking tertiary C-F bonds, defluorination is far less selective. Upon C-F cleavage and subsequent hydrolysis of perfluorocyclohexane, 1,2,4,5-tetrafluorophenol is formed in low yield. Defluorination of linear perfluorocarbons yields only NaF and elemental carbon.

Turro³¹ has shown that by photolysing perfluoroalkanes in the presence of an organic photosensitiser such as *N,N,N',N'*-tetramethyl-1,4-phenylenediamine, more selective defluorination can be performed. For example, perfluorodecalin can be converted to hexadecafluoro-bicyclo[4.4.0]dec-1(6)-ene in 35 % yield (fig 1.16).

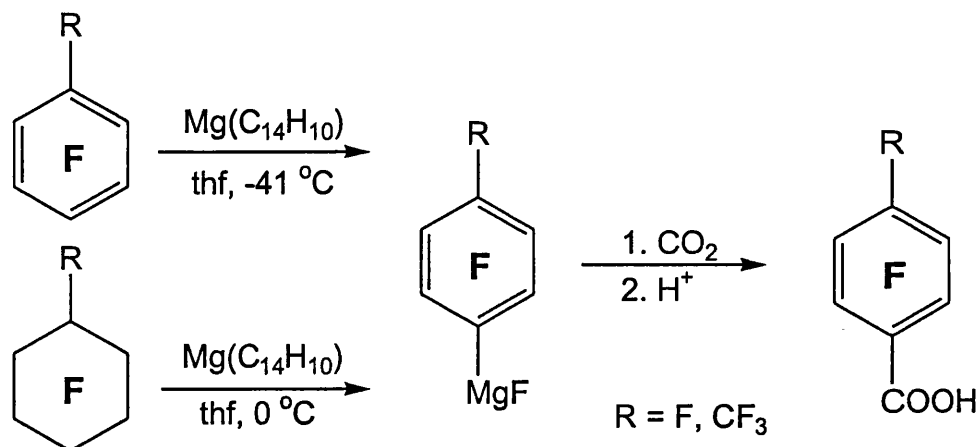
Fig 1.16 Photochemical defluorination of perfluorodecalin



The formation of the synthetically useful perfluoro-Grignard reagents from perfluoroalkanes has been reported.³² Magnesium anthracene, $\text{Mg}(\text{C}_{14}\text{H}_{10})$, a compound that is believed to act as a soluble and activated form of magnesium metal, is often used in the preparation of Grignard reagents which cannot be obtained directly from magnesium metal. The reaction of $\text{Mg}(\text{C}_{14}\text{H}_{10})$ with hexafluorobenzene or perfluorotoluene proceeds in thf at $-41\text{ }^{\circ}\text{C}$ to yield the perfluoro-Grignard *para*-FMg- $\text{C}_6\text{F}_4\text{R}$ ($\text{R} = \text{F}, \text{CF}_3$). Surprisingly, the same product is obtained in the reaction between $\text{Mg}(\text{C}_{14}\text{H}_{10})$ and perfluorocyclohexane or perfluoromethylcyclohexane in thf at $0\text{ }^{\circ}\text{C}$

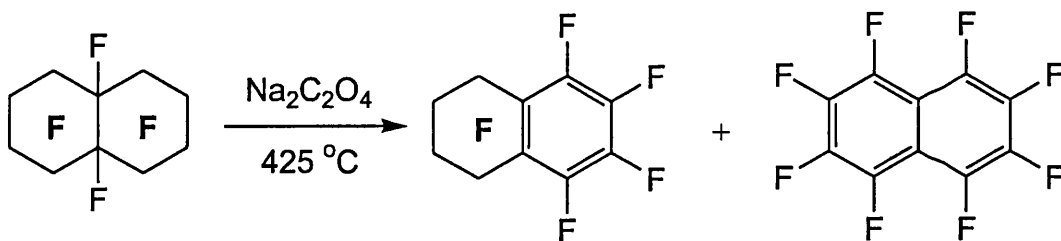
(fig. 1.17). This is the only reported conversion of perfluoroalkanes to perfluoro-Grignard reagents and provides a simple synthesis of a compound that is potentially very useful for the synthesis of novel fluorinated compounds.

Fig 1.17 Synthesis of perfluoro-Grignard reagents.



A recent report³³ has also shown, that at high temperatures, elemental carbon can act as a defluorinating agent. In a flow system containing a bed of sodium oxalate at $425\text{ }^{\circ}\text{C}$, perfluorodecalin can be aromatised to perfluorotetralin and perfluoronaphthalene (fig 1.18). Of the two sodium oxalate decomposition products, Na_2CO_3 and elemental carbon, carbon has been cited as the only plausible reducing agent.

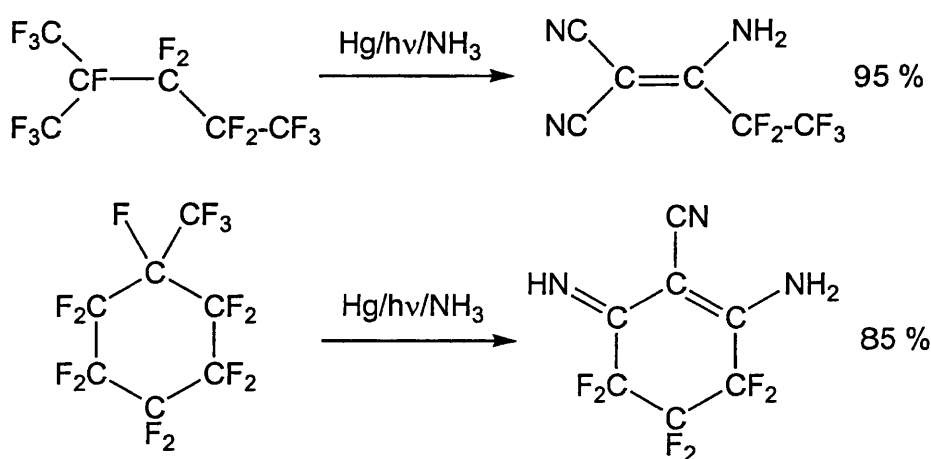
Fig 1.18 Perfluorodecalin aromatisation over hot sodium oxalate.



Fluoride is trapped as NaF, and the yields of either product can be increased by altering the carrier gases or the preheating time of the system. At 470 °C, this system has also been shown to be effective in the demineralisation of chlorofluorocarbons to NaF, NaCl and carbon.³⁴

Homolytic fluorine abstraction from a perfluorocarbon is very slow. Upon treatment of perfluoromethylcyclohexane with Hg/H₂/hν (which is an abundant source of H atoms) no formation of HF is seen.^{3a} Even though the H-F bond is far stronger (by 67 kJ mol⁻¹) than the C-F bond in perfluoromethylcyclohexane, and provides a reasonable driving force, the abstraction of HF from fluorocarbons has a high kinetic barrier. Partial reduction of perfluoroalkanes can, however, be facilitated by using ammonia gas under mercury photosensitisation to yield fluorocarbons containing imino, amino and nitrile groups³⁵ (fig 1.19).

Fig 1.19 Partial reduction of perfluoroalkanes using NH₃ and Hg photosensitisation



The abstraction of a fluorine by a H atom as mentioned above does not occur, but a detailed mechanistic study showed that reaction may occur by formation of the bis-ammonia exciplex [Hg*(NH₃)₂].³⁶ This is an efficient electron donor and fluoride ion acceptor. The electron transfer and fluoride abstraction is equivalent to fluorine

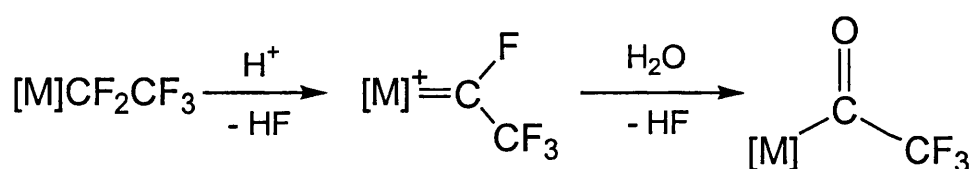
atom abstraction. The remaining functionalised perfluorocarbon then reacts with ammonia to yield the products shown above.

Introduction of oxygen into perfluoroalkanes is reported in a similar reaction using tetrabutylammonium iodide under Hg photosensitisation. The presence of a hydroxide ion, from water present in the $t\text{Bu}_4\text{NI}$, has the effect of trapping out reactive intermediates such as perfluoroenols, which readily deprotonate to perfluoroenolate salts.³⁷

1.3.2 Transition metal aliphatic C-F activations

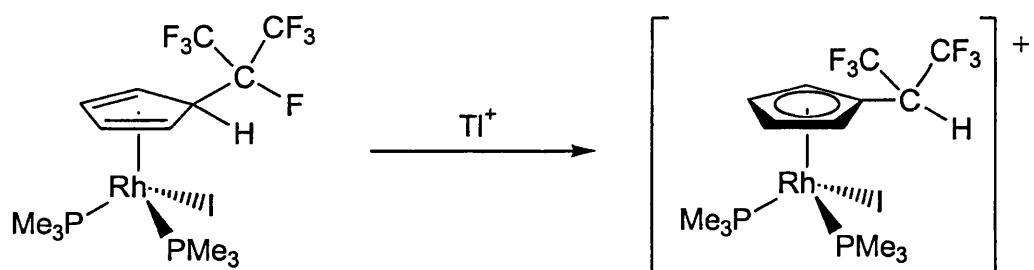
Powerful main group Lewis acids are much more effective than transition metal Lewis acids for C-F activation if the initial weak coordination is followed by a thermodynamically favoured chemical reaction. A classic example of this is the acid catalysed hydrolysis of trifluoromethylbenzene to afford benzoic acid.³⁸ The formation of HF, as shown in many cases of C-F bond cleavage, is a thermodynamic driving force in this reaction. Perfluoroalkyl ligands coordinated to transition metals have, under mild conditions, undergone C-F bond cleavage α to the transition metal leading to transition metal fluorocarbene complexes. The ability of the transition metal to stabilise carbene intermediates allows subsequent hydrolysis, made thermodynamically feasible by the formation of strong C=O and H-F bonds, to occur (fig 1.20).³⁹

Fig 1.20 Electrophilic attack on perfluoroalkyl ligand



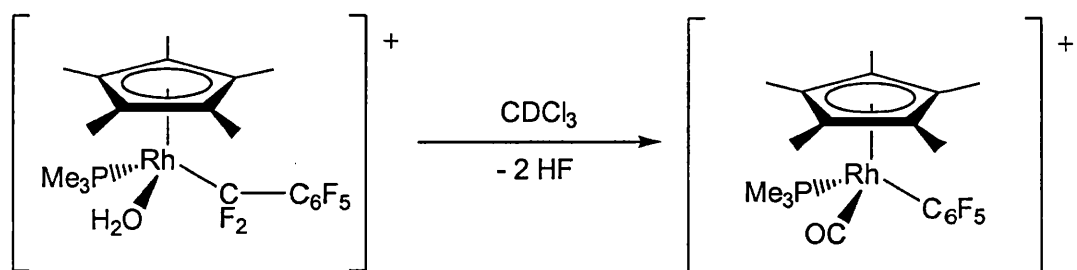
The coordination of perfluoroalkyl ligands to transition metal centres has the effect of increasing the reactivity of the aliphatic C-F bonds. The selective activation of a tertiary C-F bond is seen in the reaction of a rhodium (I) complex containing a fluoroalkylated η^4 -cyclopentadiene ligand in the presence of a thallium salt. The fluorine abstraction is followed by hydrogen transfer, which leaves a η^5 - $C_5H_4CH(CF_3)_2$ ligand. Interestingly the reaction with a silver salt leads to selective abstraction of the iodide ligand⁴⁰ (fig. 1.21).

Fig 1.21 Aliphatic C-F bond activation in a fluoroalkylated ligand



A facile intramolecular C-F activation is seen in the fluoroalkyl aqua complex, $Cp^*Rh(PMe_3)(OH_2)(CF_2C_6F_5)$.⁴¹ When this complex is dissolved in a non-coordinating solvent such as $CDCl_3$, the perfluorobenzyl ligand undergoes hydrolysis, with the α -carbon ultimately being transformed into a carbonyl ligand, the two fluorines being lost as HF (fig. 1.22).

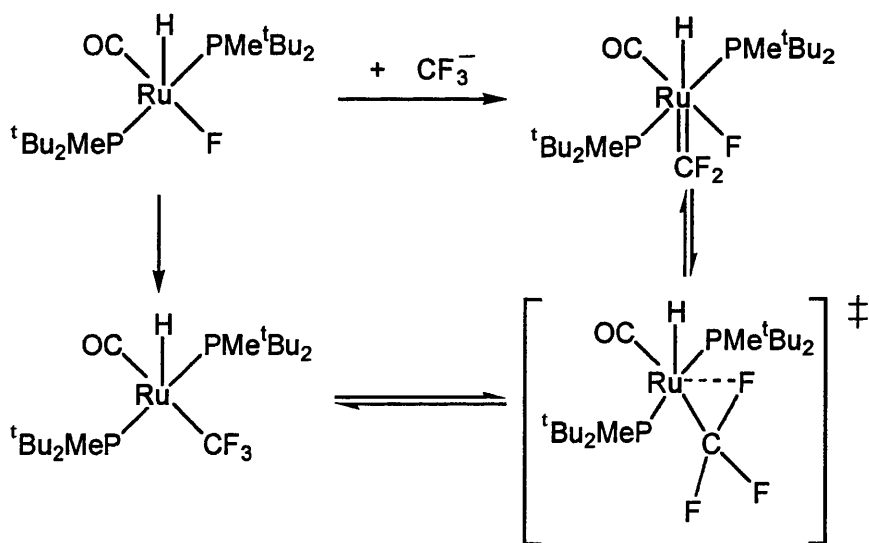
Fig 1.22 Intramolecular hydrolysis of an aliphatic C-F bond



This transformation does not occur in the more coordinating solvent d_6 -acetone, suggesting that coordinated water is responsible for the hydrolysis, its acidity being enhanced by binding to the rhodium centre.

Huang and Caulton⁴² have also reported the intramolecular C-F activation of a trifluoromethyl group bound to a coordinatively unsaturated Ru(II) phosphine complex. The reaction of $\text{Ru}(\text{PMe}^t\text{Bu}_2)_2(\text{CO})\text{HF}$ with the trifluoromethyl anion source, $\text{Me}_3\text{SiCF}_3/\text{CsF}$, at 75 °C, yields a difluorocarbene complex via α -F migration. It is proposed that electron transfer to a C-F σ^* orbital leads to facile C-F cleavage and fluoride loss via an η^2 - CF_3 transition state (fig.1.23).

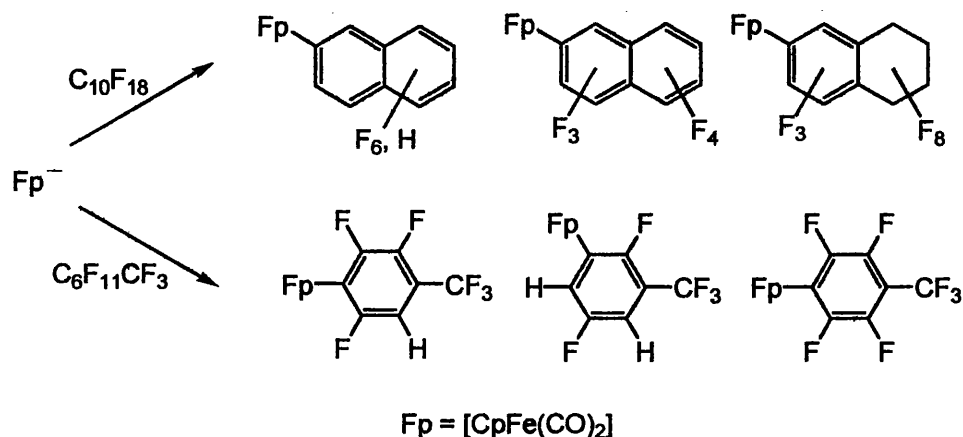
Fig 1.23 Formation of a difluorocarbene ruthenium complex



Intermolecular reactions of perfluoroalkanes and transition metals although much more difficult, have also been reported. Using a flow system to prevent over reduction, both Ni and Fe metals can aromatise cyclic perfluoroalkanes at 400-600 °C.^{3c} Under milder conditions, the organometallic nucleophile $[\text{CpFe}(\text{CO})_2]^-$ was shown by Harrison and Richmond⁴³ to be reactive towards perfluoromethylcyclohexane and

perfluorodecalin to afford fluoroaryl iron complexes (fig 1.24) providing the first example of reactions between saturated perfluorocarbons and transition metal reagents in homogeneous solution.

Fig 1.24 Products of the reaction of $[\text{CpFe}(\text{CO})_2]^-$ and perfluoroalkanes

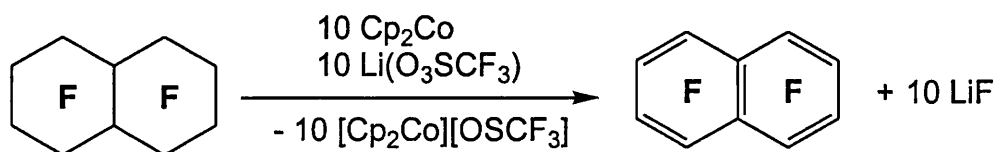


A tertiary C-F bond is necessary for such transformations to occur, since no reaction was observed with perfluorocyclohexane. The results with alternative organometallic nucleophiles ($[\text{Re}(\text{CO})_5]^-$ reacted much slower than Fp^- with perfluorodecalin, $[\text{CpMo}(\text{CO})_3]^-$ did not react) imply that the reducing power of the nucleophile is important and is consistent with single electron transfer to the fluorocarbon being the rate determining first step in the reaction mechanism.

Cobaltocene, a neutral complex, which can act as a one electron reductant, can also react with perfluorodecalin at room temperature.⁴⁴ The inorganic product from this reaction is cobaltocenium fluoride, $[\text{Cp}_2\text{Co}]\text{F}$. The reactive nature of the fluoride ion however, means that samples of this complex usually contain about 25 % $[\text{Cp}_2\text{Co}]\text{HF}_2$. The fate of the perfluorodecalin was not established, but in the presence of the fluorine scavenger $\text{Li}(\text{O}_3\text{SCF}_3)$, it was found that 10 equivalents of cobaltocene could reduce perfluorodecalin to perfluoronaphthalene in 53 % yield (fig. 1.25). Interestingly, the

cobaltocenium fluoride complex has also proved to be a source of ‘naked’ fluoride, which can be used to fluorinate organic halides, converting methyl iodide and benzoyl chloride, to methyl fluoride and benzoyl fluoride, respectively.

Fig 1.25 Reaction of cobaltocene and perfluorodecalin



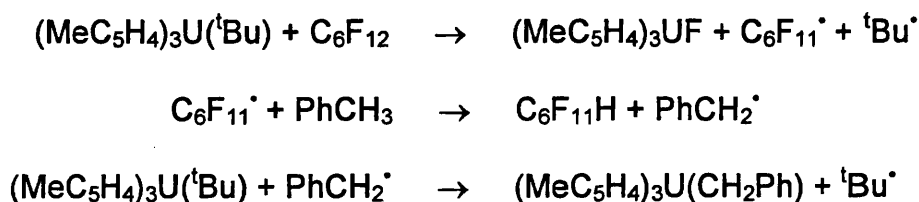
The more strongly reducing Cp^*_2Co also reacts with perfluorodecalin at a faster rate than cobaltocene. Upon testing other fluorocarbons, it was found that the perfluoroalkane must have at least one tertiary C-F bond for reaction to occur. The conversion of perfluoromethylcyclohexane to perfluorotoluene was facilitated by 6 equivalents each of Cp^*_2Co and $\text{Li}(\text{O}_3\text{SCF}_3)$.^{3c} It is proposed that an electron transfer is important in the initial C-F activation step, and that the presence of the lithium cation also has an important role in the formation of perfluoroaromatics. The tertiary C-F bond would appear to be the most reactive site for the reaction with transition metal complexes. Electrochemical measurements (Table 1.1) suggest that the initial reduction of tertiary fluorocarbons is more facile than for secondary systems.²

Table 1.1 Reduction potentials for selected perfluoroalkanes

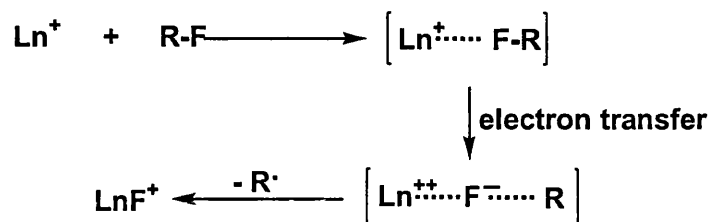
Perfluoroalkane	No. of tertiary C-F bonds	Reduction potentials (V vs Ag/0.010 M AgClO ₄)
Perfluorodecalin	2	-2.60
Perfluoromethylcyclohexane	1	-2.9
Perfluorocyclohexane	0	< -3.0

By using the uranium complex, $(\text{MeC}_5\text{H}_4)_3\text{U}(\text{tBu})$, Weydert et al.⁴⁵ showed that activation of perfluoroalkanes with no tertiary C-F bonds was possible. The reaction of $(\text{MeC}_5\text{H}_4)_3\text{U}(\text{tBu})$ and perfluorocyclohexane in toluene proceeds at room temperature over 12 h to give a 1:1 mixture of $(\text{MeC}_5\text{H}_4)_3\text{UF}$ and $(\text{MeC}_5\text{H}_4)_3\text{U}(\text{CH}_2\text{Ph})$. The fluoroorganic product was identified by GC-MS as $\text{C}_6\text{F}_{11}\text{H}$. It was proposed that fluorine is initially abstracted from the perfluorocyclohexane to form a $\text{C}_6\text{F}_{11}^\bullet$ radical, which then removes a hydrogen atom from the toluene solvent. The resulting PhCH_2^\bullet fragment then reacts with the starting material to give $(\text{MeC}_5\text{H}_4)_3\text{U}(\text{CH}_2\text{Ph})$ (fig. 1.26).

Fig 1.26 Reaction of $(\text{MeC}_5\text{H}_4)_3\text{U}(\text{tBu})$ and C_6F_{12}

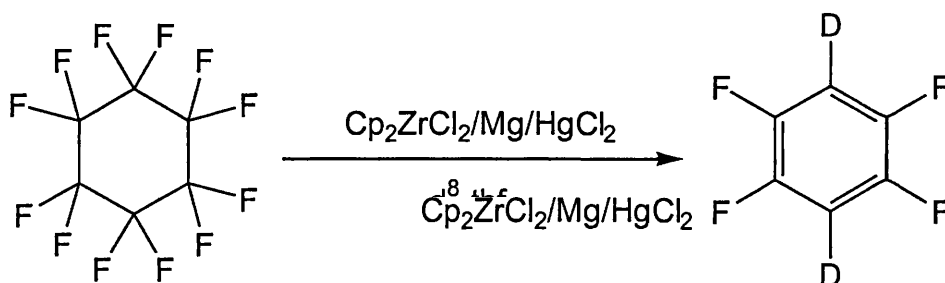


Lanthanide cations (Ce^+ , Pr^+ , Sm^+ , Ho^+ , Tm^+ , Yb^+) are seen to activate C-F bonds in saturated perfluorocarbons such as CF_4 , CF_3H , and C_2F_6 in the gas phase.⁴⁶ A ‘harpoon’ like mechanism is suggested, in which an initial electron transfer to the perfluoroalkane is followed by coordination of the fluoride and elimination of a radical substrate (fig 1.27).

Fig. 1.27 Gas phase C-F activations with lanthanide cations (Ln^+)

A recent density function calculation has suggested that the 14-electron *trans*- $\text{Ir}(\text{Cl})(\text{PH}_3)_2$ would be capable of oxidative addition of CF_4 .⁴⁷ The energy barrier for the oxidative addition is calculated to be lower than for the fluorine abstraction. This shows that the oxidative addition of saturated perfluorocarbons is theoretically possible

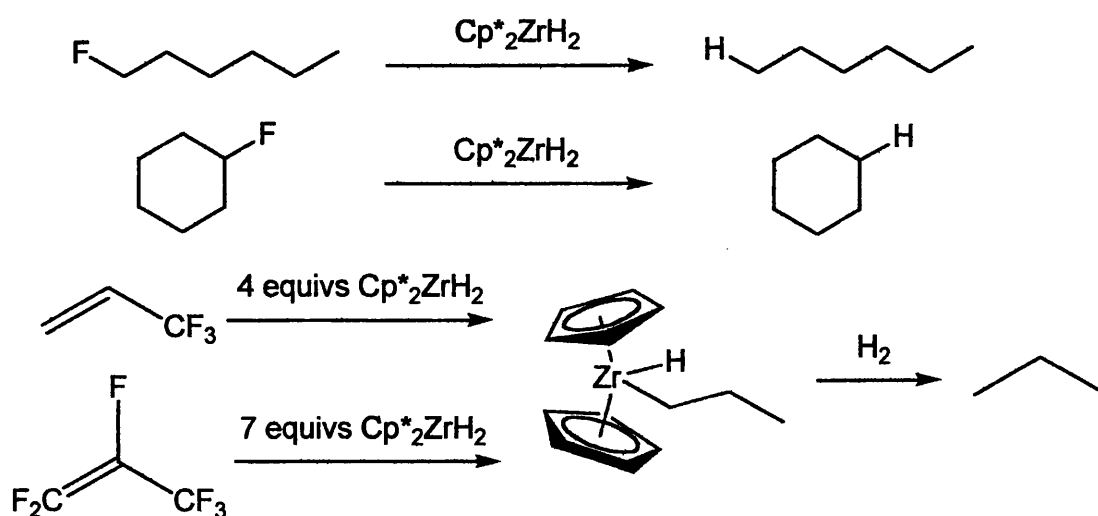
Activation of aliphatic C-F bonds in perfluoroalkanes with no tertiary C-F bonds has also been reported with early transition metallocenes. A highly active reductive defluorination system was prepared from $\text{Cp}_2\text{ZrCl}_2/\text{Mg}/\text{HgCl}_2$.⁴⁸ This was seen to defluorinate and aromatise perfluorocyclohexane to 2,3,5,6-tetrafluorobenzene, the two hydrogen atoms in the final product originating from the solvent (fig. 1.28). Zirconocene chloride is converted to zirconocene fluoride with the formation of the strong Zr-F bond providing a strong driving force for the reaction.

Fig 1.28 Reaction of perfluoroalkanes with no tertiary C-F bond.

The related zirconium complex, $\text{Cp}^*_2\text{ZrH}_2$, has also been found to activate aliphatic C-F bonds of lesser fluorinated alkanes yielding completely defluorinated

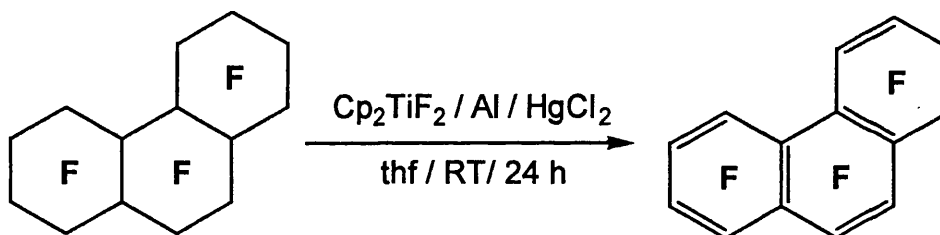
products.⁴⁹ (fig 1.29). Under 1.3 atm of H_2 and at ambient temperature, the dihydride reacted with 1-fluorohexane to form hexane. Similar C-F cleavage occurred with fluorocyclohexane and 1-fluoroadamantane, albeit at higher temperatures. The inorganic product of the reaction, in all cases, is Cp^*_2ZrHF , the strong Zr-F bond again being an obvious driving force for reaction to occur. More surprising is the ability of stoichiometric quantities of $\text{Cp}^*_2\text{ZrH}_2$ to completely defluorinate 3,3,3-trifluoropropene or perfluoropropene. In each case, $\text{Cp}^*_2\text{Zr}(\text{n-propyl})\text{H}$ was formed which eliminated propane on treatment with H_2 . Cp^*_2ZrHF has also proved to be a suitable precursor. The mechanisms for activation of the aliphatic fluorocarbons are believed to involve a bond metathesis pathway on the basis of the order of reactivity $1^\circ \text{C-F bond} > 2^\circ \text{C-F bond} > 3^\circ \text{C-F bond}$. This suggests that coordination of fluoride to the zirconium is an essential step. The fluoroalkene reactions, conversely, are suggested to occur via an insertion/ β -F elimination pathway. In every case, the origin of the hydrogen, which replaces the fluorine, is the starting dihydride.

Fig 1.29 Aliphatic C-F bond activations using $\text{Cp}^*_2\text{ZrH}_2$



The strength of the early transition metal-fluoride bond was thought to be too strong for such systems to function as catalysts. However, Richmond and Kiplinger,⁴⁸ have shown that group IV metallocene complexes can induce the catalytic defluorination of perfluoroalkanes. The reaction of Cp_2TiF_2 and perfluorodecalin in the presence of an excess of Al/HgCl_2 in thf at room temperature resulted in the catalytic production (12 turnovers) of perfluoronaphthalene. The Cp_2TiF_2 can be recovered from the reaction mixture. Under the same conditions, perfluoroperhydrophenanthrene gave the aromatised analogue, perfluorophenanthrene (fig 1.30).

Fig 1.30 Catalytic defluorination of perfluoroperhydrophenanthrene

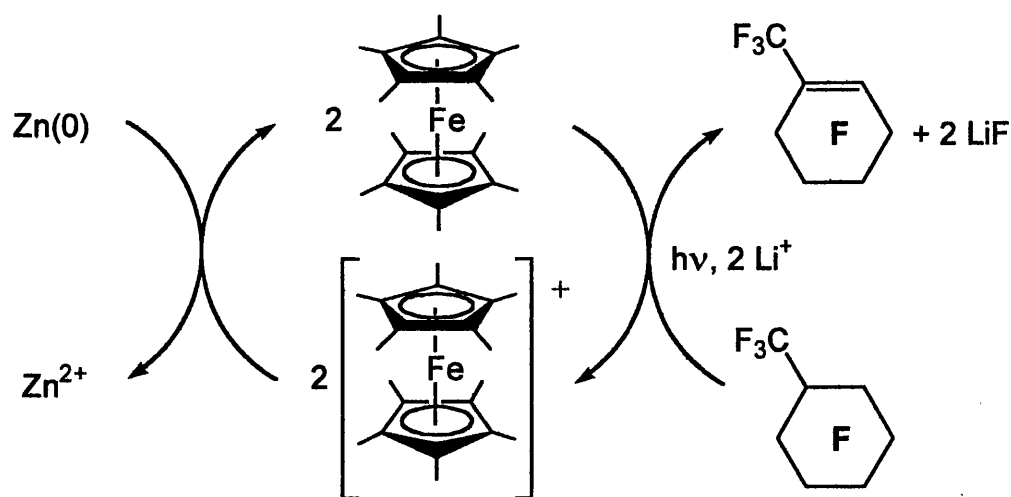


Also reported was the conversion of perfluorodecalin to perfluoronaphthalene with Cp_2ZrF_2 or Cp_2ZrCl_2 , in the presence of Mg/HgCl_2 . The fact that these reactions occur with early transition metal fluoride complexes means the strong metal-fluoride bond is not a barrier to catalysis. Successful stoichiometric conversions of perfluorodecalin with $[\text{Cp}_2\text{Ti}]$ and $[\text{Cp}_2\text{Zr}]$, generated photochemically by reductive elimination of biphenyl from Cp_2TiPh_2 and Cp_2ZrPh_2 , confirm that the nascent low-valent metallocenes mediate the defluorination process. The critical role played by the metallocene is shown by the reaction of Mg/HgCl_2 with perfluorodecalin, in the absence of a metallocene, which leads to the complete exothermic reduction of perfluorodecalin down to carbon, whereas the milder Al/HgCl_2 system requires the presence of a

metallocene. It was also noted that the cobaltocene chemistry⁴⁴ described above can be made catalytic in the presence of Al or Mg as the terminal reductant.^{3c}

Burdeniuc and Crabtree⁵⁰ have reported the defluorination of perfluoromethylcyclohexane to perfluoro-1-methylcyclohexene, upon ultraviolet irradiation in the presence of a decamethylferrocene photosensitiser. The use of $\text{Li}(\text{O}_3\text{SCF}_3)$ as a fluoride scavenger allows this conversion to occur under very mild conditions. The process can be made catalytic, with respect to iron, by adding zinc(0) which reduces $[\text{Cp}^*_2\text{Fe}]^+$ back to the active species (fig. 1.31). The reaction was performed in the presence of excess perfluoroalkane to prevent overreduction, and displayed 110 turnovers and a conversion of 12 %, which made the product difficult to separate, and only usable *in situ*.

Fig. 1.31 Catalysis of a photolytic defluorination of perfluoromethylcyclohexane



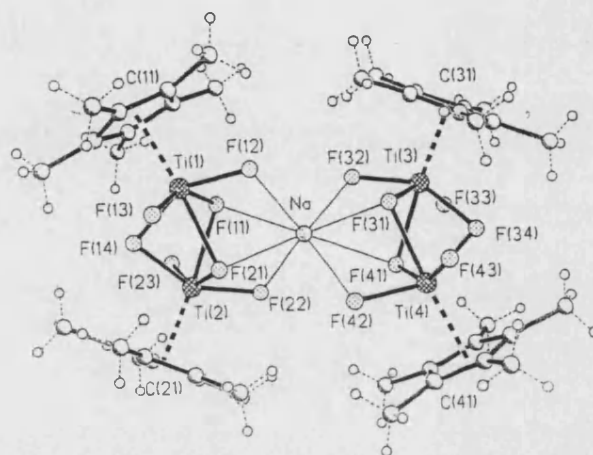
1.4 Transition metal fluorides

The second part of this introduction describes the synthesis and reactivity of late transition metal fluoride and bifluoride complexes. Transition metal fluorides are generally associated with metals in high oxidation states. Fluoride, categorised as a hard base in Hard/Soft Acid/Base theory⁵¹, has been shown to form many complexes with hard early transition metal acids like Ti^{4+} and Zr^{4+} , or give high oxidation mid-to-late transition metal complexes such as $Ru^V F_5$. Coordination of fluoride to low valent transition metals, with an oxidation state of +3 or lower, is more difficult as the lower the oxidation state the softer the transition metal acid, especially for the late transition metals. However, there has been increasing interest in using fluoride as a ligand in low oxidation state transition metal systems due to their potential as catalysts for organic transformations.^{52,53}

Introduction of fluoride into low oxidation state transition metal complexes is also problematic as there is no single methodology that is applicable across the periodic table. One route that has proved effective with early transition metal complexes is the metathesis of lower halides, such as chlorides, bromides and iodides, with Group 1 or 2 fluorides, such as NaF. However, a major problem with this method in the incorporation of fluorinating agent into the final product, making separation of the products difficult. Trimethyltin fluoride, developed by Roesky and coworkers⁵³, has been described as an ideal fluorinating agent for Group 4-6 transition metals due to its low solubility and the volatility of trimethyltin chloride. It has led to syntheses of many Group 4 organometallic fluoride species, many with exotic structures (fig 1.32). Silver fluoride has been used for later transition metal complexes, but complete exclusion of water from AgF is difficult resulting in the formation of hydroxy and aqua complexes rather

than fluoride complexes. The use of a silver salt such as AgBF_4 to abstract a halide and subsequent reaction with a source of fluorine can be used to the same effect.⁵²

Fig 1.32 X-ray structure of $[\{(\text{Cp}^*\text{TiF}_3)\}_4\text{F}_2]\text{Na}^-$



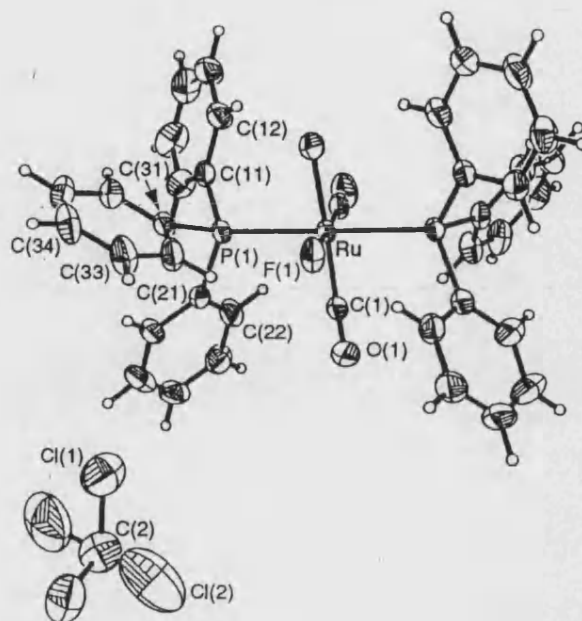
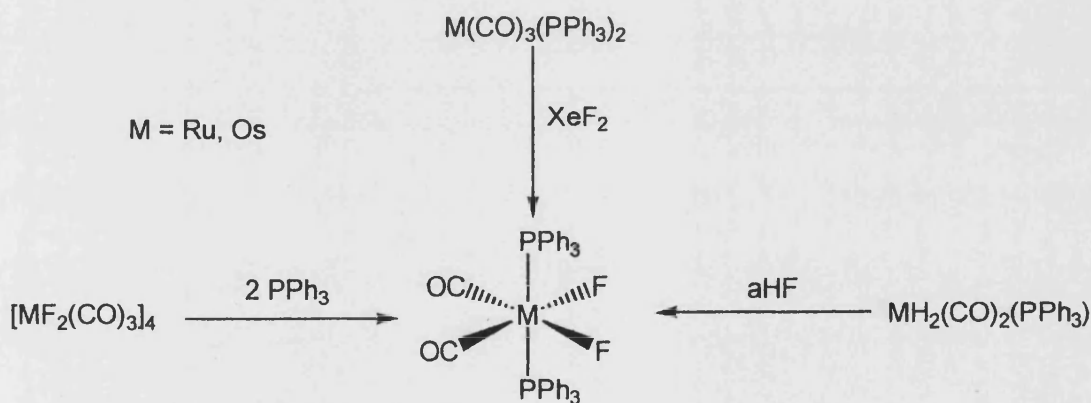
Other methods that have a wider range of activity include using anhydrous HF or amine HF reagents, or XeF_2 dissolved in HF.⁵⁴ Anhydrous HF can perform protonolysis on metal bound hydrides replacing the hydride with a fluorine, but the highly corrosive nature of HF means it is difficult to handle without specialised equipment. Amine HF salts (e.g. pyridine.HF, $\text{Et}_3\text{N} \cdot 3\text{HF}$) are mild enough to be used in glass reaction vessels and have found extensive applications in organofluorine chemistry, e.g. $\text{Et}_3\text{N} \cdot 3\text{HF}$ has been used as a fluoride source for regioselective ring opening of epoxides to give fluorohydrins.⁵⁵ The use of XeF_2 in HF creates the reactive adduct $[\text{F-Xe}][\text{HF}_2]$, which can deliver fluoride to a metal centre via oxidative addition. The ratio of XeF_2 to complex is decisive in the amount of fluorination that can occur.

As seen above, C-F bond activation can also lead to the formation of metal fluoride complexes, (e.g. $\text{Ni}(\text{PEt}_3)(\text{C}_6\text{F}_5)\text{F}^{9,10}$) although most products are usually

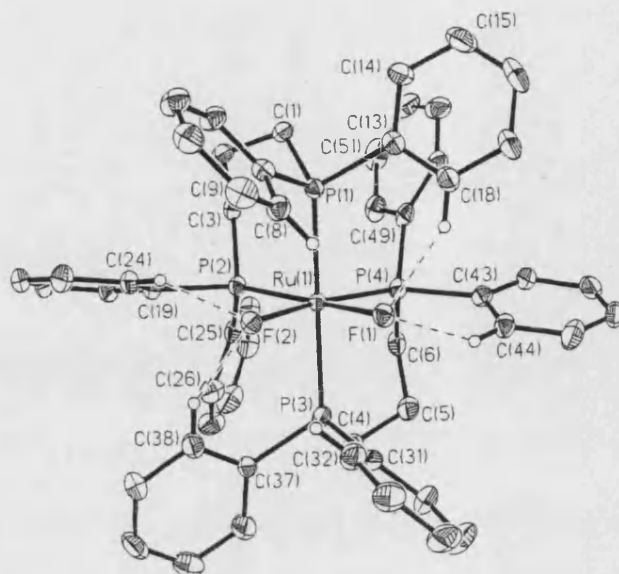
formed via serendipity rather than using a systematic approach. The following sections detail late transition metal fluorides of Groups 8, 9 and 10 that have been synthesised using some of these methods.

1.4.1 Group 8 transition metal fluorides

The difluoride complex $[\text{Ru}(\text{CO})_3\text{F}_2]_4$, prepared from RuF_5 and carbon monoxide, was first reported in 1970.⁵⁶ The same product could also be prepared as the major of three products from the controlled reaction of $\text{Ru}_3(\text{CO})_{12}$ with XeF_2 as well as two other minor products.⁵⁷ Recently, the reaction of $\text{Ru}_3(\text{CO})_{12}$ with XeF_2 in anhydrous HF has led to a reliable synthesis for *cis*- $\text{RuF}_2(\text{CO})_4$,⁵⁸ and the same methodology was used to convert $\text{Os}_3(\text{CO})_{12}$ to *cis*- $\text{OsF}_2(\text{CO})_4$.⁵⁹ Removal of solvent from the reaction mixtures yielded the moisture sensitive tetramers $[\text{M}(\text{CO})_3\text{F}_2]_4$ ($\text{M} = \text{Ru}, \text{Os}$), which have been used extensively for the synthesis of air and moisture stable ruthenium (II) and osmium (II) fluoride complexes. Treatment of these tetramers with phosphines, has yielded the fluoride complexes, $[\text{OC-6-13}][\text{MF}_2(\text{CO})_2(\text{L})_2]$, ($\text{M} = \text{Ru}, \text{L} = \text{PEtPh}_2$; $\text{M} = \text{Os}, \text{L} = \text{PPh}_3, \text{PEtPh}_2$). These difluoride complexes have also been obtained via the reaction of XeF_2 and $\text{M}(\text{CO})_3(\text{PPh}_3)_2$ (which proceed via the fluoroacyl complexes $\text{MF}(\text{COF})(\text{CO})_2(\text{PPh}_3)_2$)⁶⁰, which led to a X-ray crystal structure (fig 1.33), and upon addition of anhydrous HF to the dihydride species $\text{MH}_2(\text{CO})_2(\text{PPh}_3)_2$ ⁶¹ (fig 1.34). In each case, the six-coordinate complexes have a *cis,cis,trans* geometry. The *trans* phosphine ligands are bent towards the fluoride ligands and help stabilise the complex by intramolecular CH---F hydrogen bonding.⁶⁰

Fig 1.33 X-ray crystal structure of $[OC-6-13][RuF_2(CO)_2(L)_2]^{60}$ **Fig 1.34** Routes to $MF_2(CO)_2(PPh_3)_2$ 

Recently a ruthenium difluoride complex that is not stabilised by strong π -acceptor ligands, like CO, was reported by Mezzetti et al.⁶² The ruthenium (II) species, *cis*-Ru(dppp)₂F₂ was synthesised by treating cationic $[Ru(dppp)_2F]^+$ with a source of fluoride. Although there are no strong π acid ligands present, a combination of the electron withdrawing phenyl rings and intramolecular CH---F hydrogen bonding aids the stability of this compound (fig 1.35).

Fig 1.35 X-ray crystal structure of *cis*-Ru(dppp)₂F₂

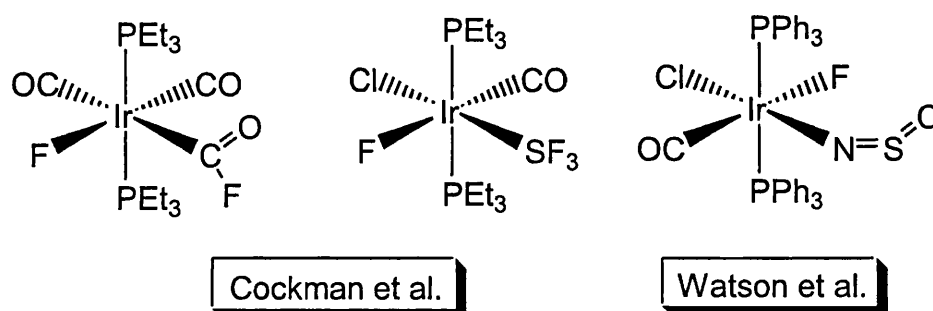
1.4.2 Group 9 transition metal fluorides

Most of the cobalt(II) fluoride complexes reported have nitrogen donor ligands present and syntheses have involved a variety of starting materials. One example is the treatment of $\text{Co}(\text{OH})_2$ with hydrazine, HF and various amines which led to the synthesis of $\text{Co}(\text{N}_2\text{H}_4)_2\text{F}_2 \cdot 2\text{H}_2\text{O}$, $\text{Co}(\text{dmpz})\text{F}_2(\text{H}_2\text{O})_2$, and $[\text{bipyH}][\text{CoF}_3(\text{bipy})] \cdot 6\text{H}_2\text{O}$.⁶³

Much of the chemistry of rhodium and iridium fluoride complexes revolves around the fluorous analogues of Vaska's complex, $\text{IrF}(\text{CO})(\text{PR}_3)_2$, and the rhodium analogue $\text{RhF}(\text{CO})(\text{PR}_3)_2$. A wide range of complexes with various phosphine ligands can be prepared by treating $\text{M}(\text{Me})(\text{CO})(\text{PR}_3)_2$ with anhydrous HF.⁵² These complexes contradict the hard/soft acid/base theory as the strength of the metal halide bond follows the order $\text{F}^- > \text{Cl}^- > \text{Br}^- > \text{I}^-$ in anhydrous dichloromethane.⁶⁴ However the fluoride ligand becomes more labile in protic solvents due to hydrogen bonding effects. These fluorous Vaska's type complexes have led to many more iridium (III) and rhodium (III) fluoride complexes by simple oxidative addition reaction with reagents such as O_2 , MeI,

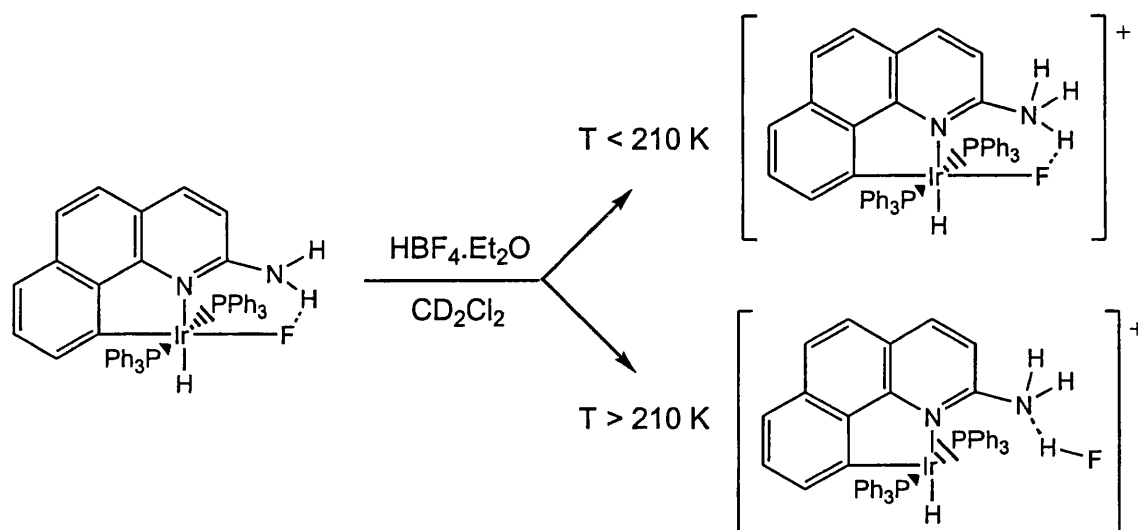
HCl and HBr.⁶⁵ Similarly, oxidative addition of XeF₂, yields the trifluoroiridium (III) complex IrF₃(CO)(PPh₃)₂.⁶⁶ Fluorination of iridium (I) phosphine carbonyl complexes with XeF₂ has led to iridium (III) fluoride complexes (fig. 1.36).

Fig 1.36 Iridium (III) fluoride complexes⁵⁸

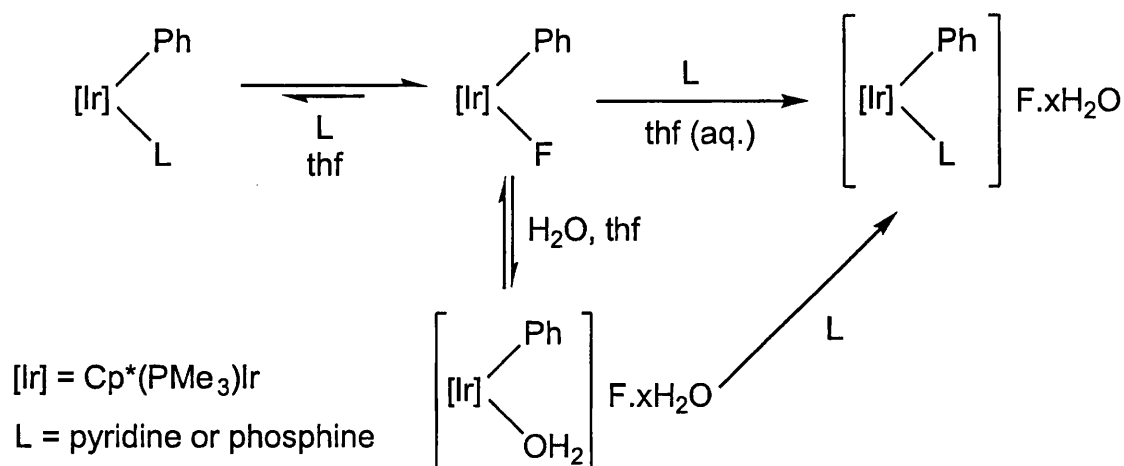


Other rhodium and iridium complexes containing fluoride ligands have also been synthesised by different routes. For example, Cp^{*}Rh(PMe₃)(C₆F₅)F was prepared via the C-F activation of hexafluorobenzene with Cp^{*}Rh(PMe₃)(C₂H₄), as mentioned earlier¹⁴ (fig. 1.8). Alkyl ammonium fluoride species have also been shown to deliver fluorine to an iridium centre. The reaction between [Ir(2-amino-7,8-benzoquinone)(PR₃)₂H(OH₂)]⁺ and ⁿBu₄NF at low temperature affords an iridium (III) fluoride.⁶⁷ Protonolysis of the pendant -NH₂ group at low temperature leads to hydrogen bonding between the NH₃⁺ group and the fluoride ligand, and as the complex warms above 210 K, the iridium-fluoride bond cleaves irreversibly to yield HF coordinated to the amine group (fig. 1.37). This emphasises the lability of fluoride in iridium complexes when dissolved in protic solvents.

Fig 1.37 Lability of an iridium (III) fluoride complex in protic conditions



The labile nature of the Ir-F bond at room temperature is also displayed in the displacement of F^- from $\text{Cp}^*\text{IrF}(\text{PMe}_3)(\text{Ph})$ under anhydrous conditions, by the addition of a Lewis base such as phosphine or pyridine.⁶⁸ An equilibrium is established between the resultant salt and the covalent starting material which favours slightly the uncharged species. The rate of establishment and the magnitude of the equilibrium constant are greatly increased on addition of water to yield the hydrate $[\text{Cp}^*\text{Ir}(\text{PMe}_3)(\text{Ph})(\text{OH}_2)]\text{F} \cdot x\text{H}_2\text{O}$, undoubtedly facilitated by strong hydrogen bonding between the water and the fluoride anion. The high reactivity of the hydrate enables these species to serve as intermediates in the water-catalysed removal of fluoride by various Lewis bases (fig 1.38).

Fig 1.38 Labile Ir-F bond in $\text{Cp}^*\text{IrF}(\text{PMe}_3)(\text{Ph})$ 

The ability of late transition metal fluorides to interact via hydrogen bonding with small molecules has led to complexes finding useful synthetic applications. For example, the iridium fluoride dihydride complex $(\text{P}^t\text{Bu}_2\text{Ph})_2\text{IrF}(\text{H})_2$, synthesised by halide metathesis between $(\text{P}^t\text{Bu}_2\text{Ph})_2\text{IrCl}(\text{H})_2$ and $[\text{NMe}_4]\text{F}$, has been shown to promote C-H activation.⁶⁹

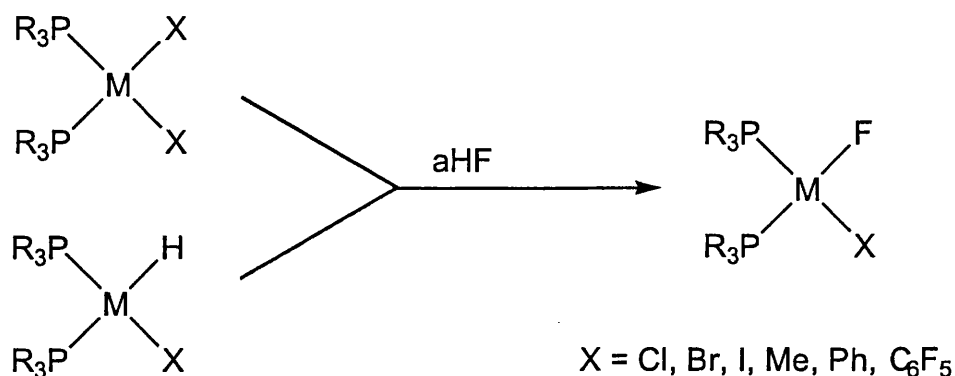
1.4.3 Group 10 transition metal fluorides

There are very few reported nickel fluoride complexes and the majority are seen to be halide bridged dimeric species. For example, the reaction between $\text{Ni}(\text{C}_6\text{F}_5)_2(\eta^6\text{-toluene})$ and NH_4F led to the crystallographically characterised halide bridged dimer, $[\text{NH}_4]_2[\{\text{Ni}(\mu\text{-F})(\text{C}_6\text{F}_5)_2\}_2]$.⁷⁰ As mentioned earlier, oxidative addition of C_6F_6 to $\text{Ni}(0)$ centres has led to formation of $(\text{PEt}_3)_2\text{Ni}(\text{C}_6\text{F}_5)\text{F}$ ^{9,10} and $(^t\text{Bu}_2\text{PCH}_2\text{CH}_2\text{P}^t\text{Bu}_2)\text{Ni}(\text{C}_6\text{F}_5)\text{F}$.¹¹

Fluoride complexes of palladium(II) and platinum(II), all of which contain phosphine ligands, can be grouped simply as neutral and cationic species. The neutral

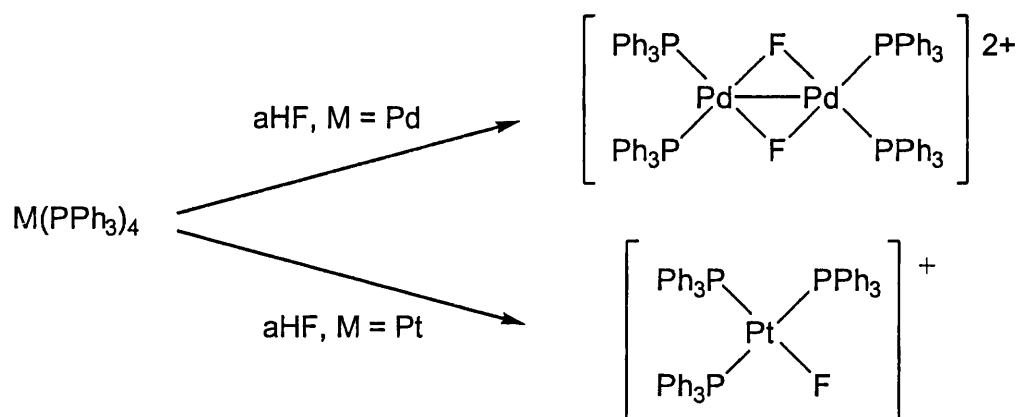
species are all of the form $[\text{MXF}(\text{phosphine})_2]$ where $\text{X} = \text{Cl}, \text{Br}, \text{I}, \text{Me}, \text{Ph}$ or C_6F_5 . The simplest route into these complexes is the addition of HF to a dihalide or hydride halide metal phosphine complex (fig. 1.39).⁶⁵

Fig 1.39 Synthesis of Pd(II) and Pt(II) fluorides.



Alternatively, halide exchange with silver fluoride and *trans*-(PPh_3)₂Pt(Me)Cl produces *trans*-(PPh_3)₂Pt(Me)F, a technique used by Grushin et al. to synthesise *trans*-(PPh_3)₂Pd(Me)F.⁷¹ The insertion of the fourteen electron platinum(0) intermediate $[\text{Pt}(\text{tBu}_2\text{PCH}_2\text{P}^t\text{Bu}_2)]$ into the C-F bond of hexafluorobenzene also gives a platinum fluoride complex, $(\text{tBu}_2\text{PCH}_2\text{P}^t\text{Bu}_2)\text{Pt}(\text{C}_6\text{F}_5)\text{F}$ as detailed earlier.¹³

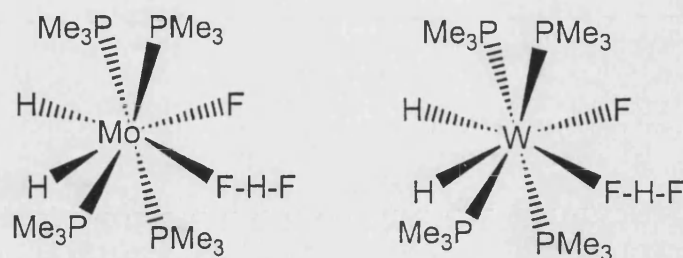
The reactions between $\text{M}(\text{PPh}_3)_4$ and HF produces different products for palladium and platinum. The use of $\text{Pd}(\text{PPh}_3)_4$ is reported to give the fluoro-bridged dimer $[\{\text{PdF}(\text{PPh}_3)_2\}_2][\text{HF}_2]_2$, while $\text{Pt}(\text{PPh}_3)_4$ gives the trisphosphine monofluorocation $[\text{Pt}(\text{PPh}_3)_3\text{F}]^+$ (fig 1.40).⁶⁵ The platinum species is very stable towards halide exchange and only decomposes in the presence of water over a period of weeks to give the hydroxide species $[\text{Pt}(\text{PPh}_3)_3(\text{OH})]^+$.⁷²

Fig 1.40 Different products from the treatment of $M(PPh_3)_4$ with HF

1.5 Transition metal bifluoride complexes

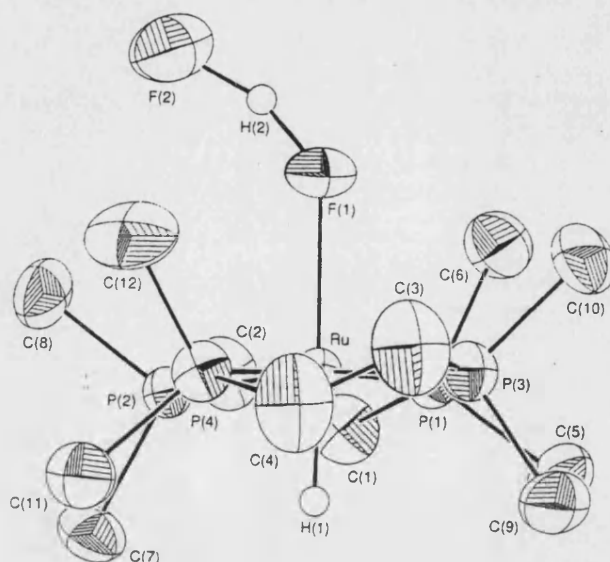
As mentioned above transition metal fluorides have the ability to form hydrogen bonds with hydrogen donors. The strongest known hydrogen bond is found in bifluoride, FHF^- .⁷³ The bonding of the HF to the metal fluoride has the ability to alter the strength of the M-F bond. The first example of a transition metal bifluoride complex, $Pt(PEt_3)_2(Ph)(FHF)$, was reported by Coulson⁷⁴ over 25 years ago. Since then only a few transition metal species containing a terminal FHF ligand have been characterised. Parkin and coworkers⁷⁵ synthesised the bifluoride complexes, $Mo(PMe_3)_4H_2F(FHF)$ and $W(PMe_3)_4H_2F(FHF)$ (fig 1.41), by treating $M(PMe_3)_5H_2$ ($M = Mo, W$) species with aqueous HF. Both complexes were characterised by X-ray crystallography. The structures appear as trigonal dodecahedra with distorted tetrahedral arrays of phosphine ligands.

Fig 1.41 Mo (IV) and W (IV) bifluoride complexes



The M-F...F angle is $\sim 134^\circ$ in both complexes. Neutron diffraction studies of the tungsten complex show the FHF ligand is asymmetric in nature, the hydrogen being located closer (0.961 \AA) to the distal fluorine, than to the metal bound proximal fluorine (1.43 \AA), and the F-H-F bond angle is 170.6° . NMR studies reveal a J_{HF} coupling of 410 Hz , which is large compared to that seen for bifluoride salts, such as $[\text{Cp}_2\text{Co}][\text{FHF}]$ which shows a coupling of 121 Hz .⁴⁴ This indicates that the hydrogen bonding is weak in the molybdenum and tungsten bifluoride complexes.

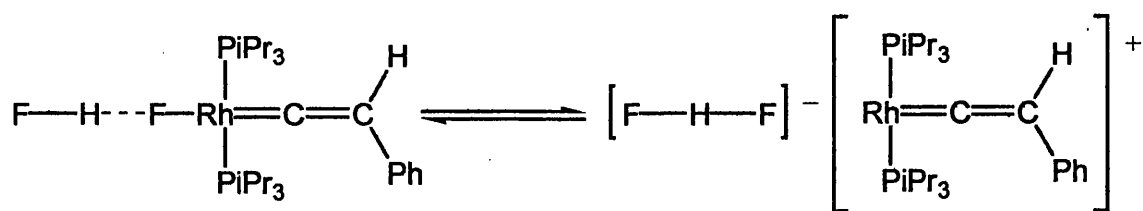
The first η^1 -bifluoride complex characterised in both solid and solution state was reported by Whittlesey et al.^{23,24} As mentioned earlier, the reaction of *cis*-Ru(dmpe)₂H₂ with highly fluorinated aromatics yielded *trans*-fluoroaryl hydride species, but was also found to yield a small amount of the bifluoride complex *trans*-Ru(dmpe)₂(FHF)H (fig 1.42).

Fig 1.42 X-ray crystal structure of *trans*-Ru(dmpe)₂(FHF)H

This complex was independently synthesised by the reaction of the dihydride with $\text{Et}_3\text{N} \cdot 3\text{HF}$. X-ray crystallography showed a $\text{Ru-F}\cdots\text{F}$ angle of 129.9° with the bifluoride ligand *trans* to the hydride. Low temperature NMR spectroscopy displayed a J_{HF} coupling constant of 274 Hz to the distal fluorine, suggesting that although the hydrogen bonding is still weak it is much stronger than that seen in the molybdenum and tungsten bifluoride complexes.

Werner et al.⁷⁶ have reported a rhodium fluoride that traps HF to give the bifluoride complex $(\text{P}^i\text{Pr}_3)_2\text{Rh}(=\text{CCHPh})(\text{FHF})$. The complex shows a rapid exchange process occurring with the bifluoride ligand dissociating readily at room temperature (fig 1.43). At 210 K, ^{19}F NMR spectroscopy shows a doublet of doublets with coupling constants $^1J_{\text{HF}} = 418$ Hz and $^2J_{\text{FF}} = 101$ Hz. This implies that the hydrogen bonding is weaker than in the ruthenium system and closer to that seen in the molybdenum and tungsten cases.

Fig 1.43 Fast exchange of rhodium bifluoride complex

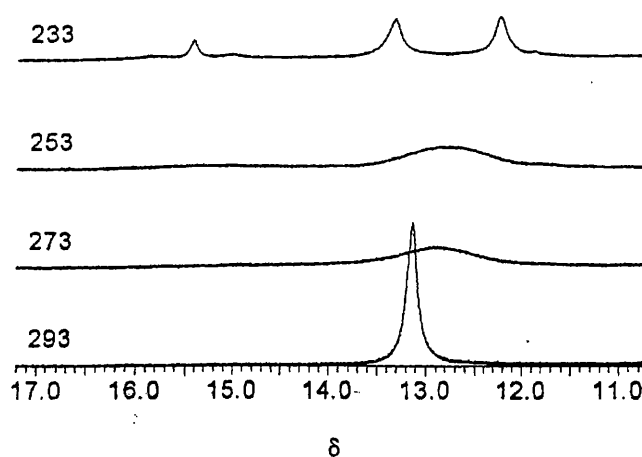


Other crystallographically characterised complexes include *trans*- $\text{Ni}(\text{PEt}_3)_2(2\text{-C}_3\text{NF}_3\text{H})(\text{FHF})$ ⁷⁷ in which the $\text{Ni-F}\cdots\text{F}$ bond has a larger angle of 156.7° compared to other bifluoride species. This is thought to be due to the residual push-pull interactions from the difluoropyrimidyl ligand. The crystal structure of $\text{Pd}(\text{PPh}_3)(\text{Ph})(\text{FHF})$ ⁷⁸ reveals a similar $\text{M-F}\cdots\text{F}$ angle (153.4°) with the same effect seen for the phenyl ligand as for the difluoropyrimidyl ligand. A dinuclear niobium complex containing two μ -

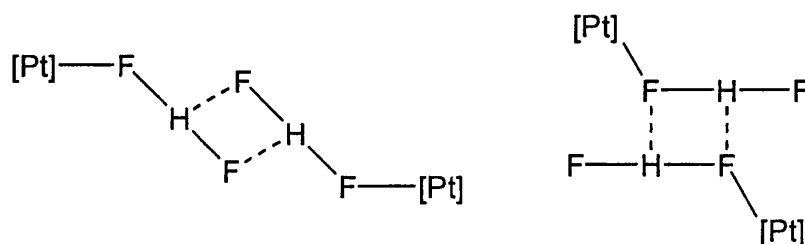
FHF ligands, $[\text{Cp}^*_2\text{Nb}_2\text{F}_6(\mu\text{-FHF})_2]$, has also been structurally characterised but no evidence has been reported for this species in solution.⁷⁹

Two very recent reports have studied the structure and solution dynamics of two related bifluoride complexes. Jasim and Perutz⁸⁰ reported the solution dynamics of the bifluoride complexes $\text{Pt}(\text{PR}_3)_2(\text{FHF})\text{H}$ ($\text{R} = \text{Cy}, ^i\text{Pr}$). Low temperature NMR spectroscopy showed the coupling of the bifluoride proton to the distal fluorine to be, in both cases, in the order of 400 Hz, suggesting a weak hydrogen bond interaction. Surprisingly though, the removal of HF is difficult and it was found that reaction with various reagents, such as organic halides or Lewis bases, actually removed the whole FHF moiety. Dynamic NMR experiments (fig 1.44) in solution showed the exchange of the distal fluoride or HF between platinum centres.

Fig 1.44 Variable temperature ^1H NMR of $\text{Pt}(\text{PCy}_3)_2(\text{FHF})\text{H} + [\text{NBu}_4]\text{FHF}$ ⁷⁷



It was proposed that this exchange process is facilitated by a transition state that has a hydrogen bonded network containing two platinum centres (fig 1.45).

Fig 1.45 Proposed transition states for distal F and HF exchange in $\text{Pt}(\text{PR}_3)_2(\text{FHF})\text{H}$ 

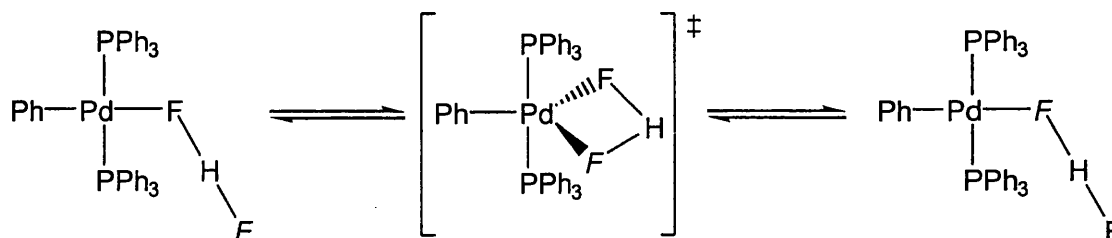
Distal fluoride exchange

HF exchange



A similar study by Grushin et al.⁷⁸ was undertaken on the palladium complex $\text{Pd}(\text{PPh}_3)(\text{Ph})(\text{FHF})$. Again low temperature NMR studies showed that the coupling between the bifluoride proton and the distal fluorine is large ($^1J_{\text{HF}} = 368 \text{ Hz}$) implying a weak hydrogen bond interaction and indeed the complex was seen to exchange HF in solution. ^{19}F NMR magnetisation transfer studies showed that the HF exchange is only a minor contributor to the exchange processes occurring in solution. The fastest exchange process was found to be independent of concentration, which suggested an intramolecular mechanism that does not involve the elimination of HF or FHF^- .

Although this type of complex is known to undergo phosphine dissociation, this was not seen in the rearrangement of the bifluoride. It was therefore proposed that the bifluoride ligand rearranges via a transition state in which the bifluoride ligand coordinates in a η^2 fashion (fig 1.46). The bent hydrogen bonding for the proposed $\mu\text{-FHF}$ palladium species does have a precedent in the X-ray structure of $[\text{Cp}^*_2\text{Nb}_2\text{F}_6(\mu\text{-FHF})_2]$.

Fig 1.46 Proposed mechanism for exchange of bifluoride in $\text{Pd}(\text{PPh}_3)(\text{Ph})(\text{FHF})$ 

The study of bifluoride complexes demonstrates the importance of hydrogen bonding to metal fluoride complexes. The possibility of hydrogen bonding should be considered as the metal-fluoride bond can be weakened by such interactions which may be important in the applications of transition metal fluoride complexes in catalysis.⁵³

1.6 An outline of the work in this thesis

This introduction has shown that there is a growing interest in the field of C-F bond activation, with most of the chemistry being reported in the last decade. Aromatic perfluorocarbons have been shown to be especially reactive to nucleophiles and to electron donors. In contrast, the activation of aliphatic C-F bonds is much more difficult, although room temperature catalytic defluorinations have been seen with early transition metallocene complexes⁴⁸ and catalytic photolytic defluorination seen using decamethylferrocene.⁵⁰

This thesis concerns the activation of C-F bonds by ruthenium phosphine hydride complexes. In chapter 2, we will describe the reactivity of the ruthenium dihydride complex, *cis*- $\text{Ru}(\text{dmpe})_2\text{H}_2$, **1**, (which was shown to thermally activate C_6F_6 at low temperature^{23,24}), towards a variety of saturated perfluorocarbons and the use of

bifluoride hydride complex, *trans*-Ru(dmpe)₂(FHF)H, as a fluorinating agent for organic and transition metal halides. Chapter 3 extends the range of dihydride complexes investigated to other *cis*-Ru(PP)₂H₂ species, where (PP) = depe, **2**; dmpm, **3**; dcpe, **4**; dppe, **5**. The thermal reactions of these dihydrides with both aromatic and aliphatic C-F bonds will be described. The importance of electron transfer processes in the reactivity of *cis*-Ru(dmpe)₂H₂ with C-F bonds^{23,24} led us to investigate the electrochemistry of the dihydride complexes. The results of these experiments and the implications for a possible reaction mechanism are discussed. There is also a short section of the fluorinating properties of the bifluoride hydride complex *trans*-Ru(depe)₂(FHF)H.

Chapter 4 is slightly different in that it reports the thermal reactions of dihydrides **1** and **4** towards perfluoroalkenes. C-F bond activation in perfluoroalkenes has been known for over 40 years, but recent studies by Jones et al.⁴⁹ suggest that novel reactions can still be found. Our studies show that the characteristics of the diphosphine ligand has a large effect on the reaction products. With dihydride **1**, a facile reaction with perfluoropropene or perfluoro-2-methyl-pentane led to a novel ruthenium bifluoride fluoride complex, whereas dihydride **4**, reacts much slower to give a ruthenium monohydride cation and a perfluoroenolate anion. As this chapter is a slight departure from the earlier work in this thesis, the first part of chapter 4 gives an introduction into C-F bond activation in perfluoroalkenes.

References

1. May, G. *Chemistry in Britain*, **1997**, 33(8), 34.
2. Marsella, J. A.; Gilicinski, A. G.; Coughlin, A. M.; Pez, G. P. *J. Org. Chem.*, **1992**, 57, 2856.
3. Recent reviews of C-F bond activation include:- a) Burdenuic, J.; Jedlicka, B.; Crabtree, R. H. *Chem. Ber./Recueil*, **1997**, 130, 145. b) Kiplinger, J.; Richmond, T. G.; Osterberg, C. E. *Chem Rev.*, **1994**, 94, 373. c) Richmond, T. G. In *Activation of Unreactive Bonds and Organic Synthesis*; Murai, S., Ed.; Springer: New York, **1999**.
4. Jones, W. D.; Feher, F. J. *J. Am. Chem. Soc.*, **1984**, 106, 1650.
5. Chambers, R. D. *Fluorine in Organic Chemistry*; Wiley: New York, **1973**; Ch. 5.
6. King, R. B.; Bisnette, M. B. *J. Organomet. Chem.*, **1964**, 2, 38.
7. Richmond, T. G.; Osterberg, C. E.; Arif, A. M. *J. Am. Chem. Soc.*, **1987**, 109, 8091.
8. Ceder, R. M.; Granell, J.; Muller, G.; FontBardia, M.; Solans, X. *Organometallics*, **1996**, 15, 4618. Ceder, R. M.; Granell, J.; Muller, G.; FontBardia, M.; Solans, X. *Organometallics*, **1995**, 14, 5544. Anderson, C. M.; Crespo, M.; Ferguson, G.; Lough, A. J., Puddephatt, R. J. *Organometallics*, **1992**, 11, 1177.
9. Fahey, D. R.; Mahan, J. E. *J. Am. Chem. Soc.*, **1977**, 99, 2501.
10. Cronin, L.; Higgitt, C. L.; Karch, R.; Perutz, R. N. *Organometallics*, **1997**, 16, 4920.
11. Bach, I.; Porschke, K. R.; Goddard, R.; Kopiske, C.; Kruger, C.; Rufinska, A.; Seevogel, K. *Organometallics*, **1996**, 15, 4959.
12. Yamamoto, T.; Alba, M. *J. Organomet. Chem.*, **1997**, 535, 209.
13. Hofmann, P.; Unfried, G. *Chem. Ber.*, **1992**, 125, 169.
14. Jones, W. D.; Partridge, M. G.; Perutz, R. N. *J. Chem. Soc., Chem. Commun.*, **1991**, 264.

-
15. Selmečzy, A. D.; Jones, W. D.; Partridge, M. G.; Perutz, R. N. *Organometallics*, **1994**, *13*, 522.
 16. Bosque, R.; Clot, E.; Fantacci, S.; Maseras, F.; Eisenstein, O.; Perutz, R. N.; Renkema, K. B.; Caulton, K. G. *J. Am. Chem. Soc.*, **1998**, *120*, 12634.
 17. Klahn, A. H.; Moore, M. H.; Perutz, R. N. *J. Chem. Soc., Chem. Commun.*, **1992**, 1699.
 18. Belt, S. T.; Helliwell, M.; Jones, W. D.; Partridge, M. G.; Perutz, R. N. *J. Am. Chem. Soc.*, **1993**, *115*, 1429.
 19. Blum, O.; Frolow, F.; Milstein, D. *J. Chem. Soc., Chem. Commun.*, **1991**, 258.
 20. Hintermann, S.; Pregosin, P. S.; Rüegger, H.; Clark, H. C. *J. Organomet. Chem.*, **1992**, *435*, 225.
 21. Burns, C. J.; Andersen, R. A. *J. Chem. Soc., Chem Commun.*, **1989**, 136.
 22. Watson, P. L.; Tulip, T. H.; Williams, I. *Organometallics*, **1990**, *9*, 1999.
 23. Whittlesey, M. K.; Perutz, R. N.; Moore, M. H. *Chem. Commun.*, **1996**, 787.
 24. Whittlesey, M. K.; Perutz, R. N.; Greener, B.; Moore, M. H. *Chem. Commun.*, **1997**, 187.
 25. Edelbach, B. L.; Jones, W. D. *J. Am. Chem. Soc.*, **1997**, *119*, 7734.
 26. Aizenberg, M.; Milstein, D. *J. Am. Chem. Soc.*, **1995**, *117*, 8674.
 27. Schlag, E. W.; Kaiser, E. W. *J. Am. Chem. Soc.*, **1965**, *87*, 1171.
 28. Zarić, S.; Hall, M. B. *J. Phys. Chem.*, **1997**, *101*, 4646.
 29. Pola, J.; Urbanová, M.; Bastl, Z.; Plzák, Z.; Šubrt, J.; Gregora, I.; Vorlíček, V. *J. Mater. Chem.*, **1998**, *8*(1), 187.
 30. MacNicol, D. D.; Robertson, C. D. *Nature*, **1988**, *332*, 59.
 31. Kaprinidis, N. A.; Turro, N. J. *Tetrahedron Lett.*, **1996**, *37*, 2372.
 32. Beck, C. M.; Park, Y.-J.; Crabtree, R. H. *Chem. Commun.*, **1998**, 693.

-
33. McAlexander, L. H.; Beck, C. M.; Burdenuic, J.; Crabtree, R. H. *J. Fluorine Chem.*, **1999**, *99*, 67.
34. Burdeniuc, J.; Crabtree, R. H. *Science*, **1996**, *271*, 340.
35. Burdeniuc, J.; Chupka, W.; Crabtree, R. H. *J. Am. Chem. Soc.*, **1995**, *117*, 10119.
36. Burdeniuc, J.; Siegbahn, P. E. M.; Crabtree, R. H. *New J. Chem.*, **1998**, 503.
37. Stoyanov, N. S.; Ramchandani, N.; Lemal, D. M. *Tetrahedron Lett.*, **1999**, *40*, 6549.
38. Richmond, T. G.; Shriver, D. F. *Organometallics*, **1984**, *3*, 305.
39. Brothers, P. J.; Roper, W. R. *Chem. Rev.*, **1988**, *88*, 1293.
40. Hughes, R. P.; Husebo, T. L.; Maddock, S. M.; Rheingold, A. L.; Guzei, I. A. *J. Am. Chem. Soc.*, **1997**, *119*, 10231.
41. Hughes, R. P.; Linder, D. C.; Rheingold, A. L.; Liable-Sands, L. M. *J. Am. Chem. Soc.*, **1997**, *119*, 11544.
42. Huang, D.; Caulton, K. G. *J. Am. Chem. Soc.*, **1997**, *119*, 3185.
43. Harrison, R. G.; Richmond, T. G. *J. Am. Chem. Soc.*, **1993**, *115*, 5303.
44. Bennett, B. K.; Harrison, R. G.; Richmond, T. G. *J. Am. Chem. Soc.*, **1994**, *116*, 11165.
45. Weydert, M.; Andersen, R. A.; Bergman, R. G. *J. Am. Chem. Soc.*, **1993**, *115*, 8837.
46. Cornehl, H. H.; Hornung, G.; Schwarz, H. *J. Am. Chem. Soc.*, **1996**, *118*, 9960.
Heinemann, C.; Goldberg, N.; Tornieporth-Oetting, I. C.; Klapötke, T. M.; Schwarz, H. *Angew. Chem. Int. Ed. Engl.*, **1995**, *34*(2), 213.
47. Su, M.-D.; Chu, S.-Y. *J. Am. Chem. Soc.*, **1999**, *121*, 1045.
48. Kiplinger, J. L.; Richmond, T. G. *J. Am. Chem. Soc.*, **1996**, *118*, 1805.
49. Kraft, B. M.; Lachicotte, R. L.; Jones, W. D. *J. Am. Chem. Soc.*, **2000**, *122*, 8559.

50. Burdeniuc, J.; Crabtree, R. H. *J. Am. Chem. Soc.*, **1996**, *118*, 2525; Burdenuic, J.; Crabtree, R. H. *Organometallics*, **1998**, *17*, 1582.
51. Pearson, R.G. *Hard and Soft Acids and Bases*, Dowden, Hutchison & Ross Inc: Stroudsburg, Pennsylvania; **1973**.
52. Clark, H. C. S.; Holloway, J. H. In *Advanced Inorganic Fluorides: Synthesis, Characterization and Applications*; Nakajima, T.; Žemva, B.; Tressaud, A., Eds.; Elsevier: **2000**.
53. Murphy, E. F.; Murugavel, R.; Roesky, H. W. *Chem. Rev.*, **1997**, *97*, 3425.
54. Brewer, S. A.; Holloway, J. H.; Hope, E. G.; Watson, P. G. *J. Chem. Soc., Chem. Commun.*, **1992**, 1577. Brewer, S. A.; Brisdon, A. K.; Holloway, J. H.; Hope, E. G.; Peck L. A.; Watson, P. G. *J. Chem. Soc., Dalton Trans.*, **1995**, 2945.
55. Wilkinson, J. A. *Chem. Rev.*, **1992**, *92*, 505.
56. Marshall, C. J.; Peacock, R. D.; Russell, D. R.; Wilson, I. L. *J. Chem. Soc., Chem. Commun.*, **1970**, 1643.
57. Hewitt, A. J.; Holloway, J. H.; Peacock, R. D.; Raynor, J. B.; Wilson, I. L. *J. Chem. Soc., Dalton Trans.*, **1976**, 579.
58. Coleman, K. S.; Holloway, J. H.; Hope, E. G. *J. Chem. Soc., Dalton Trans.*, **1997**, 1713.
59. Brewer, S. A.; Holloway, J. H.; Hope, E. G. *J. Chem. Soc., Dalton Trans.*, **1994**, 1067.
60. Brewer, S. A.; Coleman, K. S.; Fawcett, J.; Holloway, J. H.; Hope, E. G.; Russell, D. R.; Watson, P. G. *J. Chem. Soc., Dalton Trans.*, **1995**, 1073.
61. Coleman, K. S.; Holloway, J. H.; Hope, E. G.; Langer, J. *J. Chem. Soc., Dalton Trans.*, **1997**, 4555.

-
62. Barthazy, P.; Stoop, R. M.; Worle, M.; Togni, A.; Mezzetti, A. *Organometallics*, **2000**, *19*, 2844.
63. Bhattacharjee, M. N.; Chaudhuri, M. K.; Devi, M. *Polyhedron*, **1992**, *11*, 1523.
64. Forster, D. *Inorg. Chem.*, **1972**, *11*, 1686.
65. Doherty, N. M.; Hoffman, N. W. *Chem. Rev.*, **1991**, *91*, 553.
66. Cockman, R. W.; Ebsworth, E. A. V.; Holloway, J. H.; Murdoch, H.; Robertson, N.; Watson, P. G. In *Reaction of Non-metal Fluorides with some Platinum Metal Complexes*, Thrasher, J.; Strauss, S., Eds.; ACS Symposium series, ACS Books: **1994**. Watson, P. G.; Lork, E.; Mews, R. *J. Chem. Soc., Chem. Commun.*, **1994**, 1069.
67. Patel, B. P.; Crabtree, R. H. *J. Am. Chem. Soc.*, **1996**, *118*, 13105.
68. Veltheer, J. E.; Burger, P.; Bergman, R. G. *J. Am. Chem. Soc.*, **1995**, *117*, 12478.
69. Cooper, A. C.; Folting, K.; Huffman, J. C.; Caulton, K. G. *Organometallics*, **1997**, *16*, 505.
70. Brezinski, M. M.; Schneider, J.; Radonovich, L. J.; Klabunde, K. J. *Inorg. Chem.*, **1989**, *28*, 2414.
71. Fraser, S. L.; Antipin, M. Y.; Khroustalyov, V. N.; Grushin, V. V. *J. Am. Chem. Soc.*, **1997**, *119*, 4769.
72. Clark, H. C. S.; Fawcett, J.; Holloway, J. H.; Hope, E. G.; Peck, L. A.; Russell, D. *J. Chem. Soc., Dalton Trans.*, **1998**, 1249.
73. Emsley, J. *Chem Soc. Rev.*, **1980**, *9*, 91.
74. Coulson, D. R. *J. Am. Chem. Soc.*, **1976**, *98*, 3111.
75. Murphy, V. J.; Hascall, T.; Chen, J. Y.; Parkin, G. *J. Am. Chem. Soc.*, **1996**, *118*, 7428; Murphy, V. J.; Rabinovich, D.; Hascall, T.; Klooster, W. T.; Koetzle, T. F.; Parkin, G. *J. Am. Chem. Soc.*, **1998**, *120*, 4372.

76. Gil-Rubio, J.; Webendörfer, B.; Werner, H. *J. Chem. Soc., Dalton Trans.*, **1999**, 1437.
77. Braun, T.; Foxon, S. P.; Perutz, R. N.; Walton, P. H. *Angew. Chem. Int. Ed.*, **1999**, 38, 3326.
78. Roe, D. C.; Marshall, W. J.; Davidson, F.; Soper, P. D.; Grushin, V. V. *Organometallics*, **2000**, 19, 4575.
79. Roesky, H. W.; Sotoodeh, M.; Xu, Y. M.; Schrumpf, F.; Noltemeyer, M. Z. *Anorg., Allg. Chem.*, **1990**, 580, 131.
80. Jasim, N. A.; Perutz, R. N. *J. Am. Chem. Soc.*, **2000**, 122, 8685.

Chapter 2

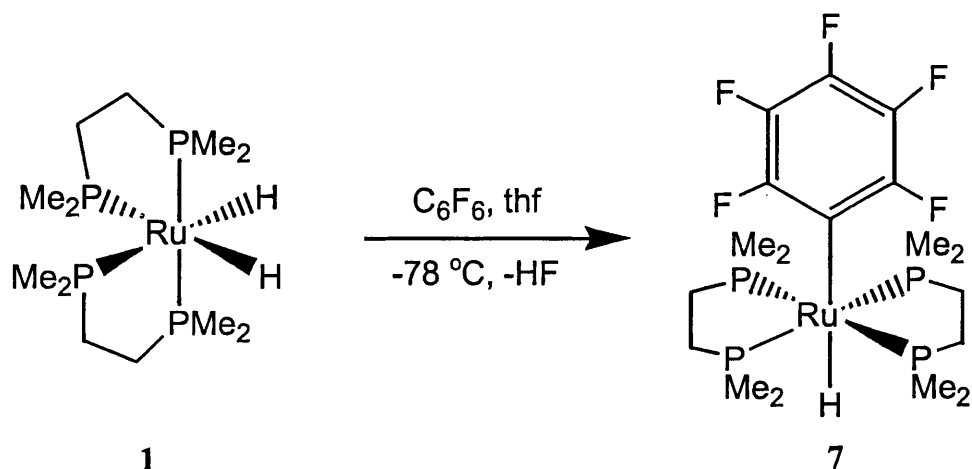
Activation of saturated C-F bonds using *cis*-Ru(dmpe)₂H₂

2 Activation of saturated C-F bonds by *cis*-Ru(dmpe)₂H₂ (1)

In this chapter, the remarkable reactivity of *cis*-Ru(dmpe)₂H₂, **1**, with aromatic C-F bonds, reported by Whittlesey et al.¹, will be discussed briefly. An electron transfer process is proposed for the mechanism of this reaction. It is known that the electron affinities of perfluoroalkanes are very similar to those of perfluoroarenes², which has led us to investigate the reactivity of **1** with an array of perfluoroalkanes, in order to facilitate the activation of saturated C-F bonds. The results of these reactions are discussed in detail below.

2.1 Introduction

As a starting point for our investigation into the activation of saturated C-F bonds we decided to probe the reactivity of the ruthenium dihydride, *cis*-Ru(dmpe)₂H₂, **1**. The reasoning for this choice was based on the work of Whittlesey et al.¹, who showed that when an excess of hexafluorobenzene was condensed into a colourless thf solution of **1** at -78 °C, an immediate reaction occurred at the remarkably low temperature to give a yellow coloured solution, which was found to contain the *trans*-fluoroaryl hydride complex, *trans*-Ru(dmpe)₂(C₆F₅)H, **7**, (Fig 2.1).

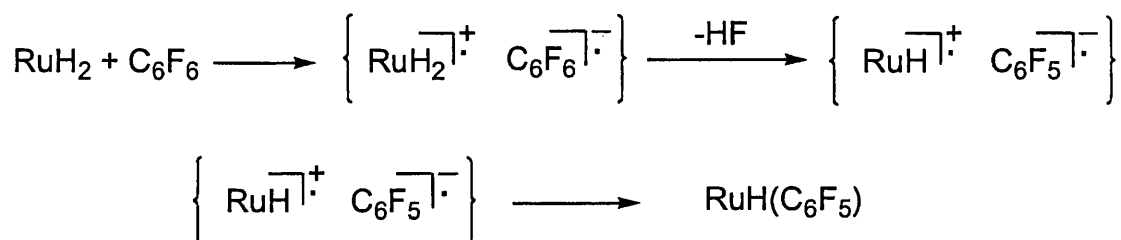
Fig 2.1 Reaction of **1** and C₆F₆

The reactivity of **1** was not limited to just C₆F₆. Other partially fluorinated arenes, C₆F₅H, 1,2,3,4-C₆F₄H₂, 1,2,3-C₆F₃H₃ and substituted arenes C₆F₅X, (X = CF₃, Ome) were seen to react with the dihydride although the reactions were slower and occurred only above -78 °C. In every case the activation of the C-F bond was preferred over activation of a C-H bond. The products of all these reactions were all *trans*-fluoroaryl hydride complexes in which the C-F bond *para* to a C-H or substituted group on the aromatic ring was selectively activated.

The favoured mechanism for the reaction of **1** with C₆F₆ is an electron transfer process, although this is not absolutely certain. Nucleophilic substitution has been ruled out by the very mild conditions employed and the lack of nucleophilicity of *cis*-Ru(dmpe)₂H₂. Likewise, oxidative addition to 16-electron [Ru(dmpe)₂] has been discounted due to the absence of *cis*-products. Also, the thermal generation of [Ru(dmpe)₂], via thermolysis of [Ru(dmpe)₂(naphthyl)H], in neat hexafluorobenzene, did not yield the pentafluorophenyl hydride complex **7**. Initial electron transfer from the electron rich metal dihydride to the C₆F₆, which has a reduction potential of -2.56 V (vs S.C.E.),² yields a radical anion and the 17-electron species [Ru(dmpe)₂H₂]^{•+}. The radical anion, [C₆F₆]^{•-}, readily loses fluoride which then abstracts hydrogen from the radical

cation to afford HF, the thermodynamic driving force for this reaction. Subsequent recombination of the radical species yields *trans*-Ru(dmpe)₂(C₆F₅)H, **7**. This is summarised in fig 2.2.

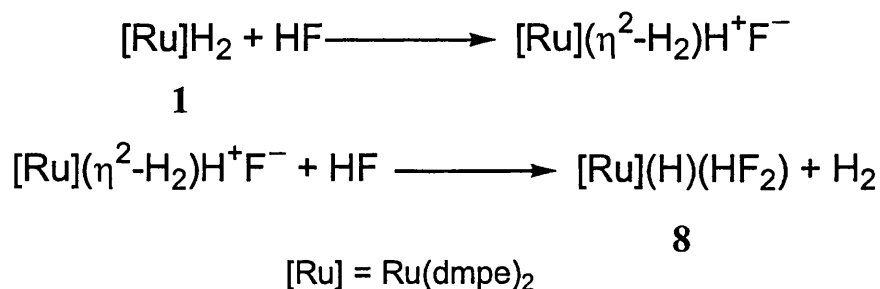
Fig 2.2 Proposed mechanism for the reaction of **1** and C₆F₆



There are, however, drawbacks with this proposed electron transfer mechanism. The free radical intermediates have not been detected, but more importantly, the initial transfer of an electron from the metal complex to the C₆F₆ has been calculated to be electrochemically uphill in excess of 2 V. The mechanism is discussed in depth in section 3.5.

There is also a secondary product formed in the reaction of **1** with fluorinated arenes. The HF that is released in the formation of **7** can react with the metal dihydride to yield the ruthenium bifluoride hydride complex, *trans*-Ru(dmpe)₂(FHF)H, **8**. This was confirmed by treating **1** with Et₃N.3HF, a mild source of HF, which yielded the same bifluoride hydride complex. The proposed mechanism of formation of this complex involves an intermediate dihydrogen hydride complex as can be seen in fig 2.3.

Fig 2.3 Proposed mechanism for formation of 8



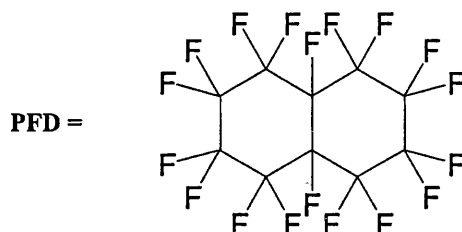
The high reactivity of **1** with aromatic C-F bonds led us to use this dihydride as a starting point for our investigations into the activation of aliphatic C-F bonds.

2.2 Preparation of *cis*-Ru(dmpe)₂H₂ (**1**)

The dihydride **1** was prepared by a reaction of a thf solution of *trans*-Ru(dmpe)₂Cl₂ using Na metal under an atmosphere of H₂. The ³¹P{¹H} NMR spectrum showed two apparent triplet resonances for the AA'BB' spin system at δ 48.4 and 39.4 (*J*_{PP} 20.1 Hz) for **1** and in a 20:1 ratio with a small singlet resonance at δ 50.2 for *trans*-Ru(dmpe)₂H₂. The ¹H NMR spectrum showed hydride resonances for **1** as a multiplet at δ -9.76 (*cis*) and a quintet at δ -10.55 (*trans*, *J*_{HP} 20.64 Hz).

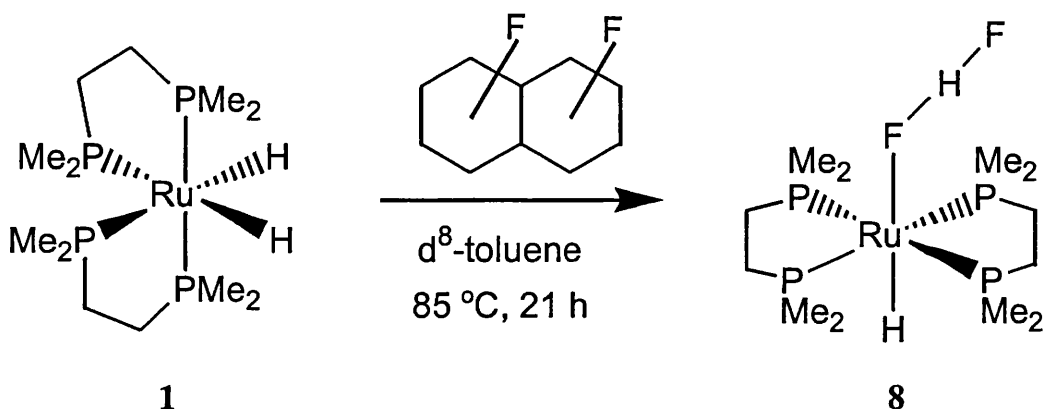
2.3 Results

2.3.1 Reaction of (1) with perfluorodecalin (PFD)



Our investigations into the activation of saturated carbon-fluorine bonds began with *cis*-Ru(dmpe)₂H₂, **1**. On addition of one equivalent of PFD to a toluene solution of **1**, in a J. Youngs resealable NMR tube, only two triplet signals originating from **1** were seen in the ³¹P{¹H} NMR spectrum even after 7 days at room temperature. When the solution was heated to 85 °C for 21 h, a colour change from colourless to yellow was observed. The main metal containing product of the reaction identified by multinuclear NMR spectroscopy was found to be the bifluoride hydride complex, *trans*-Ru(dmpe)₂(HF₂)H, **8**.

Reaction 2.1



The ³¹P{¹H} NMR spectrum of **8** (fig 2.4) shows a broad singlet at δ 46.6 for the four equivalent phosphorus atoms but, more distinctively, the ¹H NMR spectrum shows

a triplet at δ 14.2 (fig 2.5). The large triplet splitting of 274 Hz is typical of a $^1J_{\text{HF}}$ coupling. A broad multiplet is also seen at δ -25.6 for the hydride resonance.

Fig 2.4 $^{31}\text{P}\{^1\text{H}\}$ NMR spectrum of **8** (*d*₈-toluene, 270 MHz)

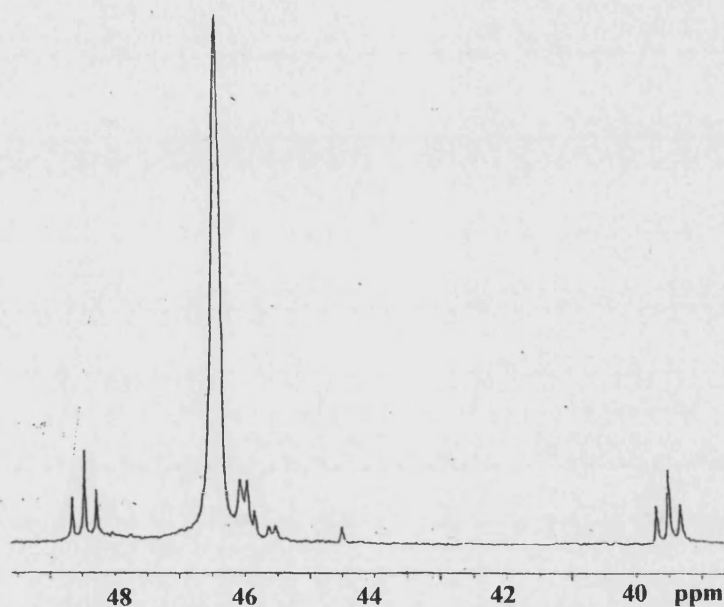
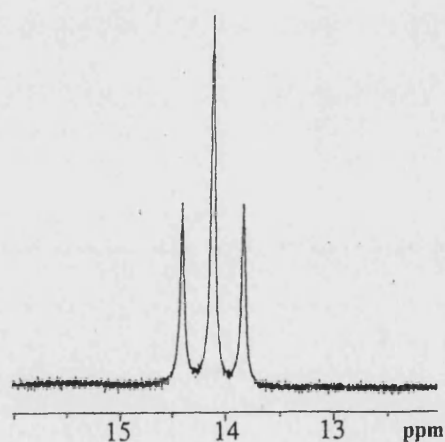


Fig 2.5 ^1H NMR spectrum of **8** showing bifluoride proton triplet (*d*₈-toluene, 270 MHz)



The appearance of the acidic proton of **8** is different to that reported by Whittlesey et al.¹, from the reaction of **1** and Et₃N.3HF, where a broad singlet is observed at room temperature. We interpret that the triplet resonance that we observe is indicative of intermolecular and/or intramolecular exchange processes. Low

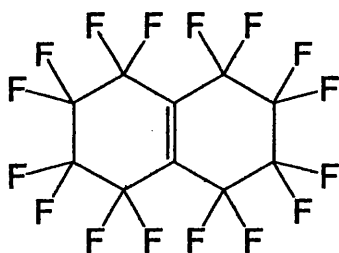
temperature NMR spectra, which have not yet been performed, are required to resolve this problem.

This reaction is very different to that of **1** and C₆F₆. Obviously, the reaction with PFD does not occur as easily as with C₆F₆, requiring a relatively high temperature over a long period of time and, instead of forming a species with a perfluorocarbon ligand, we form the bifluoride hydride species **8** as the only metal containing product. This is only seen as a by-product in the reaction with C₆F₆.

The bifluoride hydride is assumed to be produced by reaction of **1** with HF generated in the reaction process. This would imply that HF reacts with dihydride **1** more easily than any perfluorocarbon fragment present.

The fate of the PFD could not be established. The ¹⁹F NMR spectrum of the reaction solution showed new resonances in the δ -104 to -110 and δ -128 to -137 regions for the fluoroorganic products. Resonances occurring in these areas of the spectrum usually correlate to perfluoroalkene species but products such as perfluoronaphthalene and hexadecafluoro-bicyclo[4.4.0]dec-1(6)-ene³ (fig 2.6), chosen because the loss of two fluorines would correspond with the gain of two fluorines in the formation of **8**, can be ruled out as the reported data for the ¹⁹F NMR spectra does not match the products we have observed.

Fig 2.6 Hexadecafluoro-bicyclo[4.4.0]dec-1(6)-ene

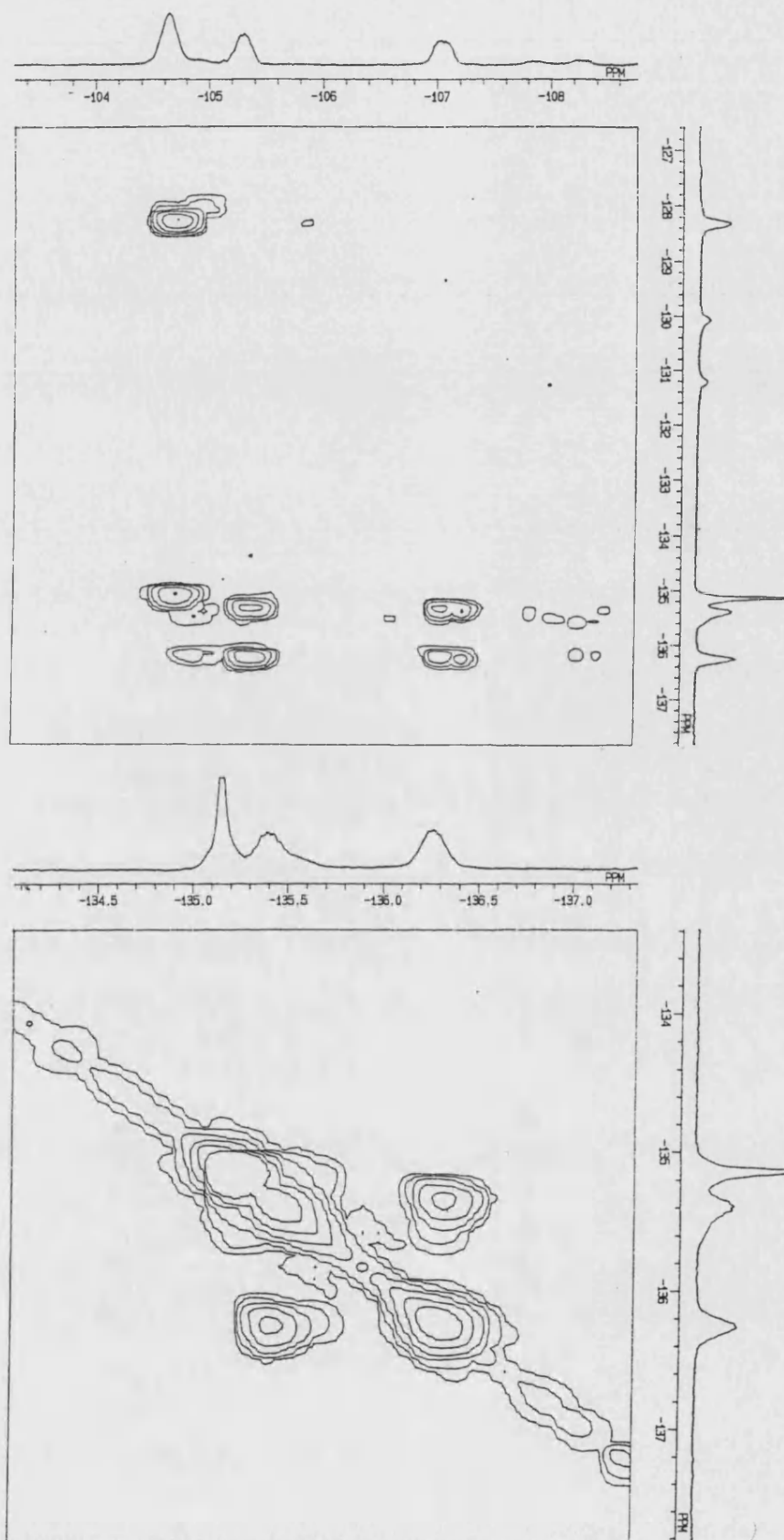


products that remain must be unsaturated as there is no evidence in the ¹H NMR spectrum that substitution by hydrogen atoms occurs. Also the fact that these products are involatile under vacuum may infer that they have a high molecular weight or they are polymeric in nature.

From the ¹⁹F-¹⁹F COSY NMR spectrum (fig 2.7) it would appear that peaks in both areas correlate to each other and that there are probably two or three different fluoroorganic products.

Attempts to identify the products by GC-MS have been fruitless, possibly because of this. Similar difficulties in identifying fluoroorganic products of PFD were observed by Deacon et al.,⁴ in the reaction of the PFD with ytterbium(II) aryloxides [Yb(OAr)₂(thf)₃], and Bennett⁵ et al in the reaction of PFD and Cp₂Co. The reactions yield bis(aryloxo)fluoroytterbium(III) dimers, [Yb(OAr)₂F(thf)]₂, and [Cp₂Co]F respectively, but the fate of the fluoroorganic substrate was not identified. The problem was resolved in the case of Cp₂Co by adding Li[O₃SCF₃] to scavenge the cobaltocenium fluoride. The result was that 10 equivalents of Cp₂Co was found to defluorinate PFD to octafluoronaphthalene. We tried adding Li[O₃SCF₃] to reaction 2.1 but **1** was seen to react with the triflate salt in preference to PFD.

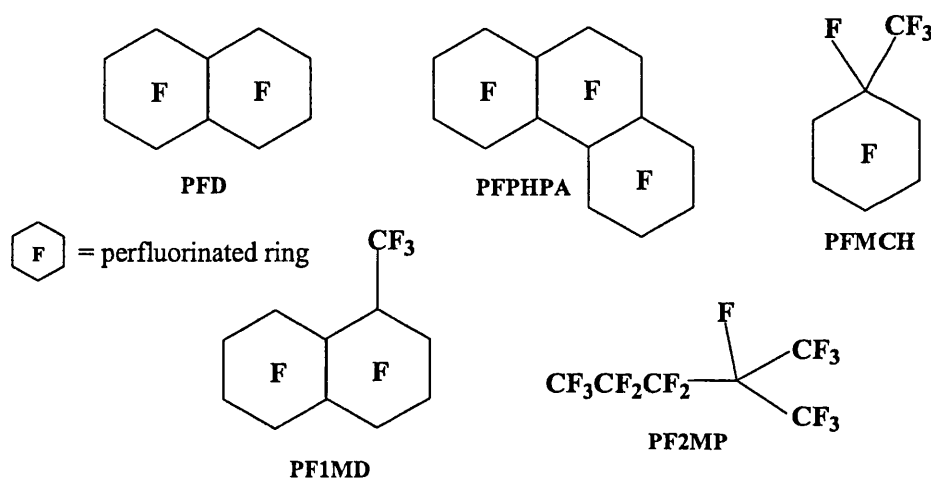
Fig 2.7 ¹⁹F-¹⁹F COSY NMR spectrum of fluoroorganic products from reaction 2.1



2.3.2 Reactions with other perfluoroalkanes

Toluene and benzene solutions of **1** were also treated with 1 equivalent of a range of different saturated perfluorocarbons (fig 2.8).

Fig 2.8 Saturated perfluorocarbons used in reactions with **1**



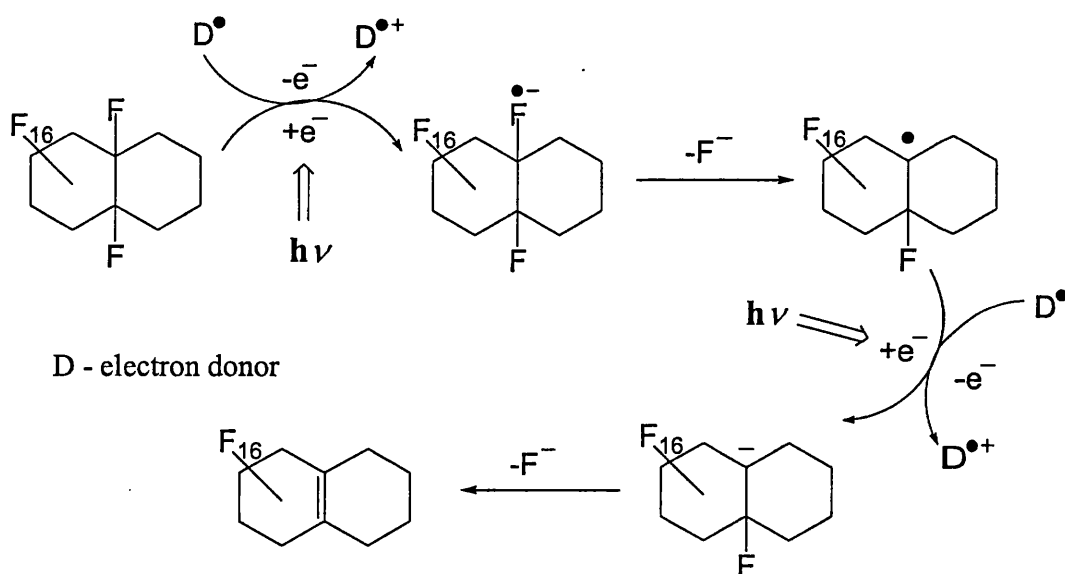
In each case no reaction was seen at room temperature but on heating certain perfluorocarbons reacted to yield the bifluoride hydride species **8**. Successful reactions were observed with the three-ringed perfluoroperhydrophenanthrene (PFPHPA), (120 h at 85 °C) and perfluoro-1-methyldecalin (PF1MD), (ca. 30 h at 85 °C).

The fluorinated products for PFPHPA appear in a similar region to those seen for PFD although the complicated ¹⁹F NMR resonances of the PFPHPA itself make it very difficult to interpret these. In the case of the PF1MD, the ¹⁹F NMR spectra again showed resonances in the same regions as seen for PFD, except that the number of products is greater. In the cases of perfluoromethylcyclohexane (PFMCH) and perfluoro-2-methylpentane (PF2MP), no bifluoride hydride formation was seen after a 3 weeks of heating at 85 °C.

On inspection of the perfluorocarbons that do react with **1** (PFD, PFPHPA and PF1MD) and those that do not (PFMCH and PF2MP), there appears to be a structural feature that allows the conversion of **1** to **8**. The results suggest that there is a need for two vicinal tertiary fluorines for the reaction to occur. A similar requirement is seen for the photolytic C-F activation of PFD, in the presence of electron donors, reported by Turro.³ It is reported that under UV irradiation and in the presence of a photosensitizing amine, the tertiary C-F bonds in PFD are selectively cleaved to give hexadecafluoro-bicyclo[4.4.0]dec-1(6)-ene (fig 2.6), the proposed reaction mechanism of which is given in fig. 2.9.

Even though hexadecafluoro-bicyclo[4.4.0]dec-1(6)-ene was ruled out as a product from reaction 2.1, from what is seen above it may be that the perfluoroalkene is an intermediate which can react further with **1** to yield the fluoroorganic products that we find.

Fig 2.9 Mechanism for photolytic C-F activation of PFD



2.3.3 Effect of base on the reaction of *cis*-Ru(dmpe)₂H₂ (1) with PFD

Base was used by Milstein⁶ to try and alter fluoroorganic and inorganic products in the reaction of Rh(PMe₃)₄H with hexafluorobenzene. The presence of a base removed HF, which resulted in the development of a catalytic cycle for the conversion of C₆F₆ to C₆F₅H. It is obvious that HF plays an important part in the reaction of 1 and PFD. Therefore the original 1:1 reaction of 1 and PFD was repeated in the presence of a 5x molar amount of pyridine, with the aim of trapping out HF and in turn halting the formation of the bifluoride hydride. This, we hoped, would lead to formation of a metallic product containing a perfluorocarbon ligand, which might be isolable. On heating the solution for 21 h at 85 °C the ³¹P{¹H} NMR showed that the major metal containing product was still *trans*-Ru(dmpe)₂(FHF)H, 8. However, the spectrum also showed a small amount of a new product as a singlet resonance at δ 40.4.

When a much greater excess of pyridine was present (30 equivalents), all of the starting material reacted after 20 h at 85 °C, and the ³¹P{¹H} NMR spectrum (fig 2.10) now showed the major metal containing species to be the one displaying the resonance at δ 40.4; the bifluoride hydride 8 was present in a smaller amount. The ¹H NMR spectrum showed that the new product was a metal hydride complex, which displayed a quintet resonance at δ -20.80 (²J_{HP} = 20.8 Hz). Further inspection of the ¹H NMR spectrum revealed resonances corresponding to coordinated pyridine at δ 8.54 (m, 2 *ortho* H), 7.00 (m, 1 *para* H), and 6.67 (m, 2 *meta* H) in a 2:1:2 ratio and also a very broad triplet resonance at very low field (δ 17.8, ¹J_{HF} = 117 Hz). The ¹⁹F NMR spectrum showed a broad doublet at δ -148 with the same coupling constant of 117 Hz

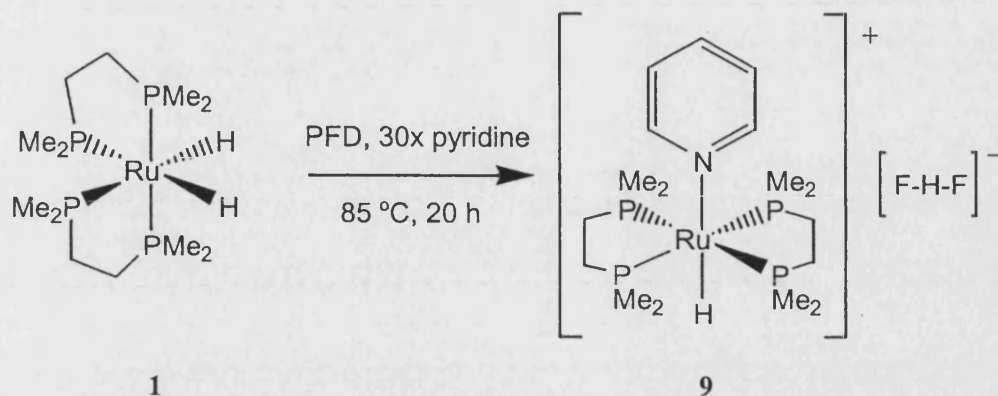
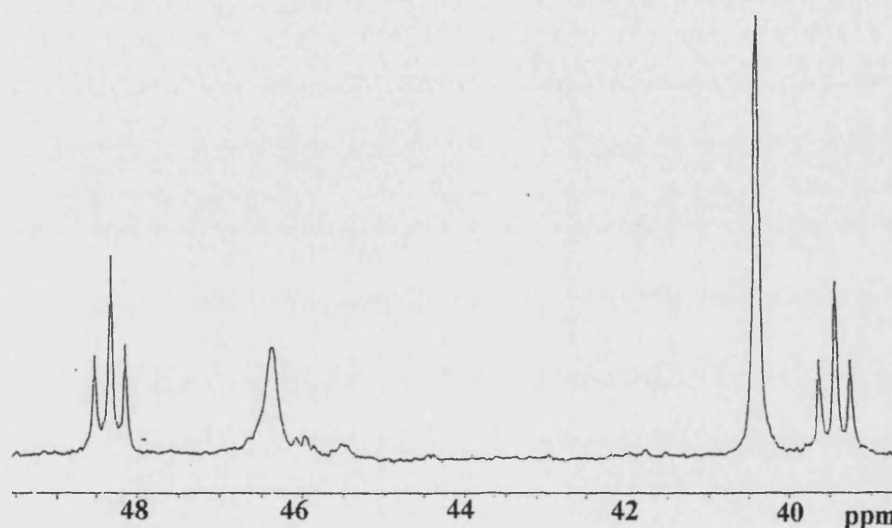
consistent with the presence of free HF₂⁻. These signals for HF₂⁻ compare well to other reported bifluoride salts, table 2.1.

Table 2.1 ¹⁹F and ¹H NMR data for salts of HF₂⁻

Bifluoride salt	Solvent	Chemical Shift (ppm)		<i>J</i> _{HF} (Hz)
		¹⁹ F NMR	¹ H NMR	
[Me ₄ N]HF ₂ ⁷	CH ₃ CN	-145.6	16.3	122
[Et ₃ NH]HF ₂ ⁸	CH ₃ CN	-152	14.9	139
[ⁿ Bu ₄ N]HF ₂ ⁹	CH ₃ CN	-144	16.3	121
9	C ₆ D ₆	-148	17.8	117
[Cp ₂ Co]HF ₂ ⁵	CD ₂ Cl ₂	-153.6	16.1	121

The only other peaks in the ¹⁹F NMR spectrum were due to the same fluoroorganic products seen in the original reaction of **1** and PFD done in the absence of base. This showed that the excess of pyridine had the effect of forming the cationic pyridine hydride complex *trans*-[Ru(dmpe)₂(C₅H₅N)H]⁺, **9**, with free bifluoride being present as a counterion.

Reaction 2.2

Fig 2.10 $^{31}\text{P}\{^1\text{H}\}$ NMR of reaction 2.2 (C_6D_6 , 270 MHz)

It would appear that the base had little effect on the reaction between **1** and PFD but it did react with the bifluoride hydride displacing the bifluoride group with a coordinated pyridine. The reaction yielded small yellow needle like crystals in 59 % yield. A single crystal X-ray analysis confirmed the product of the reaction as *trans*-[Ru(dmpe)₂(C₅H₅N)H]⁺[HF₂]⁻, **9** (fig 2.11). Data collection parameters are given in table 2.2, while selected bond lengths and angle are give in table 2.3.

Fig 2.11 X-Ray crystal structure of *trans*-[Ru(dmpe)₂(C₅H₅N)H]⁺[HF₂]⁻, 9.

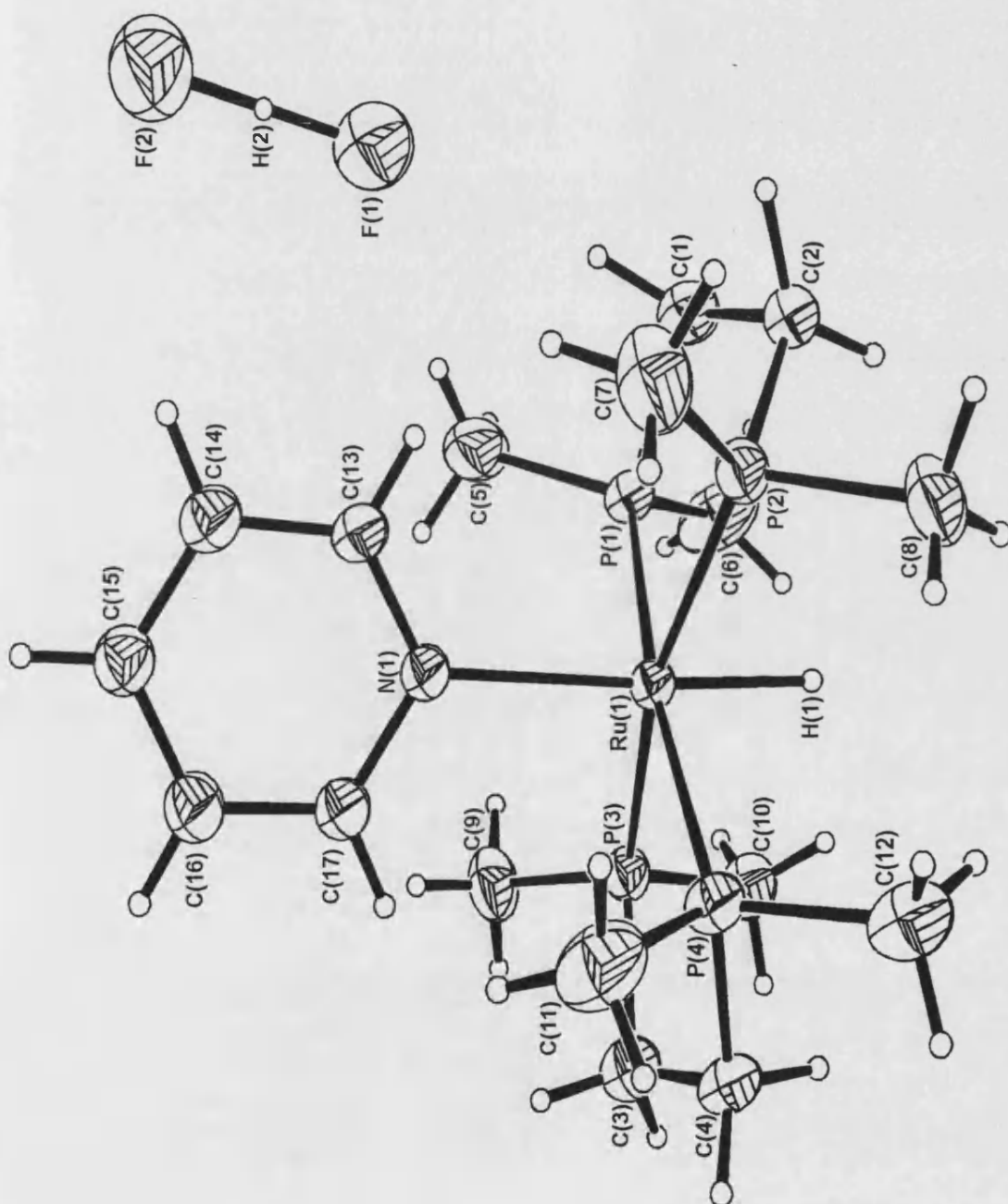


Table 2.2 Crystal data and structure refinement parameters for **9**.

Empirical formula	C ₁₇ H ₃₉ F ₂ N P ₄ Ru
Formula weight	520.44
Temperature	293(2) K
Wavelength	0.71073 Å
Crystal system	Monoclinic
Space group	P2 ₁ /c
Unit cell dimensions	a = 8.957(3) Å α = 90° b = 25.809(6) Å β = 96.96(4)° c = 10.584(6) Å γ = 90°
Volume	2429(2) Å ³
Z	4
Density (calculated)	1.423 Mg/m ³
Absorption coefficient	0.926 mm ⁻¹
F(000)	1080
Crystal size	0.3 x 0.1 x 0.1 mm
Theta range for data collection	3.71 to 25.37°.
Index ranges	-10 ≤ h ≤ 10; -30 ≤ k ≤ 31; -12 ≤ l ≤ 12
Reflections collected	13265
Independent reflections	3995 [R(int) = 0.0846]
Absorption correction	None
Refinement method	Full-matrix least-squares on F ²
Data / restraints / parameters	3994 / 0 / 264
Goodness-of-fit on F ²	1.027
Final R indices [I > 2σ(I)]	R ₁ = 0.0432 wR ₂ = 0.1077
R indices (all data)	R ₁ = 0.0729 wR ₂ = 0.1243
Extinction coefficient	0.0019(7)
Largest diff. peak and hole	0.309 and -0.335 e.Å ⁻³

Table 2.3 Selected bond lengths [Å] and angles [°] for **9**.

Ru(1)-N(1)	2.276(4)	Ru(1)-P(3)	2.315(2)
Ru(1)-P(1)	2.320(2)	Ru(1)-P(4)	2.324(2)
Ru(1)-P(2)	2.328(2)	P(1)-C(1)	1.816(8)
P(1)-C(5)	1.831(8)	P(1)-C(6)	1.836(8)
P(2)-C(7)	1.803(8)	P(2)-C(2)	1.803(14)
P(3)-C(10)	1.834(6)	P(3)-C(9)	1.820(6)
P(4)-C(11)	1.807(7)	P(3)-C(3)	1.838(8)
P(4)-C(12)	1.843(8)	P(4)-C(4)	1.838(11)
N(1)-C(13)	1.336(7)	N(1)-C(17)	1.366(7)
C(1)-C(2)	1.52(2)	C(3)-C(4)	1.500(13)
C(13)-C(14)	1.396(8)	C(15)-C(16)	1.375(10)
C(14)-C(15)	1.380(10)	C(16)-C(17)	1.396(9)
N(1)-Ru(1)-P(3)	96.87(13)	N(1)-Ru(1)-P(1)	93.26(13)
P(3)-Ru(1)-P(1)	95.17(7)	N(1)-Ru(1)-P(4)	95.11(12)
P(3)-Ru(1)-P(4)	83.45(7)	P(1)-Ru(1)-P(4)	171.62(6)
N(1)-Ru(1)-P(2)	97.55(13)	P(3)-Ru(1)-P(2)	165.57(6)
P(1)-Ru(1)-P(2)	83.30(7)	P(4)-Ru(1)-P(2)	95.97(7)
C(1)-P(1)-C(5)	101.2(4)	C(1)-P(1)-C(6)	100.7(4)
C(5)-P(1)-C(6)	102.1(5)	C(1)-P(1)-Ru(1)	110.3(3)
C(5)-P(1)-Ru(1)	120.9(3)	C(6)-P(1)-Ru(1)	118.5(4)
C(7)-P(2)-C(8)	94.0(6)	C(2)-P(2)-C(7)	112.5(6)
C(7)-P(2)-Ru(1)	123.9(3)	C(2)-P(2)-Ru(1)	108.6(4)
C(9)-P(3)-C(3)	102.3(4)	C(8)-P(2)-Ru(1)	116.6(5)
C(9)-P(3)-Ru(1)	122.9(3)	C(9)-P(3)-C(10)	99.8(3)
C(3)-P(3)-Ru(1)	109.8(2)	C(10)-P(3)-C(3)	101.7(4)
C(11)-P(4)-C(12)	99.8(4)	C(10)-P(3)-Ru(1)	117.4(2)
C(11)-P(4)-Ru(1)	120.5(3)	C(11)-P(4)-C(4)	108.3(5)
C(12)-P(4)-Ru(1)	120.3(3)	C(4)-P(4)-C(12)	95.0(5)
C(13)-N(1)-C(17)	116.4(5)	C(4)-P(4)-Ru(1)	109.6(3)
C(17)-N(1)-Ru(1)	121.0(4)	C(13)-N(1)-Ru(1)	122.6(4)
C(2)-C(1)-P(1)	113.0(7)	C(3)-C(4)-P(4)	111.2(7)
C(1)-C(2)-P(2)	111.1(8)	N(1)-C(13)-C(14)	123.9(6)
C(4)-C(3)-P(3)	110.8(6)	C(16)-C(15)-C(14)	118.0(6)
C(15)-C(14)-C(13)	119.2(7)	N(1)-C(17)-C(16)	122.3(7)
C(15)-C(16)-C(17)	120.1(6)		

Symmetry transformations used to generate equivalent atoms: N/A

The crystal structure of **9** shows a six coordinate cationic ruthenium (II) centre with a distorted octahedral geometry. The imbalance between the size of the coordinated pyridine and the hydride ligand imparts an average N-Ru-P angle of 95.70(13) °. A similar trait has been seen for other crystallographically characterised *trans*-Ru(dmpe)₂HL species as shown in table 2.4.

Table 2.4 Crystal data for *trans*-Ru(dmpe)₂HX species

<i>Trans</i> -Ru(dmpe) ₂ HL L =	Average P-Ru-X angle (°) (X = coordinated atom)	Ru-X bond length (Å)
-C ₆ F ₅ (7) ^{1a}	96.34(7)	2.250(4)
-NH ₃ (cation) ¹⁰	93.3(2)	2.268(7)
-N=C=CH(<i>p</i> -C ₆ H ₄ CF ₃) ¹⁰	93.4(3)	2.13(2)
-CHCH ₂ CH ₂ C=O ¹⁰	95.00(9)	2.338(3)
-O(<i>p</i> -C ₆ H ₄ Me) ¹¹	92.56(5)	2.239(2)
3-methylindole- <i>N</i> ¹²	~96	Not given
5-methoxyindole- <i>N</i> ¹²	~95	Not given

The two bidentate phosphorus ligands lie in the equatorial position and the average Ru-P bond length is 2.322(2) Å and the plane of the pyridine ring bisects the backbones of the dmpe ligand in a similar way to the perfluorophenyl ring in *trans*-Ru(dmpe)₂(C₆F₅)H. The Ru-N bond length is 2.276(4) Å which compares well to the Ru-N bond length of 2.252(7) Å reported for a similar cationic complex *trans*-[Ru(dmpe)₂(NH₃)H]⁺ very recently described by Fulton et al.¹⁰ This was formed from the reaction of *trans*-[Ru(dmpe)₂(NH₂)H] with fluorene, the organic fragment forming a fluorenyl counterion for the system. Comparisons with the Ru-X bond lengths shown

in table 2.4 are also quite close although the cationic nature of **9** is better matched with the *trans*-[Ru(dmpe)₂(NH₃)H]⁺ complex.

In **9**, the counterion to the cationic complex is free bifluoride. The separation between the two fluorines in the anion is 2.202 Å. Apart from NMR evidence for the bifluoride anion, IR spectroscopy shows a sharp peak at 1591 cm⁻¹ for the asymmetric F-H-F vibration.¹³ A weak Ru-H stretching band is also seen in the IR spectrum at 1925 cm⁻¹, which again compares well to *trans*-[Ru(dmpe)₂(NH₃)H]⁺, for which $\nu_{\text{Ru-H}}$ appears at 1916 cm⁻¹.

The presence of the bifluoride as a counterion and the fact that, in the ¹⁹F NMR spectrum, no change was seen in the fluoroorganic products of the reaction, implies that the pyridine does not prevent the formation of the bifluoride hydride **8** but does react with it displacing the bifluoride ligand and coordinating *trans* to the hydride.

The 1:1 reaction of **1** and PFD was also repeated in the presence of another base, triethylamine. On repeating reaction 2.1 in the presence of 5 equivalents of Et₃N, the ³¹P{¹H} NMR spectrum showed conversion of dihydride **1** to bifluoride hydride **8** as before after 25 h at 85 °C. When the amount of base added to reaction 2.1 was increased to 20 equivalents, dihydride **1** completely reacted after 26 h at 85 °C. The ³¹P{¹H} NMR spectrum showed in addition to bifluoride hydride **8**, formation of a new product as a broad singlet resonance at δ 45.5 in a 1:1 ratio. The ¹H NMR spectrum indicated that the new product was a metal hydride complex with a broad multiplet resonance being seen at δ -27.8. The ¹⁹F NMR spectrum also showed a new broad peak at δ -179. Elsewhere in the ¹⁹F NMR spectrum the fluoroorganic products found were the same as found for the original 1:1 reaction of **1** and PFD.

These results imply that the presence of relatively low concentrations of Et₃N had no effect on the conversion of **1** to **8**. As with pyridine, higher concentrations of

base result in the reaction of **8** to give new metal hydride species, *trans*-Ru(dmpe)₂HX. The multiplet nature of the hydride resonance suggests that X must have a spin of $I = \frac{1}{2}$ otherwise the hydride would appear as a simple quintet. It is possible that the Et₃N removes HF from the bifluoride forming [Et₃NH]F and *trans*-Ru(dmpe)₂HF. The ¹⁹F NMR spectrum shows no evidence for a fluoride ligand at room temperature but the broad singlet at δ -179 could be due to the [Et₃NH]F. The reported value⁸ measured in CH₃CN is given as δ -150.5, however it has been shown that ¹⁹F NMR chemical shifts of fluorides and HF species are very susceptible to changes in solvent, e.g. the chemical shift range for fluoride anions is δ -75 to -150.⁷ The ¹H NMR spectrum however shows no evidence for [Et₃NH]F at room temperature.

2.3.4 Other modifications to reaction 2.1

The reaction between *cis*-Ru(dmpe)₂H₂, **1**, and PFD was also carried out in the presence of 10 equivalents of the radical trap 9,10-dihydroanthracene (DHA). Two reactions were run side-by-side, one with DHA and the other free of DHA. The reaction mixture containing the DHA was found to react at the same rate as the reaction mixture free of DHA, converting **1** to **8** in 21 h at 85 °C. This showed that the DHA had no effect on the formation of the bifluoride hydride species **8**. However this would not necessarily rule out an electron transfer mechanism, if, as proposed for the reaction of **1** and hexafluorobenzene, it occurs within a solvent cage.¹

Due to the higher temperature of this reaction compared to that of **1** and C₆F₆, it was necessary to rule out any involvement of the fluoroborosilicate glass, in the NMR tube, in the reaction. A J. Youngs resealable NMR tube was lined with a length of

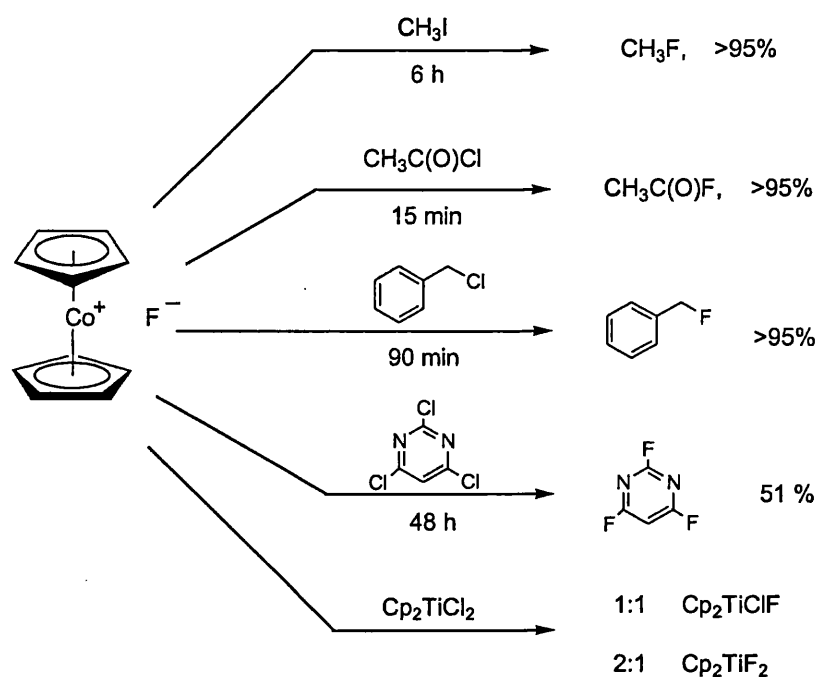
sealed FEP tubing, but the reaction was seen to proceed no differently in terms of reaction time or products to reaction 2.1.

Reaction 2.1 was also carried out in d₆-benzene and d₈-thf. In each case formation of bifluoride hydride **8** was seen on heating with no noticeable difference in the time taken for the reaction to go to completion. Therefore, any effect of the solvents in the reaction can be ruled out.

2.4 Bifluoride hydride (**8**) as a fluorinating agent

Richmond et al.⁵ reported C-F bond activation of perfluorodecalin with cobaltocene, Cp₂Co, after 4 h at room temperature to form cobaltocenium fluoride, [Cp₂Co]⁺F⁻. It was found that [Cp₂Co]⁺F⁻ was capable of fluorinating small organic halides and transition metal halides under mild conditions (fig 2.12). However, under the same conditions, the bifluoride salt, [Cp₂Co]HF₂, was unable to perform these fluorinations.

Fig 2.12 Fluorinations with [Cp₂Co]⁺F⁻



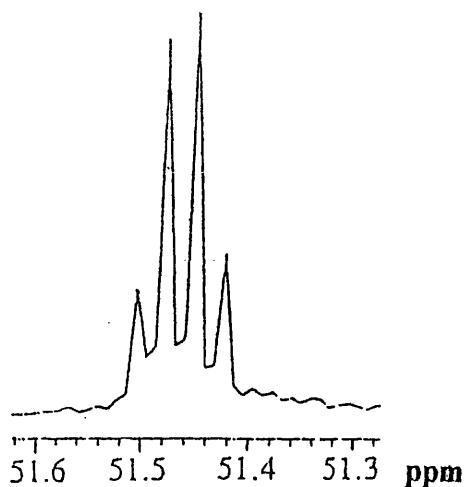
By comparison, the fluorination of trichloropyrimidine with KF requires 2 h at 310 °C in the presence of antimony oxide, whereas with the HF adduct of 1,8-bis(dimethylamino)naphthalene fluorination occurs at a rate similar to that shown by [Cp₂Co]F.

Grushin¹⁴ has also shown fluorination of dichloromethane by ‘naked’ fluoride ions generated from the fluoropalladium complex [(Ph₃P)₂Pd(Ph)F]. Addition of a chloride to this complex in a CH₂Cl₂ solution under mild conditions, resulted in the generation of fluoride ions in high concentrations which fluorinated the solvent to CH₂ClF and CH₂F₂.

We decided to investigate whether bifluoride hydride **8**, formed in the reaction of **1** and PFD was capable of similar fluorinations to small organic and transition metal halides.

2.4.1 Reaction of *trans*-Ru(dmpe)₂(FHF)H (**8**) and CH₃C(O)Cl

Bifluoride hydride **8** was synthesised via the reaction of **1** and PFD as detailed above making sure that no dihydride remained. The volatiles were then removed under vacuum, the bifluoride hydride weighed and d₆-benzene added to give a solution of **8**. Two equivalents of dry CH₃C(O)Cl were then added to this solution. The reaction proceeded rapidly at room temperature, with the solution turning from a pale yellow to a dark yellow. After ~ 10 mins at room temperature, the ¹⁹F NMR spectrum showed only one resonance, a distinctive quartet at δ 51.5 (³J_{HF} 7.3 Hz) (fig 2.13), which confirmed that **8** had successfully converted CH₃C(O)Cl to CH₃C(O)F.

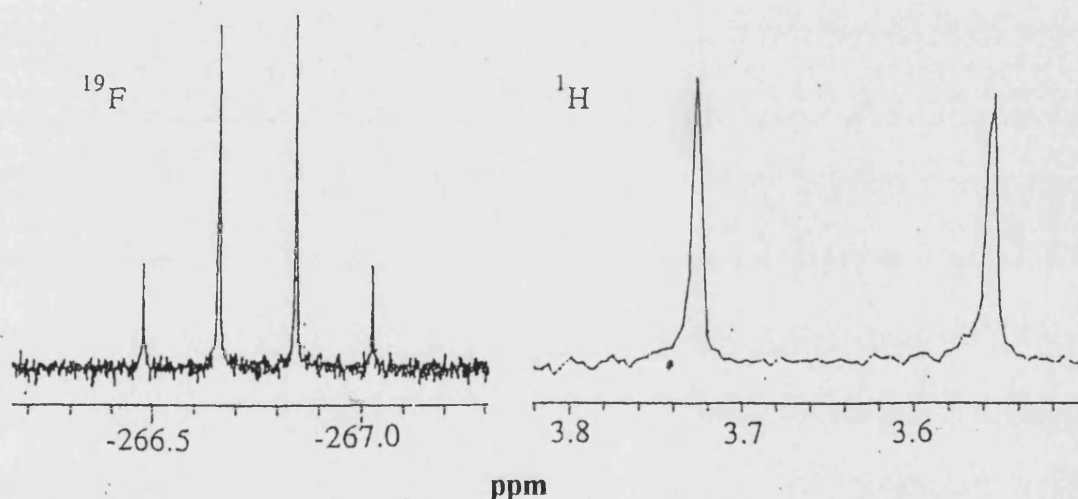
Fig 2.13 ¹⁹F NMR spectrum of CH₃C(O)F (C₆D₆, 270 MHz)

³¹P{¹H} NMR spectroscopy showed that **8** had completely reacted and displayed two new products in a 1:5 ratio, a new singlet resonance at δ 44.5 and a pair of triplet resonances at δ 49.3 and 40.1 (J_{PP} 23.2 Hz). The two triplets have a coupling constant close to that reported¹⁵ for *cis*-Ru(dmpe)₂Cl₂ (J 22.8 Hz) which would be a product we might expect. The singlet at δ 44.5 appeared to be a metal hydride species since the ¹H NMR spectrum showed a quintet in the hydride region at δ -20.71 (J_{HP} 23.7 Hz). As chlorine is in abundance and the hydride resonance is a simple quintet it is proposed that this product is *trans*-Ru(dmpe)₂HCl, although there is no literature evidence to confirm this. The conversion of acetyl chloride is believed to be > 90 % due to the ratio of the chloride containing products formed from the total conversion of **8**.

2.4.2 Reaction of *trans*-Ru(dmpe)₂(FHF)H (**8**) and CH₃I

To J. Youngs resealable NMR tube containing d₆-benzene solution of **8**, prepared from the reaction of **1** and PFD, 2 equivalents of CH₃I were added. The reaction was complete after 2 h at room temperature fluorinating the methyl iodide to yield methyl fluoride, which was detected in the ¹⁹F NMR spectrum as a quartet at δ -266.7 (²J_{FH} 46.5 Hz) and in the ¹H NMR spectrum as a doublet at δ 3.64 (²J_{HF} 46.5 Hz) (fig 2.14).

Fig 2.14 ¹⁹F and ¹H NMR spectra of CH₃F (C₆D₆, 270 MHz)



Four ruthenium phosphine compounds were seen in the ³¹P{¹H} NMR spectrum at δ 45.4 (t, *J* 17.8 Hz), 40.1 (d, *J* 19.1 Hz), 38.7 (s) and 27.3 (s). The singlet at δ 38.7 was identified as *trans*-Ru(dmpe)₂HI by comparison with the literature.¹⁶ This was confirmed by a quintet resonance for the hydride at δ -18.39 (*J*_{HP} 21.5 Hz). This product disappears on addition of an excess of CH₃I increasing the yield of the product at δ 27.3, identified as *trans*-Ru(dmpe)₂I₂. This was deduced by running a ³¹P{¹H} NMR spectrum of the reaction of *cis*-Ru(dmpe)₂H₂, **1**, and CH₃I reported by Chatt et al.¹⁷ which yields both *cis* and *trans* forms of the diiodide and the hydride iodide. The

two remaining resonances are of lesser intensity and do not contain hydrides. The coupling constants are typical of a phosphorus-fluorine coupling, which indicates that these products could contain fluoride ligands, and may, for example, be *trans*-Ru(dmpe)₂F₂ and *trans*-Ru(dmpe)₂FI.

The ¹H NMR spectrum shows none of the starting CH₃I present at the end of the reaction suggesting a quantitative conversion. The presence of the ruthenium phosphine products deemed to contain fluoride ligands could imply that a small amount of methane is also formed by reaction of the CH₃I with the hydride ligand of **8**, however this was not investigated at the time.

2.4.3 Reaction of *trans*-Ru(dmpe)₂(FHF)H (**8**) and Cp₂TiCl₂

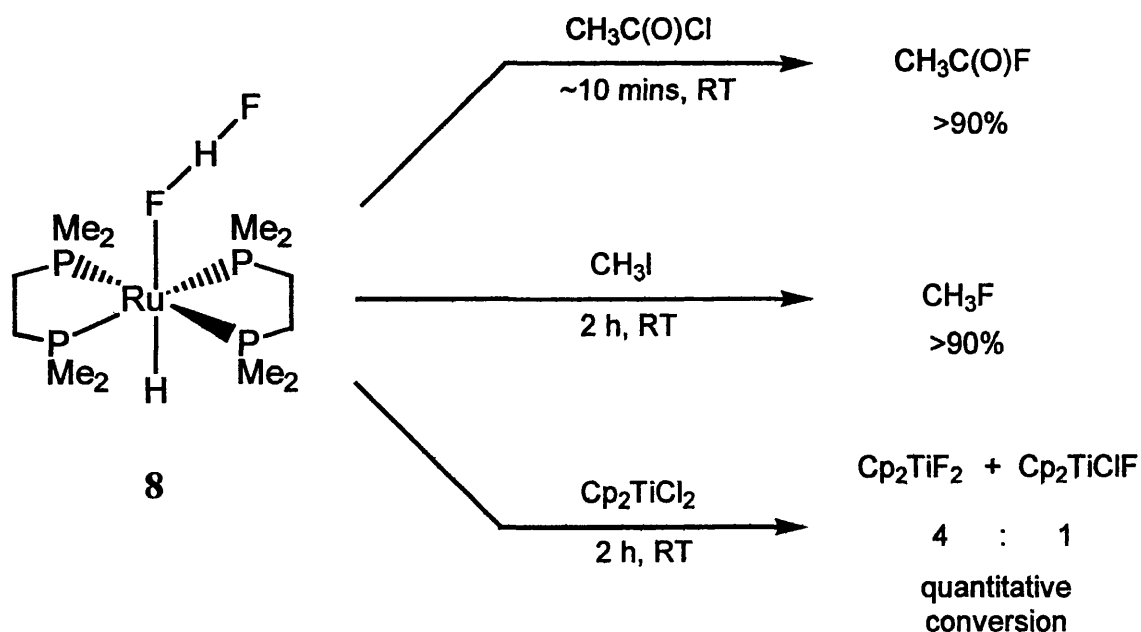
Into a d₆-benzene solution of **8** in a J. Youngs resealable NMR tube one equivalent of Cp₂TiCl₂ was added. The tube was warmed slightly to dissolve the titanium dichloride complex. After 2 h at room temperature, the solution had turned from red, due to the Cp₂TiCl₂, to a yellow colour and a yellow precipitate was formed.

The yellow solid was isolated and dissolved in thf. The ¹⁹F NMR spectrum showed the presence of two resonances at δ 85.73 and 138.35 that integrated in a ratio of 8:1. In the ¹H NMR spectrum two slightly broad cyclopentadienyl resonances at δ 6.32 and 6.40, which integrated in a ratio of 4:1. From these resonances it was deduced that Cp₂TiCl₂ had reacted with **8** to form Cp₂TiF₂ (¹⁹F δ 83.73, 2F; ¹H 6.32, 10H) and Cp₂TiClF (¹⁹F δ 138.35 1F; ¹H δ 6.40, 10H) in a 4:1 ratio. The NMR data matches closely that reported for both Cp₂TiClF and Cp₂TiF₂ reported by Seyam et al.¹⁸ but unfortunately the small couplings of 1.5 Hz that were reported were not detected in our spectra.

The $^{31}\text{P}\{^1\text{H}\}$ NMR of the solution was very similar to that seen in the reaction of **8** with $\text{CH}_3\text{C}(\text{O})\text{Cl}$, showing two triplet resonances at δ 49.3 and 40.1 (J_{PP} 23.2 Hz) and a broad singlet at δ 44.5, thought to be *cis*-Ru(dmpe)₂Cl₂ and *trans*-Ru(dmpe)₂HCl respectively. The ^1H NMR spectrum showed the quintet resonance for the hydride chloride at δ -20.71 (J_{HP} 23.2 Hz).

The ^1H NMR spectrum at the end of the reaction showed that none of the starting Cp_2TiCl_2 remained indicating a quantitative conversion to the fluorinated products.

Fig 2.15 Schematic of the fluorination reactions seen with *trans*-Ru(dmpe)₂(FHF)H, **8**.



2.4.4 Reaction of *trans*-Ru(dmpe)₂(FHF)H (**8**) and CH₂Cl₂

Addition of one equivalent of CH₂Cl₂ to a d₆-benzene solution of **8**, unlike in the reaction reported by Grushin¹⁴, showed no reaction by NMR spectroscopy after a week of heating at 85 °C.

2.5 Discussion

The reaction between *cis*-Ru(dmpe)₂H₂, **1**, and PFD proceeds very differently to that of **1** and C₆F₆. With the fluoroarene, reaction occurs at -78 °C but with the PFD prolonged heating at 85 °C is needed to drive the reaction to completion. The reaction products however do have some similarity. The bifluoride hydride species *trans*-Ru(dmpe)₂(FHF)H, **8**, is seen as a secondary product in the reaction with C₆F₆ and this same species is seen as the only metal containing product in the reaction of **1** and PFD. This would suggest that the PFD reaction has some similarities to that of C₆F₆. i.e. in both reactions an electron transfer occurs, a fluoride is released which then abstracts a hydrogen from the acidic radical cation to form HF. The HF can then attack dihydride **1** to yield bifluoride hydride **8**. Obviously, in the reaction with C₆F₆ the reaction path to form *trans*-Ru(dmpe)₂(C₆F₅)H is far more favourable.

A similar reaction path with the PFD molecule cannot be as favourable. This could be due to two factors. The size of the PFD molecule may mean that coordination of the larger fluoroorganic fragment is sterically restricted. There have been no reports of a saturated C-F bond being cleaved and the subsequent coordination of the remaining fragment. Also, if an electron transfer mechanism is involved, C₆F₆ will form a stable radical anion due to delocalisation of the extra electron around the aromatic ring. A PFD radical anion would be unable to give any delocalisation to the extra electron and therefore would be far more unstable. This would mean a radical recombination as seen in the reaction of **1** and C₆F₆ is unlikely. Therefore the reaction of **1** and PFD is more likely to form bifluoride hydride **8** than a complex with a fluoroorganic ligand.

Although the fluoroorganic products of the reaction of **1** and PFD were not identified, it can be concluded from NMR evidence that these products are unsaturated

in nature and do not contain substituted hydrogens. The stoichiometry of the reaction also suggests that each perfluorodecalin ‘gives up’ more than two fluorines in the course of the reaction. It is suspected that the organofluorine products may well be polymeric, which would explain their involatility.

The reactivity of other saturated perfluorocarbons with **1** showed that only fluorocarbons containing two vicinal tertiary C-F bonds displayed any reactivity, converting **1** to bifluoride hydride **8**. In the cases where this moiety was not seen in the fluorocarbon no reaction was seen on prolonged heating over 3 weeks. A similar reactivity pattern was found in the case of the photolytic activation of perfluoroalkanes using photosensitising amines reported by Turro.³ However, the use of [CpFe(CO)₂]⁻¹⁹ or cobaltocene⁵ only requires one tertiary C-F bond, and reactions with magnesium anthracene²⁰ and (MeC₅H₄)₃U(^tBu)²¹ with perfluoroalkanes, do not require any tertiary C-F bonds for C-F activation to occur.

A base was added to the reaction of **1** and PFD in an attempt to halt the formation of bifluoride hydride **8** and see if a complex with a fluoroorganic ligand could be isolated. Instead of this, an addition of a 30 x molar excess of pyridine to the original reaction yield the pyridine hydride complex *trans*-[Ru(dmpe)₂(C₅H₅N)H]⁺, **9**. The counterion to this complex was free bifluoride. This implied that the pyridine had little effect in halting the formation of **8**, but did react with **8**, displacing the bifluoride ligand with a pyridine molecule, leaving the bifluoride to be present as a counterion. The use of triethylamine as the base had a similar effect. The conversion of **1** to **8** was not affected but Et₃N did react with **8** yielding a new metal hydride species.

No effect on the conversion of **1** to **8** was seen on addition of the radical trap 9,10-dihydroanthracene (DHA) but this does not rule out the possibility of an electron transfer mechanism if the reaction occurs within a solvent cage. If the reaction does

occur within a solvent cage this would also explain why pyridine does not affect the formation of **8**. Further detailed discussion of the mechanism of reaction 2.1 will be discussed in chapter 3.

It is also important to note that no reaction is seen with the fluoroborosilicate glassware, and there is no effect on the reaction on changing the solvent.

With *trans*-Ru(dmpe)₂(FHF)H, **8**, we found we were able to readily fluorinate CH₃C(O)Cl, CH₃I and Cp₂TiCl₂ at room temperature to CH₃C(O)F, CH₃I and Cp₂TiF₂/Cp₂TiClF respectively. In the reactions involving chlorides **8** was converted to *cis*-Ru(dmpe)₂Cl₂ and *trans*-Ru(dmpe)₂HCl, whereas when an iodide was used the main products were *trans*-Ru(dmpe)₂I₂ and *trans*-Ru(dmpe)₂HI were found.

The activity of **8** as a fluorinating agent is comparable to the reactivity of [Cp₂Co]F reported by Bennett et al.⁵ Interestingly, whereas the cobaltocenium bifluoride complex does not perform such fluorination bifluoride hydride **8** does. The reactivity of Grushin's¹⁴ 'naked' fluoride, converting CH₂Cl₂ to CH₂ClF and CH₂F₂, was not seen for bifluoride hydride **8**. The use of transition metal fluoride or bifluoride complexes as fluorinating agents has an advantage over conventional fluorinating agents as there is the possibility of developing catalytic cycles for the transfer of fluorine from saturated perfluorocarbons to organic and transition metal halides. Unfortunately in our case, a one-pot system containing **1**, PFD and the halide is not possible due to the high reactivity of **1** towards the halide species.

2.6 Conclusions

- *cis*-Ru(dmpe)₂H₂, **1**, was seen to react with perfluorodecalin at 85 °C to yield the bifluoride hydride, *trans*-Ru(dmpe)₂(FHF)H, **8**, as the only inorganic product.
- The fluoroorganic products are involatile and appear in the δ -104 to -110 and δ -128 to -137 regions of the ¹⁹F NMR spectrum implying that these products are unsaturated and possibly polymeric.
- *cis*-Ru(dmpe)₂H₂, **1**, will only react with perfluoroalkanes that contain two vicinal tertiary C-F bonds.
- Addition of pyridine to the reaction of **1** and PFD led to the formation of the cationic pyridine hydride species *trans*-[Ru(dmpe)₂(C₅H₅N)H]⁺. The pyridine reacts with the bifluoride hydride that is formed and the displaced bifluoride unit remains as a counterion.
- *trans*-Ru(dmpe)₂(FHF)H, **8**, can act as a fluorinating agent, converting CH₃I, CH₃C(O)Cl and Cp₂TiCl₂ to CH₃F, CH₃C(O)F and Cp₂TiFX (X = F, Cl) respectively.

References

1. Whittlesey, M. K.; Perutz, R. N.; Moore, M. H. *Chem. Commun.*, **1996**, 787.
Whittlesey, M. K.; Perutz, R. N.; Greener, B.; Moore, M. H.; *Chem. Commun.*, **1997**, 187.
2. Marsella, J. A.; Gilicinski, A. G.; Coughlin, A. M.; Pez, G. P. *J. Org. Chem.*, **1992**, 57, 2856.
3. Kaprinidis, N. A.; Turro, N. J. *Tetrahedron Lett.*, **1996**, 37(14), 2373.
4. Deacon, G. B.; Meyer, G.; Stellfeldt, D. *Eur. J. Inorg. Chem.*, **2000**, 1061.
5. Bennett, B. K.; Harrison, R. G.; Richmond, T. G. *J. Am. Chem. Soc.*, **1994**, 116, 11165.
6. Aizenberg, M.; Milstein, D. *J. Am. Chem. Soc.*, **1995**, 117, 8674.
7. Christe, K. O.; Wilson, W. W. *J. Fluorine Chem.*, **1990**, 46, 339. Christe, K. O.; Wilson, W. W. *J. Fluorine Chem.*, **1990**, 47, 117.
8. Gouin, L.; Cousseau, J.; Smith, J. A. S. *J. Chem. Soc., Faraday Trans. 2*, **1977**, 1878.
9. Martin, J. S.; Fujiwara, F. Y. *Canad. J. Chem.*, **1971**, 49, 3071.
10. Fulton, J. R.; Bouwkamp, M. W.; Bergman, R. G. *J. Am. Chem. Soc.*, **2000**, 122, 8799.
11. Burn, M. J.; Fickes, M. G.; Hollander, F. J.; Bergman, R. G. *Organometallics*, **1995**, 14, 137.
12. Hsu, G. C.; Kosar, W. P.; Jones, W. D. *Organometallics*, **1994**, 13, 385.
13. Emsley, J. *Chem Soc Rev.*, **1980**, 9, 91.
14. Grushin, V. V. *Angew. Chem. Int. Ed.*, **1998**, 37, 994.
15. Clark, S. F.; Petersen, J. D. *Inorg. Chem.*, **1983**, 22, 620.
16. Kaplan, A. W.; Bergman, R. G. *Organometallics*, **1998**, 17, 5072.

17. Chatt, J.; Davidson, J. M. *J. Chem. Soc.*, **1965**, Pt.1, 843.
18. Seyam, A.; Sahma, H.; Hodali, H. *Gazz. Chim. Ital.*, **1990**, 120, 527.
19. Harrison, R. G.; Richmond, T. G. *J. Am. Chem. Soc.*, **1993**, 115, 5303.
20. Beck, C. M.; Park Y.-J.; Crabtree, R. H. *Chem. Commun.*, **1998**, 693.
21. Weydert, M.; Andersen, R. A.; Bergman, R. G. *J. Am. Chem. Soc.*, **1993**, 115, 8837.

Chapter 3

Activation of C-F bonds with other ruthenium dihydrides

3 Activation of C-F bonds with other ruthenium dihydrides

3.1 Introduction

Following the observations that **1** reacted with both aromatic and aliphatic C-F bonds, we investigated the effect of changing the substituents on the phosphorus atoms and changes in the backbone of the bidentate ligands. Thus, *cis*-Ru(depe)₂H₂ (**2**, depe = 1,2-bis(diethylphosphino)ethane), *cis*-Ru(dmpm)₂H₂ (**3**, dmpm = 1,2-bis(dimethylphosphino)methane), *cis*-Ru(dcpe)₂H₂ (**4**, dcpe = 1,2-bis(dicyclohexylphosphino)ethane; *cis*-Ru(dppe)₂H₂ (**5**, dppe = 1,2-bis(diphenylphosphino)ethane), and *cis*-Ru(PMe₃)₄H₂ (**6**) were prepared and probed for C-F activation chemistry.

Below the reactivity of this series of dihydrides towards aromatic and aliphatic C-F bonds is described. This chapter also describes cyclic voltammetry studies aimed at establishing the oxidation potentials of compounds **1-6**. The possibility of metal dihydrides to effect C-F bond activation through electron transfer processes has been described earlier.

3.2 Reactivity of *cis*-Ru(depe)₂H₂ (**2**)

3.2.1 Preparation of *cis*-Ru(depe)₂H₂ (**2**)

This dihydride was synthesised in a very similar manner to that used for dihydride **1**. A thf solution of *trans*-Ru(depe)₂Cl₂ was reduced under a hydrogen atmosphere using Na metal which yielded a 4:1 mixture of the *cis*- and *trans*-Ru(depe)₂H₂ species respectively.¹ The ³¹P{¹H} NMR spectrum showed a pair of apparent triplet resonances for the AA'BB' spin system at δ 77.1 and 64.3 (*J*_{PP} 18.2 Hz) for the *cis* isomer and a singlet resonance at δ 85.2 for the *trans* isomer. The hydride resonances were observed in the ¹H NMR spectrum at δ -10.12 (*trans* species, qnt, *J*_{HP} 19.7 Hz) and δ -10.53 (*cis* species, m).

3.2.2 Reaction with hexafluorobenzene

Addition of one equivalent of C₆F₆ to a benzene solution of Ru(depe)₂H₂ **2** in a J. Youngs resealable NMR tube, gave, on the basis of ³¹P{¹H} NMR spectroscopy, no immediate reaction at low or room temperature. However, upon leaving the NMR tube to stand for 3 days at room temperature the solution had turned from colourless to yellow. Analysis of the NMR spectra showed that the reaction had proceeded in a similar way to that reported for **1**.²

The ³¹P{¹H} NMR spectrum (fig 3.1) displayed a triplet at δ 71.6 (*J*_{FP} = 9.5 Hz) assigned to *trans*-Ru(depe)₂(C₆F₅)H, **10**, in a 4:1 ratio with another product, a singlet at δ 67.7, assigned as the bifluoride hydride complex *trans*-Ru(depe)₂(FHF)H, **11**.

The ³¹P{¹H} NMR spectrum shows that both *cis* and *trans* isomers of **2** react to give these products.

Reaction 3.1

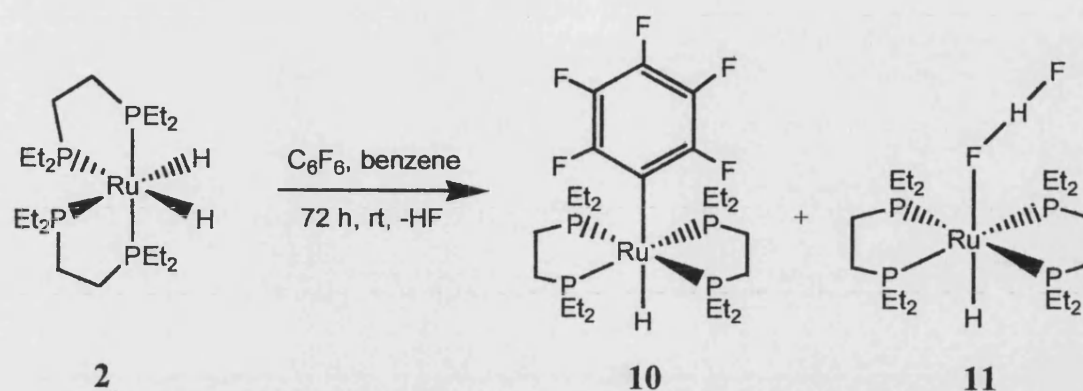
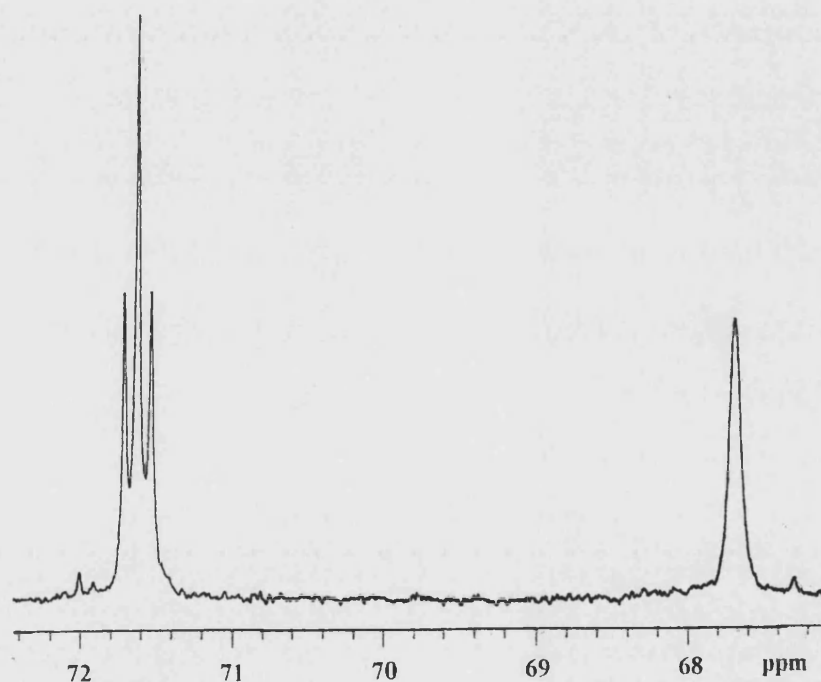


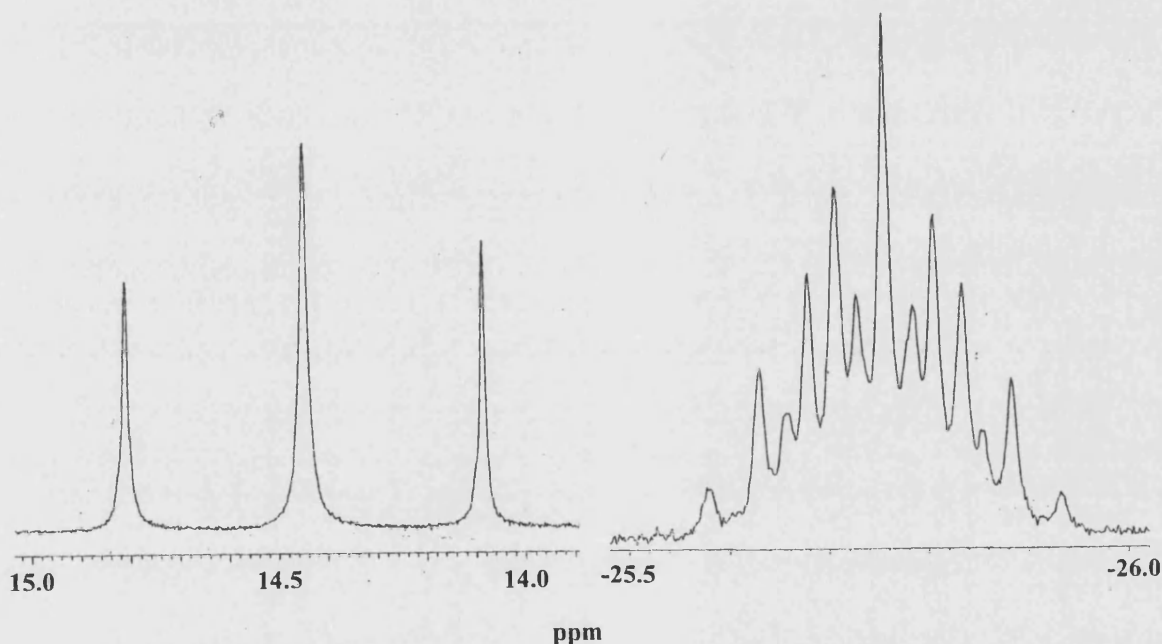
Fig 3.1 $^{31}\text{P}\{^1\text{H}\}$ NMR spectrum of reaction 3.1 products (C_6D_6 , 270 MHz)



The ^1H NMR spectrum showed the hydride resonance for *trans*- $\text{Ru}(\text{depe})_2(\text{C}_6\text{F}_5)\text{H}$, **10**, at δ -15.16 (tqnt, J_{HF} 11.0 Hz, J_{HP} 21.9 Hz). The bifluoride proton of **11** was observed as a distinctive triplet at δ 14.45 (J_{HF} 144.9 Hz) and the hydride was seen as a multiplet at δ -25.76. When a $^1\text{H}\{^{31}\text{P}\}$ NMR spectrum was recorded the hydride resonance simplified to a triplet (J_{HF} 31.2 Hz). Reviewing the ^1H

NMR spectrum we observed the hydride peak to be a triplet of quintets, the quintet splitting being J_{HP} 19.7 Hz. Both these proton resonances are shown in fig 3.2. The triplet splitting indicates that the bifluoride fluorines are equivalent at room temperature.

Fig 3.2 Sections of ^1H NMR spectrum of **11** showing the hydride and bifluoride proton resonances (C_6D_6 , 400 MHz)



The ^{19}F NMR spectrum showed a broad multiplet at δ -429.9 for fluoride resonances of **11** and some well defined peaks for the coordinated C_6F_5 group in **10** at δ -92.8 (m, 2 *ortho* F), δ -162.5 (m, 2 *meta* F), δ -163.7 (t, $J_{\text{FF}} = 20.3$ Hz, 1 *para* F). There were also resonances at δ -137.8 (m), -152.7 (m) and -161.0 (m), which were assigned to $\text{C}_6\text{F}_5\text{H}$ by comparison with published results.³ The proton for the pentafluorobenzene was detected in the ^1H NMR spectrum as a multiplet at δ 5.74. We see that the reaction follows a similar course to that of *cis*- $\text{Ru}(\text{dmpe})_2\text{H}_2$, **1**, and C_6F_6 yielding analogous products to those reported by Whittlesey et al.² and thus we did not follow up and

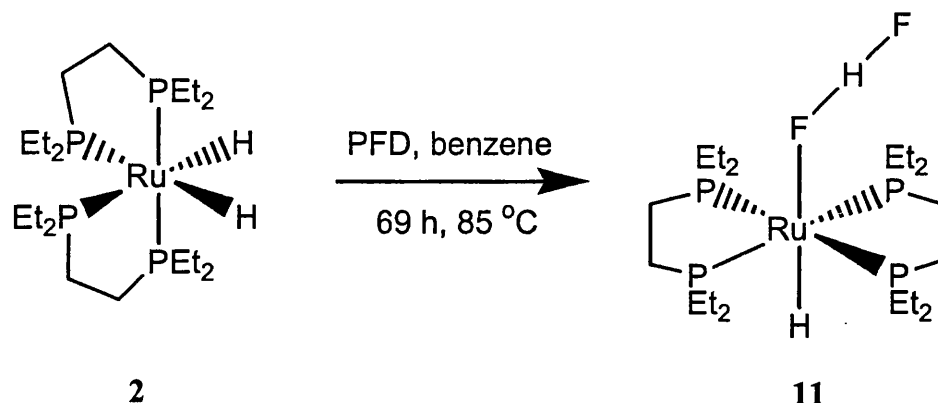
isolate **10**. The similarity also led us to investigate the reactivity of **2** with saturated perfluorocarbons.

3.2.3 Reaction with Perfluorodecalin

When one equivalent of PFD was added to a J. Youngs resealable NMR tube containing a benzene solution of *cis*-Ru(depe)₂H₂, **2**, no reaction was observed between -78 and 25 °C. This was not unexpected as *cis*-Ru(dmpe)₂H₂, **1**, needed 21 h at 85 °C for all the dihydride to react. It was found that **2** did react with PFD but at a much slower rate to that of **1**, 69 h at 85 °C was needed for all of the dihydride to react. As expected the reaction proceeded in a similar way to that of **1** and PFD. The major product in the ³¹P{¹H} NMR spectrum was a singlet at δ 67.7 attributable to the bifluoride hydride complex **11**. As seen for reaction 3.1 the ¹H NMR spectrum displays the bifluoride proton at δ 14.45 (t, *J*_{FH} 144.9 Hz) and the hydride was seen as a multiplet at δ -25.76 (tqnt, *J*_{HF} 31.2 Hz, *J*_{HP} 19.7 Hz).

In the ¹⁹F NMR spectrum a broad multiplet at δ -429.9 was found for the fluoride resonances of **11**. Infrared spectroscopy of *trans*-Ru(depe)₂(FHF)H, **11**, also confirmed the presence of the bifluoride ligand displaying broad bands at 1881 and 2433 cm⁻¹, which are close to those reported for the Pt(P^{*i*}Pr₃)₂(FHF)H complex.⁴

The ¹⁹F NMR spectrum also showed that all the PFD had not reacted and as before in the case of *cis*-Ru(dmpe)₂H₂, **1**, with PFD (chap. 2) new resonances for the fluoroorganic products appeared in the δ -100 to -110 and δ -130 to -140 regions of the spectrum.

Reaction 3.2

The fluoroorganic products seen in the ^{19}F NMR spectrum were the same as found in the reaction of **1** and PFD and similar problems occurred in trying to identify these products (chapter 2). The stoichiometry of the reaction was similarly complicated to that found for **1**. Whereas a 1:1 ratio of dihydride **2** and PFD in benzene did not consume all the PFD a 10:1 mixture reacted consuming all the PFD, converting **2** to the bifluoride hydride complex **11**.

The reactivity of **2** towards other saturated perfluoroalkanes was also investigated. Unsurprisingly, perfluoroalkanes with two adjacent tertiary C-F bonds, PFPHPA and PF1MD, were seen to react on heating to yield bifluoride hydride complex **11** and the same fluoroorganic products as seen in their reactions with **1**. Perfluoroalkanes, such as perfluoromethylcyclohexane (PFMCH), lacking two adjacent tertiary C-F groups, showed no reaction even on prolonged heating at 85 °C for several weeks.

The effect of a base on the reaction of **2** and PFD was studied to try and halt the formation of the bifluoride hydride complex **11**. On repeating reaction 3.2 in the presence of a 30 x molar excess of pyridine, conversion of **2** to **11** was complete after 150 h at 85 °C as shown by the loss of the starting dihydride. Analysis of the $^{31}\text{P}\{^1\text{H}\}$ NMR spectrum showed no evidence for the bifluoride hydride complex **11**, but instead,

two separate singlets were observed at δ 65.6 and 62.1. The resonance at δ 65.6 was by far the strongest by a ratio of 4:1 and coupled to a quintet resonance in the ^1H NMR spectrum at δ -20.72 (J_{HP} 19.9 Hz) on the basis that both these resonances appeared together in the early stages of the reaction before the appearance of the δ 62.1 resonance which showed no resonances in the hydride region. This suggested the presence of a *trans*- RuP_4HX species and a non hydridic ruthenium phosphine complexes. The ^{19}F NMR spectrum did show a small amount of the fluoroorganic products seen for the original reaction but also a sharp singlet at δ -134.3. No evidence for a bifluoride cation as seen in the analogous reaction with **1** was seen.

When the reaction 3.2 was carried out in a 1:1 solution of pyridine and C_6D_6 the reaction proceeded much faster with all dihydride **2** lost after 16 h at 80 °C. The $^{31}\text{P}\{^1\text{H}\}$ NMR spectrum showed that the peaks at δ 65.6 and 62.1 were present again only this time the singlet resonance at δ 62.1 was strongest in a ratio ca. 3:1. The ^1H NMR spectrum showed no hydride resonance coupling for the δ 62.1 peak, only the resonance at δ -20.72 for the δ 65.6 peak. Clearly, the effect of adding pyridine (either 30 equivalents or a larger excess) leads to a different reaction profile in the case of **2** and PFD compared to **1** and PFD.

On addition of a different base, triethylamine, in a 30 x molar excess to reaction 3.2 the major product seen after 19 h at 80 °C in the $^{31}\text{P}\{^1\text{H}\}$ NMR spectrum was the same peak seen in the pyridine reactions at δ 65.6. The ^1H NMR spectrum showed the same quintet at δ -20.72 (J_{HP} 19.9 Hz) as before. After 61 h of heating, all of the dihydride had reacted and the main product was now the bifluoride hydride **11** at δ 67.9, in a 10:1 ratio with the product seen at δ 65.6. The ^1H NMR spectrum displayed both hydride (δ -25.76) and bifluoride proton (δ 14.45) resonances for **11** and the hydride

resonance at δ -20.72 for the δ 65.6 species. The ^{19}F NMR spectrum again showed the same fluoroorganic products as seen in the original reaction of **2** and PFD.

These results indicate that base has an effect on this reaction that is different to that seen for **1** and PFD where the pyridine hydride, *trans*-[Ru(dmpe)₂(C₅H₅N)H]⁺, **9**, is formed. In the case of *cis*-Ru(depe)₂H₂, **2**, and PFD, the effect of the base on the reaction seems to initially form a *trans*-Ru(depe)₂HX species which appears as a singlet in the $^{31}\text{P}\{^1\text{H}\}$ NMR spectrum at δ 65.6 and a quintet in the ^1H NMR spectrum at δ -20.72. With Et₃N as the base this species appears to react further to ultimately form the bifluoride hydride complex **11**. With pyridine as the base, the *trans*-Ru(depe)₂HX species reacts further to form a non-hydridic complex seen as a singlet in the $^{31}\text{P}\{^1\text{H}\}$ NMR spectrum at δ 62.1 (s) which was not conclusively identified. In the *trans*-Ru(depe)₂HX species we thought that as before for the 1:PFD:pyridine (30x) reaction a pyridine may be coordinated to the metal centre to give a cationic pyridine hydride complex, however the same product is seen in the reaction with Et₃N. The hydride resonance for this species at δ -20.72 appears as a quintet so no coupling is seen from a ligand coordinated trans to the hydride. It may be that the coordination site is vacant giving a five coordinate [Ru(depe)₂H]⁺. For this cationic species to be present a suitable anion must be available. No bifluoride anion was detected but it could be that the strong singlet seen in the ^{19}F NMR spectrum at δ -134.3 is a fluoride anion. Cobaltocenium fluoride⁵ appears at δ -110 in the ^{19}F NMR spectrum but data collected by Christe et al.⁶ investigating the solvent effect on the fluoride resonance suggest a chemical shift range of δ -75 to δ -150 for the fluoride anion.

3.3 Reactivity with *cis*-Ru(dmpm)₂H₂ (3)

This dihydride was chosen as it closely resembles dihydride 1 apart from one less carbon in the chelate bridge. The substituent ‘ears’ are the same size as in 1 and smaller than in 2 so it was expected that *cis*-Ru(dmpm)₂H₂, 3, would be very reactive towards C-F bonds.

3.3.1 Preparation of *cis*-Ru(dmpm)₂H₂ (3)

This dihydride was prepared using a method described by Hartwig et al.⁷ Two equivalents of dmpm are added to (PPh₃)₂Ru(OAc)₂ to form a dimer which is then thermolysed to *cis*-Ru(dmpm)₂(OAc)₂. Treatment of the diacetate with LiAlH₄ yields pure *cis*-Ru(dmpm)₂H₂, 3, as a pale yellow powder in 59 % yield. The ³¹P{¹H} NMR spectrum of 3 shows two apparent triplet resonances for the AA'BB' spin system at δ -16.4 and -28.9 (*J*_{PP} 46.5 Hz). The ¹H NMR spectrum shows the hydride resonances at δ -8.24 (dq, *J*_{HP} 77.8 Hz, *J*_{HP} 22.2 Hz).

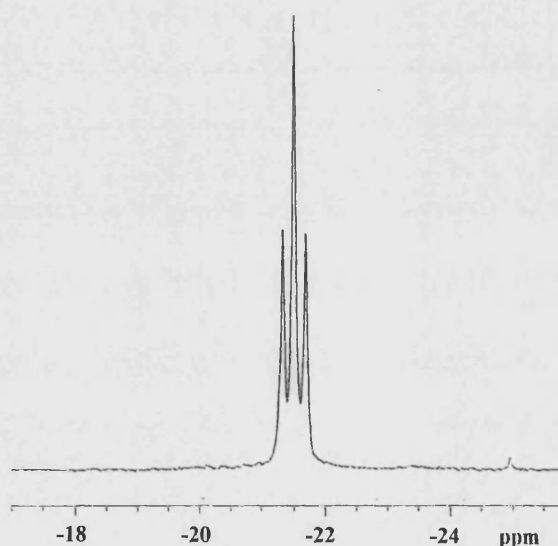
3.3.2 Reaction with hexafluorobenzene

When C₆F₆ was condensed into a colourless benzene solution of 3 in a J. Youngs resealable NMR tube, an immediate reaction was observed on thawing from -78 °C, with the formation of a yellow homogeneous solution. The ³¹P{¹H} NMR spectrum (fig 3.3) showed complete disappearance of the starting dihydride, and the formation of a new triplet resonance at δ -21.5 (*J*_{PF} 20.0 Hz) as the only product. The ¹H NMR spectrum displayed a new broadened multiplet signal at δ -9.32, while in the ¹⁹F NMR

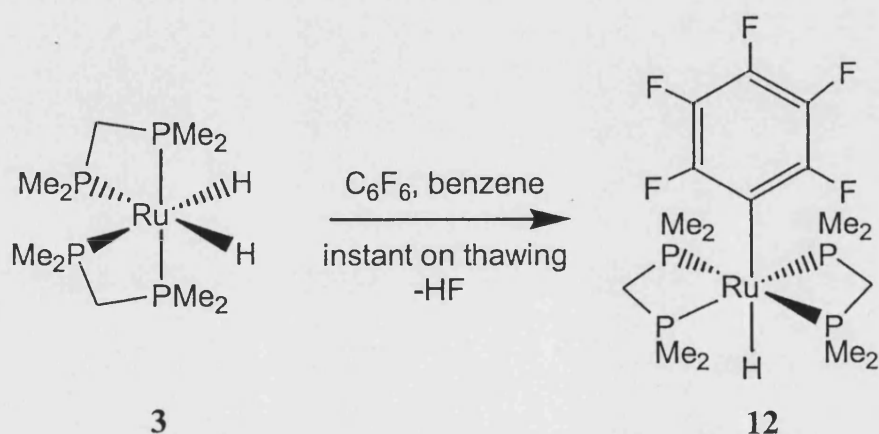
spectrum, peaks at δ -99.7 (m, 2 *ortho* F), -164.9 (m, 2 *meta* F), and -165.7 (t, 1 *para* F, J_{FF} 20.31 Hz) were consistent with a coordinated pentafluorophenyl group. The data was consistent with the formation of *trans*-Ru(dmpm)₂(C₆F₅)H, **12**. Also present in both the ¹⁹F and ¹H NMR spectra were signals for C₆F₅H as seen in the reactions of both **1** and **2** with C₆F₆.

One important difference was seen in the reaction of **3** with C₆F₆ compared to dihydrides **1** and **2**. At no point was any evidence seen in the NMR spectra for the formation of a bifluoride hydride species.

Fig 3.3 ³¹P{¹H} NMR spectrum of *trans*-Ru(dmpm)₂(C₆F₅)H, **12**. (C₆D₆, 270 MHz)



Reaction 3.3



From the reaction mixture, small colourless crystals were obtained in 89 % yield. A single crystal X-ray analysis confirmed the structure of **12** as *trans*-Ru(dmpm)₂(C₆F₅)H (fig 3.4). The structure has a mirror plane running through the Ru metal, the bridging carbons in the chelating phosphines, the coordinated carbon and the *para* carbon and fluorine atoms. It can be seen that the structure is a six coordinate ruthenium complex with a distorted octahedral geometry, the imbalance between the sizes of the hydride and pentafluorophenyl ligands enforcing an average P-Ru-C angle of 98.85(4) °, a trait that was discussed in chapter 2. The average Ru-P bond distance in **12** is 2.3003(4) Å, essentially identical to the average Ru-P bond length of 2.3082(4) Å in *trans*-Ru(dmpe)₂(C₆F₅)H, **7**. However, the Ru-C bond in **12** (2.1807(19) Å) is much shorter compared to 2.250(4) Å in the dmpe analogue. This is due to the positioning of the chelating phosphines ligands. In **12** the average C-Ru-P angle of 98.85(4) ° means that the dmpm ligand bridge bends away from the coordinated C₆F₅ also pulling away the methyl ‘ears’ from the coordination site. This allows the fluorinated ligand to get closer to the metal than in *trans*-Ru(dmpe)₂(C₆F₅)H, **7**, where the steric constraints of having two carbons in the chelate bridge means the average C-Ru-P angle is only 96.34(7) °. The shorter Ru-C distance in **12** also affects the Ru-H bond distance. The freely refined hydride in **12** was found to be 1.64(3) Å from the ruthenium metal, slightly longer than seen for *trans*-Ru(dmpe)₂(C₆F₅)H, **7**, (1.56 Å) .

Fig 3.4 X-ray crystal structure of *trans*-Ru(dmpm)₂(C₆F₅)H (12)

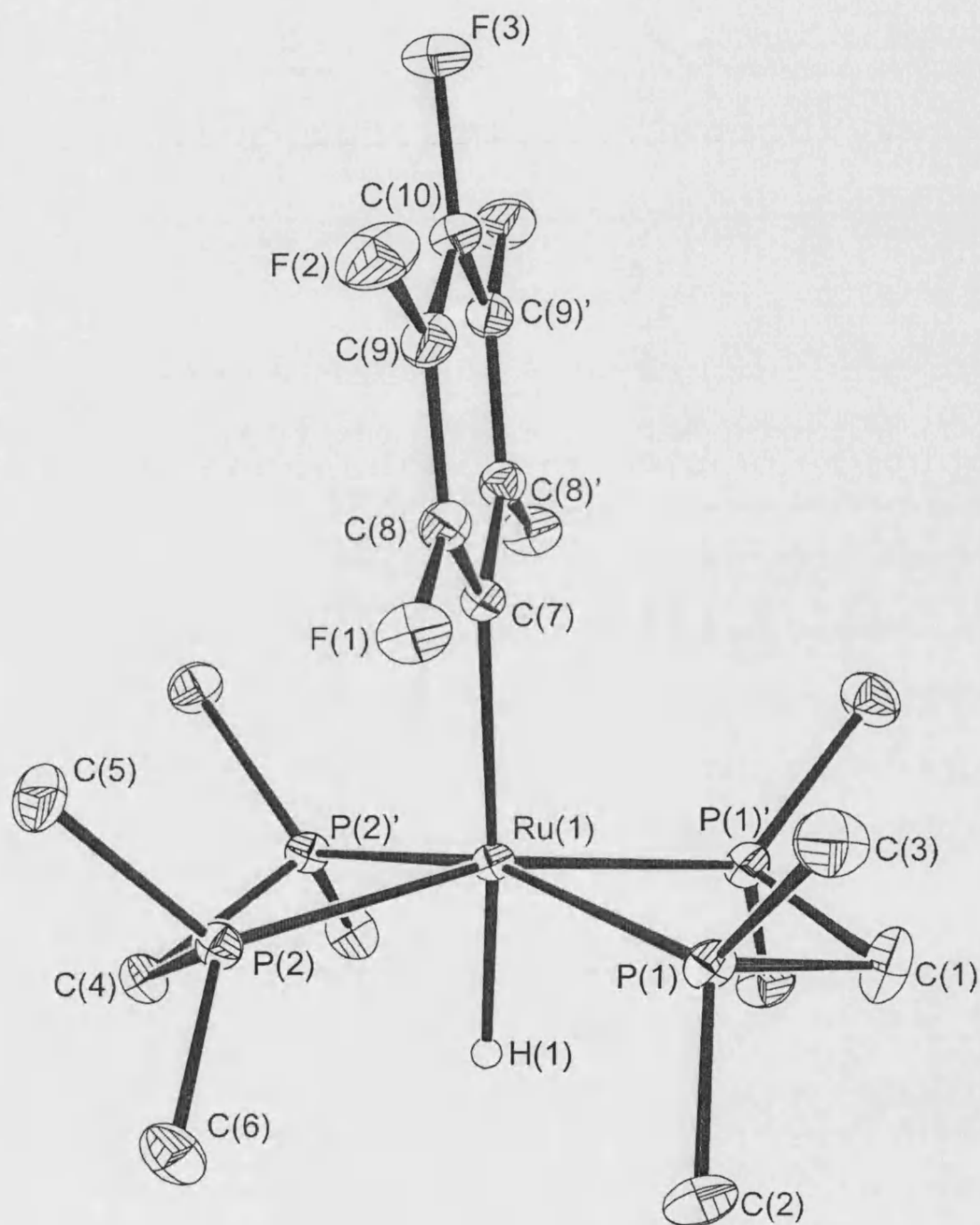


Table 3.1. Crystal data and structure refinement parameters for **12**

Empirical formula	C ₁₆ H ₂₉ F ₅ P ₄ Ru
Formula weight	541.34
Temperature	170(2) K
Wavelength	0.71070 Å
Crystal system	Orthorhombic
Space group	Pcmn
Unit cell dimensions	a = 8.8090(1) Å α = 90° b = 15.8140(2) Å β = 90° c = 16.0680(3) Å γ = 90°
Volume	2238.36(6) Å ³
Z	4
Density (calculated)	1.606 Mg/m ³
Absorption coefficient	1.026 mm ⁻¹
F(000)	1096
Crystal size	0.33 x 0.33 x 0.25 mm
Theta range for data collection	3.67 to 27.48 °
Index ranges	-10 ≤ h ≤ 11; -20 ≤ k ≤ 20; -20 ≤ l ≤ 20
Reflections collected	35518
Independent reflections	2652 [R(int) = 0.0294]
Reflections observed (>2σ)	2529
Absorption correction	Multiscan
Max. and min. transmission	
Refinement method	Full-matrix least-squares on F ²
Data / restraints / parameters	2652 / 0 / 135
Goodness-of-fit on F ²	1.001
Final R indices [I > 2σ(I)]	R ₁ = 0.0191 wR ₂ = 0.0529
R indices (all data)	R ₁ = 0.0204 wR ₂ = 0.0540
Largest diff. peak and hole	0.442 and -0.475 e.Å ⁻³

N.B. Asymmetric unit = ½ molecule. Atoms Ru1, H1, C1, C4, C7, C10 and F3 located on crystallographic mirror plane at y = ¼.

H1 located in Difference map and freely refined. Ru1–H1 1.64(2) Å.

Table 3.2 Bond lengths [Å] and angles [°] for **12**

Ru(1)-C(7)	2.1807(19)	Ru(1)-P(1)	2.3048(4)
Ru(1)-P(2)	2.2957(4)	Ru(1)-P(1)#1	2.3048(4)
Ru(1)-P(2)#1	2.2957(4)	Ru(1)-H(1)	1.64(3)
P(1)-C(2)	1.8208(16)	C(1)-P(1)#1	1.8441(15)
P(1)-C(3)	1.8290(16)	C(4)-P(2)#1	1.8544(14)
P(1)-C(1)	1.8441(15)	C(7)-C(8)#1	1.3901(18)
P(2)-C(6)	1.8243(16)	C(7)-C(8)	1.3901(18)
P(2)-C(5)	1.8318(16)	C(8)-C(9)	1.390(2)
P(2)-C(4)	1.8544(14)	C(9)-C(10)	1.374(2)
P(2)-P(2)#1	2.6928(7)	C(10)-C(9)#1	1.374(2)
F(1)-C(8)	1.3645(16)	F(3)-C(10)	1.352(2)
F(2)-C(9)	1.3530(18)		
C(7)-Ru(1)-P(2)	98.09(4)	C(6)-P(2)-C(4)	107.83(8)
C(7)-Ru(1)-P(2)#1	98.09(4)	C(5)-P(2)-C(4)	102.42(9)
P(2)-Ru(1)-P(2)#1	71.818(19)	C(6)-P(2)-Ru(1)	122.96(6)
C(7)-Ru(1)-P(1)	99.61(4)	C(5)-P(2)-Ru(1)	124.69(6)
P(2)-Ru(1)-P(1)	162.285(15)	C(4)-P(2)-Ru(1)	94.47(5)
P(2)#1-Ru(1)-P(1)	104.846(13)	C(6)-P(2)-P(2)#1	140.49(6)
C(7)-Ru(1)-P(1)#1	99.61(4)	C(5)-P(2)-P(2)#1	110.44(6)
P(2)-Ru(1)-P(1)#1	104.846(13)	C(4)-P(2)-P(2)#1	43.44(5)
P(2)#1-Ru(1)-P(1)#1	162.284(15)	Ru(1)-P(2)-P(2)#1	54.091(9)
P(1)-Ru(1)-P(1)#1	72.833(18)	P(1)#1-C(1)-P(1)	95.80(11)
C(7)-Ru(1)-H(1)	176.2(11)	P(2)#1-C(4)-P(2)	93.11(9)
P(2)-Ru(1)-H(1)	78.9(9)	C(8)#1-C(7)-C(8)	111.73(18)
P(2)#1-Ru(1)-H(1)	78.9(9)	C(8)#1-C(7)-Ru(1)	124.10(9)
P(1)-Ru(1)-H(1)	83.4(9)	C(8)-C(7)-Ru(1)	124.10(9)
P(1)#1-Ru(1)-H(1)	83.4(9)	F(1)-C(8)-C(9)	114.28(12)
C(2)-P(1)-C(3)	100.41(8)	F(1)-C(8)-C(7)	120.31(13)
C(2)-P(1)-C(1)	105.88(10)	C(9)-C(8)-C(7)	125.40(14)
C(3)-P(1)-C(1)	103.56(11)	F(2)-C(9)-C(10)	119.12(14)
C(2)-P(1)-Ru(1)	120.97(6)	F(2)-C(9)-C(8)	121.42(14)
C(3)-P(1)-Ru(1)	127.32(6)	C(10)-C(9)-C(8)	119.45(14)
C(1)-P(1)-Ru(1)	95.38(5)	F(3)-C(10)-C(9)	120.69(10)
C(6)-P(2)-C(5)	101.20(8)	F(3)-C(10)-C(9)#1	120.69(10)

Symmetry transformations used to generate equivalent atoms:

#1 x,-y+1/2,z

The structure also shows that the coordinated C_6F_5 in **12** sits twisted by approximately 90° to the position seen in the crystal structure of **7**.¹ The mean bite angle of dmpm in the structure of **12** is $72.33(19)^\circ$, which compares well to reported bite angles found in the crystal structures of *cis*- $\text{Ru}(\text{dmpm})_2\text{H}_2$ ($72.03(7)^\circ$)⁸ and *trans*- $[\text{Ru}(\text{dmpm})_2(\eta^1\text{-dmpm})\text{H}]\text{PF}_6$ ($72.0(7)^\circ$)⁹, two of only five ruthenium dmpm complexes that have been crystallographically characterised and reported.¹⁰ This means that the average of the remaining *cis* P-Ru-P angles is $104.85(13)^\circ$. This shows a marked difference to the crystal structure of *trans*- $\text{Ru}(\text{dmpe})_2(\text{C}_6\text{F}_5)\text{H}$, **7**¹, where the larger bite angle of dmpe ($83.89(5)^\circ$) means the remaining *cis* P-Ru-P bond angles average at $94.60(5)^\circ$. This substantial difference is probably the reason behind the difference in orientation of the C_6F_5 group between the two crystal structures. In *trans*- $\text{Ru}(\text{dmpe})_2(\text{C}_6\text{F}_5)\text{H}$, **7**, the plane of the fluorophenyl ring bisects the backbone of the dmpe ligand. However in **12**, the space provided by the larger *cis* P-Ru-P angles means the planar pentafluorophenyl ligand can coordinate more strongly by being perpendicular to the position seen in the dmpe analogue.

3.3.3 Reaction with pentafluorobenzene

Considering the high reactivity of *cis*- $\text{Ru}(\text{dmpm})_2\text{H}_2$, **3**, towards C_6F_6 it was deemed important to react **3** with pentafluorobenzene to see if the aromatic C-F activation was selective over aromatic C-H activation.

To a J. Youngs resealable NMR tube containing a benzene solution of **3**, one equivalent of pentafluorobenzene was added. No immediate reaction was seen at low temperatures but after 2 h at room temperature, $^{31}\text{P}\{^1\text{H}\}$ NMR spectroscopy indicated

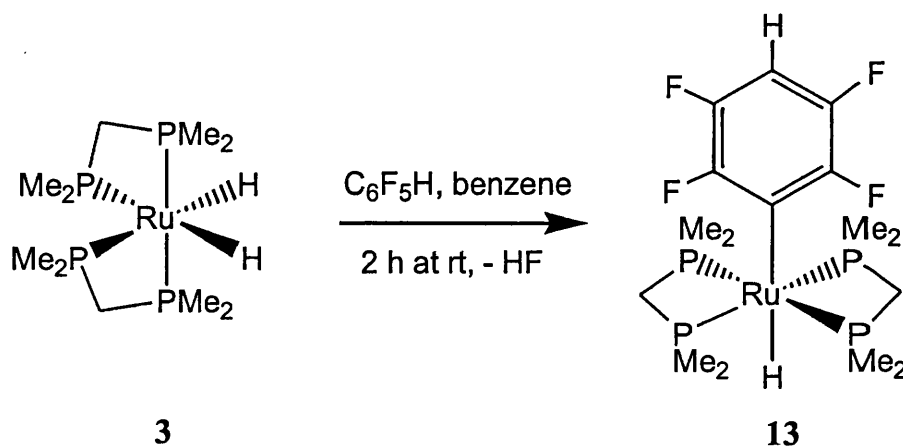
that all the starting dihydride had depleted to give a single product that appeared as a triplet at δ -21.1 (J_{PF} 19.3 Hz). This was assigned as *trans*-Ru(dmpm)₂(*p*-C₆F₄H)H, **13**.

The ¹H NMR spectrum showed a broadened multiplet hydride resonance at δ -9.15 and a resonance at δ 6.68 (tt, J_{HF} 6.78, J_{HF} 9.15) for the *para* proton on the coordinated C₆F₄H ring. The ¹⁹F NMR spectrum showed resonances for the coordinated C₆F₄H at δ -101.7 (m, 2 *ortho* F) and δ -143.0 (m, 2 *meta* F). The reaction also yielded a small amount of 1,2,4,5-C₆F₄H₂, which was seen as an apparent quintet at δ 6.06 (tt, J_{HF} 8.78 Hz) in the ¹H NMR spectrum and an apparent triplet at δ -139.7 (dd, J_{HF} 8.78 Hz) in the ¹⁹F NMR spectrum, which matched reported data¹¹

for what?

The reaction is slower than with C₆F₆ but it does show that *cis*-Ru(dmpm)₂H₂, **3**, reacts comparably to *cis*-Ru(dmpe)₂H₂, **1**, in the reaction with C₆F₅H. The aromatic C-F activation is preferred over C-H activation and occurs *para* to the C-H bond in the pentafluorobenzene ring. Also, once again there was no evidence, by NMR spectroscopy, during the reaction for the formation of a bifluoride hydride species.

Reaction 3.4



3.3.4 Reaction with perfluorodecalin (PFD)

The high reactivity of *cis*-Ru(dmpm)₂H₂ towards aromatic C-F bonds led us to investigate its reactivity towards perfluorodecalin. As no evidence of a bifluoride hydride was seen in the reactions with C₆F₆ or C₆F₅H it was important to see if such a complex could be formed. One equivalent of PFD was added to a J.Youngs resealable NMR tube containing a benzene solution of **3**. No immediate reaction was seen at room temperature, but on heating at 85 °C, the colourless solution slowly turned yellow. After 20 h at 85 °C, the ³¹P{¹H} NMR spectrum showed that all of the starting dihydride had been consumed but more than one product had been formed as displayed by the number of weak broad resonances seen in the δ 10 to –40 region. Analysis of the ¹H NMR also showed five broad lumps in the hydride region but the products were very weak. The ¹⁹F NMR spectrum showed that most of the PFD remained so it was decided that the reaction was not worth pursuing.

3.4 Reactivity of *cis*-Ru(dcpe)₂H₂ (**4**), *cis*-Ru(dppe)₂H₂ (**5**), and *cis*-Ru(PMe₃)₄H₂ (**6**)

3.4.1 Preparation of dihydrides **4**, **5** and **6**

These dihydrides were synthesised using literature methods.¹² Benzene solutions of each dihydride show two apparent triplets in their ³¹P{¹H} NMR spectra for the AA'BB' spin system and a multiplet hydride resonance in their ¹H NMR spectra (table 3.3). In the preparation of **5** a 20:1 ratio of *cis:trans* isomers is formed. Both **4** and **6** are formed as *cis* only dihydrides.

Table 3.3 NMR data for dihydrides **4**, **5** and **6**

Ruthenium dihydride	$^{31}\text{P}\{^1\text{H}\}$ NMR data	^1H NMR of hydrides
4	δ 65.8 (t), δ 90.2 (t) J_{PP} 13.0 Hz	δ -12.31 (m)
5	δ 79.0 (t), δ 65.0 (t) J_{PP} 15.1 Hz (<i>cis</i>) δ 83.4 (s) (<i>trans</i>)	δ -8.33 (m) (<i>cis</i>) δ -8.17 (qnt, J_{HP} = 17 Hz) (<i>trans</i>)
6	δ 0.1 (t), δ -7.4 (t) J_{PP} 26.1 Hz	δ -9.71 (m)

3.4.2 Reaction with hexafluorobenzene

When one equivalent of hexafluorobenzene was added to J.Youngs resealable NMR tubes containing benzene solutions of any of these three dihydrides, no reactions were seen, by NMR spectroscopy, at room temperature, nor upon heating at 85 °C for several weeks.

3.4.3 Reaction with perfluorodecalin

Even though no reaction was seen between the three dihydrides and hexafluorobenzene, it was important to make sure that there was no reaction with perfluorodecalin. On addition of one equivalent of PFD to J.Youngs resealable NMR tubes containing benzene solutions of the dihydrides, no reactions were seen by NMR spectroscopy, upon heating at 85 °C for several weeks

The phosphine ligand characteristics appear to make dihydrides **1**, **2** and **3** capable of C-F bond activation but not **4**, **5** and **6**. With *cis*-Ru(dcpe) $_2$ H $_2$ **4** and *cis*-

$\text{Ru}(\text{dppe})_2\text{H}_2$, **5**, it would appear that the size of the substituent ‘ears’ is a factor. It was noticed that even by just adding an extra carbon into these ‘ears’, from dmpe to depe , the rate of reaction, with both hexafluorobenzene and perfluorodecalin, decreased significantly and that the larger ears of **4** and **5** restrict any similar reaction process. Also, more surprisingly is the fact that no reaction is seen with *cis*- $\text{Ru}(\text{PMe}_3)_2\text{H}_2$, **6**, which implies that the dihydride is only reactive towards C-F bonds when chelating diphosphine ligands are present.

3.5 Cyclic voltammetry of the series of dihydrides

As mentioned in chapter 2 the proposed mechanism for the reaction of *cis*- $\text{Ru}(\text{dmpe})_2\text{H}_2$, **1**, and C_6F_6 is initiated by an electron transfer from the electron rich transition metal hydride to the fluorocarbon.² Thus we decided to measure the first oxidation potentials for the series of dihydrides **1-6** we had used by cyclic voltammetry.

All measurements were carried out in an oxygen and moisture free glovebox to protect the dihydride from decomposition. In each case a small amount (~ 2 mg) was added to a thf solution containing 0.2 M $[\text{Bu}_4\text{N}][\text{BF}_4]$ as an electrolyte. Firstly measurements were carried out using a silver wire electrode and a vitreous carbon electrode (area = 0.0707 cm²), then the measurements referenced using a SCE (standard calomel electrode).

The cyclic voltammetry traces are shown in fig 3.5 and the first oxidation potentials are given in table 3.4.

Fig 3.5 Cyclic voltamograms of dihydrides 1-6

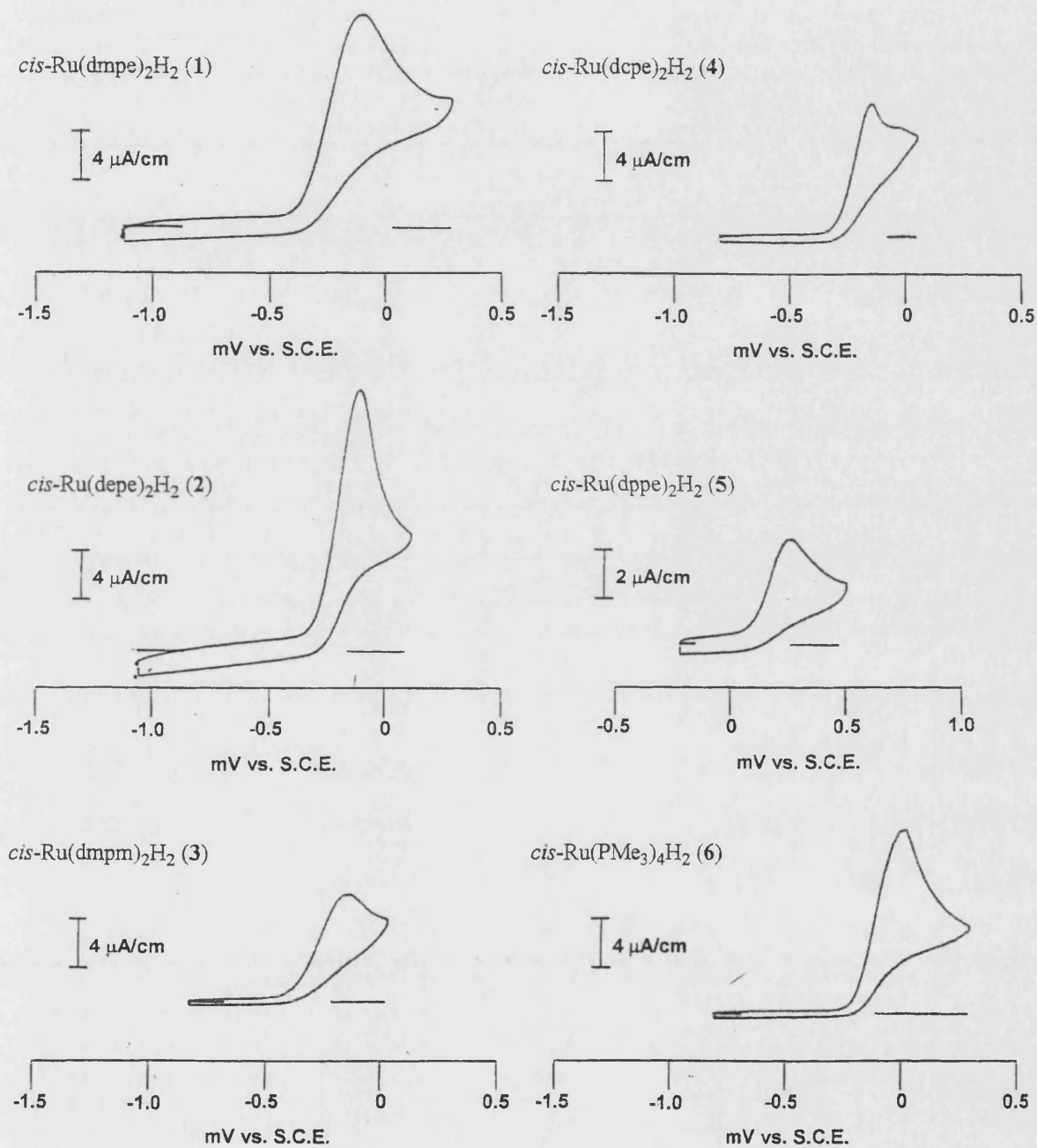


Table 3.4 First oxidation potentials for dihydrides 1-6

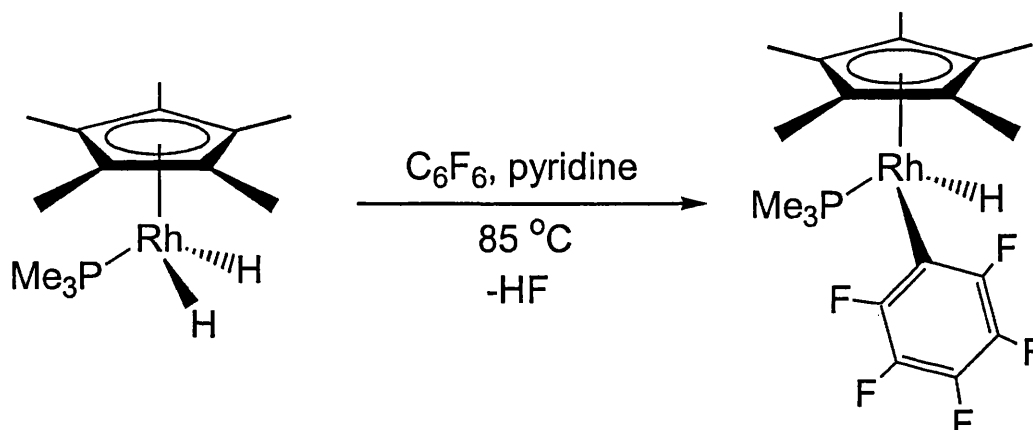
<i>cis</i> -RuH ₂ (P ₄) where P ₄ =	First oxidation potential (V vs. S.C.E.)	Reversible (<i>R</i>) or Irreversible (<i>I</i>)
(dmpe) ₂ (1)	- 0.10	<i>I</i>
(depe) ₂ (2)	- 0.12	<i>I</i>
(dmpm) ₂ (3)	- 0.13	<i>I</i>
(dcpe) ₂ (4)	- 0.14	<i>I</i>
(dppe) ₂ (5)	+0.24	<i>I</i>
(PMe ₃) ₄ (6)	0.00	<i>I</i>

The diagrams show that for each of the chosen dihydrides the first oxidation potential peak is irreversible, so the electron transfer from the dihydride cannot be reversed. It is seen that the chelating phosphines with alkyl groups lead to the more electron donating dihydride complexes. Two chelating diphosphine ligands seem to affect the metal centre more than four monophosphine ligands in increasing the electron donating properties, and the smaller the bite angle of the diphosphine the lower the oxidation potential (i.e. 3 vs. 1). The substituent ‘ears’ on the diphosphine ligands are also seen to affect the oxidation potential. The electron withdrawing phenyl ‘ears’ increase the oxidation potential of *cis*-Ru(dppe)₂H₂ to +0.24 V vs S.C.E., whereas the non-electron withdrawing alkyl ‘ears’ of dihydrides 1-4 make these more electron donating. In dihydrides 1, 2 and 4 the electron-pushing inductive effect of the alkyl groups can be also be seen. The increasing inductive effect from *methyl* < *ethyl* < *cyclohexyl* makes the order of decreasing oxidation potentials 4 < 2 < 1.

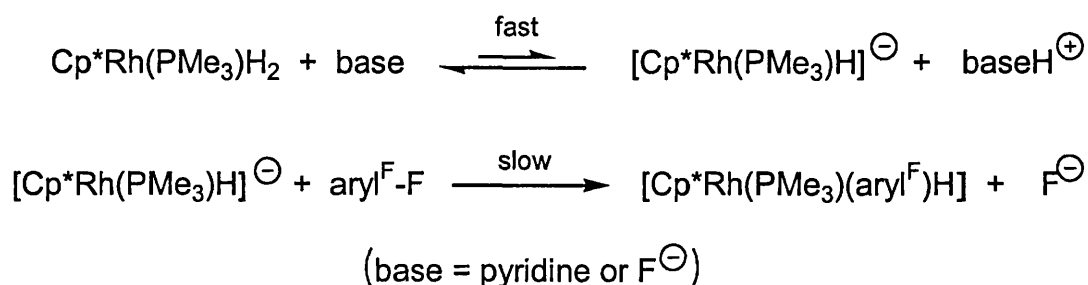
Our investigations showed that the dihydrides that reacted with C₆F₆ all reacted in a similar way to give a *trans*-Ru(P-P)₂(C₆F₅)H species with the rate of reactivity

being $3 \geq 1 > 2$. Dihydrides **4**, **5** and **6** were not seen to react. If the proposed mechanism of activation is correct then we would expect the more electron donating dihydrides to react more readily with hexafluorobenzene. With **5** and **6** no reaction is seen which agrees with this fact. However the oxidation potentials of the other four dihydride increases in the order $4 < 3 < 2 < 1$. This would imply that hexafluorobenzene would react more readily with *cis*-Ru(dcpe)₂H₂, **4**, and *cis*-Ru(depe)₂H₂, **2**, than with *cis*-Ru(dmpe)₂H₂, **1**. We have shown that *cis*-Ru(dcpe)₂H₂, **4**, does not react with C₆F₆ and that *cis*-Ru(depe)₂H₂, **2**, takes 3 days at room temperature to completely react with C₆F₆. Considering that the reaction of *cis*-Ru(dmpe)₂H₂, **1**, reacts with C₆F₆ at -78 °C, it would seem that, if electron transfer is the initial step then the rate of the reaction is affected by the steric effect of the substituent alkyl 'ears' in the chelating diphosphine ligand.

This being said the reduction potentials of perfluoroarenes reported by Pez¹³ show C₆F₆ to have a irreversible reduction potential of -2.56 V (vs S.C.E) and perfluorodecalin an irreversible reduction potential of -2.31 V (vs S.C.E). This shows that an electron transfer from any of the dihydrides to either perfluorocarbon would be uphill in excess of 2 V. A similar problem is reported by Jones et al.¹⁴ in the reaction of (C₅Me₅)Rh(PMe₃)H₂ and perfluoroarenes. The rhodium dihydride reacts with the perfluoroarene, on heating at 85 °C in a pyridine solution, cleaving an aromatic C-F bond, to yield a rhodium complex with a perfluorinated ligand, in a manner very similar to that seen in the reactions of **1**, **2** and **3** with C₆F₆ (fig 3.6). Therefore, an electron transfer mechanism as shown in chapter 2 could be suggested. However, the irreversible oxidation potential of the rhodium complex is reported to be at -0.336 V (vs Ferrocene/Ferrocenium Ion couple), which means that an electron transfer from the rhodium complex to C₆F₆ would also be uphill by more than 2 V.

Fig 3.6 Example of aromatic C-F activation shown by $(C_5Me_5)Rh(PMe_3)H_2$ 

Due to this electrochemical stumbling block, Jones¹⁴ put forward an alternative mechanism for the reaction of $(C_5Me_5)Rh(PMe_3)H_2$ and perfluoroarenes. Kinetic studies showed that by adding fluoride to the reaction an increase in the rate of dihydride consumption is seen. Also when the solvent is only 50% pyridine in benzene the rate of consumption decreases. As both pyridine and fluoride are basic, a deprotonation of the starting dihydride is suggested. The resulting nucleophilic anion can then attack the perfluoroaryl ring generating a fluoride ion (fig 3.7). The substitution would occur with the same regiochemistry as seen in an electron transfer mechanism.

Fig 3.7 Proposed anionic nucleophilic mechanism

The anion $[Cp^*Rh(PMe_3)H]^\ominus$, was prepared and was seen to react with perfluoroarenes readily at room temperature yielding identical products to that formed with the starting dihydride. The radical trap 9,10-dihydroanthracene has no effect on the

reaction but this would be the case if a caged radical process was involved. The reaction also appears to follow a product-catalysed behaviour. It is suggested that this is because the stoichiometric product, HF, reacts with starting dihydride during the reaction to produce fluoride. The presence of this fluoride increases the basicity of the reaction speeding up the first step of the proposed reaction. This would mean that once the reaction is underway, the presence of the fluoride ions would carry the cycle. However, the presence of a base can also act to sequester HF, as shown by Milstein³ in the development of $\text{Rh}(\text{PMe}_3)_4\text{H}$ as a catalyst for conversion of C_6F_6 to $\text{C}_6\text{F}_5\text{H}$ which is also thought to be initiated by electron transfer.

Applying this type of mechanism to the reaction of dihydrides **1** and **3** with C_6F_6 seems difficult due to the fact that reaction occurs rapidly at -78°C . A deprotonation of either dihydride at such a rate would surely require a very strong base of which none is added in these reactions. Also the metal anion would have to be so nucleophilic that it reacts at -78°C . In the reaction of **1** and PFD the addition of pyridine or Et_3N did not appear to have the as large an effect on the rate of reaction as seen for the $(\text{C}_5\text{Me}_5)\text{Rh}(\text{PMe}_3)\text{H}_2$ and perfluoroarenes reactions. When the reaction of **2** and PFD was performed in a 1:1 C_6D_6 :pyridine solution the starting material did disappear at a much faster rate, however the products that were formed were not the bifluoride hydride formed without the addition of base. The trouble with the suggested anionic nucleophilic mechanism is that it needs to be initiated and the reactions of **1** and **3** with C_6F_6 appear to occur without any source of this initiation.

This brings back the idea of the electron transfer process. Although the initial electron transfer is uphill in excess of 2 V, the irreversibility of both the dihydride oxidation and the perfluorocarbon reduction should be taken into consideration. The effective concentration of the radical anion is very low as it loses fluoride readily

through the loss of HF. By using the Nernst equation (fig 3.8) we can see the thermodynamics of the electron transfer can be reduced significantly.

Fig 3.8 Nernst equation

$$E = E^{\ominus} - \frac{RT}{nF} \ln Q$$

E = effective potential; E^{\ominus} = standard potential; R = Molar gas constant;
 T = temperature; n = no. of electrons; F = Faraday constant

If, $a\text{Ox}_A + b\text{Red}_B \rightarrow a'\text{Red}_A + b'\text{Ox}_B$ then,

$$Q \text{ (reaction quotient)} = \frac{[\text{Red}_A]^{a'}[\text{Ox}_B]^{b'}}{[\text{Ox}_A]^a[\text{Red}_B]^b}$$

Hence, if the concentration of the radical anion was 1×10^{-20} M then the potential difference would be altered by 0.059×20 V at room temperature, i.e. ~ 1.2 V. This would make the initial electron transfer more favourable. This is probably why hexafluorobenzene is also seen to oxidise typically electron rich complexes like $\text{Cr}(\text{C}_6\text{H}_6)_2$ and Cp_2Co , so the proposed electron transfer process cannot be discounted. Also the fact that **1** and **2** react with perfluoroalkanes, which are seen to react mostly via electron transfer pathways, supports an electron transfer process in the reactions of **1** and **2** with perfluorocarbons. The problem of initiation in the mechanism of the reactions of $(\text{C}_5\text{Me}_5)\text{Rh}(\text{PMe}_3)\text{H}_2$ and perfluoroarenes may also be solved by an electron transfer from the dihydride to the perfluoroarenes.

3.6 Fluorinations using *trans*-Ru(depe)₂(FHF)H (11)

In chapter 2 it was shown that *trans*-Ru(dmpe)₂(FHF)H, **8**, was able to transfer fluorine to organic and transition metal hydrides to give organic fluorides and transition metal fluorides. The similarities seen between reactions where the ligand is dmpe and depe led us to investigate whether bifluoride hydride **11** was capable of similar fluorinations.

3.6.1 Reaction of *trans*-Ru(depe)₂(FHF)H (11) and CH₃C(O)Cl

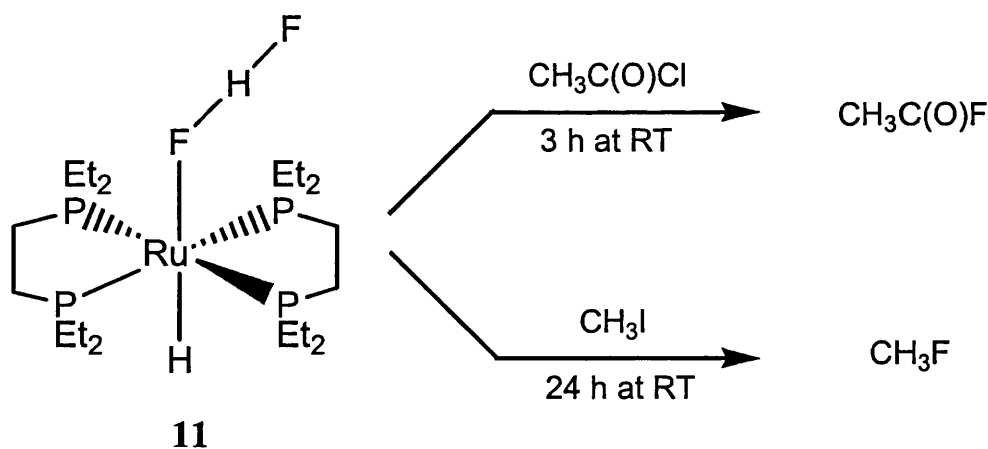
Two equivalents of CH₃C(O)Cl were added to a C₆D₆ solution of **11** in a J. Youngs resealable NMR tube. After 3 h at room temperature the pale yellow solution had darkened and the ¹⁹F NMR spectrum displayed a quartet resonance at δ 51.5 (³J_{FH} 7.3 Hz) for CH₃C(O)F as seen in the reaction of **8** and CH₃C(O)Cl (fig 2.13). The ³¹P{¹H} NMR spectrum showed that all of the bifluoride hydride had reacted to give two triplet resonances at δ 59.6 and 48.1 (*J*_{PP} 22.2 Hz), attributable to *cis*-Ru(depe)₂Cl₂ by comparison with the literature^{12b}, and a singlet resonance at δ 65.6. The ¹H NMR spectrum showed a quintet resonance for a hydride at δ -20.67 (*J*_{HP} 19.3 Hz). It is believed that the second product is *trans*-Ru(depe)₂HCl, similar to that seen in the reaction of **8** and CH₃C(O)Cl, but there is no literature evidence to confirm this.

3.6.2 Reaction of *trans*-Ru(depe)₂(FHF)H (11) and CH₃C(O)Cl

To a J. Youngs resealable NMR tube containing a C₆D₆ solution of **11**, two equivalents of CH₃I were added. After 24 h at room temperature the pale yellow

solution slowly turned dark orange and the presence of CH_3F identified by resonances in the ^{19}F and ^1H NMR spectra by resonances at δ -266.7 (q, $^2J_{\text{FH}}$ 46.5 Hz) and δ 3.64 (d, $^2J_{\text{HF}}$ 46.5 Hz) respectively. In the $^{31}\text{P}\{^1\text{H}\}$ NMR spectrum the bifluoride hydride **11** had been replaced by a pair of triplet resonances at δ 67.1 and 47.7 (J_{PP} 22.5 Hz) and a singlet resonance at δ 59.2. The ^1H NMR showed a broad multiplet resonance at δ -18.56. It is believed that the triplet peaks correspond to *cis*- $\text{Ru}(\text{depe})_2\text{I}_2$, which is reported to be dark orange in colour¹⁵, and the singlet to *trans*- $\text{Ru}(\text{depe})_2\text{HI}$ on account that the chemical shift of hydride is comparable to that seen for the reported *trans*- $\text{Ru}(\text{dmpe})_2\text{HI}$.¹⁶

Fig 3.9 Fluorinations using *trans*- $\text{Ru}(\text{depe})_2(\text{FHF})\text{H}$ (**11**)



Bifluoride hydride **11** can fluorinate small organic halides in a manner similar to bifluoride hydride **8** but at a slower rate, e.g., **8** converts $\text{CH}_3\text{C}(\text{O})\text{Cl}$ to $\text{CH}_3\text{C}(\text{O})\text{F}$ in ~10 mins at room temperature whereas the same conversion with **11** takes three hours. The larger steric bulk of the depe ligand is probably a factor in this difference. One other difference observed are the inorganic products formed in the reactions of **8** and **11** with CH_3I . Assuming our observations are correct, with dmpe as the ligand the diiodide

produced has a *trans* geometry whereas when depe is the ligand the diiodide has a *cis* geometry. This implies that although similar products are formed in both cases the reaction pathway may be slightly different.

3.7 Discussion

The results put forward in this chapter show that ruthenium dihydrides **1**, **2**, and **3** show C-F bond activation and dihydrides **4**, **5** and **6** do not. The reasons for the changes in reactivity are believed to be due to oxidation potentials of the dihydrides and the steric effects of the substituent ‘ears’ on the chelating phosphines.

Both aromatic and aliphatic C-F bond activation was seen with *cis*-Ru(depe)₂H₂, **2**. The products obtained from the reactions with C₆F₆ and PFD were *trans*-Ru(depe)₂(C₆F₅)H, **10**, and *trans*-Ru(depe)₂(FHF)H, **11**, respectively, similar to those products obtained in the same reactions with **1**. The fluoroorganic products from the reaction of **2** and PFD are the same as the reaction of **1** and PFD, and the perfluoroalkane must contain two vicinal tertiary C-F bonds for reaction with **2** to occur. This implies both dihydrides react via the same pathway. However, the rates of the reactions with **2** were much slower than those observed for **1** (chapter 2). Also, the first oxidation potential of **2** suggests that if anything these reactions should proceed more quickly. It is therefore thought that the greater steric effect of ethyl, compared with methyl, substituent ‘ears’ in the diphosphine ligand slows down these reactions. The effect of base on the **2**:PFD reaction was different to that seen for the reaction of **1**:PFD:pyridine (30x). The reasons for this are unclear. It may be possible that the larger ethyl ‘ears’ on the diphosphine ligand may be too large and sterically hinder coordination of a pyridine sized ligand, and form a cationic ruthenium monohydride species, [Ru(depe)₂H]⁺.

With *cis*-Ru(dmpm)₂H₂, **3**, where the ligand has one less carbon in the backbone than in **1**, aromatic C-F bond activation was seen under the same conditions as for **1**, at a comparable rate. Of particular interest was the orientation of the pentafluorophenyl ring in the *trans*-Ru(dmpm)₂(C₆F₅)H, **12**, which was twisted 90 ° compared to the dmpe

analogue. The smaller size of the dmpm ligand allowed the ring to sit in parallel with the diphosphine backbones which meant the Ru-C bond was also shorter than in *trans*-Ru(dmpe)₂(C₆F₅)H, **7**. C-F bond activation was seen to be selective over C-H bond activation in the reaction with C₆F₅H, but unfortunately on reaction with PFD the ³¹P{¹H} NMR spectrum only showed a range of broad lumps, which were not identified.

The other dihydrides used, *cis*-Ru(dcpe)₂H₂, **4**, *cis*-Ru(dppe)₂H₂, **5**, and *cis*-Ru(PMe₃)₄H₂, **6**, showed no reactivity towards aromatic or aliphatic C-F bond activation. The lack of reactivity of **4** contradicts the evidence provided by the cyclic voltammetry experiments, which on its own, would suggest that **4** would react more readily than the other ruthenium dihydrides. This was not the case however and showed that there were characteristics needed for this type of ruthenium dihydride to be reactive towards C-F bonds. Firstly, the dihydride must have two chelating diphosphine ligands, not four monophosphines, the substituent 'ears' on the diphosphine ligand should not be electron withdrawing, and finally the substituent 'ears' should not be too large that they hinder the reaction with their steric bulk.

Finally, it has been shown that *trans*-Ru(depe)₂(FHF)H, **11**, can act as a fluorinating agent in a similar way to that seen for *trans*-Ru(dmpe)₂(FHF)H, **8**, although the conversions of CH₃C(O)Cl and CH₃I to CH₃C(O)F and CH₃F respectively proceed at a slower rate.

3.8 Conclusions

- *cis*-Ru(depe)₂H₂, **2**, reacts with hexafluorobenzene over 3 days at room temperature to give a 4:1 ratio of *trans*-Ru(depe)₂(C₆F₅)H, **10**, and *trans*-Ru(depe)₂(FHF)H, **11**, whereas the reaction with perfluorodecalin at 85 °C yields only the bifluoride hydride complex, **11**.
- The fluoroorganic products from the reaction of **2** and PFD are the same as seen for the reaction of **1** and PFD.
- *cis*-Ru(dmpm)₂H₂, **3**, reacts with hexafluorobenzene rapidly on thawing to give *trans*-Ru(dmpm)₂(C₆F₅)H, **12**, as the only inorganic product. The reaction of **3** and pentafluorobenzene reacts over 2 h at room temperature to give *trans*-Ru(dmpm)₂(*p*-C₆F₄H)H, **13**. No bifluoride hydride species is formed in either reaction.
- Cyclic voltammetry shows the order of reducing ability for the dihydrides is **4** > **3** > **2** > **1** > **6** > **5**. The ability for C-F cleavage however also depends on the size of the substituent 'ears' on the phosphine ligand.
- *trans*-Ru(depe)₂(FHF)H can act as a fluorinating agent, converting CH₃I and CH₃C(O)Cl to CH₃F and CH₃C(O)F respectively.

References

1. Cronin, L.; Nicasio, M. C.; Perutz, R. N.; Peters, R. G.; Roddick, D. M.; Whittlesey, M. K. *J. Am. Chem. Soc.*, **1995**, *117*, 10047.
2. Whittlesey, M. K.; Perutz, R. N.; Moore, M. H. *Chem. Commun.*, **1996**, 787;
Whittlesey, M. K.; Perutz, R. N.; Greener, B.; Moore, M. H. *Chem. Commun.*, **1997**, 187.
3. Aizenberg, M.; Milstein, D. *J. Am. Chem. Soc.*, **1995**, *117*, 8674.
4. Jasim, N. A.; Perutz, R. N. *J. Am. Chem. Soc.*, **2000**, *122*, 8685.
5. Bennett, B. K.; Harrison, R. G.; Richmond, T. G. *J. Am. Chem. Soc.*, **1994**, *116*, 11165.
6. Christe, K. O.; Wilson, W. W. *J. Fluorine Chem.*, **1990**, *46*, 339.
7. Hartwig, J. F.; Andersen, R. A.; Bergman, R. G. *Organometallics*, **1991**, *10*, 1710.
8. Nicasio, M. C.; Perutz, R. N.; Walton, P. H. *Organometallics*, **1997**, *16*, 1410.
9. Wong, W. K.; Chiu, K. W.; Wilkinson, G.; Howes, A. J.; Motevalli, M.;
Hursthouse, M. B. *Polyhedron*, **1985**, *4*, 603.
10. Other ruthenium dmpm complexes reported on the Cambridge Crystallographic Database, (a) $[\text{Ru}_3(\mu\text{-dmpm})_3(\text{dmpm})_3]\text{Cl}_6\text{C}_7\text{H}_8\cdot\text{C}_2\text{H}_6$ and $[\text{RuCl}_2(\text{dmpm})_2]_4$; van Rooyen, P. H.; Ashworth, T. V.; Hietkamp, S.; Sparrow, N. *Acta Cryst., C (Cr. Str. Comm.)*, **1992**, *48*, 545, (b) $[\text{RuCp}(\text{PPh}_3)(\text{dmpm})]\text{Cl}$; Mague, J. T.; Balakrishna, M. S. *Polyhedron*, **1996**, *15*, 4259.
11. Olah, G. A.; Mo, Y. K. *J. Org. Chem.*, **1973**, *38(18)*, 3212.
12. Dihydride preparations. (a) **4**, Nolan, S. P.; Belderrain, T. D.; Grubbs, R. H. *Organometallics*, **1997**, *16*, 5569; (b) **5**, Bautista, M. T.; Cappellani, E. P.; Drouin, S. D.; Morris, R. H.; Schweitzer, C. T.; Sella, A.; Zubkowski, J. *J. Am. Chem.*

- Soc.*, **1991**, *113*, 4876; (c) **6**, Hartwig, J. F.; Andersen, R. A.; Bergman, R. G. *J. Am. Chem. Soc.*, **1991**, *113*, 6492.
13. Marsella, J. A.; Gilicinski, A. G.; Coughlin, A. M.; Pez, G. P. *J. Org. Chem.*, **1992**, *57*, 2856.
14. Edelbach, B. L.; Jones, W. D. *J. Am. Chem. Soc.*, **1997**, *119*, 7734.
15. Chatt, J.; Hayter, R. G. *J. Chem. Soc.*, **1961**, 896.
16. Kaplan, A. W.; Bergman, R. G.; *Organometallics*, **1998**, *17*, 5072.

Chapter 4

Reactions of ruthenium dihydrides with perfluoroalkenes

4 Reactions of $\text{RuH}_2(\text{PP})_2$ with perfluoroalkenes

Following the reactivity of *cis*- $\text{Ru}(\text{dmpe})_2\text{H}_2$, **1**, towards fluoroaromatics, reported by Perutz et al.¹, in which aromatic C-F bonds are cleaved readily, and the work described in chapter 2 on the reactivity of **1** towards perfluoroalkanes, where the activation of sp^3 C-F bonds is seen to be more difficult, we decided to look at the possibility of cleaving C-F bonds in perfluoroalkenes. In this chapter we discuss the reactions of *cis*- $\text{Ru}(\text{dmpe})_2\text{H}_2$, **1**, and *cis*- $\text{Ru}(\text{dcpe})_2\text{H}_2$, **4**, towards two perfluoroalkenes, $\text{CF}_3\text{CF}=\text{CF}_2$ and $(\text{CF}_3)_2\text{C}=\text{CFCF}_2\text{CF}_3$.

A general introduction to the organic chemistry of perfluoroalkenes is outlined below, which helps to explain the reactivity that is seen with the dihydride species, followed by an overview of reactions reported of metal complexes with perfluoroalkenes.

4.1 Introduction

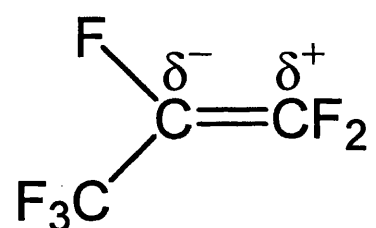
In contrast to saturated perfluorocarbons, the chemistry of perfluoroalkenes is plentiful. Substitution of hydrogen by fluorine in an alkene leads to an increased reactivity for many processes. For example, the heat of polymerisation for tetrafluoroethene is around 71.4 kJmol^{-1} higher than that of ethene.²

Observations like this have been attributed to destabilisation of the π system by electron pairs on the vinylic fluorines, increasing reactivity, even though the C-F bond strength increases on changing from a saturated system to an alkene. That carbon increases in electronegativity in the series $\text{sp}^3 > \text{sp}^2 > \text{sp}$ implies that C-F bond strengths would increase in unsaturated systems.³ Therefore, it is unsurprising that the chemistry

of such perfluoroalkenes is rich. In this chapter we have used perfluoropropene (PFP) and known dimers of this as reagents so the main focus will be on these perfluoroalkenes in this introduction.

PFP was one of the earliest perfluorocarbons produced and was prepared commercially by low-pressure pyrolysis of tetrafluoroethene as far back as 1963.⁴ The replacement of one of the vinylic fluorines in tetrafluoroethene by a CF₃ group not only increases stability of the alkene but also imparts a polarity on the group (fig. 4.1).

Fig 4.1 Polarity in perfluoropropene



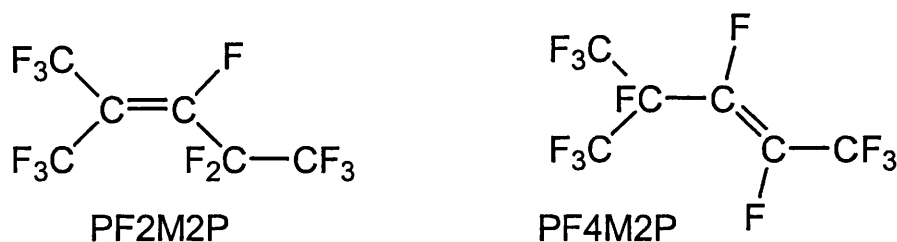
This is due to back bonding effect of the vinylic fluorines, which outweighs their inductive effect and the inductive and hyperconjugative effects of the CF₃ group.³

4.1.1 Nucleophilic attack on perfluoroalkenes

The effect of the polarity can be seen in the nucleophilic attack on the double bond. Perfluoroalkenes are more susceptible to this than hydrocarbon analogues as the double bond is relatively electron poor. In particular attack by metal fluorides^{5,6,7} has been shown to give dimers and trimers of PFP with a mechanism which involves the formation of an intermediate perfluorocarbanion. The dimers formed, perfluoro-4-

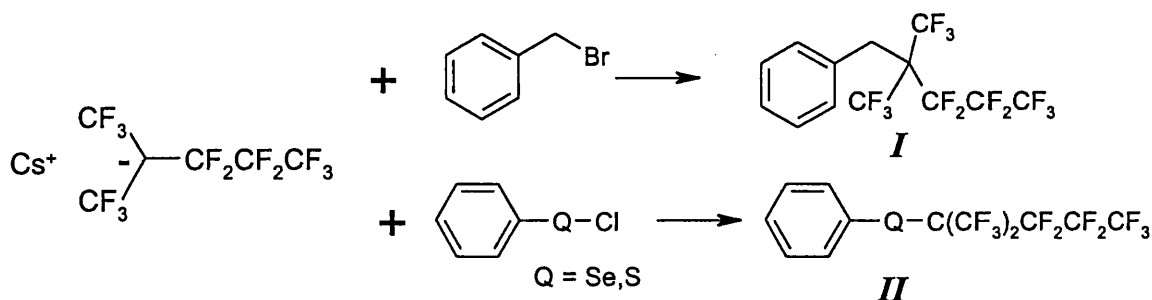
methyl-2-pentene, (PF4M2P), the kinetic product, and perfluoro-2-methyl-2-pentene, (PF2M2P) from thermodynamic isomerisation of the kinetic product (fig. 4.2),⁸ indicate that the nucleophilic attack of fluoride and perfluorocarbanion is directed towards the CF₂ end of the double bond.

Fig 4.2 Dimers of PFP



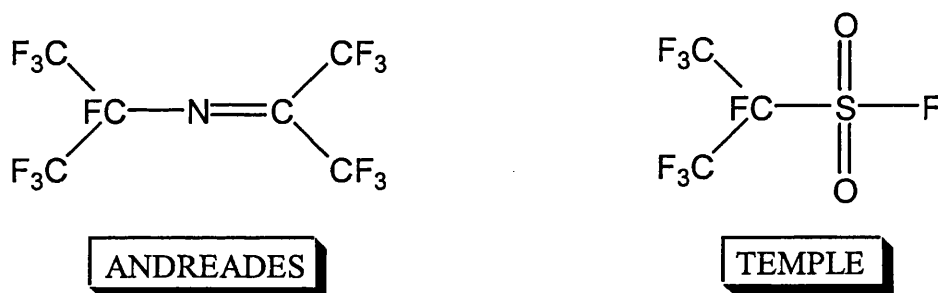
The perfluorocarbanion formed in this reaction and other perfluorocarbanions have been isolated as tris(dimethylamino)sulfonium salts⁹ and caesium salts.^{10,11} These have been used to introduce perfluoroalkyl moieties into organic and inorganic molecules. For example, Chambers¹⁰ has prepared a perfluoroalkylated methyl benzene (*I*), while Suzuki¹² has reported the preparation of fluorinated thio- and selenoethers (*II*) (fig 4.3).

Fig 4.3 Reactions using perfluorocarbanion



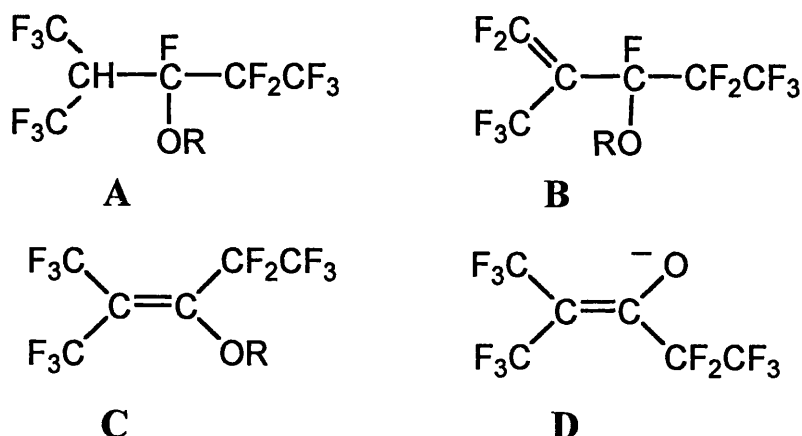
The perfluorocarbanion is also thought to be a key intermediate in the reactions of PFP with nitrosyl fluoride¹³ and sulfuryl fluoride.¹⁴ Initial attack by fluoride forms the carbanion, which then reacts rapidly via radical pathways to give a perfluoroazaalkene in the case of nitrosyl fluoride, and a perfluorosulfonyl fluoride on reaction with sulfuryl fluoride (fig 4.4).

Fig 4.4 Products from reactions of PFP with nitrosyl fluoride and sulfuryl fluoride



The susceptibility of PFP and dimers to nucleophilic attack has also led to much work being done with differing nucleophiles. Ishikawa⁸ has shown that in the presence of triethylamine, alcohols and phenols react with PF2M2P via nucleophilic attack to give a mixture of addition and substitution products. They include fluorinated ethers (A,B), enols (C) and a perfluoroenolate (D) (fig. 4.5).

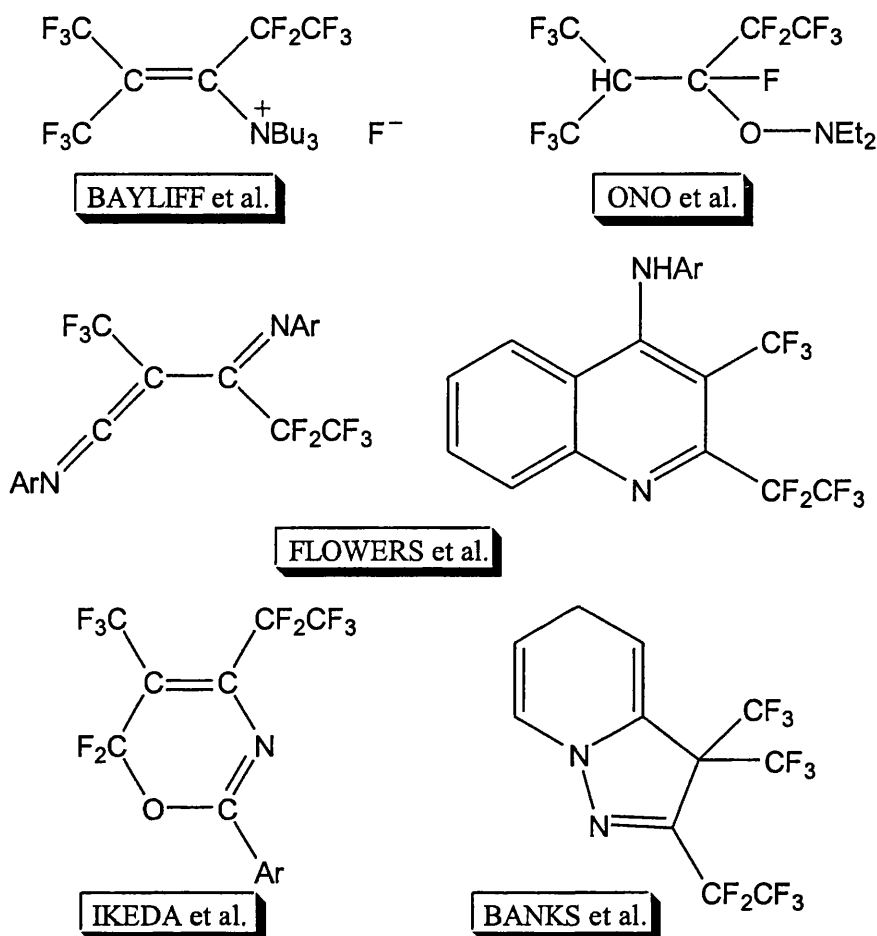
Fig 4.5 Products of Ishikawa reactions



Many O- and N- nucleophiles have been shown to react with perfluoroalkenes, yielding new fluorine containing molecules. Figure 4.6 shows a few of the products that have been reported from such reactions.^{10,15,16,17,18,19}

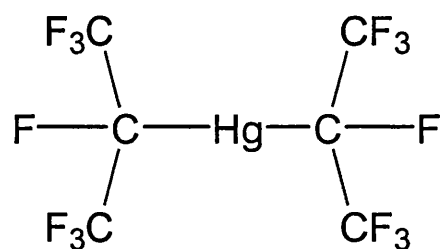
The reaction Ono reports between PF₂M₂P and HONe_t shows that there is a preference for the perfluoroalkene to react with an oxygen nucleophile, therefore forming the adduct shown in fig. 4.6. It can also be seen that the perfluoroalkyl moieties can be incorporated into heterocycles.

This is desirable as the presence of perfluoroalkyl moieties in such molecules can impart profound changes on physical, chemical and biological properties as shown in chapter 1. The nucleophilic attack on these perfluoroalkenes is a key reaction for this introduction.

Fig. 4.6 Fluorine containing molecules generated by reactions with perfluoroalkenes

4.1.2 Electrophilic attack on perfluoroalkenes.

Although electrophilic attack on hydrocarbon alkenes is common, the analogous attack on a fluorocarbon π system is relatively rare. However treatment of perfluoropropene with HgF_2 in an HF solution at 85°C results in electrophilic attack by a mercury cation, which yields bisheptafluoroisopropylmercury (fig. 4.7), via an intermediate cyclic mercurinium ion.²⁰

Fig 4.7 Bisheptafluoroisopropylmercury

In general though, perfluoroalkenes are more resistant to attack by reagents classed as electrophilic in hydrocarbon chemistry, in particular hydrogen halides.

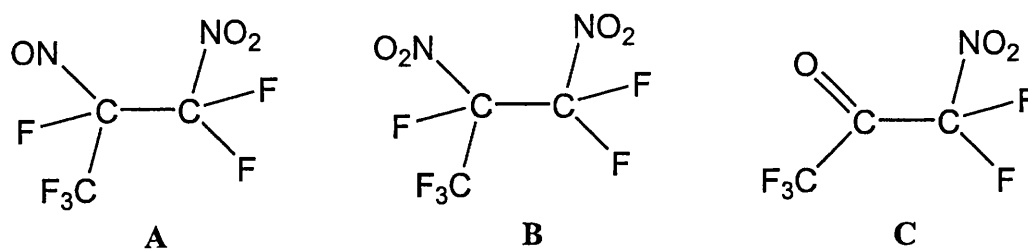
4.1.3 Free radical chemistry of perfluoroalkenes

Free radical attack on the fluorocarbon double bond proceeds with ease with the polarity of unsymmetrical perfluoroalkenes influencing the direction of attack. A study of radical addition to PFP shows some interesting properties.³ The more reactive the radical the less selective it should be; however, it is seen to be more discriminative towards the CF_2 site. Also as the alkene is more susceptible to nucleophilic attack, it is expected that the more nucleophilic radical will react quicker; however, the rate of reaction seems more based on the polarity of the free radical. In PFP there is little difference in the stability of the two intermediate radicals that can be formed, so polarity of the free radical becomes important in determining the site of attack. Also as PFP is highly sensitive to nucleophilic attack at the CF_2 site the more nucleophilic the free radical the more it is likely to attack the CF_2 site.

Free radical reactions of PFP with nitric oxide have been reported by Park²¹ and Bagley.²² Isolated compounds included hexafluoro-1-nitro-2-nitrosopropane (**A**),

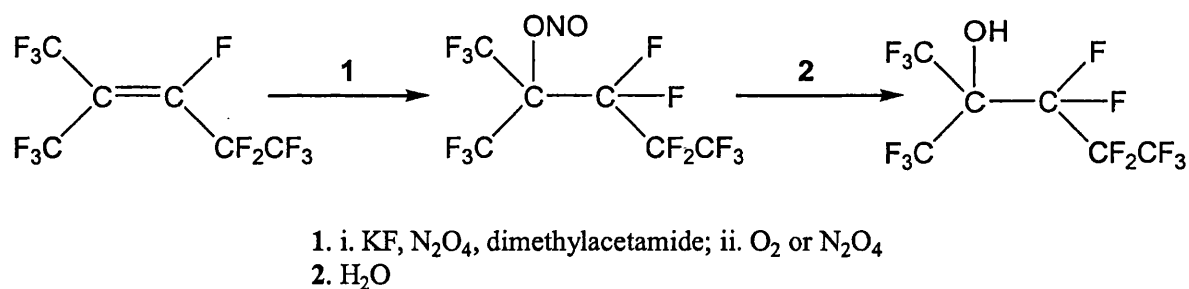
hexafluoro-1,2-dinitropropane (**B**) and pentafluoronitroacetone (**C**), depending upon the reaction conditions employed (fig. 4.8).

Fig 4.8 Products reported by Park and Bagley



More recently, Scherer²³ has used perfluoro-2-methyl-2-pentene with N_2O_4 to give a perfluoronitrite. This was shown to hydrolyse to perfluoro-2-methyl-2-pentanol and provided a simple route to a perfluorinated tertiary alcohol (fig. 4.9).

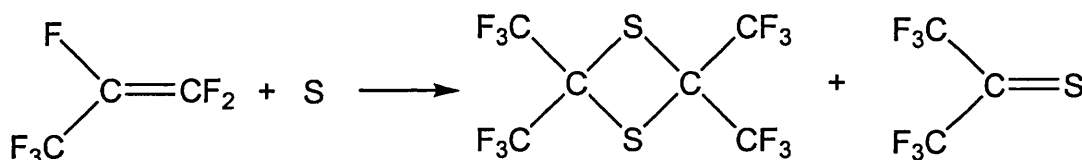
Fig 4.9 Formation of perfluoro-2-methyl-2-pentanol



4.1.4 Reaction by rearrangement

Martin²⁴ reported a reaction where perfluoropropene and sulfur vapour react at 425 °C in the presence of activated carbon. The result of this was the formation of hexafluorothioacetone as a monomer and as a dimer (fig 4.10).

Fig 4.10 Reaction of perfluoropropene and sulfur vapour



It is suggested that the reaction proceeds by the rearrangement of the alkene to a perfluorocarbene, which then reacts with the sulfur vapour. However, it is more likely that the sulfur adds across the double bond to give an episulfide, followed by migration of fluorine to give the product.

4.1.5 Reaction with metal complexes

In comparison, again, to saturated perfluorocarbons, perfluoroalkenes have been widely investigated for their interactions with metal centres.

i) Coordination of perfluoroalkenes

Stone et al. showed that using neutral transition metal carbonyl complexes the reaction with perfluoroalkenes resulted in coordination to the metal centre of the

fluorinated π system. Elimination of a carbonyl ligand led to occupation of the vacant site by a perfluoroalkene. They synthesised complexes such as $(\text{cod})\text{Ni}(\text{CF}_3\text{CF}=\text{CF}_2)^{25}$, where the cyclooctadiene can be replaced on reaction with 2 equivalents of triphenylphosphine or triethylphosphine. They suggest that these complexes are Ni(II) complexes, as the PFP is not replaced. Use of tetrafluoroethene in these complexes leads to the formation of octafluoronickelacyclopentane complexes (fig. 4.11). Other ligand systems were used to try and alter the properties, including tridentate systems²⁶ but the same type of products were seen even if the coordination sphere had increased.

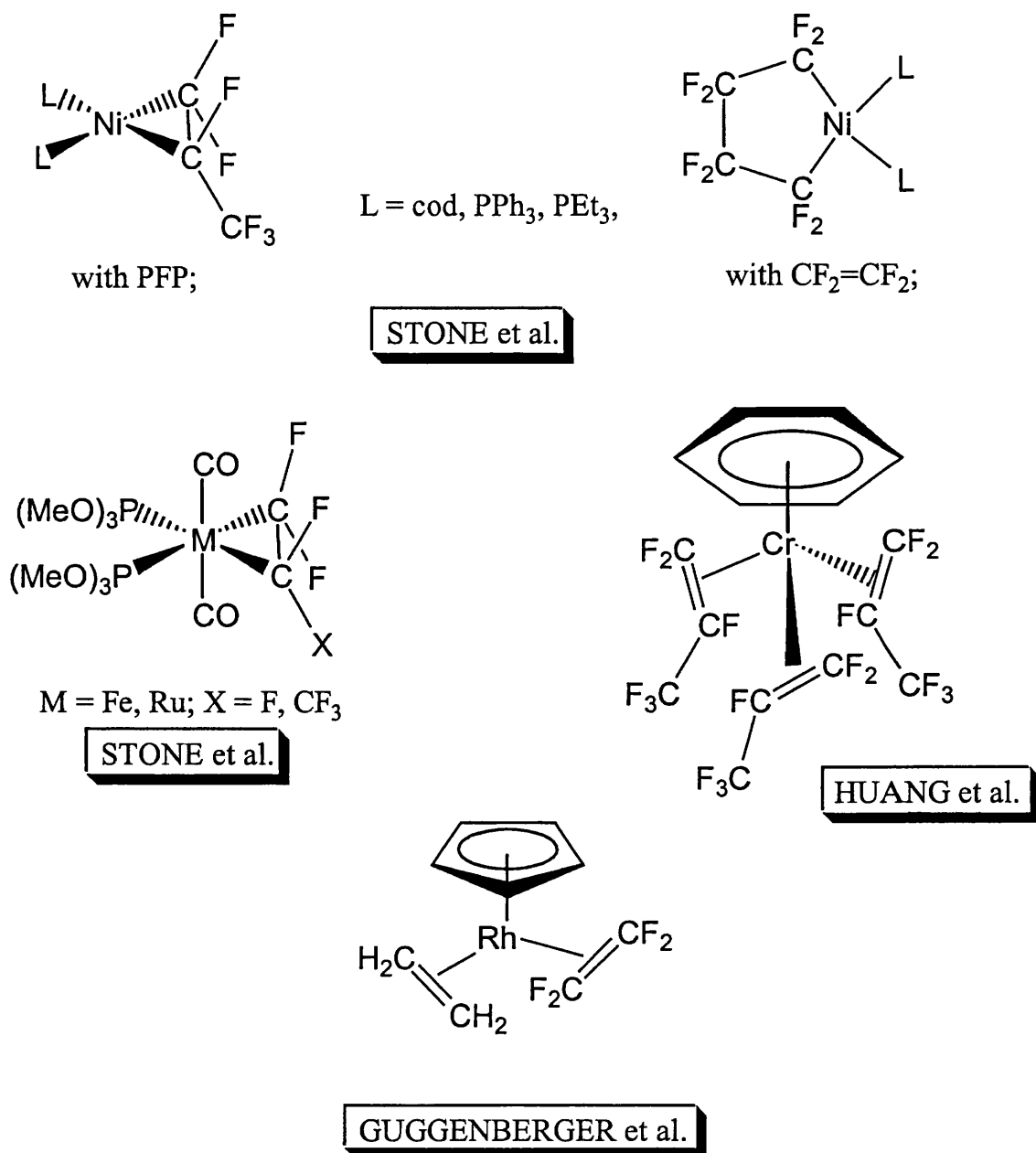
Similar activity to that seen in the case of the nickel compounds was observed for $\text{M}(\text{CO})_3(\text{P}(\text{OMe})_3)_2$ ($\text{M} = \text{Fe}, \text{Ru}$),²⁷ with the formation of $\text{M}(\text{CO})_2(\text{P}(\text{OMe})_3)_2(\text{CF}_3\text{CF}=\text{CF}_2)$. However for reactions with tetrafluoroethene, there is no evidence for a five-membered metallacycle, and in fact, the product appears to have a three-membered ring (Fig 4.11).

Huang²⁸ reported that $(\eta^6\text{-C}_6\text{H}_6)_2\text{Cr}$ catalyses the dimerisation and trimerisation of PFP. The proposed reaction scheme involves the loss of a coordinated benzene and coordination of two or three PFP molecules to give an intermediate $(\eta^6\text{-C}_6\text{H}_6)\text{Cr}(\text{CF}_3\text{CF}=\text{CF}_2)_x$ complex ($x = 2, 3$). This then reductively eliminates the coordinated perfluoroalkenes as dimers or trimers. This intermediate species has not been isolated, but is the only example of more than two perfluoroalkenes being coordinated to a metal centre.

Probably the most interesting complex involving the coordination of C_2F_4 is $\text{CpRh}(\text{C}_2\text{H}_4)(\text{C}_2\text{F}_4)$.²⁹ This complex has been used as a paradigm for illustrating the differences between the bonding of ethene and tetrafluoroethene, in particular, showing that the activation barrier for propeller rotation is much higher for the fluoroalkene,

suggesting the proposed tendency for the $\text{Rh}(\text{C}_2\text{F}_4)$ moiety to be more like a metallocyclopropane in character.

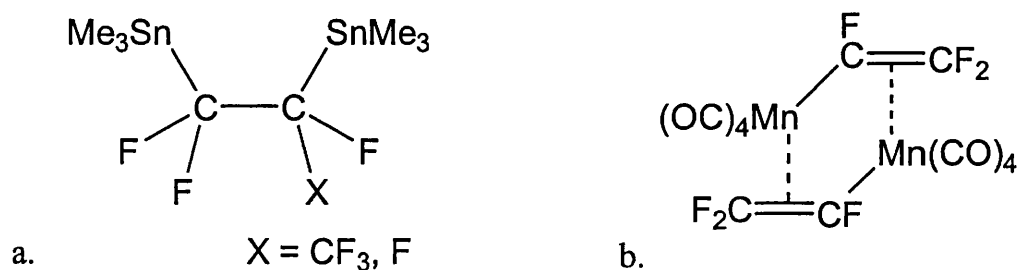
Fig 4.11 Transition metal perfluoroalkene complexes



ii) Activation of perfluoroalkenes

One of the earliest examples involved the reaction of Sn_2Me_6 with tetrafluoroethene or PFP.³⁰ On heating in a sealed silica tube at 70 °C under ultraviolet radiation, the perfluoroalkene inserts into the Sn-Sn bond to give 1,2-bis(trimethylstannyl)perfluoroethane or -propane (fig. 4.12a). Similarly, the reaction of the tetrafluoroethene with $\text{Me}_3\text{Sn-Mn}(\text{CO})_5$ leads to alkene insertion into the Mn-Sn bond to form $\text{Me}_3\text{SnCF}_2\text{CF}_2\text{Mn}(\text{CO})_5$. Subsequent C-F cleavage yields the dimer $[(\text{CO})_4\text{Mn-CF}=\text{CF}_2]_2$, where the manganese is coordinated to the π system of the fluoroalkene moiety (fig.4.12b). This rearrangement is thermodynamically driven by the formation of Me_3SnF .

Fig 4.12 C-F bond cleavage products

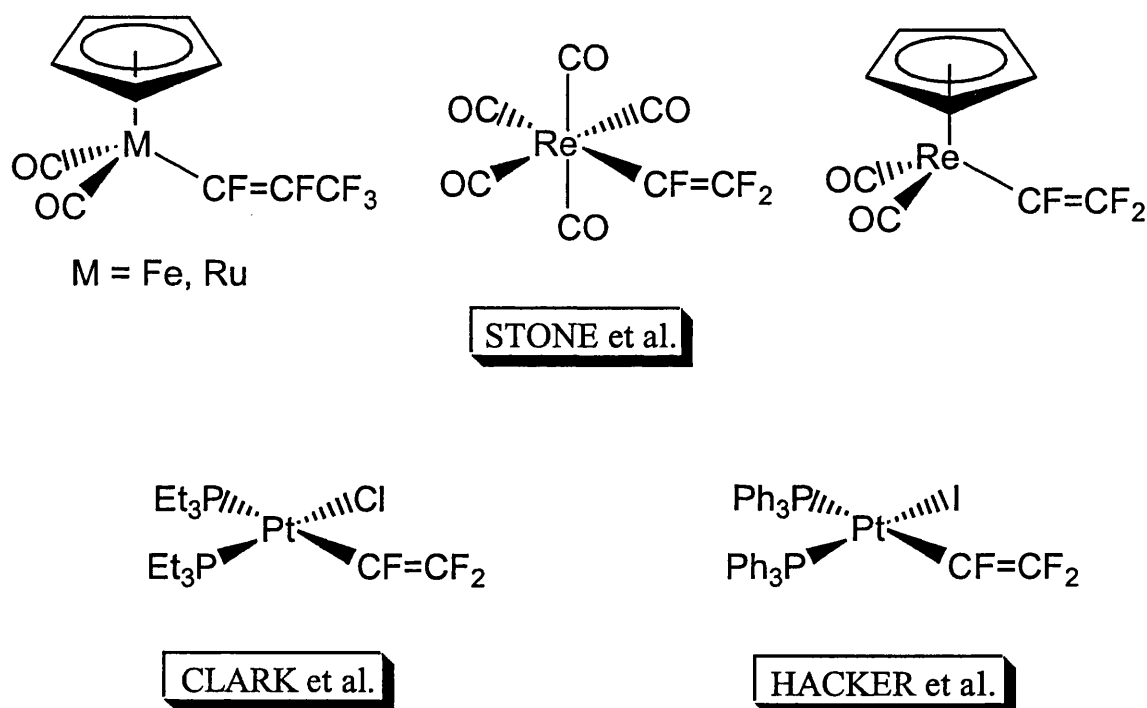


The nucleophilic attack of silver fluoride on perfluoroalkenes has also been reported.³¹ This yields perfluoroalkyl silver complexes, which are relatively stable compared to hydrocarbon analogues. These were found to thermally decompose to perfluoroalkyl radicals, which are useful as synthetic intermediates.

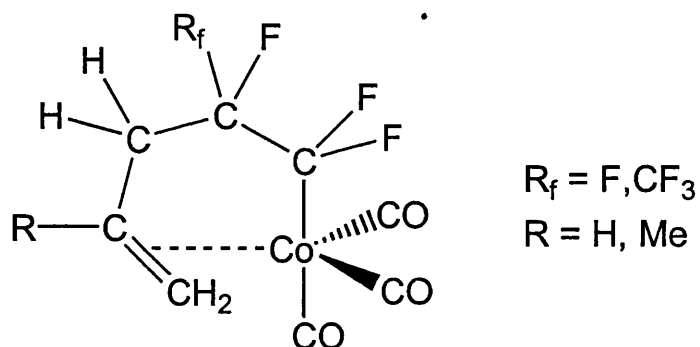
Nucleophilic attack by anionic transition metal complexes has also been seen to give perfluorovinyl complexes. Stone^{32,33} showed that $[\text{CpM}(\text{CO})_2]_2$ ($\text{M} = \text{Fe}, \text{Ru}$) treated with sodium amalgam to give $[\text{CpM}(\text{CO})_2]^-$, acts as a nucleophile for attack at

the CF_2 site of PFP to give fluorocarbon complexes $\text{CpM}(\text{CO})_2\text{CF}=\text{CFCF}_3$. This product and other examples are shown in fig. 4.13.³⁴

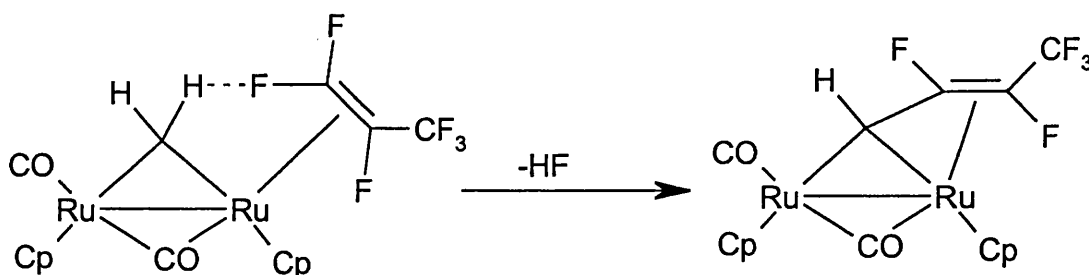
Fig 4.13 Perfluorovinyl complexes



A very different reaction with perfluoroalkenes is seen with $(\eta^3\text{-C}_3\text{H}_5)\text{Co}(\text{CO})_3$.³⁵ Loss of a carbonyl ligand allows the initial coordination of the perfluoroalkene, followed by double bond insertion into the cobalt-carbon bond to form complexes where the fluorocarbon moiety is attached directly to the cobalt centre (fig. 4.14).

Fig 4.14 Product of perfluoroalkene insertion into Co-C bond

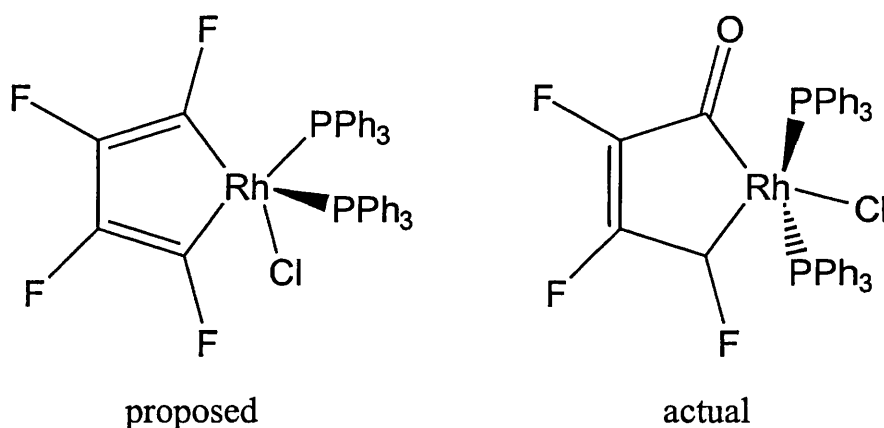
C-F bond activation under very mild conditions is seen in a coordinated perfluoroalkene attached to a diruthenium complex³⁶ (fig 4.15). The complex, $[\text{Cp}_2\text{Ru}_2(\text{CO})(\text{MeCN})(\mu\text{-CH}_2)(\mu\text{-CO})]$, loses acetonitrile and perfluoropropene fills the vacant site. Interaction between a vinylic fluorine and a hydrogen on the methylene bridge leads to elimination of HF and the formation of a carbon-carbon bond.

Fig 4.15 C-F bond activation of coordinated PFP

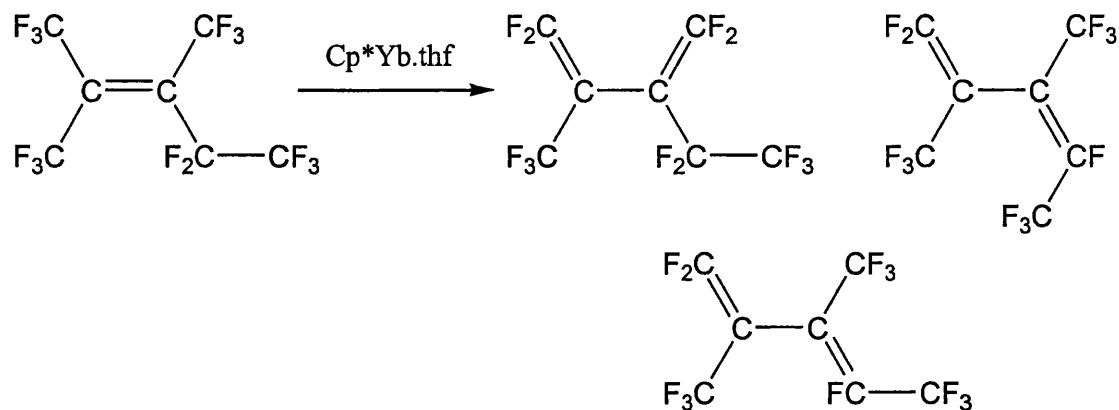
Wilkinson's catalyst, $\text{Rh}(\text{PPh}_3)_3\text{Cl}$, has also been reported to show activity with perfluoroalkenes. In the reaction with hexafluorobutadiene, two C-F bonds are broken en route to the product.³⁷ When heated in benzene with hexafluorobutadiene, the rhodium complex was originally reported to have lost a PPh_3 group and two fluorines. A proposed product had the rhodium as part of a tetrafluorometallocyclopentadiene ring

with two phosphines and a chloride. Reinvestigation of this reaction showed that the product actually contained a tetrafluorometallocyclopentenone moiety (fig. 4.16). The ketone was postulated to come about from hydrolysis, since repeating the reaction using rigorously dry conditions yielded the expected hexafluororhodacyclopentene species. Thus in the steps to form the ketone, two C-F bonds are broken on the carbon α to the metal. This reaction emphasises the susceptibility of coordinated perfluoroalkenes to hydrolysis.

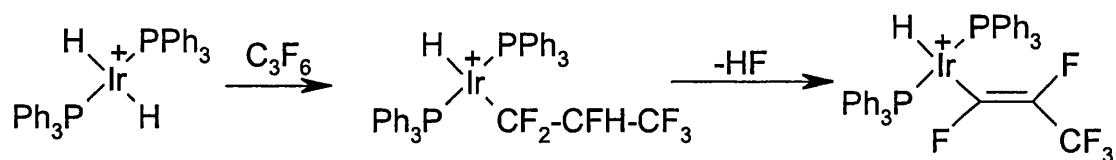
Fig 4.16 Proposed and actual product of $\text{Rh}(\text{PPh}_3)_3\text{Cl}$ and hexafluorobutadiene



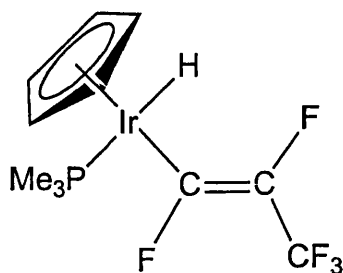
The divalent lanthanoids $\text{MCp}^*_2\cdot\text{L}$ ($\text{M} = \text{Yb}, \text{Eu}, \text{Sm}$; $\text{L} = \text{THF}$ or Et_2O) have been reported to abstract fluorine from perfluoroalkenes to form the monofluoride complexes $\text{MCp}^*_2\text{F}\cdot\text{L}$.³⁸ These reactions occur under mild conditions and the mechanism is thought to be analogous to the halide extraction seen in the reaction of these complexes with other haloalkanes, i.e. via a radical abstraction. The resultant fluoroorganic products are usually a series of perfluorodiene isomers (fig. 4.17).

Fig 4.17 C-F activation with a divalent lanthanoid complex*iii) Activation by metal hydrides*

The activity of a transition metal hydride with a perfluoroalkene was first reported in 1989.³⁹ The heterogeneous reaction between $[(\text{Ph}_3\text{P})_2\text{IrH}_2]_3[\text{PW}_{12}\text{O}_{40}]$ and PFP also gives an example of a carbon-fluorine bond being broken (fig 4.18). The alkene is inserted into the Ir-H bond and subsequent elimination of HF leads to a coordinated perfluoroalkene, similar to that seen for the nucleophilic addition of Stone's ruthenium anion.

Fig 4.18 C-F activation by iridium hydride

A very similar product (fig. 4.19) was observed by Peterson et al.⁴⁰ in the reaction of $\text{Cp}^*(\text{PMe}_3)\text{Ir}(\text{Li})(\text{H})$ with perfluoropropene.

Fig 4.19 Product of reaction of $\text{Cp}^*(\text{PMe}_3)\text{Ir}(\text{Li})(\text{H})$ with perfluoropropene.

This again proceeds under mild conditions with insertion into the Ir-Li bond. The formation of LiF is the driving force behind this and a perfluorovinyl complex is the result.

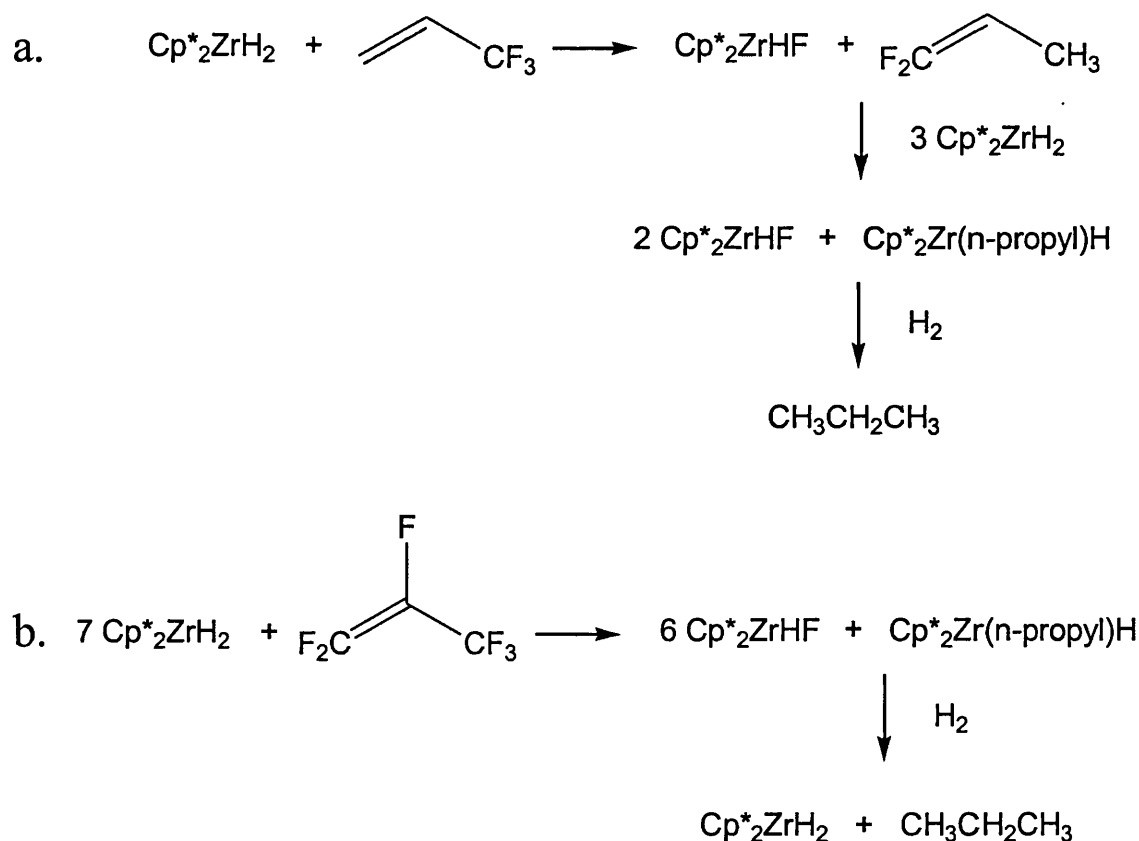
The most recent and the most remarkable activity seen of transition metals with perfluoropropene has been reported by Jones.⁴¹ As mentioned earlier in chapter 1, the complex $\text{Cp}^*_2\text{ZrH}_2$ has been shown to activate aliphatic carbon-fluorine bonds, e.g. the conversion of 1-fluorohexane to hexane and fluorocyclohexane to hexane. In each case Cp^*_2ZrHF was found to be the metallic product. The same dihydride also showed increased reactivity with fluorinated alkenes. When 3,3,3-trifluoropropene is treated with one equivalent of $\text{Cp}^*_2\text{ZrH}_2$, a C-F bond is cleaved resulting in 1,1-difluoropropene and Cp^*_2ZrHF . However, the use of four equivalents of the dihydride leads to complete defluorination of the alkene in less than ten minutes at room temperature (fig 4.20a). On addition of H_2 to the zirconium propyl hydride complex formed from the defluorinated alkene, propane is released.

The reaction of $\text{Cp}^*_2\text{ZrH}_2$ with perfluoropropene follows along a similar route. Treatment with one equivalent of the dihydride leads to the selectively defluorinated product, *trans*- $\text{CF}_3\text{CF}=\text{CFH}$. Again though, treatment with 7 equivalents of the dihydride leads to the complete defluorination of the perfluoroalkene and formation of

the zirconium propyl hydride after 15 minutes at room temperature. Addition of H₂ to the reaction at this point yields propane (fig 4.20b).

The driving force behind these reactions is the formation of the strong Zr-F bond and at the moment it is suggested that a bond metathesis pathway is the most likely mechanism.

Fig 4.20 Reactions of Cp*₂ZrH₂ and perfluoropropene



The reactions shown above show that certain transition metal hydrides can readily activate C-F bonds in perfluoroalkenes. We have shown previously that both *cis*-Ru(dmpe)₂H₂, **1**, and *cis*-Ru(depe)₂H₂, **2**, can activate aromatic and aliphatic C-F bonds. We therefore set out to see whether C-F activation would occur in perfluoroalkenes with

both **1** and **2** and also *cis*-Ru(dcpe)₂H₂, **4**. The latter dihydride was chosen as the different size of the substituent ‘ears’ on the chelating diphosphine provides a series of dihydrides with increasing stericity, a property that was seen to be important in the reactions of **1**, **2** and **4** with both hexafluorobenzene and perfluorodecalin.

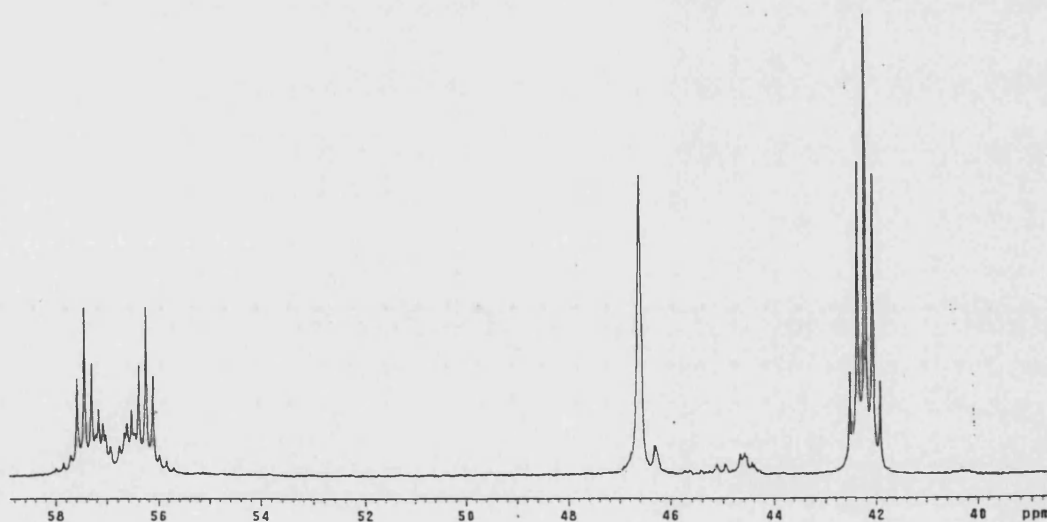
4.2 Results

4.2.1 Reaction of *cis*-Ru(dmpe)₂H₂ (**1**) and perfluoroalkenes

4.2.1.1 Reaction with perfluoro-2-methyl-2-pentene (PF2M2P)

When a C₆D₆ solution of *cis*-Ru(dmpe)₂H₂, **1** was treated with 1 equivalent of PF2M2P at room temperature in a J. Youngs resealable NMR tube, the colourless solution immediately turned yellow. The ³¹P{¹H} NMR spectrum showed that **1** had completely reacted with the formation of two ruthenium containing products. A singlet at δ 46.6 was characteristic of the *trans*-bifluoride hydride complex **8**, seen in the reaction of **1** with perfluorodecalin. The second product displayed two resonances, a quintet at δ 42.2 and a complex second pattern at δ 56.8 (fig 4.21).

Fig. 4.21 ³¹P{¹H} NMR spectrum of reaction 4. (C₆D₆, 400 MHz)

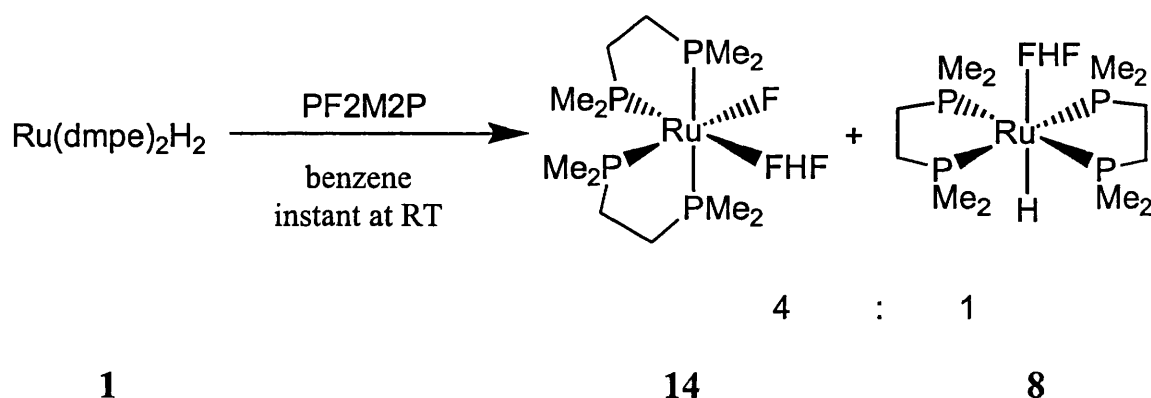


³¹P-³¹P COSY NMR spectroscopy showed that these two resonances were coupled to each other. The complexity of the ³¹P{¹H} NMR spectrum was inconsistent with the formation of a *trans* product and can only arise from a product with a *cis*

geometry. The ^1H NMR spectrum showed a broadened doublet at δ 14.2 ($J_{\text{HF}} = 344.0$ Hz) and a corresponding doublet in the ^{19}F NMR spectrum at δ -175.2, which indicated the presence of HF. The ^{19}F NMR spectrum also showed two broad multiplet signals at δ -343 and -362. More importantly the ^1H NMR spectrum showed no hydride resonances for this new product.

The NMR spectra indicated that the bifluoride fluoride complex *cis*- $\text{Ru}(\text{dmpe})_2\text{F}(\text{F}.. \text{HF})$, **14**, had been formed. This was later confirmed by X-ray crystallography. Interpretation of the NMR spectra of **14** are described in detail below, while the X-ray structure is described in section (ii).

Reaction 4.1

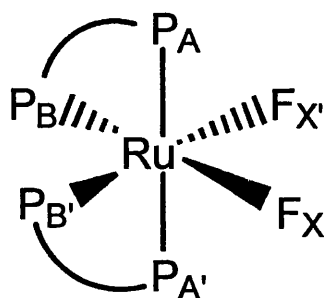


(i) Interpretation of NMR spectra

The two different resonances in the $^{31}\text{P}\{^1\text{H}\}$ NMR spectrum arise from the two different sets of phosphorus nuclei (fig. 4.22). The axial phosphorus signal appears as an apparent quintet at δ 42.2 due to J_{PP} and J_{PF} being similar, around 22-23 Hz. The equatorial phosphorus signal at δ 56.8 is more complicated and coupling constants for the rest of the molecule were derived from a simulation using the *gNMR* simulation

software.⁴² In the simulation, the ‘bare’ difluoride, *cis*-Ru(dmpe)₂F₂, was used to establish coupling constants as we believe the Ru-F...HF interaction in solution is only

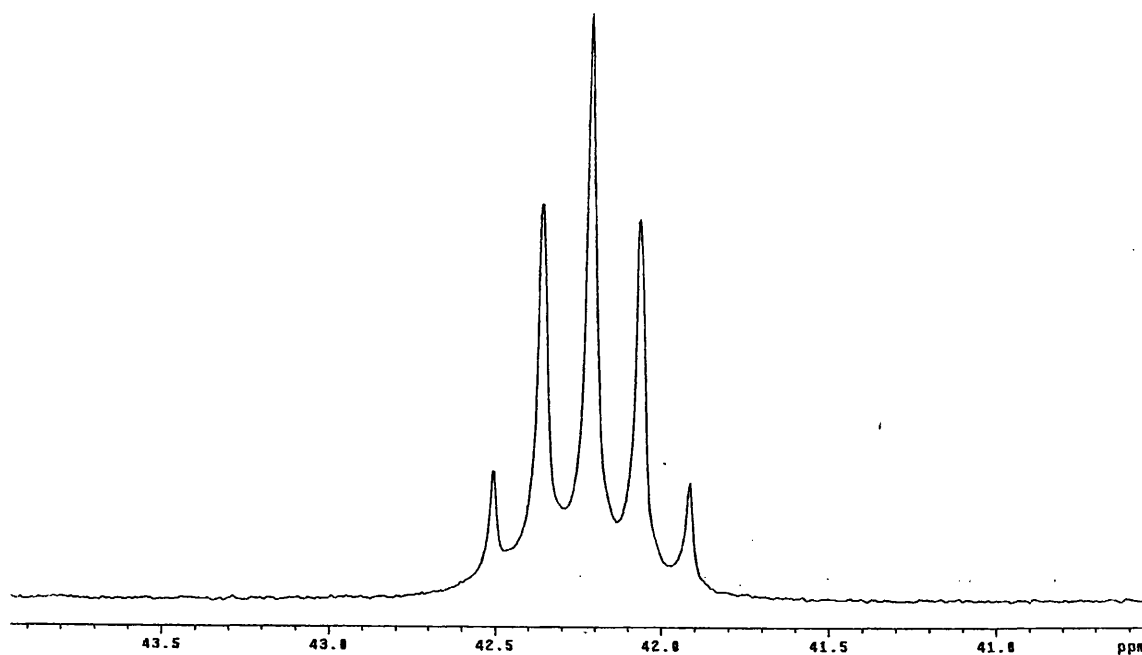
Fig 4.22 Spin system of *cis*-Ru(dmpe)₂F₂



weak on the grounds that the HF resonance only appears as a doublet in the ¹H NMR spectrum and no triplet is seen as for *trans*-Ru(dmpe)₂(FHF)H, **8**, where a strong interaction is known (chap. 2). However, in the solid state the interaction is much stronger (see later). Figure 4.23 shows the comparison between the experimental and simulated spectra from which we have obtained coupling constants for the *cis*-Ru(dmpe)₂F₂ molecule (table 4.1). Clearly the two metal bound fluorines in **14** are chemically and magnetically inequivalent but in the modelled *cis*-Ru(dmpe)₂F₂ complex they are only magnetically inequivalent. This will be discussed further at the end of this section. (p. 156)

Fig. 4.23 Spectra and coupling constants obtained from simulation of spectra using *gNMR* simulation software.

i.a Experimental $^{31}\text{P}\{^1\text{H}\}$ NMR spectra (δ 42.2) (400 MHz)



i.b Simulated $^{31}\text{P}\{^1\text{H}\}$ NMR spectra (δ 42.2) (400 MHz)

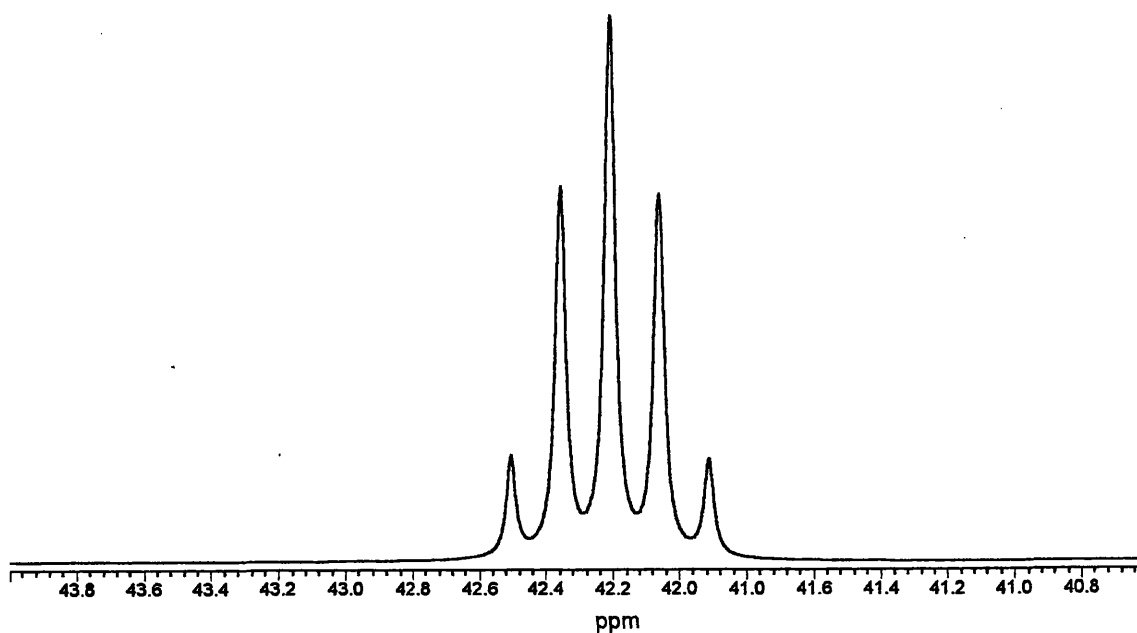
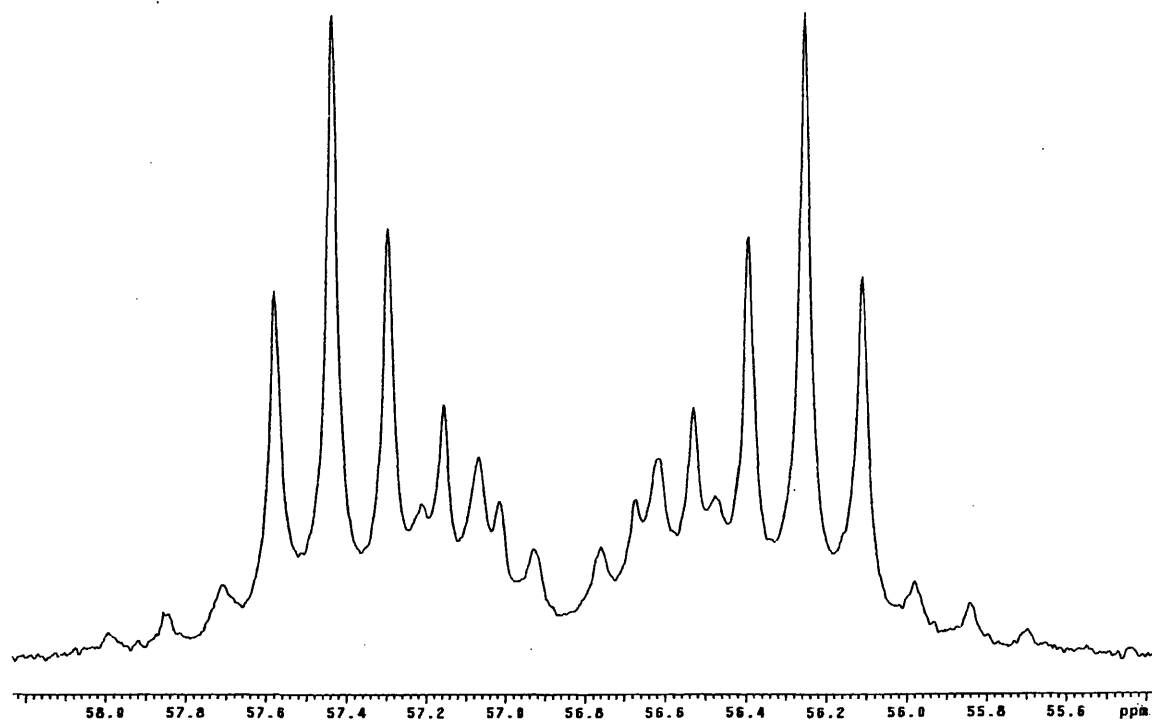


Fig 4.23 (cont.)

ii.a Experimental $^{31}\text{P}\{^1\text{H}\}$ NMR spectrum (δ 56.8) (400 MHz)



ii.b Simulated $^{31}\text{P}\{^1\text{H}\}$ NMR spectrum (δ 56.8)

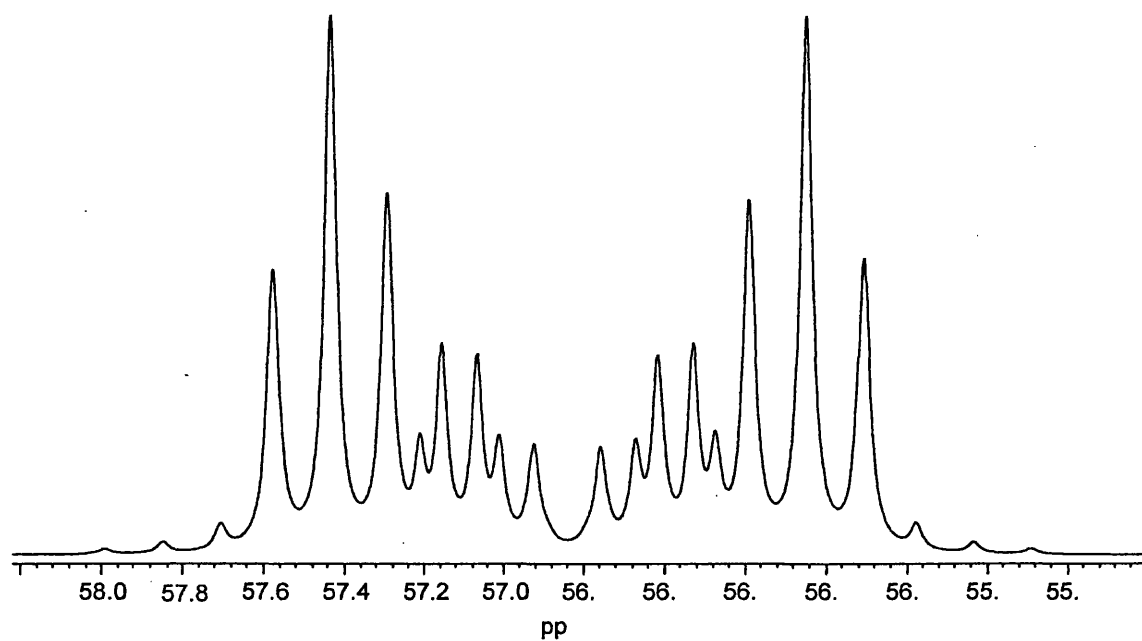
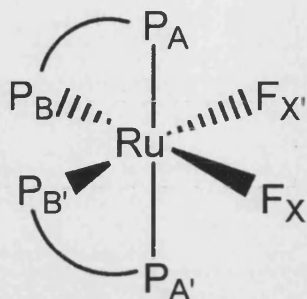


Table 4.1 Spin coupling constants for *cis*-Ru(dmpe)₂F₂

Nucleus	No.	Symbol	Chemical Shift δ	J (Hz)			
				A	B	B'	X
³¹ P _{axial}	2	A/A'	42.21	-			
³¹ P _{equatorial}	1	B	56.84	21.85	-		
³¹ P _{equatorial}	1	B'	56.84	21.84	-59.46	-	
¹⁹ F	1	X	-357.40	23.23	-151.00	-29.47	-
¹⁹ F	1	X'	-357.40	23.21	-29.47	-151.00	-43.57

The figures in table 4.1 confirm the fact that coupling constants between the two axial phosphorus and two equatorial phosphorus and fluorines are similar leading to the apparent quintet at δ 42.2. The spin system can be classified as an AA'BB'XX' system, the two equatorial phosphorus and fluorines are slightly unsymmetrical leading to the complicated multiplet at δ 56.8. This is likely to be due to the constraints imposed by the bidentate ligand. Coupling between an equatorial phosphorus and the fluorine is larger when they are mutually *trans* rather than when they are mutually *cis*. It should also be noted that although no coupling is given between the two axial phosphorus,

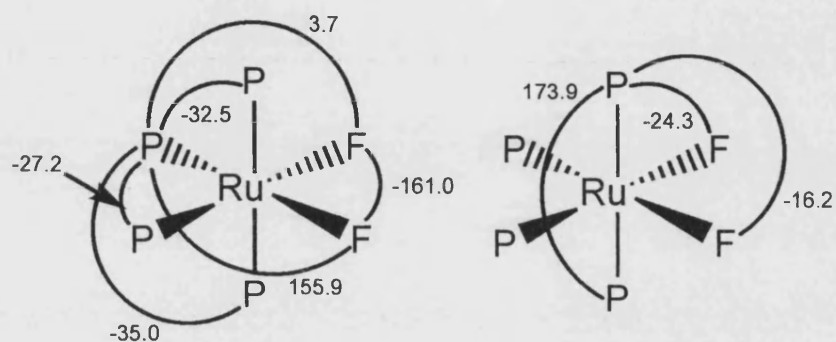
introduction of an estimated coupling into the simulation showed no change in the simulated spectra.

The product **14** is unusual as it is a ruthenium fluoride complex that is not stabilised by π -acceptor ligands. The only other example of this is *cis*-Ru(dppp)₂F₂ (dppp = Ph₂PCH₂CH₂CH₂PPh₂) very recently reported by Mezzetti et al.⁴³, synthesised by treating cationic [Ru(dppp)₂F]⁺ with a source of fluoride. A comparison of coupling constants and ³¹P{¹H} NMR spectra of **14**, *cis*-Ru(dppp)₂F₂, and another d⁶-metal difluoride, [*cis*-Ir(dppe)F₂]⁺ synthesised by Holloway et al.⁴⁴ is shown in fig. 4.24.

Fig. 4.24 Schematic of reported coupling constants and $^{31}\text{P}\{^1\text{H}\}$ NMR spectra of d^6 -metal difluoride complexes

***cis*-Ru(dppp) $_2$ F $_2$**

a) Coupling constants (Hz)



b) $^{31}\text{P}\{^1\text{H}\}$ NMR spectrum (400 MHz, reproduced from published data⁴³ using gNMR)

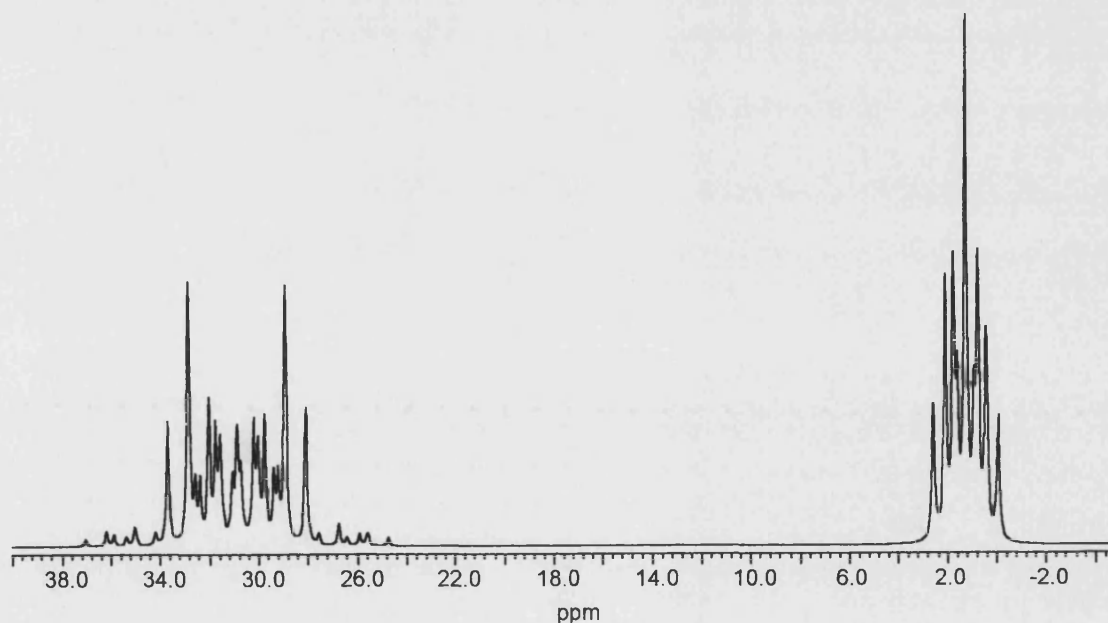
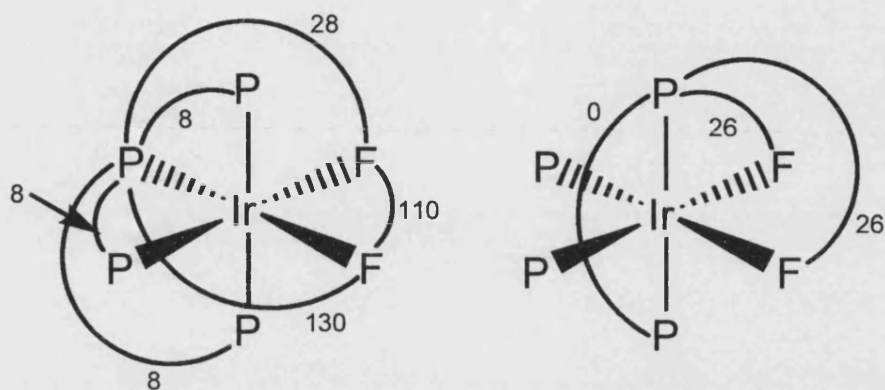


Fig 4.24 (cont.)



a) Coupling constants (Hz)



b) $^{31}\text{P}\{^1\text{H}\}$ NMR spectrum (400 MHz, reproduced from spin data using gNMR)

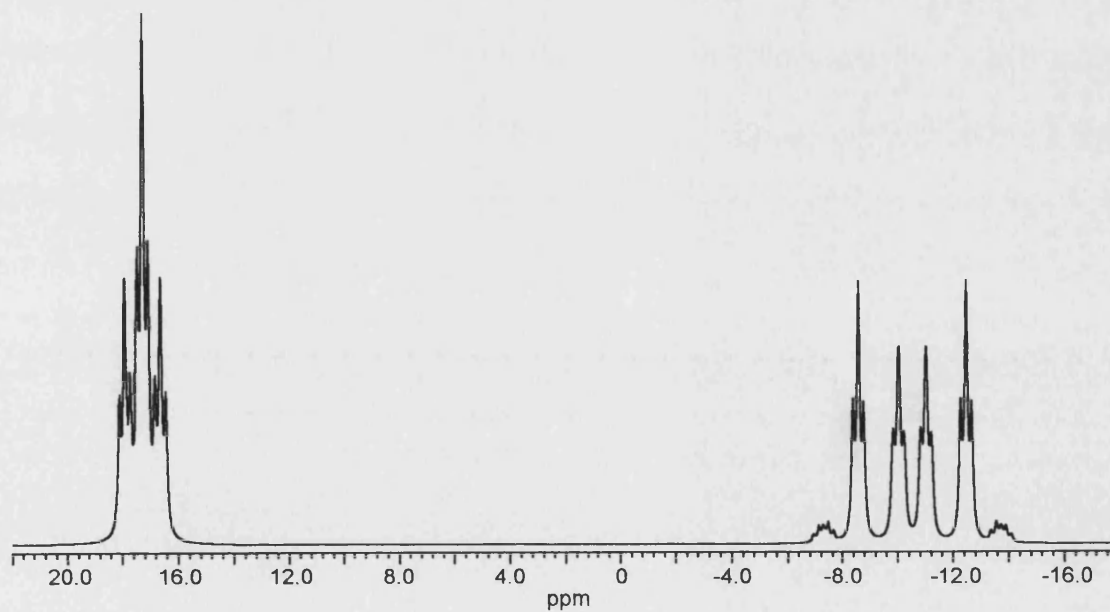
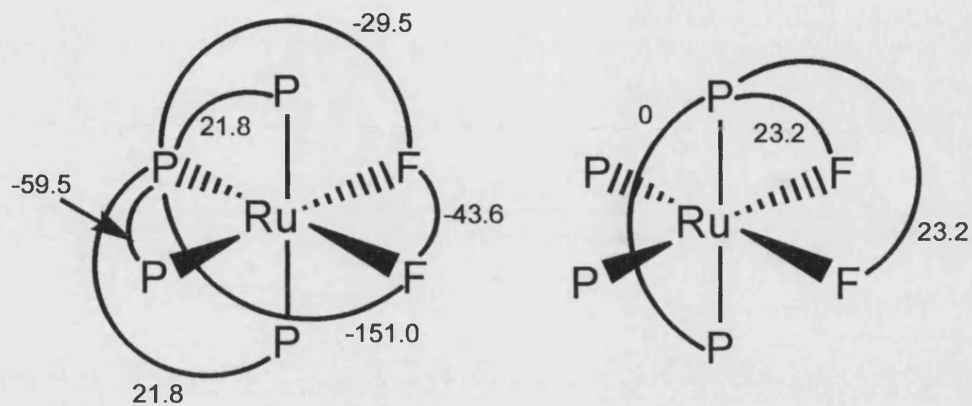
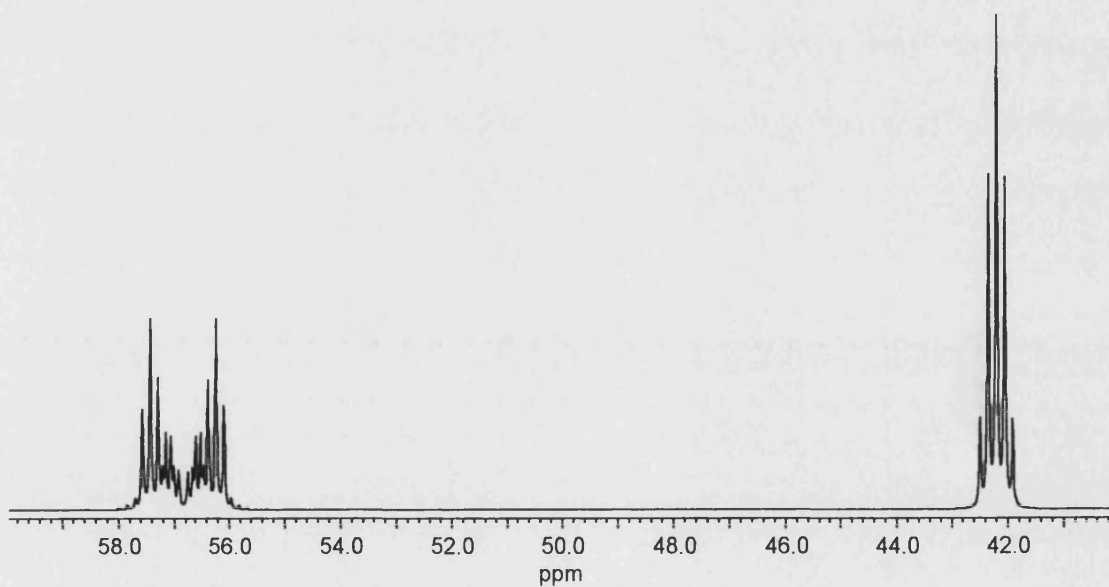


Fig 4.24 (cont.)

cis*-Ru(dmpe)₂F₂ (in *cis*-Ru(dmpe)₂(FHF)F)*a) Coupling constants (Hz)****b) ³¹P{¹H} NMR spectrum (400 MHz, reproduced from spin data using gNMR)**

1.



The $^{31}\text{P}\{^1\text{H}\}$ NMR spectra for all three difluorides show the apical phosphorus resonances to be at least half the width of the equatorial phosphorus resonances. This is due to the *trans* J_{PF} constant being much larger than the *cis* J_{PF} constant as shown in the coupling constant diagrams. Apart from this, the complexes show completely different couplings. The change between the two ruthenium complexes is due to the different ligands. The dppp ligand is much larger than the dmpe ligand (bite angles:- dppp = $91(2)^\circ$ ⁴⁵, dmpe = $\sim 84^\circ$ ⁴⁶) and therefore forces a different geometry on the metal centre, and it is noticed that the two axial phosphines are slightly inequivalent in the *cis*-Ru(dppp)₂F₂. The $^{31}\text{P}\{^1\text{H}\}$ NMR spectra shows that the *cis*-Ru(dppp)₂F₂ phosphorus resonances appear to be more complex as a result.

The [*cis*-Ir(dppe)F₂]⁺ complex also has a slightly larger ligand system (bite angle of dppe = $85(3)^\circ$ ⁴³) but is also cationic which will also lead to a difference in the coupling constants due to shorter bonds between the metal and its ligands.

(ii) X-ray crystal structure of *cis*-Ru(dmpe)₂F(F..HF), **14**.

When the reaction of *cis*-Ru(dmpe)₂H₂, **1**, with PF₂M₂P was repeated in the presence of tenfold equivalent of Et₃N, the $^{31}\text{P}\{^1\text{H}\}$ NMR spectrum indicated that *trans*-Ru(dmpe)₂(FHF)H, **8**, was no longer formed and that *cis*-Ru(dmpe)₂(F..HF)F, **14**, was the only transition metal species present. From this reaction mixture, yellow needle-like crystals formed in 70 % yield after two days. A single crystal X-ray structure confirmed the *cis* disposition of the two fluorides in the distorted octahedral geometry around the ruthenium centre and the strong interaction of one of these with HF in the solid state (fig. 4.25). Data collection parameters for **14** are given in Table 4.2 while selected bond lengths and angles are given in table 4.3.

Fig. 4.25 X-ray crystal structure of *cis*-Ru(dmpe)₂F(F..HF), 14.

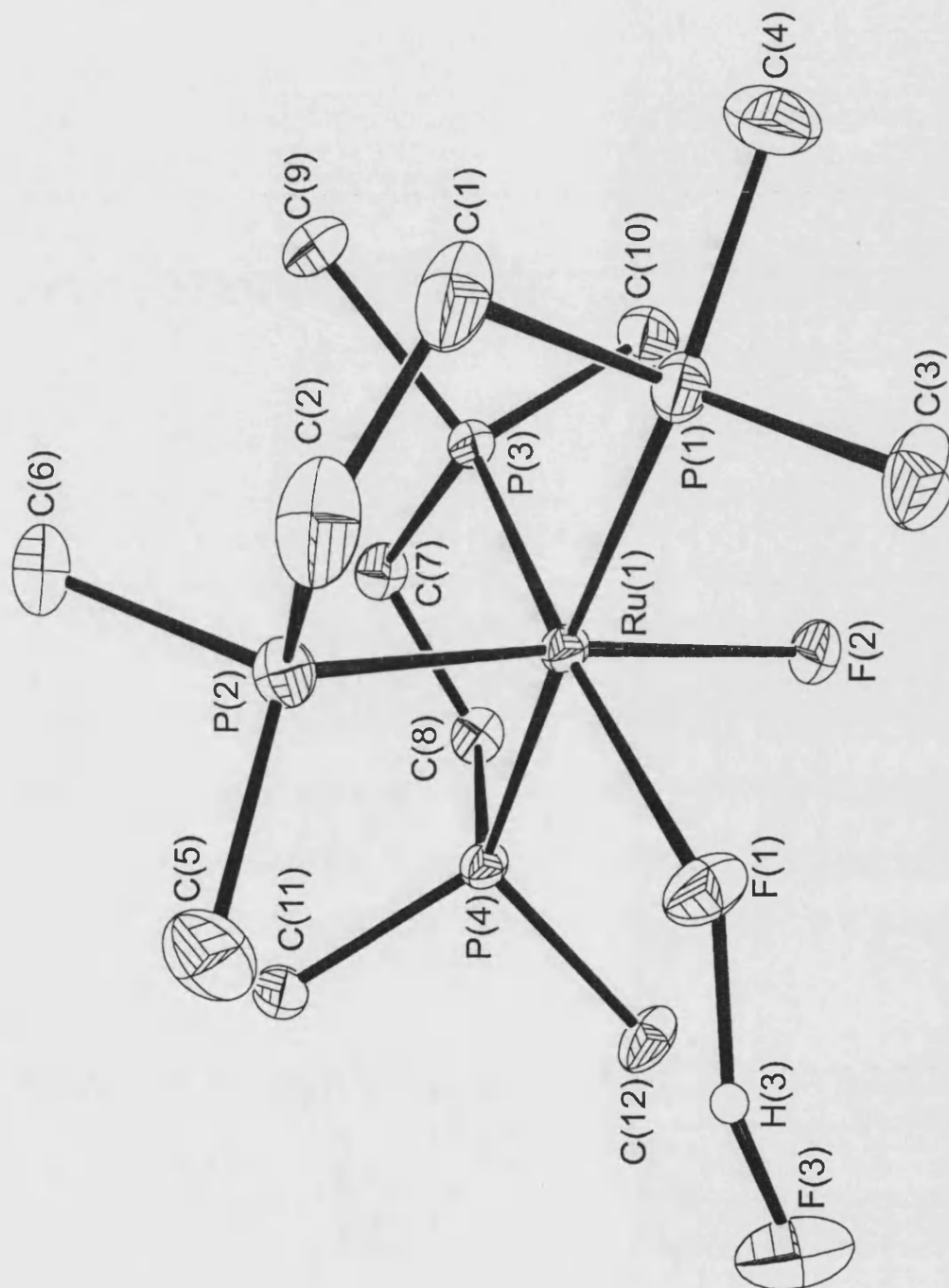


Table 4.2 Crystal data and structure refinement for *cis*-Ru(dmpe)₂F(F..HF), **14**.

Empirical formula	C ₁₂ H ₃₃ F ₃ P ₄ Ru
Formula weight	459.33
Temperature	133(2) K
Wavelength	0.71073 Å
Crystal system	Monoclinic
Space group	Cc
Unit cell dimensions	a = 9.071(1) Å α = 90° b = 17.621(2) Å β = 106.061(2)° c = 13.805(2) Å γ = 90°
Volume	1965.2(4) Å ³
Z	4
Density (calculated)	1.553 Mg/m ³
Absorption coefficient	1.138 mm ⁻¹
F(000)	944
Crystal size	0.10 x 0.10 x 0.08 mm
Theta range for data collection	2.61 to 28.32 °.
Index ranges	-11 ≤ h ≤ 11; -8 ≤ k ≤ 23; -15 ≤ l ≤ 14
Reflections collected	5399
Independent reflections	4105 [R(int) = 0.0221]
Reflections observed (>2σ)	3938
Absorption correction	Multiscan
Max. and min. transmission	0.9195 and 0.8947
Refinement method	Full-matrix least-squares on F ²
Data / restraints / parameters	4105 / 2 / 193
Goodness-of-fit on F ²	1.005
Final R indices [I > 2σ(I)]	R ₁ = 0.0322 wR ₂ = 0.0770
R indices (all data)	R ₁ = 0.0335 wR ₂ = 0.0775
Absolute structure parameter	0.03(3)
Largest diff. peak and hole	1.006 and -0.397 e.Å ⁻³

Note: HF proton located and freely refined.

Hydrogen bonds with H..A < r(A) + 2.000 Angstroms **and** <DHA > 110 deg.

D-H	d(D-H)	d(H..A)	<DHA	d(D..A)	A
F3-H3	1.05(11)	1.30(11)	155(10)	2.293(4)	F1

Table 4.3 Bond lengths [Å] and angles [°] for *cis*-Ru(dmpe)₂F(F..HF), **14**.

Ru(1)-F(2)	2.101(3)	P(2)-C(5)	1.832(6)
Ru(1)-F(1)	2.168(3)	P(2)-C(2)	1.841(5)
Ru(1)-P(3)	2.249(1)	P(3)-C(9)	1.818(4)
Ru(1)-P(2)	2.350(1)	P(3)-C(10)	1.820(5)
Ru(1)-P(1)	2.320(1)	P(3)-C(7)	1.845(4)
Ru(1)-P(4)	2.332(1)	P(4)-C(11)	1.814(5)
P(1)-C(1)	1.815(5)	P(4)-C(12)	1.824(4)
P(1)-C(3)	1.817(5)	P(4)-C(8)	1.835(4)
P(1)-C(4)	1.821(6)	C(1)-C(2)	1.516(9)
P(2)-C(6)	1.817(5)	C(7)-C(8)	1.537(6)
F(2)-Ru(1)-F(1)	85.4(1)	C(6)-P(2)-C(2)	102.5(3)
F(2)-Ru(1)-P(3)	87.19(8)	C(5)-P(2)-C(2)	100.0(3)
F(1)-Ru(1)-P(3)	172.33(9)	C(6)-P(2)-Ru(1)	135.8(2)
F(2)-Ru(1)-P(2)	171.63(8)	C(5)-P(2)-Ru(1)	115.9(2)
F(1)-Ru(1)-P(2)	86.33(9)	C(2)-P(2)-Ru(1)	108.4(2)
P(3)-Ru(1)-P(2)	101.09(4)	C(9)-P(3)-C(10)	101.0(2)
F(2)-Ru(1)-P(1)	93.45(8)	C(9)-P(3)-C(7)	102.6(2)
F(1)-Ru(1)-P(1)	86.51(8)	C(10)-P(3)-C(7)	101.6(2)
P(3)-Ru(1)-P(1)	96.07(4)	C(9)-P(3)-Ru(1)	125.7(2)
P(2)-Ru(1)-P(1)	84.51(5)	C(10)-P(3)-Ru(1)	112.6(2)
F(2)-Ru(1)-P(4)	83.57(8)	C(7)-P(3)-Ru(1)	110.4(1)
F(1)-Ru(1)-P(4)	92.74(8)	C(11)-P(4)-C(12)	103.5(2)
P(3)-Ru(1)-P(4)	84.32(4)	C(11)-P(4)-C(8)	102.3(2)
P(2)-Ru(1)-P(4)	98.37(4)	C(12)-P(4)-C(8)	106.0(2)
P(1)-Ru(1)-P(4)	176.98(5)	C(11)-P(4)-Ru(1)	124.5(2)
C(1)-P(1)-C(3)	105.4(3)	C(12)-P(4)-Ru(1)	112.7(2)
C(1)-P(1)-C(4)	101.0(3)	C(8)-P(4)-Ru(1)	106.2(1)
C(3)-P(1)-C(4)	101.6(3)	C(2)-C(1)-P(1)	108.5(4)
C(1)-P(1)-Ru(1)	108.4(2)	C(1)-C(2)-P(2)	109.7(4)
C(3)-P(1)-Ru(1)	113.2(2)	C(8)-C(7)-P(3)	107.8(3)
C(4)-P(1)-Ru(1)	125.2(2)	C(7)-C(8)-P(4)	107.5(3)
C(6)-P(2)-C(5)	101.8(3)		

It is interesting to compare the crystal structure of **14** with the crystal structure of *cis*-Ru(dppp)₂F₂. The steric bulk of the dppp ligand has a greater effect on the geometry than the dmpe ligand. The F-Ru-F angle is closed down to 78.2 ° in *cis*-Ru(dppp)₂F₂ compared to 85.4 ° in **14** and the *trans* P-Ru-P angle is also bent to 169.7 ° compared with 177.0 ° in **14**. This shows that *cis*-Ru(dmpe)₂F(F..HF), **14**, is closer to an octahedral geometry than the *cis*-Ru(dppp)₂F₂. The Ru-P bond lengths in **14** (average 2.313(1) Å) are also slightly shorter on average compared to *cis*-Ru(dppp)₂F₂ (average Ru-P length 2.350(2) Å) again due to steric constraints.

Perhaps more importantly the data shows that both Ru-F bonds in **14** are long due to the lack of stabilising π -acceptor ligands. Also the Ru-F..HF bond (2.168(3) Å) is longer than the unperturbed Ru-F bond (2.101(3) Å) due to the hydrogen bonding to the HF group. Both these distances are significantly longer than those seen for *cis*-Ru(dppp)₂F₂ (average 2.06 Å) and the complexes *cis*-RuF₂(CO)₂L₂ (L = PPh₃, PEtPh₂) synthesised by Coleman et al.,⁴⁷ where average Ru-F bond lengths are around 2.01 Å. This shows the effect of stabilising π -accepting ligands on ruthenium fluoride species. In the carbonyl species it is seen that in both cases strongly π -accepting carbonyl ligands are found *trans* to the π -donating fluoride ligands. This shortens the Ru-F bond and stabilises the fluoride ligand. In fact both species are air and moisture stable.

Slightly longer Ru-F distances are seen in the *cis*-Ru(dppp)₂F₂ species as there are no strongly π -accepting ligands *trans* to the fluoride ligands. However, the presence of phenyl rings allows the chelating phosphine ligands to be weakly π -accepting which gives some stabilisation to the fluoride ligands. There is also evidence of intramolecular hydrogen bonding between the fluorides and the phenyl hydrogens to aid the stability of the species. Unsurprisingly, this complex is less stable than the *cis*-RuF₂(CO)₂L₂

complexes being susceptible to moisture. However, crystallisation could be carried out in a CH_2Cl_2 /hexane solution.

The longest Ru-F bond is seen in *cis*-Ru(dmpe)₂F(F..HF), **14**, where there are not any weakly π -accepting ligands to stabilise the fluoride ligands. There is a difference of ~ 0.1 Å between the bond lengths shown for these difluoride species. Some stabilisation must come about from the presence of the hydrogen bonded HF, which effectively creates a bifluoride ligand. This type of ligand is far less π -donating than a fluoride ligand, as pointed out by Grushin et al.⁴⁸ and therefore maybe crucial to the stability of the complex. That being said, this complex is extremely air and moisture sensitive and in the presence of chlorinated solvents decomposed to give unidentified products.

In the bifluoride ligand of **14**, the distance between the two fluorines is 2.292(8) Å. This is comparable to that of the bifluoride hydride **8**, (2.276(8) Å), and shorter than other reported bifluoride complexes (table 4.4). This seems to suggest that **14** is best described as a bifluoride fluoride complex, rather than a difluoride..HF complex. Also, the infrared spectrum of **14** shows two broad bands at 2452 and 1915 cm^{-1} , which can be attributed to a bifluoride ligand.⁴⁹ The angle of the M-F...F bonds is typically around 130-134° in the compounds shown in table 4.4. In the cases of the nickel and palladium complexes residual push-pull interactions from the difluoropyrimidyl and phenyl ligands respectively are thought to be responsible for the higher angle. For **14**, the angle is 141.7°, which is within the range seen for previously characterised bifluoride complexes. The bifluoride proton was freely refined and showed a F-H-F angle of 155(10)°. The bifluoride unit appears unsymmetrical but the error on the H-F bond lengths is high so this cannot be stated accurately. The related molybdenum and tungsten bifluoride complexes (table 4.4) show asymmetry in the F-H-F unit.^{50,51} The

proton of the tungsten bifluoride species was detected by neutron diffraction studies, which is reported to be more reliable than the X-ray detection of the proton in the molybdenum bifluoride species, as the presence of a polar axis can make X-ray structure refinements fall into a false minimum.⁵¹

Table 4.4 Parameters for structurally characterised bifluoride complexes

Bifluoride complex	F...F distance in bifluoride ligand (Å)	M-F...F bond angle (°)
Ru(dmpe) ₂ H(FHF), 8	2.276(8)	129.9
<i>cis</i> -Ru(dmpe) ₂ F(F..HF), 14	2.292(8)	141.7
Pd(PPh ₃)(Ph)(FHF) ⁴⁷	~ 2.35	153.4
Mo(PMe ₃) ₄ H ₂ F(FHF) ⁵⁰	2.351(8)	~ 134
W(PMe ₃) ₄ H ₂ F(FHF) ⁵¹	2.390(13)	134.1
Ni(PEt ₃) ₂ (2-C ₅ NF ₃ H)(FHF) ⁵²	2.400(6)	156.7

Note on use of cis-Ru(dmpe)₂F₂ in simulation exercises

The results of carbon/hydrogen microanalysis on **14** found the product to be % C 32.5, % H 7.28, which is actually closer to *cis*-Ru(dmpe)₂F₂ (expected % C 32.8, % H 7.34) than *cis*-Ru(dmpe)₂F(F..HF). This suggested that HF must be lost prior to the sample being weighed for microanalysis. A reaction between *cis*-Ru(dmpe)₂H₂, **1**, and PF₂M₂P was prepared in thf and after the reaction occurred, the solution was left to slowly evaporate in a glovebox, which yielded an off-white residue remained. The ³¹P{¹H} NMR spectrum of the residue in thf gave the same complex pattern as observed for **14**. However, HF was not observed, and in the ¹⁹F NMR spectrum, where only one broad signal was seen at δ -357 for the two fluorides. Elemental analysis of the powder confirmed that it was *cis*-Ru(dmpe)₂F₂.

The fact that the difluoride gave an almost identical $^{31}\text{P}\{^1\text{H}\}$ NMR spectrum to **14**, and that the ^{19}F and ^1H NMR spectra of **14** show HF only as a doublet, i.e. no coupling is seen to the fluorides, suggested that HF had little effect on the six-atom spin system around the ruthenium metal. Therefore the simpler *cis*-Ru(dmpe)₂F₂ system was used in the simulation exercises.

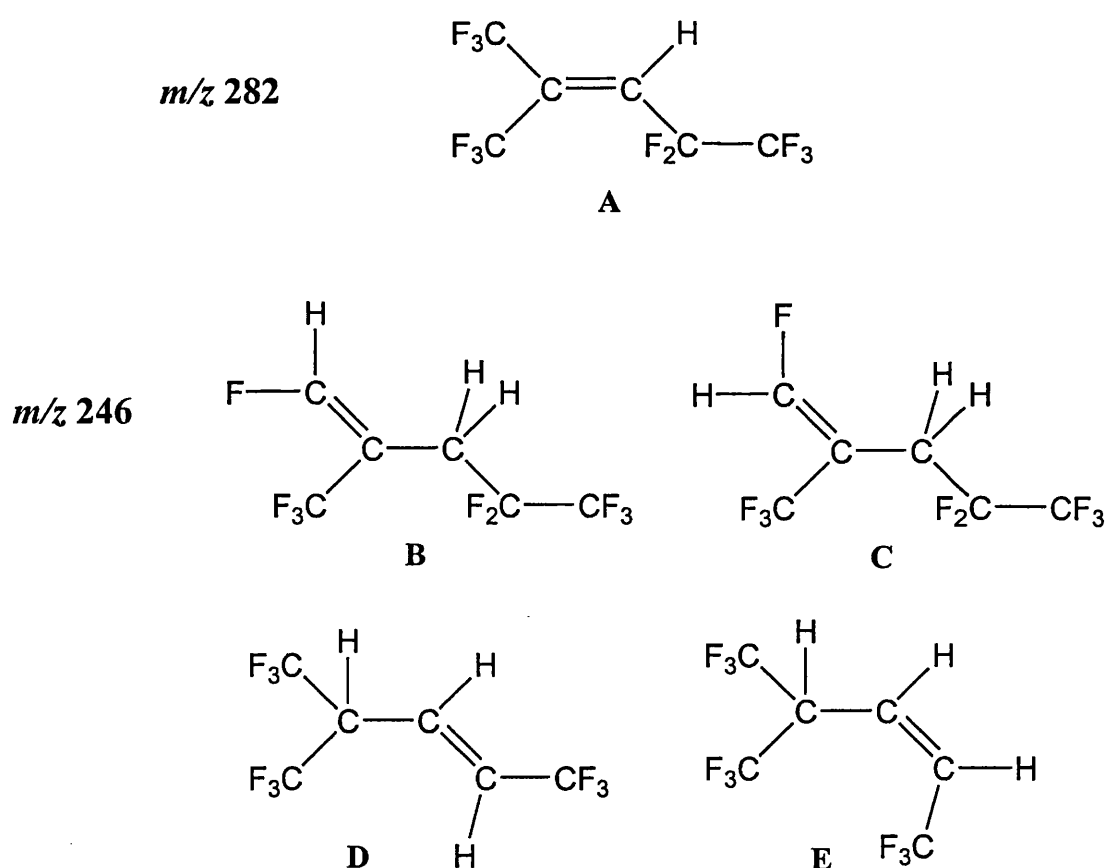
Also the ‘lability’ of the HF suggests that in solution, **14** can be called a difluoride..HF complex, and on crystallisation, a bifluoride fluoride complex, although distinguishing between the two may simply be a case of semantics.

(iii) Fluoroorganic products

The ^{19}F NMR spectrum of the fluoroorganic products from the PF₂M₂P in reaction 4.1, condensed off from the inorganic products, was very complex but selectively decoupled ^{19}F NMR experiments suggested the formation of four products. The ^1H NMR spectrum indicated that some, if not all, of these products resulted from exchange of fluorine for hydrogen. Due to the complexity of the NMR spectra, GC and GC-MS techniques were used to try and identify possible products. The reaction was repeated in both dodecane and toluene as the volatile products had a low retention time and these solvents would stay on the column while the reaction products were detected. In both cases the same fluoroorganic products were seen by ^{19}F NMR spectroscopy as when the reaction was done in thf or C₆D₆. Gas chromatography, on a non chiral column (DB-1), identified the presence of four main products. Using GC-MS these four products were found to have *m/z* values of 246, the equivalent to the loss of three fluorines and the gain of three hydrogens in the PF₂M₂P (*m/z* = 300) molecule. Another product was also found in a smaller amount. The *m/z* value for this is 282, i.e. loss of one fluorine and gain of one hydrogen.

A report by Snegirev et al.⁵³ details the reaction of NaBH₄ with PF₂M₂P, which results in the partial defluorination of the perfluoroalkene giving products that have lost up to six fluorines by replacement with hydrogen. In the list of products there are examples of partially defluorinated products with molecular masses equivalent to those found in the GC-MS of the reaction products of **1** and PF₂M₂P (fig. 4.26). Compound **A** corresponds to the observation of a small amount of a product with mass of 282. This implies that the vinylic fluorine is the most reactive and would be replaced first.

Fig 4.26 Fluoroorganic products of reaction 4.1



The other four products arise then, from further reaction of **A**. The double bond is attacked by another hydride, which moves the double bond to form new vinylic

fluorines, which in turn can be replaced by hydrogen. Depending on which end of the double bond is attacked, two pairs of isomers, **B/C** and **D/E**, are formed.

Compounds **B** and **C** are reported to each show a distinctive set doublets and triplets in the ^1H NMR spectrum. These are seen at **B** : δ 8.83 (d, 73.8 Hz), δ 3.81 (t, 17.8 Hz) and **C** : δ 6.62 (d, 75.7 Hz), δ 2.17 (t, 17.1 Hz). The large coupling in the doublets is typical of a coupling of $=\text{CFH}$ group, seen in compounds **B** and **C**. Compounds **D** and **E** were not reported by Snegirev, however, these are proposed as the third and fourth products as they both have m/z of 246, and can be produced by a similar route to the products **B** and **C**, the only difference being the site of hydrogen attack on the double bond in **A**.

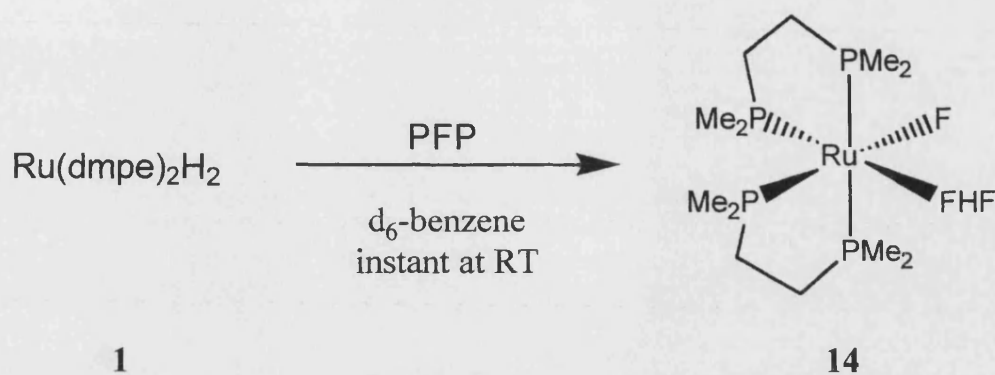
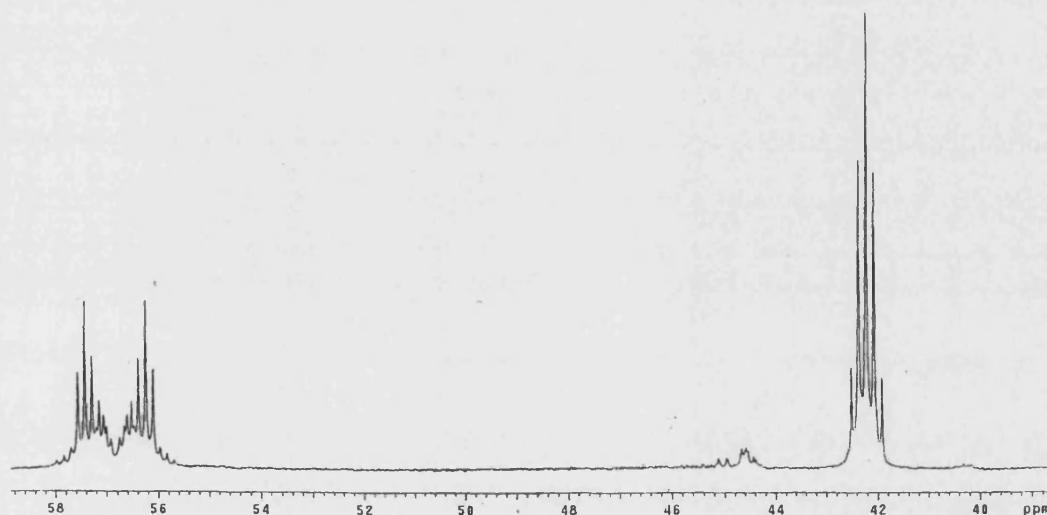
It should also be noted in this reaction that the products are always the same irrespective of the choice of solvent, whether deuterated in the cases of d_6 -benzene or d_8 -thf or protonated as in toluene and dodecane, which would imply that the source of the hydrogen is the dihydride species and not the solvent.

Therefore the compounds shown in fig. 4.26 are proposed to be formed from the reaction of **1** and $\text{PF}_2\text{M}_2\text{P}$.

4.2.1.2 Reaction of *cis*- $\text{Ru}(\text{dmpe})_2\text{H}_2$ (**1**) with perfluoropropene (PFP)

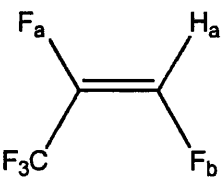
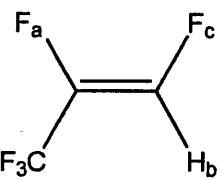
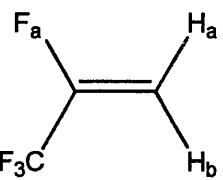
The reaction of **1** with $\text{CF}_2=\text{CF}(\text{CF}_3)$ was carried out in order to simplify the fluorinated products. A thf solution of **1** in a resealable NMR tube was treated with 1 atm PFP (~ 2 equivalents) and, at room temperature, the solution became yellow immediately. The $^{31}\text{P}\{^1\text{H}\}$ NMR spectrum of the solution showed that the reaction had yielded *cis*- $\text{Ru}(\text{dmpe})_2\text{F}(\text{FHF})$, **14**, as the only metal containing species with no bifluoride hydride, **8**, being produced.

Reaction 4.2

Fig. 4.27 $^{31}\text{P}\{^1\text{H}\}$ NMR spectrum of reaction 4.2 (C_6D_6 , 400 MHz)

As expected, the fate of the PFP was more easily established by ^1H and ^{19}F NMR than in reaction 4.1. Fewer possibilities were available for fluoroorganic products and most had been reported.⁵⁴ Three partially fluorinated products were found and identified, using the literature, as *trans*- and *cis*- $\text{CF}_3\text{CF}=\text{CFH}$ and $\text{CF}_3\text{CF}=\text{CH}_2$, in a 4:1:3 ratio. The chemical shifts for the three products and their coupling constants are given in table 4.5.

Table 4.5 Fluoroorganic products of reaction 4.2

Fluoroorganic products from reaction 4.2			
Product ratio	4	1	3
CF ₃	δ -69.5 dd J_{FFa} 11.9 Hz J_{FFb} 20.6 Hz	δ -72.2 dd J_{FFa} 14.5 Hz J_{FFc} 5.7 Hz	δ -73.9 d J_{FFa} 10.3 Hz J_{FHa} unresolved
F _a	δ -181.8 ddq J_{FFa} 11.9 Hz J_{FaFb} 134.3 Hz J_{FaHa} 4.1 Hz	δ -161.3 ddq J_{FFa} 14.5 Hz J_{FaFc} 9.8 Hz J_{FaHb} 16.7 Hz	δ -125.1 ddq J_{FFa} 10.3 Hz J_{FaHa} 15.5 Hz J_{FaHb} 43.4 Hz
F _b	δ -163.5 ddq J_{FFb} 20.6 Hz J_{FaFb} 134.3 Hz J_{FbHa} 68.2 Hz	-	-
F _c	-	δ -152.9 ddq J_{FFc} 5.7 Hz J_{FaFc} 9.8 Hz J_{FcHb} 66.1 Hz	-
H _a	δ 8.45 dd J_{FaHa} 4.1 Hz J_{FbHa} 68.2 Hz	-	δ 4.52 dd J_{FaHa} 15.5 Hz J_{HaHb} 5.0 Hz
H _b	-	δ 7.44 dd J_{FaHb} 16.7 Hz J_{FcHb} 66.1 Hz	δ 4.47 ddq J_{FHa} 1.6 Hz J_{FaHb} 43.4 Hz J_{HaHb} 5.0 Hz

The stoichiometry of this reaction was changed in an attempt to compare the chemistry reported by Jones³⁹ with the zirconocene dihydride complex. However, on reaction of ~ 10 equivalents of **1** with PFP in a resealable NMR tube, there was only a small amount of conversion of **1** to *cis*-Ru(dmpe)₂F(F..HF), **14**. Further additions of PFP to the NMR tube in small quantities showed the formation of *trans*-

$\text{Ru}(\text{dmpe})_2\text{H}(\text{FHF})$, **8**, at first then the formation of bifluoride fluoride, **14**. The fluorocarbon products obtained did not differ from those seen in table 4.3.

A reaction using **1** with either PF2M2P or PFP in the presence of 9,10-dihydroanthracene, showed some inhibition of production of **14**. Bifluoride hydride **8** is seen to become more prevalent. This indicates the possibility of a radical process in the reaction mechanism.

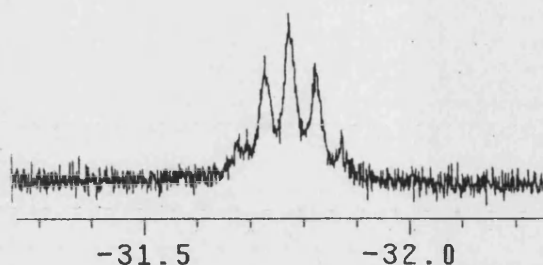
4.2.2 Reaction of *cis*-Ru(dcpe)₂H₂ (**4**) and perfluoroalkenes

4.2.2.1 Reaction with perfluoro-2-methyl-2-pentene (PF2M2P)

The facile activation of PF2M2P and PFP by *cis*-Ru(dmpe)₂H₂, **4**, led us to investigate the reactivity of similar ruthenium dihydride complexes with the same perfluoroalkenes. On addition of 1 equivalent of PF2M2P to a C₆D₆ solution of *cis*-Ru(dcpe)₂H₂, **2**, the ³¹P{¹H} NMR spectrum showed a forest of peaks indicating multiple products being formed. This reaction was not pursued any further.

Reaction of *cis*-Ru(dcpe)₂H₂, **4**, which showed no reactivity with C₆F₆ even on heating (Ch. 3), with 1 equivalent of PF2M2P in benzene yielded an orange solution over a period of 24 hours at room temperature from which small orange needle like crystals were isolated. The ³¹P{¹H} NMR spectrum of the remaining solution showed only the presence of starting dihydride **4**. However, on repeating the reaction in d₈-thf, a homogenous solution was formed and no solid was precipitated. The ³¹P{¹H} NMR spectrum now showed the presence of a singlet at δ 73.4, although the starting dihydride was still the main metal containing species. Careful investigation of the ¹H NMR spectrum (fig 4.28) showed a quintet resonance at very high field (δ -31.78, *J*_{HP} = 19.2 Hz) consistent with the formation of cationic [Ru(dcpe)₂H]⁺. The BPh₄ and PF₆ salts of this have previously been reported by Winter⁵⁵ and Mezzetti⁵⁶ respectively.

The fate of the perfluoroalkene was identified from the ¹⁹F NMR spectrum. This showed the formation of the perfluoro-2-methyl-2-en-3-olate anion as seen in fig 4.4 (D). The spectrum showed four signals at δ -45.5 (tq, *J*_{FF} 10.7 Hz, *J*_{FF} 19.6 Hz, 3F, CF₃), δ -51.3 (q, *J*_{FF} 10.7 Hz, 3F, CF₃), δ -77.8 (s, 3F, CF₃) and δ -113.6 (q, *J*_{FF} 19.6 Hz, 2F, CF₂). This data corresponds well to the previously reported ammonium and alkali metal salts.^{7,57}

Fig. 4.28 ^1H NMR spectrum of $[\text{Ru}(\text{dcpe})_2\text{H}]^+$ ($\text{d}_8\text{-thf}$, 400 MHz)

X-ray crystallographic analysis of the crystals obtained from the reaction in benzene (27 % yield) confirmed that the reaction product was $[\text{Ru}(\text{dcpe})_2\text{H}][(\text{CF}_3)_2\text{C}=\text{C}(\text{O})\text{CF}_2\text{CF}_3]$, **15**, (fig. 4.29). The reaction of **4** with PF2M2P (reaction 4.3) is noticeably different to that of **1** with PF2M2P. Data collection parameters are shown in table 4.6 while selected bond lengths and angles are given in table 4.7

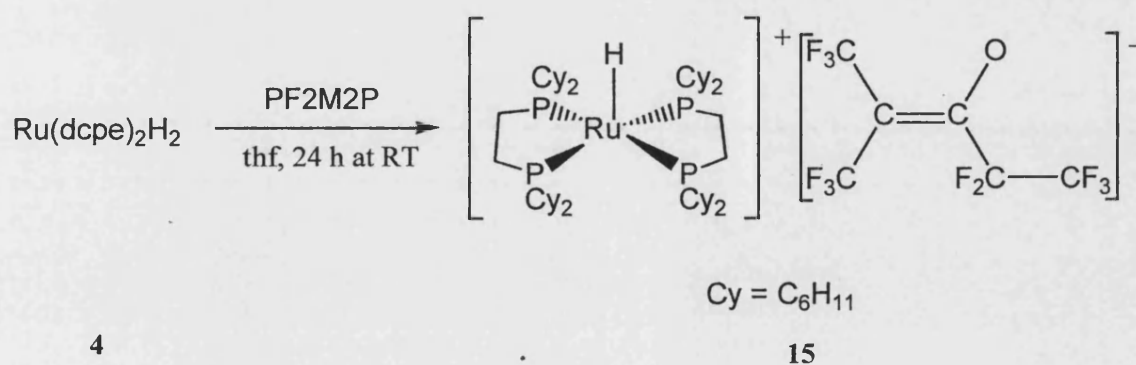
Reaction 4.3

Fig. 4.29 X-ray crystal structure of $[\text{Ru}(\text{dcpe})_2\text{H}][(\text{CF}_3)_2\text{C}=\text{C}(\text{O})\text{CF}_2\text{CF}_3]$, **15**.

Note:- Hydrogen atoms have been removed for clarity.

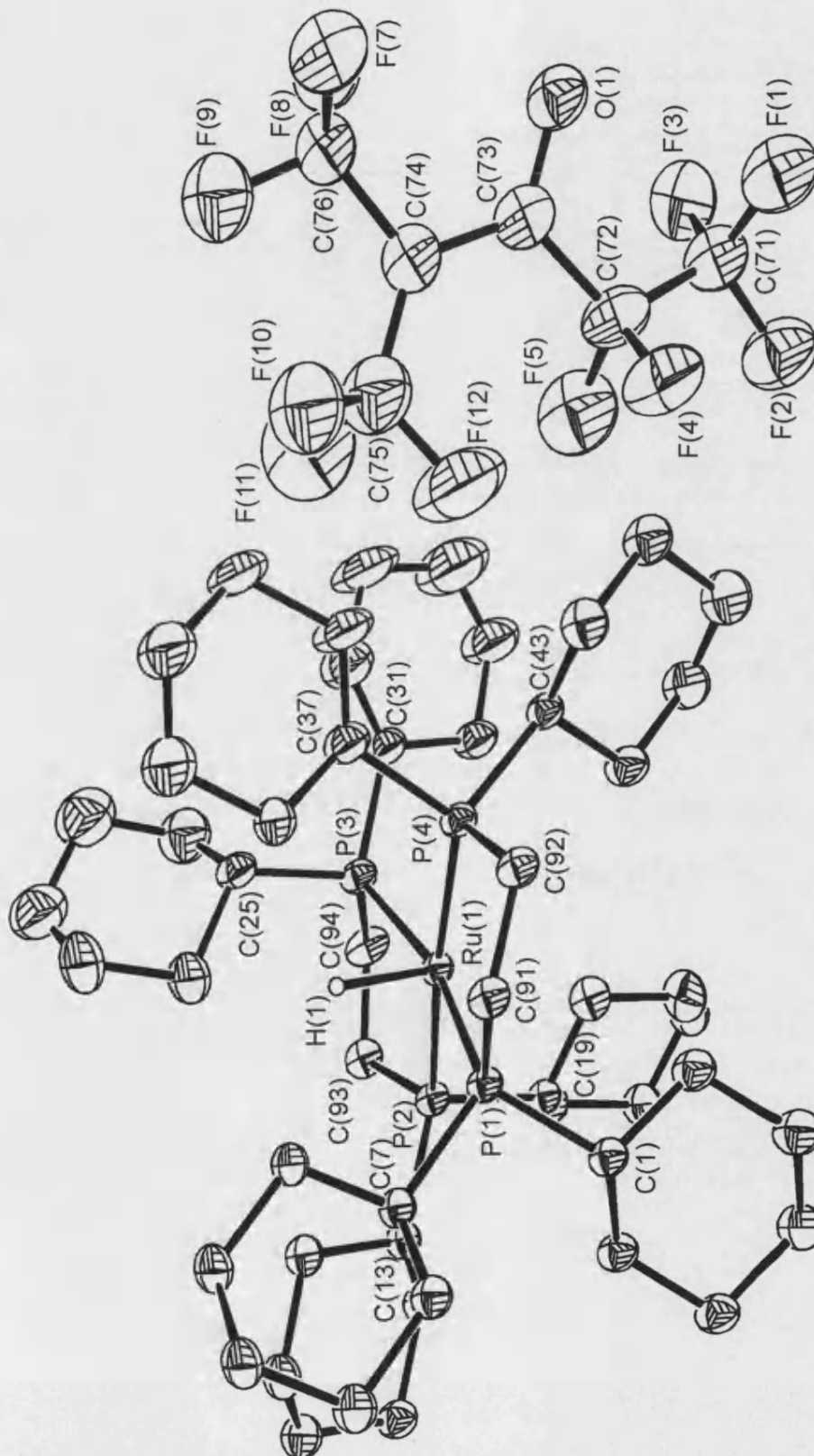


Table 4.6 Crystal data and structure refinement parameters for **15**.

Empirical formula	C ₇₀ H ₁₀₉ F ₁₁ O P ₄ Ru
Formula weight	1400.52
Temperature	170(2) K
Wavelength	0.71073 Å
Crystal system	Triclinic
Space group	P-1
Unit cell dimensions	a = 12.3863(3) Å α = 106.140(2) ^o b = 13.6610(4) Å β = 93.171(2) ^o c = 21.9070(6) Å γ = 93.832(2) ^o
Volume	3542.23(17) Å ³
Z	2
Density (calculated)	1.313 Mg/m ³
Absorption coefficient	0.381 mm ⁻¹
F(000)	1480
Crystal size	0.15 x 0.10 x 0.08 mm
Theta range for data collection	3.52 to 23.82 ^o .
Index ranges	-14 ≤ h ≤ 14; -15 ≤ k ≤ 15; -24 ≤ l ≤ 24
Reflections collected	33863
Independent reflections	10742 [R(int) = 0.0441]
Reflections observed (>2σ)	8993
Absorption correction	Multiscan
Max. and min. transmission	0.9720 and 0.9450
Refinement method	Full-matrix least-squares on F ²
Data / restraints / parameters	10742 / 25 / 843
Goodness-of-fit on F ²	1.041
Final R indices [I > 2σ(I)]	R ₁ = 0.0571 wR ₂ = 0.1511
R indices (all data)	R ₁ = 0.0694 wR ₂ = 0.1613
Largest diff. peak and hole	1.629 and -0.761 e.Å ⁻³

Table 4.7 Selected bond lengths [Å] and angles [°] for **15**.

Ru(1)-P(4)	2.3501(12)	Ru(1)-P(1)	2.3522(11)
Ru(1)-P(2)	2.3600(12)	Ru(1)-P(3)	2.3690(12)
P(1)-C(91)	1.852(4)	P(1)-C(1)	1.866(4)
P(1)-C(7)	1.875(4)	P(2)-C(13)	1.844(5)
P(2)-C(93)	1.846(4)	P(2)-C(19)	1.865(4)
P(3)-C(94)	1.842(5)	P(3)-C(31)	1.865(5)
P(3)-C(25)	1.865(5)	P(4)-C(37)	1.849(5)
P(4)-C(92)	1.849(5)	P(4)-C(43)	1.868(4)
F(1)-C(71)	1.306(8)	F(2)-C(71)	1.331(8)
F(3)-C(71)	1.331(9)	F(4)-C(72)	1.362(8)
F(5)-C(72)	1.376(8)	O(1)-C(73)	1.228(7)
F(7)-C(76)	1.330(7)	F(8)-C(76)	1.354(8)
F(9)-C(76)	1.342(7)	F(10)-C(75)	1.346(11)
F(11)-C(75)	1.357(11)	F(12)-C(75)	1.324(12)
C(91)-C(92)	1.525(6)	C(93)-C(94)	1.519(7)
P(4)-Ru(1)-P(1)	83.56(4)	P(4)-Ru(1)-P(2)	173.59(4)
P(1)-Ru(1)-P(2)	98.43(4)	P(4)-Ru(1)-P(3)	98.00(4)
P(1)-Ru(1)-P(3)	165.47(4)	P(2)-Ru(1)-P(3)	81.62(4)
F(1)-C(71)-F(3)	108.8(7)	F(1)-C(71)-F(2)	107.1(6)
F(3)-C(71)-F(2)	107.8(6)	F(1)-C(71)-C(72)	111.8(6)
F(3)-C(71)-C(72)	112.3(6)	F(2)-C(71)-C(72)	108.9(7)
F(4)-C(72)-F(5)	106.5(6)	F(4)-C(72)-C(73)	112.7(6)
F(5)-C(72)-C(73)	112.7(6)	F(4)-C(72)-C(71)	105.0(6)
F(5)-C(72)-C(71)	103.9(6)	C(73)-C(72)-C(71)	115.2(6)
O(1)-C(73)-C(74)	125.0(6)	O(1)-C(73)-C(72)	112.7(6)
F(12)-C(75)-F(10)	102.7(10)	F(12)-C(75)-F(11)	107.1(9)
F(10)-C(75)-F(11)	100.6(8)	F(12)-C(75)-C(74)	116.8(8)
F(10)-C(75)-C(74)	114.3(8)	F(11)-C(75)-C(74)	113.6(10)
F(7)-C(76)-F(9)	105.0(6)	F(7)-C(76)-F(8)	104.2(6)
F(9)-C(76)-F(8)	102.6(5)	F(7)-C(76)-C(74)	116.7(5)
F(9)-C(76)-C(74)	112.4(6)	F(8)-C(76)-C(74)	114.5(6)

Symmetry transformations used to generate equivalent atoms: N/A

The X-ray crystal structure shows a 16-electron five-coordinate monohydride ruthenium cation with a perfluoro-2-methyl-2-en-3-olate anion. The cation displays a distorted square planar arrangement of the four P atoms around the Ru centre (average bond length of 2.358(1) Å) giving an overall square pyramidal structure. The hydride ligand was not localised but is expected to sit in an apical position as suggested in the crystal structure. The anion, although reported before, has not been previously characterised by X-ray crystallography. It is similar to the starting PF₂M₂P molecule apart from the vinyl fluorine that has been replaced by an oxygen atom creating an anion. The cation is unique in that the metal does not sit above or below the plane of the four basal P atoms, a characteristic usually associated with five coordinate square pyramidal complexes. Winter⁵⁴ attributes this to the steric bulk of the cyclohexyl groups on the ligands and the small size of the apical hydride. If all the P atoms did bend away from the metal centre this would cause unfavourably close contacts between the cyclohexyl rings.

The gross structure is similar to the cation [Ru(dcpe)₂H]⁺ previously reported by Winter⁵⁴ as the [BPh₄] salt and Mezzetti⁵⁵ as the [PF₆] salt. Our X-ray crystallographic parameters are slightly different but we attribute this to packing within the crystal. The only other ruthenium cation of this type has been reported by Jimenez et al.⁵⁸ They report the [Ru(dippe)₂H]⁺ cation as the [BPh₄] salt, and also a [Ru(dippe)₂H(η²-O₂)]⁺ cation which forms on exposure to air. They also report the conversion of [Ru(dcpe)₂H]⁺ with exposure to air to form the analogous [Ru(dcpe)₂H(η²-O₂)]⁺. Complex **15** is also seen to undergo a similar reaction with oxygen. A ¹H NMR spectrum of a benzene solution of the off-white powder, formed on exposure of **15** to air, shows a quintet at δ -5.94 (*J*_{HP} 21.3 Hz), which is consistent with the reported NMR data⁵⁸, while the ³¹P{¹H} NMR spectrum shows a singlet resonance at δ 66.8 which was

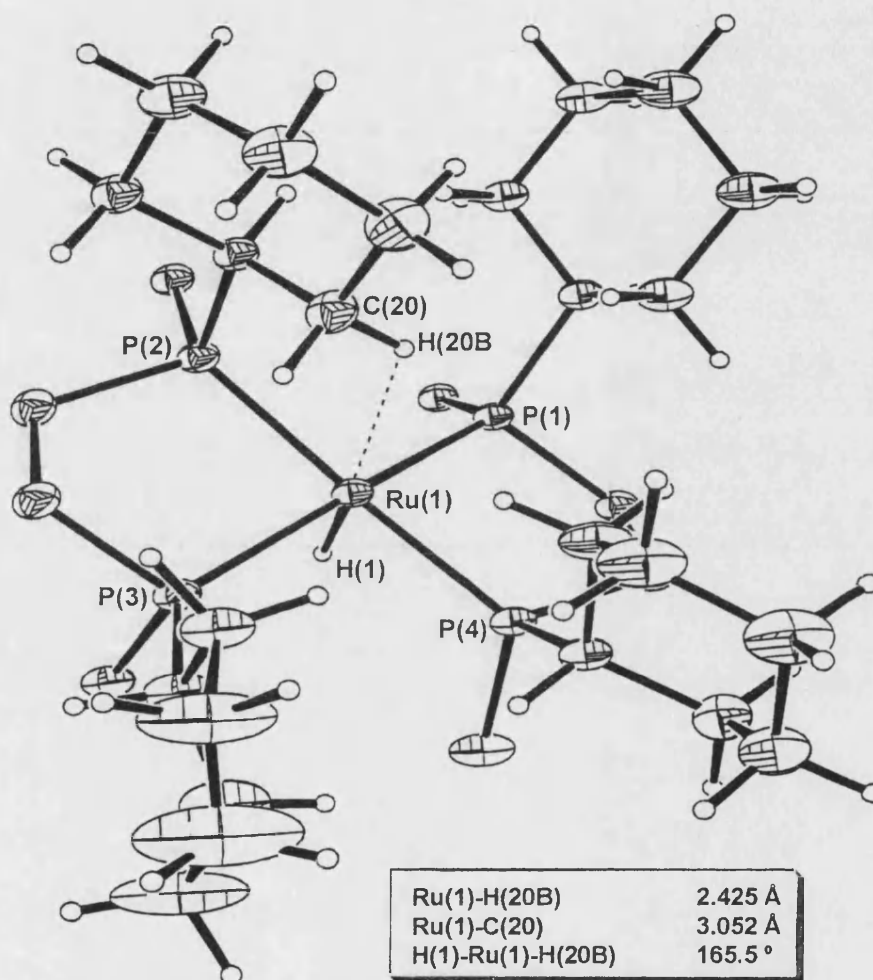
unreported. This addition of O₂ occurs because the five-coordinate ruthenium cation has only 16 electrons so oxygen addition fulfils the 18-electron rule.

This implies that there is a stabilising agostic interaction in the [Ru(dcpe)₂H]⁺ cation. This has been observed by Mezzetti⁵⁵ in the [PF₆] salt. In this crystal structure, two short Ru...H contacts, 2.59(5) Å and 2.84(5) Å, between the Ru and cyclohexyl hydrogens, are observed on the opposite side of the RuP₄ plane to the hydride. The two contacts can interchange with a minor rearrangement. It is proposed that these contacts provide a weak γ-agostic interaction. Analysis of our crystal structure shows a Ru...H-C interaction of 2.42 Å between the metal and a hydrogen on a cyclohexyl ring, in the vacant site (fig 4.30). This implies that a slightly stronger γ-agostic interaction occurs in our cation than in Mezzetti's structure. Mezzetti also states that the agostic interaction is responsible for the position of the Ru metal in relation to the P₄ plane since in the much more crowded crystal structure of *trans*-Ru(dcpe)₂Cl₂ the rotational freedom of the cyclohexyl rings releases the strain.

Ogasawara⁵⁹ and Ashworth⁶⁰ have both shown that coordinatively unsaturated ruthenium complexes can be stabilised by agostic interactions. Ogasawara showed that [RuH(dppb)₂]PF₆ is stabilised by a hydrogen in the backbone of the bidentate ligand and Ashworth reported that [Ru(η³-C₈H₁₃)(P(OMe)Ph₂)₃]PF₆ can be stabilised by a hydrogen from the cycloalkenyl ring. In the latter case the distance of the interaction Ru...H-C is 2.08 Å which is only slightly shorter than the interaction in 15.

Fig 4.30 View of suggested agostic interaction in $[\text{Ru}(\text{dcpe})_2\text{H}]^+$.

Note:- cyclohexyl rings on hydride side of the RuP_4 plane removed for clarity.

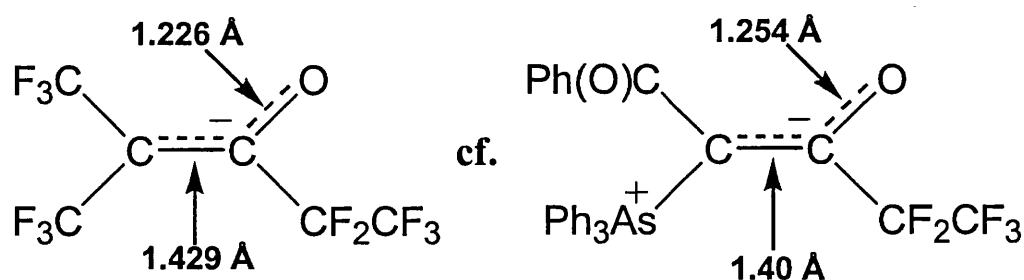


The agostic interaction in $[\text{Ru}(\text{dcpe})_2\text{H}][\text{PF}_6]^{55}$ was also observed in the ^1H NMR spectrum at $-90\text{ }^\circ\text{C}$ as a broad lump at δ -0.36. This implies that some interaction is retained in solution, at least at low temperature, albeit weak. A similar broad lump is seen in the room temperature ^1H NMR spectrum of **15** at $\sim \delta$ -0.6 which again implies that the γ -agostic interaction is slightly stronger in **15**. However, the hydride signal at δ -31.78 is in the range usually attributed to five coordinate complexes whereas related

complexes displaying strong agostic interactions in the vacant site have considerably lower field resonances around δ -12.⁶¹

In the previously structurally uncharacterised perfluoroenolate ion the shortening of the C-O bond (1.226(7) Å) and lengthening of the C=C bond (1.429(9) Å) suggests delocalisation over the C=C-O moiety. A similar delocalisation is seen in the X-ray crystal structure of a fluorinated arsonium ylide, where a negative charge is delocalised over C-C-O system (fig. 4.31).⁶²

Fig 4.31 Comparable bond lengths of perfluoroenolate anion and arsonium ylide



The presence of an oxygen atom in the product led us to investigate its source. The addition of 10 equivalents of degassed water to a 1:1 mixture of **4** and PF2M2P in thf resulted in quantitative conversion of **4** to **15**. Two $^{31}\text{P}\{^1\text{H}\}$ NMR time course experiments were conducted in order to follow the reaction of **4** with PF2M2P: in one case degassed water (10 equivalents) was added (experiment X), and in the second case, water was excluded with the usual degree of care (experiment Y). The stacked spectra of the two reactions are shown in figs. 4.32 and 4.33.

In experiment X, at T = 0 the spectrum displays the starting dihydride **4** as two apparent triplets at δ 65.8 and δ 90.3 but also a small amount of a singlet resonance which was not seen before at δ 75.8. At T = 15 min, most of **4** had disappeared and the

singlet peak at δ 75.8 is the main species present. Also the first sign of **15** is seen as a singlet at δ 73.4. From $T = 30$ mins to $T = 3$ h the amount of **15** increases at the expense of the singlet at δ 75.8 and after 3 h no further change is seen. The peak at δ 75.8, which had not been detected before and displayed a broad hydride resonance at δ -6.18 in the ^1H NMR spectrum is either an intermediate of the reaction or a product of a reversible side reaction between **4** and H_2O . On addition of an excess of PF2M2P it was shown that the yield of **15** was increased at the expense of the singlet at δ 75.8 in a period of 1 h (fig 4.32a).

In comparison experiment Y only showed any reactivity after $T = 45$ mins, with a very small amount of **15** seen at δ 73.4. The amount of **15** gradually increases over 12 h, but is still only seen in a 1:7 ratio with the starting dihydride **4**. A small amount of the singlet at δ 75.8 is observed after 2 h but does not appear in the amount seen in experiment X.

These time course experiments show that the presence of added water not only increases the yield of the conversion from **4** to **15** but also increases the rate at which the conversion occurs. In the case of the added water all the dihydride reacts within 30 mins. Both spectra also display a singlet resonance at δ 75.8 which in experiment X is the main product after 15 mins. This species converts to **15** over time and also by addition of a second equivalent of PF2M2P. It is thought that this species is either an intermediate in the reaction or the product of a reversible reaction between **4** and H_2O . It is thought the latter is the case as the excess of water in experiment X seemed to inhibit the 1:1 reaction of **4** and PF2M2P and meant excess PF2M2P had to be added to increase the yield of **15**.

Fig 4.32 $^{31}\text{P}\{^1\text{H}\}$ NMR time course spectrum for experiment X

Fig 4.32a $^{31}\text{P}\{^1\text{H}\}$ NMR time course spectrum for experiment X after addition of second equivalent of PF2M2P.

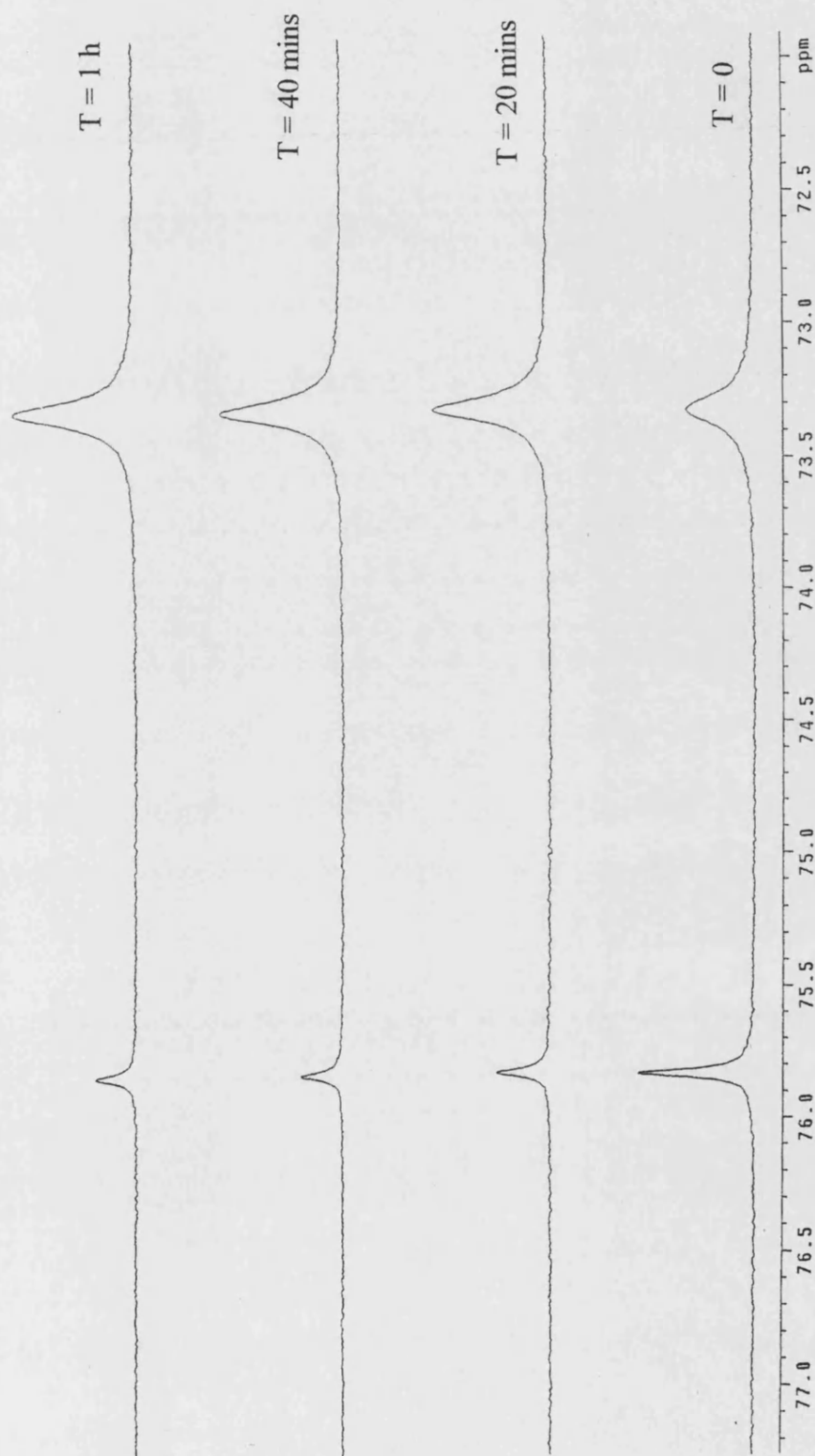
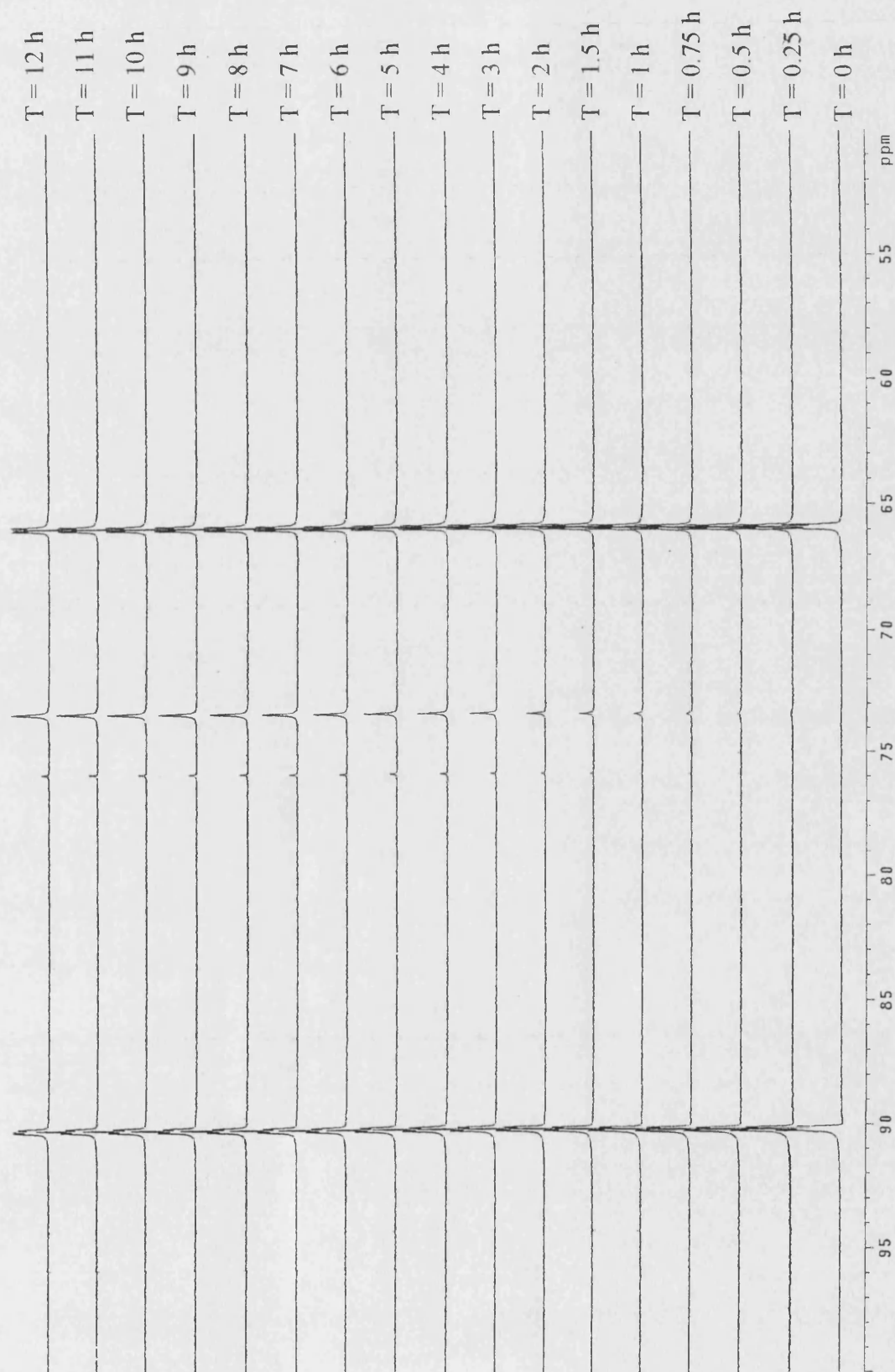


Fig 4.33 $^{31}\text{P}\{^1\text{H}\}$ NMR time course spectrum for experiment Y



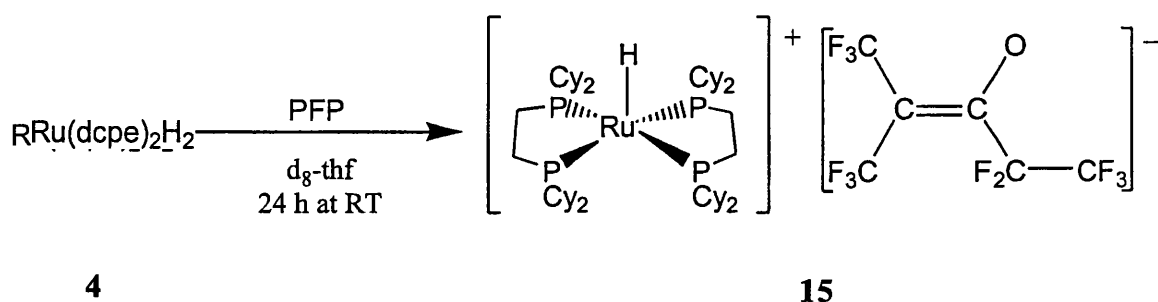
The yield of crystals of **15** from reaction 4.3 in d_6 -benzene was low (27 %), but on repeating the reaction in benzene with 10 equivalents of water present, the solution turned from colourless to orange in less than half an hour with orange crystals in 93 % yield being formed after only 3 h.

These results serve to confirm our suspicions that the presence of an oxygen atom in **15** arises from the presence of adventitious water in the NMR glassware.

4.2.2.2 Reaction of *cis*-Ru(dcpe)₂H₂ (**4**) with perfluoropropene (PFP)

The change in reactivity from **1** to **4** with PF2M2P, led us to expect a similar change in the reactivity from **1** to **4** with PFP. A thf solution of **4** in a J. Youngs resealable NMR tube was placed under 1 atm of PFP (~ 2 equivalents). After 24 h at room temperature, the solution had become an orange colour similar to that observed in the reaction with PF2M2P. Analysis of the ³¹P {¹H} and ¹H NMR spectra indicated the formation of the [Ru(dcpe)₂H]⁺ cation. However, in the ¹⁹F NMR spectrum, instead of seeing a perfluoropropenolate, as we might have expected, we found the same four signals that were observed in reaction 4.3.

Reaction 4.4



This implied that $[(\text{CF}_3)_2\text{C}=\text{C}(\text{O})\text{CF}_2\text{CF}_3]^-$ had been formed as the counterion again. It would appear that the perfluoropropene undergoes a dimerisation in the course of the reaction to yield the perfluoroenolate ion. The fact that a dimerisation occurs would suggest that the reaction proceeds via a nucleophilic attack on the PFP, leading to a fluorocarbanion which can then dimerise.

Addition of an excess of degassed water to this reaction shows an increase in the conversion of **4** to **15** as seen for reaction 4.3, which implies that the presence of water facilitates the reaction, and that in the absence of added water, adventitious water from the glassware or solvent is responsible for the formation of **15**.

The conversion of **4** to **15**, using PF2M2P in 27 % yield would appear too high for the reaction to be facilitated by ‘adventitious water’ as suggested. However, the reactions of both *cis*-Ru(dmpe)₂H₂ and *cis*-Ru(dcpe)₂H₂ with the perfluoroalkenes were conducted on NMR tube scales, typically with 10-15 mg starting material. Thus, under these small-scale conditions, the presence of ‘adventitious water’ on the glassware (NMR solvents were dried from potassium/benzophenone, liquid perfluoroalkene from 4 Å molecular sieves) could be sufficient to give a respectable 27% yield of product in reaction 4.3.

4.3 Discussion

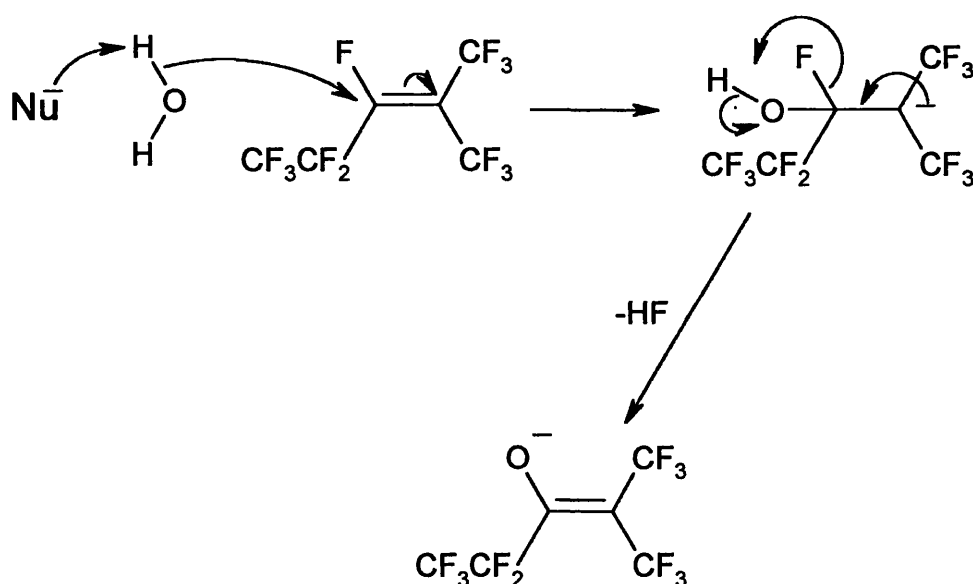
The results show that the activity of ruthenium dihydrides towards perfluoroalkenes can be greatly affected by a change in the substituent ‘ears’ on the bidentate phosphines ligands.

The formation of *cis*-Ru(dmpe)₂F(F..HF), **14**, from the reaction of **1** with perfluoroalkenes is in complete contrast to the reaction of **1** with hexafluorobenzene and saturated perfluorocarbons. Both hydrides are seen to be active and are replaced by fluorines in the course of the reaction. The fluoroorganic products formed from the reaction of **1** and PFP show activation of vinylic fluorines at the CF₂ site only. This would suggest that the mechanism of the reaction proceeds via a nucleophilic or free radical attack (see introduction). It may also be possible that we get an insertion of the alkene into the Ru-H bond similar to the insertion seen for the iridium hydrides^{37,38}, followed by elimination of a partially fluorinated product. The main fluoroorganic products from the reaction of **1** with PF2M2P are four isomers of the formula C₆F₉H₃ where three fluorines are replaced by hydrogen. Again these come about by a nucleophilic or radical attack at the vinylic fluorine. A further attack on the double bond by another hydrogen nucleophile or radical creates two new vinylic fluorines, which themselves can be replaced.

The reaction of *cis*-Ru(dcpe)₂H₂, **4**, with both perfluoroalkenes leads to the formation of a five coordinate ruthenium monohydride cation and a perfluoroenolate anion, [Ru(dcpe)₂H][(CF₃)₂C=C(O)CF₂CF₃], **15**. The ruthenium cation appears to have a weak γ -agostic interaction between the Ru and a cyclohexyl hydrogen of 2.425 Å which was tentatively identified in the ¹H NMR spectrum. The formation of the perfluoroenolate anion in reactions with both these alkenes and the necessity for water

to be present suggests that the reaction proceeds by a nucleophilic addition. The formation of the cationic monohydride leads us to propose that the basic dihydride deprotonates water, forming a dihydrogen hydride complex, which can readily lose H_2 to yield the monohydride species, and an ^-OH group, which attacks PF2M2P at the carbon containing the vinylic fluorine. A further rearrangement sees the elimination of HF, a strong driving force, which yields the perfluoroenolate (fig.4.34)

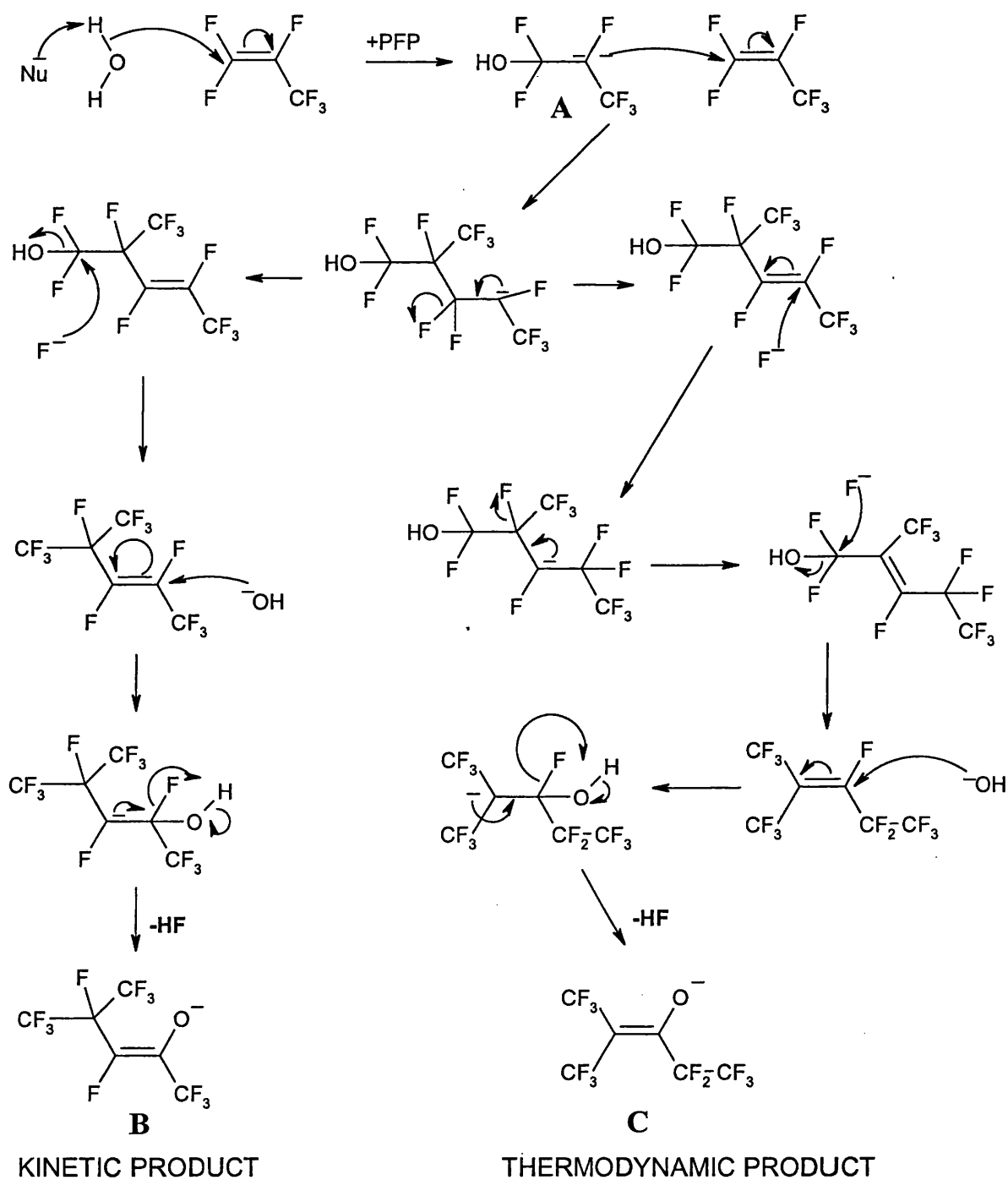
Fig 4.34 Proposed reaction mechanism reaction of 4 with PF2M2P



The fact that the same product is seen when we start with PFP is not surprising, if the mechanism for dimerisation to PF2M2P is taken into consideration.⁶ This is initiated by nucleophilic attack by a fluoride ion. This forms the $(\text{CF}_3)_2\text{CF}^-$ carbanion, which reacts with another molecule of PFP to form perfluoro-4-methyl-2-pentene as the kinetic product, and then the thermodynamically favoured PF2M2P via a rearrangement. It is suggested here that attack by the ^-OH forms a similar carbanion (A), which reacts with another PFP molecule, and a series of rearrangements occur to

give both a kinetically favoured perfluoroenolate (**B**) and the thermodynamically favoured perfluoroenolate (**C**) seen in the reaction of **4** with PF2M2P (fig. 4.35).

Fig. 4.35 Proposed mechanism for reaction of **4** with PFP



In this proposed reaction mechanism formation of two different products is possible. This accounts for the fact that crystals, obtained from the reaction, were unsuitable for X-ray diffraction as a small amount of the kinetically favoured perfluoroenolate is present. Again in both mechanisms, the elimination of HF is seen, which drives the reaction process.

On submitting a paper⁶³ on the above work, we were asked how the presence of adventitious water could give a yield of 27 % in the conversion of **4** to **15**. The reactions of both *cis*-Ru(dmpe)₂H₂ and *cis*-Ru(dcpe)₂H₂ with the perfluoroalkenes were conducted on NMR tube scales, typically with 10-15 mg starting material. Thus, under these small-scale conditions, the presence of ‘adventitious water’ on the glassware (NMR solvents were dried from potassium/benzophenone, liquid perfluoroalkene from molecular sieve) could be sufficient to give a respectable 27% yield of product in reaction 4.3. We have performed the reactions of the perfluoroalkenes with **1** or **4** side by side, using both standard Schlenk and high-vacuum techniques, and also in a glovebox, to ensure that the two processes do genuinely proceed differently i.e. if ‘adventitious water’ is present in one case, then it is also present in the other. Finally, when we took stringent precautions and flame dried all glassware, we did reduce the yield of [Ru(dcpe)₂H][(CF₃)₂C=C(O)CF₂CF₃] down to tiny amounts (ca. < 5%), in contrast to reaction 4.1 which affords Ru(dmpe)₂F(F..HF) in the same yield found under less stringent conditions. Thus, we are confident, that the reaction of perfluoroalkenes with **1** or **4** proceed via different routes.

4.4 Conclusions

- *cis*-Ru(dmpe)₂H₂, **1**, reacts quickly at room temperature with both PFP and PF2M2P to give the novel *cis*-Ru(dmpe)₂(FHF)F, **14**, species.
- The fluoroorganic products of these reactions, in both cases, are lesser fluorinated alkenes.
- *cis*-Ru(dcpe)₂H₂, **4**, reacts at room temperature with both PFP and PF2M2P to give the five-coordinate ruthenium monohydride cation [Ru(dcpe)₂H]⁺ and a perfluoroenolate anion, [(CF₃)₂C=C(O)CF₂CF₃]⁻.
- The rate of reaction of **4** with both PFP and PF2M2P is increased in the presence of degassed water. The water also increases the yield of the product, [Ru(dcpe)₂H][(CF₃)₂C=C(O)CF₂CF₃], **15**.

References

1. Whittlesey, M. K.; Perutz, R. N.; Moore, M. H. *Chem. Commun.*, **1996**, 787;
Whittlesey, M. K.; Perutz, R. N.; Greener, B.; Moore, M. H. *Chem. Commun.*, **1997**, 187.
2. Montgomery, L. K.; Schueller, K.; Bartlett, P. D. *J. Am. Chem. Soc.*, **1964**, 86, 622.
3. Chambers, R. D. *Fluorine in Organic Chemistry* (Wiley, 1973) pp 140-142.
4. Banks, R. E. *Fluorocarbons and their Derivatives* (Oldbourne, 1964) Ch 2.
5. Dresdner, R. D.; Tlumac, R. N.; Young, J. A. *J. Org. Chem.*, **1965**, 30, 3524.
6. Brunskill, W.; Flowers, W. T.; Gregory, R.; Haszeldine, R. N. *Chem. Commun.*, **1970**, 1444.
7. Chambers, R. D.; Lindley, A. A.; Fielding, H. C.; Moilliet, J. S.; Whittaker, G. *J. Chem. Soc., Perkin Trans. 1*, **1981**, 1064.
8. Ishikawa, N.; Nagashima, A. *Bull. Chem. Soc. Jpn.*, **1976**, 49(2), 502.
9. Smart, B. E.; Middleton, W. J.; Farnham, W. B. *J. Am. Chem. Soc.*, **1986**, 108, 4905.
10. Chambers, R. D.; Magron, C.; Sandford, G. *J. Chem. Soc., Perkin Trans. 1*, **1999**, 283.
11. Bayliff, A. E.; Chambers, R. D. *J. Chem. Soc., Perkin Trans. 1*, **1988**, 201.
12. Suzuki, H.; Satake, H.; Uno, H.; Shimizu, H. *Bull. Chem. Soc. Jpn.*, **1987**, 60, 4471.
13. Andreades, S. *J. Org. Chem.*, **1962**, 27, 4163.
14. Temple, S. *J. Org. Chem.*, **1968**, 33(1), 344.
15. Flowers, W. T.; Haszeldine, R. N.; Owen, C. R.; Thomas, A. *J. Chem. Soc., Chem. Comm.*, **1974**, 134.
16. Ono, T.; Henderson, P. B.; *Chem. Commun.*, **1996**, 763.

17. Yanagida, S.; Noji, Y.; Okahara, M. *Tetrahedron Lett.*, **1977**, 2337.
18. Ikeda, I.; Umino, M.; Okahara, M. *J. Org. Chem.*, **1986**, *51*, 569, and references therein.
19. Banks, R. E.; Hitchen, S. M. *J. Chem. Soc., Perkin Trans. 1*, **1982**, 1593.
20. Miller, Freedman, Fried, Koch, *J. Am. Chem. Soc.*, **1961**, *83*, 4105; Miller, Freedman, *J. Am. Chem. Soc.*, **1963**, *85*, 180.
21. Park, J. D.; Stefani, A. P.; Crawford, G. H.; Lacher, J. R. *J. Org. Chem.*, **1961**, *26*, 3316.
22. Bagley, E.; Birchall, J. M.; Haszeldine, R. N. *J. Chem. Soc. (C)*, **1966**, 1232.
23. Scherer, K.; Terranova, T. F.; Lawson, D. D. *J. Org. Chem.*, **1981**, *46*, 2379.
24. Martin, K. V. *J. Chem. Soc.*, **1964**, 2944.
25. Cundy, C. S.; Green, M.; Stone, F. G. A. *J. Chem. Soc. (A)*, **1970**, 1647.
26. Maples, P. K.; Green, M.; Stone, F. G. A. *J. Chem. Soc., Dalton Trans.*, **1973**, 388.
27. Burt, R.; Cooke, M.; Green, M. *J. Chem. Soc. (A)*, **1970**, 2975.
28. Huang, Y.; Li, J.; Zhou, J.; Zhu, Z.; Hou, G. *J. Organomet. Chem.*, **1981**, *205*, 185.
29. Guggenberger, L. J.; Cramer, R. *J. Am. Chem. Soc.*, **1972**, *94*, 3779.
30. Clark, H. C.; Tsai, J. H. *J. Chem. Soc., Chem. Comm.*, **1965**, *6*, 111.
31. Miller Jr., W. T.; Burnard, R. J. *J. Am. Chem. Soc.*, **1968**, *90*, 7367.
32. Jolly, P. W.; Bruce, M. I.; Stone, F. G. A. *J. Chem. Soc.*, **1965**, 5830.
33. Blackmore, T.; Bruce, M. I.; Stone, F. G. A. *J. Chem. Soc. (A)*, **1968**, 2158.
34. Brisdon, A. K.; Banger, K. K. *J. Fluorine Chem.*, **1999**, *100*, 35. and references therein.
35. Greco, A.; Green, M.; Stone, F. G. A. *J. Chem. Soc. (A)*, **1971**, 3476.

36. Howard, J. A. K.; Knox, S. A. R.; Terrill, N. J.; Yates, M. I. *J. Chem. Soc., Chem. Comm.*, **1989**, 640.
37. Thrasher, J. S.; Strauss, S. H. *Inorganic Fluorine Chemistry – Towards the 21st Century*, ACS Symposium series no. 555, **1994**, Ch. 15.
38. Watson, P. L.; Tulip, T. H.; Williams, I. *Organometallics*, **1990**, *9*, 1999.
39. Siedle, A. R.; Newmark, R. A. *Organometallics*, **1989**, *8*(6), 1442.
40. Peterson, T. H.; Golden, J. T.; Bergman, R. G. *Organometallics*, **1999**, *18*, 2005.
41. Kraft, B. M.; Lachicotte, R. J.; Jones, W. D. *J. Am. Chem. Soc.*, **2000**, *122*, 8559.
42. gNMR NMR simulation software v.4.0.1. ©1995-8. Budzelaar P.H.M. Published by Cherwell Scientific.
43. Barthazy, P.; Stoop, R. M.; Worle, M.; Togni, A.; Mezzetti, A. *Organometallics*, **2000**, *19*, 2844.
44. Thrasher, J. S.; Strauss, S. H. *Inorganic Fluorine Chemistry – Towards the 21st Century*, ACS Symposium series no. 555, **1994**, Ch. 20, p328. Coupling constants obtained by private communication with Dr. Paul Watson at the Universität Bremen, Germany.
45. Dierkes, P.; van Leeuwen, P. W. N. M. *J. Chem. Soc., Dalton Trans.*, **1999**, 1519.
46. Nicasio, M. C.; Perutz, R. N.; Walton, P. H. *Organometallics*, **1997**, *16*, 1410.
47. Coleman, K. S.; Fawcett, J.; Holloway, J. H.; Hope, E. G.; Russell, D. R. *J. Chem. Soc., Dalton Trans.*, **1997**, 3557.
48. Roe, D. C.; Marshall, W. J.; Davidson, F.; Soper, P. D.; Grushin, V. V. *Organometallics*, **2000**, *19*, 4575.
49. Jasim, N. A.; Perutz, R. N. *J. Am. Chem. Soc.*, **2000**, *122*, 8685.

50. Murphy, V. J.; Hascall, T.; Chen, J. Y.; Parkin, G. *J. Am. Chem. Soc.*, **1996**, *118*, 7428.
51. Murphy, V. J.; Rabinovich, D.; Hascall, T.; Klooster, W. T.; Koetzle, T. F.; Parkin, G. *J. Am. Chem. Soc.*, **1998**, *120*, 4372.
52. Braun, T.; Foxon, S. P.; Perutz, R. N.; Walton, P. H. *Angew. Chem. Int. Ed.*, **1999**, *38*, 3326.
53. Snegirev, V. F.; Makarov, K. N.; Zabolotskikh, V. F.; Sorokina, M. G.; Knunyants, I. L. *Bull. Acad. Sci. USSR Div. Chem. Sci. (Engl.)*, **1983**, *32(12)*, 2489.
54. Burton, D. J.; Spawn, T. D.; Heinze, P. L.; Bailey, A. R.; Shin-Ya, S. *J. Fluorine Chem.*, **1989**, *44*, 167; Montanari, V.; DesMarteau, D. D. *J. Org. Chem.*, **1992**, *57*, 5018.
55. Winter, R. F.; Hornung, F. M. *Inorg. Chem.*, **1997**, *36*, 6197.
56. Marteletti, A.; Gramlich, V.; Zürcher, F.; Mezzetti, A. *New J. Chem.*, **1999**, 199.
57. Snegirev, V. F.; Galakhov, M. V.; Petrov, V. A.; Makarov, K. N.; Bakhmutov, V. I. *Bull. Acad. Sci. USSR Div. Chem. Sci. (Engl.)*, **1986**, *35(6)*, 1194.
58. Jiminez-Tenorio, M.; Puerta, M. C.; Valerga, P. *J. Am. Chem. Soc.*, **1993**, *115*, 9794; Jiminez-Tenorio, M.; Puerta, M. C.; Valerga, P. *Inorg. Chem.*, **1994**, *33*, 3515.
59. Ogasawara, M.; Aoyagi, K.; Saburi, M. *Organometallics*, **1993**, *12*, 3393.
60. Ashworth, T. V.; Liles, D. C.; Singleton, E. *Organometallics*, **1984**, *3*, 1851.
61. Ogasawara, M.; Saburi, M. *Organometallics*, **1994**, *13*, 1911.
62. Burton, D. J.; Yang, Z.-Y.; Qui, W. *Chem. Rev.*, **1996**, *96*, 1641.

Chapter 5

Experimental Section

5 Experimental

5.1 General methods

All manipulations of oxygen sensitive compounds were carried out using air and moisture free gloveboxes or standard Schlenk techniques in an argon atmosphere. All solvents were distilled and stored under nitrogen; from Na (hexane, diethylether, toluene), Na and benzophenone (thf, benzene), Mg/I₂ (methanol and ethanol), CaH₂ (*sec*-butanol, *tert*-butanol). NMR solvents were purchased from Aldrich Chemicals Ltd. and dried (Na and benzophenone for d₆-benzene, d₈-toluene and d₈-thf, CaH₂ for d₂-dichloromethane), degassed and stored under argon. The phosphines Me₂PCH₂CH₂PMe₂ (dmpe), Et₂PCH₂CH₂PEt₂ (depe), Me₂PCH₂PMe₂ (dmpm), and PMe₃ were purchased from Strem Chemicals Inc and used without further purification. Ph₂PCH₂CH₂PPh₂ (dppe) was purchased from Aldrich Chemicals Ltd and recrystallised from hot ethanol prior to use. Cy₂PCH₂CH₂PCy₂ (dcpe) was kindly donated by Dr. J. Lynam (University of Bath). Perfluorocarbon liquids were purchased from Fluorochem Ltd. and Aldrich Chemicals Ltd. and were dried over 4 Å molecular sieves and degassed prior to use. Perfluoropropene gas was purchased from Aldrich Chemical Ltd. and used without any purification.

The metal salt RuCl₃.xH₂O was loaned by Johnson Matthey Plc. The ruthenium starting materials, RuCl₂(PPh₃)₃, [Ru(COD)Cl₂]₂ and Ru(DMSO)₄Cl₂ were all prepared according to literature methods.¹

Physical and analytical measurements

NMR spectra were recorded on JEOL GX-270 MHz FT-NMR and Varian Mercury 400 MHz NMR spectrometers. The ^{31}P NMR spectra were referenced to external 85 % H_3PO_4 . The ^1H NMR spectra were reference to deuterated solvents used in the reactions. The ^{19}F NMR spectra were referenced to external CFCl_3 . IR spectra were recorded on a Nicolet Nexus FT-IR spectrometer as nujol mulls. Elemental analyses were carried out at the University of Bath. Electrospray mass spectra were recorded on a Fison VG Autospec mass spectrometer in a 1:1 $\text{H}_2\text{O}/\text{CH}_3\text{OH}$ with 1 % acetic acid. Gas Chromatography was carried out on a Fisons 8000 GC and GC-MS recorded by Dr. Trevor Dransfield on a Fison VG Autospec mass spectrometer at the University of York. Cyclic voltammetry was performed with a Hi-Tek Instruments DT2101 potentiostat in conjunction with a Hi-Tek Instruments Waveform PPRI generator, with the help of Dr C. Pickett and Dr. S. Ibrahim and the Nitrogen Fixation Laboratory, John Innes Research Park, Norwich.

5.2 Preparation of the ruthenium bis(diphosphine) dihydrides.

5.2.1 *cis*- $\text{Ru}(\text{dmpe})_2\text{H}_2$ (1)

An argon filled three-necked round bottom flask was charged with 0.56 g (2.1 mmol) of $\text{RuCl}_3 \cdot x\text{H}_2\text{O}$, and magnetic stirrer bar. 100 mL of dry ethanol was then added followed by the addition of 1,2-bis(dimethylphosphino)ethane (dmpe) (1 g, 6.7 mmol). The dark solution was then refluxed under argon for ca. 3 h or until a bright orange colour was seen. The air stable solution was filtered while hot and the solvent removed using a rotary evaporator. Orange crystals of *trans*- $\text{Ru}(\text{dmpe})_2\text{Cl}_2$ were obtained by recrystallisation from a 3:1 ethanol/water solvent mixture. Yield from three recrystallisations, 0.622 g (56.5 %).

0.300 g (0.64 mmol) of *trans*-Ru(dmpe)₂Cl₂ was transferred to an argon filled ampoule and dissolved in 10 mL dry THF. ~0.3 g of Na metal (~ 20 equivalents) was added, the solvent degassed and placed under 1 atm of H₂. The solution was stirred for ~ 2 days until a dark purple/black colouration was seen. Addition of H₂ was repeated if necessary. The solvent was removed and the remaining solid extracted with 3 x 10 mL dry hexane. The hexane was removed and Ru(dmpe)₂H₂ isolated as a white solid (20:1 *cis/trans*, 0.170 g, 66.1 %) upon vacuum sublimation (Hg diffusion pump, 80 °C, dry ice/acetone cold finger). ³¹P{¹H} NMR (C₆D₆): *cis* AA'BB' δ 48.4 (t, *J*_{PP} 20.1 Hz), 39.4 (t, *J*_{PP} 20.1 Hz); *trans* δ 50.2 (s). ¹H NMR (C₆D₆): *cis* δ -9.76 (m); *trans* δ -10.55 (qnt, *J*_{HP} 20.6 Hz).

5.2.2 *cis*-Ru(depe)₂H₂ (2)

A similar procedure to 5.2.1 was used to prepare 2. RuCl₃.xH₂O (0.43 g, 1.64 mmol) was suspended in 100 mL of dry ethanol and 1,2-bis(diethylphosphino)ethane, (depe) (1 g, 4.85 mmol) added. The dark solution was then refluxed under argon for ca. 3 h or until a bright orange colour was seen. The air stable solution was filtered while hot. The solvent was removed using a rotary evaporator, and *trans*-Ru(depe)₂Cl₂ obtained as orange crystals (0.574 g, 57.6 %) by recrystallisation from a 3:1 ethanol/water solvent mixture.

0.300 g (0.51 mmol) of *trans*-Ru(depe)₂Cl₂ was transferred to an argon filled ampoule and dissolved in 10 mL dry THF. ~0.3 g of Na metal was added, the solvent degassed and placed under 1 atm of H₂. The solution was stirred until a dark purple/black colouration was seen. The solvent was removed and the remaining solid extracted with 3 x 10 mL dry hexane. The hexane solution was reduced to ~ 3 mL and 0.120 g (45.4 %) of Ru(depe)₂H₂ was obtained as white crystalline blocks (4:1 *cis/trans*)

upon cooling to $-78\text{ }^{\circ}\text{C}$. $^{31}\text{P}\{^1\text{H}\}$ NMR (C_6D_6): *cis* AA'BB' δ 77.1 (t, J_{PP} 18.15 Hz), 64.3 (t, J_{PP} 18.2 Hz); *trans* δ 85.2 (s). ^1H NMR (C_6D_6): *cis* δ -10.53 (m); *trans* δ -10.12 (qnt, J_{HP} 19.7 Hz).

5.2.3 *cis*-Ru(dmpm) $_2$ H $_2$ (3)

The complex was prepared using the literature method reported by Hartwig et al.² Using a pestle and mortar, 1.5 g (1.56 mmol) $\text{Ru}(\text{PPh}_3)_3\text{Cl}_2$ was ground together with 2.11 g (15.5 mmol) $\text{Na}(\text{OAc})\cdot 3\text{H}_2\text{O}$ and then refluxed under argon in 100 mL dry *tert*-BuOH for 1 h to form an orange precipitate. The solution was cooled to $\sim 30\text{ }^{\circ}\text{C}$ and the liquid decanted off. The remaining small orange crystals were washed into a sinter with diethyl ether and subsequently washed with water, methanol and diethyl ether. The orange product was dried in vacuo yielding 0.817 g (62.1 %) $\text{Ru}(\text{PPh}_3)_2(\text{OAc})_2$.

In an ampoule, 400 mg (0.54 mmol) $\text{Ru}(\text{PPh}_3)_2(\text{OAc})_2$ was suspended in 10 mL hexane. 170 μL (1.07 mmol) of 1,2-bis(dimethylphosphino)methane (dmpm) was then added to the ampoule and the suspension heated for 6 h at $60\text{--}65\text{ }^{\circ}\text{C}$ until a pale yellow solid formed. The solvent was filtered off and the solid residue washed with hexane. The solid, $[(\eta^2, \mu^2\text{-dmpm})(\eta^2, \mu^1\text{-dmpm})\text{Ru}(\eta^1\text{-OAc})_2]_2$ was dried under vacuum (0.216 g, 82.0 %) and then suspended in 10 mL dry benzene. The suspension was degassed using three freeze-pump-thaw cycles and heated under vacuum at $100\text{--}110\text{ }^{\circ}\text{C}$ for 2 h until the yellow solution became homogeneous. The solvent was then removed leaving 180 mg (83.3 %) of *cis*-Ru(dmpm) $_2$ (OAc) $_2$, as a yellow solid.

180 mg (0.37 mmol) of *cis*-Ru(dmpm) $_2$ (OAc) $_2$ was suspended in 10 mL diethyl ether. 183 μL (0.18 mmol) of a 1.0 M LiAlH_4 solution in Et_2O was added and the solution stirred for 3 h. The solvent was removed and the solid extracted with hexane (3

x 5 mL). The hexane was removed under vacuum to yield 60 mg (40.1 %) of *cis*-Ru(dmpm)₂H₂ as a pale yellow powder, judged pure by NMR spectroscopy. ³¹P{¹H} NMR (C₆D₆): AA'BB' δ -16.4 (t, *J*_{PP} 46.5 Hz), -28.9 (t, *J*_{PP} 46.5 Hz). ¹H NMR (C₆D₆): δ -8.24 (dq, *J*_{HP} 77.8 Hz, *J*_{HP} 22.2 Hz).

5.2.4 *cis*-Ru(dcpe)₂H₂ (4)

Complex 4 was prepared according to the literature method of Grubbs et al.³ A Schlenk tube was charged with 200 mg (0.47 mmol) of dcpe, 66 mg (0.12 mmol) [Ru(COD)Cl₂]₂, 189 mg (4.73 mmol) of NaOH, and a magnetic stirrer bar. 30 mL of degassed *sec*-butanol was then added to form a brown suspension. The suspension was heated at 80 °C under a slight vacuum for 3 h or until a white suspension was observed. Degassed water (20 mL) was then added to dissolve up the excess NaOH/NaCl. The suspension was filtered over a medium porosity collection frit and washed with 3 x 10 mL dry methanol. The off white solid was then dried in vacuo yielding 120 mg (54.1 %) of spectroscopically pure *cis*-Ru(dcpe)₂H₂. ³¹P{¹H} NMR (C₆D₆): AA'BB' δ 65.8 (t, *J*_{PP} 13.0 Hz), 90.2 (t, *J*_{PP} 13.0 Hz). ¹H NMR (C₆D₆): δ -12.31 (m).

5.2.5 *cis*-Ru(dppe)₂H₂ (5)

Complex 5 was prepared using the procedure reported by Bautista et al.⁴ 0.500 g of Ru(DMSO)₄Cl₂ (1.03 mmol) and 0.830 g (2.02 mmol) dppe were dissolved in 20 mL of dichloromethane and stirred for 2 h. The yellow solution was filtered through celite and the solvent removed under vacuum and washed with hexane. The yellow solid, which contained a 3:1 ratio of *cis/trans*-Ru(dppe)₂Cl₂ was redissolved in the least amount of CH₂Cl₂ and layered with hexane. Upon cooling, the solution yielded 0.454 mg (45.4 %) of *cis*-Ru(dppe)₂Cl₂ as small yellow cubic crystals.

In an ampoule, 0.240 g (0.24 mmol) of *cis*-Ru(dppe)₂Cl₂ was dissolved in a mixture of 8 mL THF and 2 mL ethanol. 70 mg (1.03 mmol) of NaOEt was added to the solution, the ampoule placed under 1 atm of H₂, and the solution stirred for 30 mins. The solvent was removed and the yellow solid redissolved in benzene. The solution was filtered through Celite to remove any NaCl, reduced to 2 mL and layered with hexane. Ru(dppe)₂H₂ was precipitated as a cream coloured solid (*cis/trans* 20:1, 0.095 g, 42.6 %). ³¹P{¹H} NMR (C₆D₆): *cis* AA'BB' δ 79.0 (t, *J*_{PP} 15.1 Hz), 65.0 (t, *J*_{PP} 15.1 Hz); *trans* δ 83.4 (s). ¹H NMR (C₆D₆): *cis* δ -8.33 (m); *trans* δ -8.17 (qnt, *J*_{HP} 17.1 Hz).

5.2.6 *cis*-Ru(PMe₃)₄H₂ (6)

Complex 6 was prepared using methods reported by Mainz et al.⁵ and Hartwig et al.⁶ 0.750 g (0.78 mmol) of Ru(PPh₃)₃Cl₂ was ground together with 0.107 g (0.78 mmol) of Na(OAc).3H₂O with a pestle and mortar and exposed to vacuum in a three necked round bottom flask for 30 mins. The flask was then filled with argon and 50 mL of dry *tert*-BuOH. The solution was refluxed for 1 h with rapid stirring, and on cooling, a brown-pink precipitate was formed. The product was isolated by filtration in air and washed successively with Et₂O, water, MeOH and Et₂O and dried under vacuum yielding 0.632 g (81.8 %) of Ru(PPh₃)₃(OAc)Cl.

0.500 g (0.51 mmol) of Ru(PPh₃)₃(OAc)Cl was added to an argon purged Schlenk tube and 50 mL of dry hexane added. To this solution 25 μL (0.26 mmol) of PMe₃ was added and the Schlenk tube sealed under a slight vacuum. The reaction mixture was heated to 80 °C for 1 h. Upon cooling, small white crystals 0.250 g (99 %) of Ru(PMe₃)₄(OAc)Cl were precipitated. These were isolated by filtration, washed with hexane and dried under vacuum.

0.250 g (0.50 mmol) of $\text{Ru}(\text{PMe}_3)_4(\text{OAc})\text{Cl}$ was weighed in to a three-necked round bottom flask dissolved in 50 mL of Et_2O . The solution was stirred and 125 μL (0.25 mmol) of a 1.0 M solution of LiAlH_4 in Et_2O added. The yellow solution was stirred at room temperature for 1 h over which time the solution cleared and a white precipitate formed. The solvent was removed under vacuum and the residue extracted with hexane. The hexane was removed to form 0.096 g (46.9 %) of spectroscopically pure *cis*- $\text{Ru}(\text{PMe}_3)_4\text{H}_2$ as a white powder. $^{31}\text{P}\{^1\text{H}\}$ NMR (C_6D_6): AA'BB' δ 0.1 (t, J_{PP} 26.1 Hz), -7.4 (t, J_{PP} 26.1 Hz). ^1H NMR (C_6D_6): δ -9.71 (m).

5.3 Reactions of ruthenium dihydride complexes with perfluorocarbons

5.3.1 Reactions of *cis*- $\text{Ru}(\text{dmpe})_2\text{H}_2$ (1) with perfluoroalkanes

i) *cis*- $\text{Ru}(\text{dmpe})_2\text{H}_2$ (1) and PFD (1:1); 0.010 g (0.025 mmol) of 1 was added to a J.Youngs NMR tube and dissolved in d_8 -toluene. 6.3 μL (0.025 mmol) of PFD was added to the solution and the NMR tube heated at 85 °C for 21 h. The solution turned yellow and contained *trans*- $\text{Ru}(\text{dmpe})_2(\text{FHF})\text{H}$, 8, as the only inorganic product. $^{31}\text{P}\{^1\text{H}\}$ NMR (d_8 -toluene): δ 46.6 (s, 4 P). ^1H NMR (d_8 -toluene): δ -25.6 (br m, 1 H, Ru-H), 1.34 (s, 12 H, 4 x CH_3), 1.47 (s, 12 H, 4 x CH_3), 1.54 (br s, 4 H, 4 x PCHH), 1.74 (br s, 4 H, 4 x PCHH), 14.22 (t, $^1J_{\text{HF}}$ 274 Hz, 1 H, F-H-F). ^{19}F NMR (d_8 -toluene): Peaks for 8 not seen at 298 K, Unidentified fluoroorganic products seen at δ -104.6 (br), -104.9 (br), -105.3 (br), -107.1 (br), -107.8 (br), -108.3 (br), -128.3 (br), -130.1 (br), -131.2 (br), -135.1 (sh), -135.4 (br), -136.3 (br). Volatiles removed from NMR tube and involatiles dissolved in d_8 -toluene to record ^{19}F - ^{19}F COSY NMR spectrum. This reaction was repeated in d_8 -thf yielding the same products in the same period of time.

ii) ***cis*-Ru(dmpe)₂H₂ (1) and PFD (10:1)**; 0.050 g (0.125 mmol) of **1** was added to a J.Youngs NMR tube and dissolved in d₈-toluene. 3.2 μL (0.0125 mmol) of PFD was added to the solution and the NMR tube heated at 85 °C for 21 h. The solution turned yellow and ³¹P{¹H} and ¹H NMR spectroscopy showed the presence of **1** and **8** in a ratio ~ 6.2:1. ¹⁹F NMR spectroscopy showed no remaining PFD and gave the same fluoroorganic products as detailed in the 1:1 reaction above.

iii) ***cis*-Ru(dmpe)₂H₂ (1) and PFPHPA**; 0.010 g (0.025 mmol) of **1** was added to a J.Youngs NMR tube and dissolved in d₈-toluene. 8.0 μL (0.025 mmol) of PFPHPA was added to the solution and the NMR tube heated at 85 °C for 120 h. The solution turned yellow and ³¹P{¹H} NMR spectroscopy showed that **1** had been completely converted to *trans*-Ru(dmpe)₂(FHF)H, **8**, as the only inorganic product. ¹⁹F NMR: Unidentified fluoroorganic products seen in similar regions as for **1**/PFD reaction but obscured by resonances of PFPHPA.

iv) ***cis*-Ru(dmpe)₂H₂ (1) and PFMCH**; 0.010 g (0.025 mmol) of **1** was added to a J.Youngs NMR tube and dissolved in d₈-toluene. 4.8 μL (0.025 mmol) of PFMCH was added to the solution and the NMR tube heated at 85 °C for three weeks. No reaction was seen by ³¹P{¹H} NMR spectroscopy.

v) ***cis*-Ru(dmpe)₂H₂ (1) and PF1MD**; 0.010 g (0.025 mmol) of **1** was added to a J.Youngs NMR tube and dissolved in d₈-toluene. 6.6 μL (0.025 mmol) of PF1MD was added to the solution and the NMR tube heated at 85 °C for 30 h. The solution turned yellow and contained *trans*-Ru(dmpe)₂(FHF)H, **8**, as the only inorganic product by ³¹P{¹H} NMR spectroscopy. ¹⁹F NMR (d₈-toluene): Unidentified fluoroorganic products at δ -69.6 (m), -69.7 (m), -70.0 (m), -110.9 (br), -113.0 (br), -122.7 (br), -126.0 (br), -131.2 (br), -135.7 (sh), -141.2 (br), -142.5 (br).

vi) *cis*-Ru(dmpe)₂H₂ (1) and PF2MP; 0.010 g (0.025 mmol) of **1** was added to a J.Youngs NMR tube and dissolved in d₈-toluene. 4.9 μL (0.025 mmol) of PFMCH was added to the solution and the NMR tube heated at 85 °C for three weeks. No reaction was seen by ³¹P{¹H} NMR spectroscopy.

vii) *cis*-Ru(dmpe)₂H₂ (1) and PFD plus 5 equivalents of pyridine; 0.010 g (0.025 mmol) of **1** was added to a J.Youngs NMR tube and dissolved in d₆-benzene. 10.1 μL (0.125 mmol) of dry pyridine was added followed by 6.3 μL (0.025 mmol) of PFD. The NMR tube was heated at 85 °C for 21 h. The solution turned yellow and contained *trans*-Ru(dmpe)₂(FHF)H, **8**, and a trace amount of *trans*-[Ru(dmpe)₂(C₅H₅N)H][FHF], **9**. ³¹P{¹H} NMR (d₆-benzene): **8**, δ 46.6 (s); **9**, δ 40.4 (s).

viii) *cis*-Ru(dmpe)₂H₂ (1) and PFD plus 30 equivalents of pyridine; 0.010 g (0.025 mmol) of **1** was added to a J.Youngs NMR tube and dissolved in d₆-benzene. 60 μL (0.743 mmol) of dry pyridine was added followed by 6.3 μL (0.025 mmol) of PFD. The NMR tube was heated at 85 °C for 20 h. The solution turned yellow and ³¹P{¹H} NMR spectroscopy showed that it contained *trans*-[Ru(dmpe)₂(C₅H₅N)H][FHF], **9** in a 2:1 ratio with *trans*-Ru(dmpe)₂(FHF)H, **8**. On leaving the NMR tube to stand at room temperature for one day, 0.007 g (53.8 %) of yellow needle-like crystals of **9** were obtained. ³¹P{¹H} NMR (d₆-benzene): **9**, δ 40.4 (s, 4 P). ¹H NMR (d₆-benzene): δ - 20.80 (qnt, ²J_{HP} 20.8 Hz, 1H, Ru-H), 1.0-1.7 (br m, 28 H, dmpe H), 6.67 (m, 2 H, *meta* pyridine H), 7.00 (m, 1 H, *para* pyridine H), 8.54 (m, 2 H, *ortho* pyridine H), 17.8 (t, ¹J_{HF} 117 Hz, 1 H, F-H-F). ¹⁹F NMR (d₆-benzene): δ -148 (br d, ¹J_{FH} 117 Hz, F-H-F). IR (Nujol): 1925 (m, ν(Ru-H)), 1591 (w, ν (FHF)) cm⁻¹. Elemental analysis, found (calculated): %C 38.6 (39.2), %H 7.60 (7.48), %N 2.70 (2.74).

ix) *cis*-Ru(dmpe)₂H₂ (1) and PFD plus 5 equivalents of Et₃N; 0.010 mg (0.025 mmol) of **1** was added to a J.Youngs NMR tube and dissolved in d₆-benzene. 17.5 μL (0.125

mmol) of dry Et₃N was added followed by 6.3 μL (0.025 mmol) of PFD. The NMR tube was heated at 85 °C for 25 h. The solution turned yellow and contained *trans*-Ru(dmpe)₂(FHF)H, **8**, as the only inorganic product.

x) *cis*-Ru(dmpe)₂H₂ (1) and PFD plus 20 equivalents of Et₃N; 0.010 g (0.025 mmol) of **1** was added to a J.Youngs NMR tube and dissolved in d₆-benzene. 58 μL (0.50 mmol) of dry Et₃N was added followed by 6.3 μL (0.025 mmol) of PFD. The NMR tube was heated at 85 °C for 26 h. The solution turned yellow and contained a new ruthenium phosphine hydride product in a 1:1 ratio with *trans*-Ru(dmpe)₂(FHF)H, **8**. ³¹P{¹H} NMR (d₆-benzene): δ 45.5 (s). ¹H NMR (d₆-benzene): δ -27.8 (br m, 1H, Ru-H). ¹⁹F NMR (d₆-benzene): δ -179 (br s), and unidentified fluoroorganic products seen in the reaction of **1** and PFD.

xi) *cis*-Ru(dmpe)₂H₂ (1) and PFD with and without 5 equivalents of 9,10-dihydroanthracene; NMR tube A: 0.010 g (0.025 mmol) of **1** was added to a J.Youngs NMR tube and dissolved in d₈-toluene and 6.3 μL (0.025 mmol) of PFD was added. NMR tube B: 0.010 g (0.025 mmol) of **1** and 0.022 g (0.125 mmol) of 9,10-dihydroanthracene were added to a J.Youngs NMR tube and dissolved in d₈-toluene. 6.3 μL (0.025 mmol) of PFD was then added. Both tubes were heated, side by side, at 85 °C. Complete conversion of **1** to **8** was found in in 21 h according to ³¹P{¹H} NMR spectroscopy. PFD and unidentified fluoroorganic products as seen in reaction of **1** and PFD were also present.

xii) *cis*-Ru(dmpe)₂H₂ (1) and PFD with FEP lining in NMR tube; 0.010 g (0.025 mmol) of **1** was added to a J.Youngs NMR tube that had been lined with a length of sealed FEP tubing. Addition of d₈-toluene and 6.3 μL (0.025 mmol) of PFD followed by thermolysis for 21 h at 85 °C gave the same products as seen in the reaction of **1** and PFD.

5.3.2 Reactions of *cis*-Ru(depe)₂H₂ (2) with perfluorocarbons

i) *cis*-Ru(depe)₂H₂ (2) and hexafluorobenzene; 0.010 g (0.019 mmol) of 2 was added to a J.Youngs resealable NMR tube, dissolved in d₆-benzene and 2.2 μL (0.019 mmol) of C₆F₆ was added. After 3 days at room temperature, the solution had turned from colourless to yellow and 2 had been converted to a 4:1 ratio of *trans*-Ru(depe)₂(C₆F₅)H, 10, and *trans*-Ru(depe)₂(FHF)H, 11.

trans-Ru(depe)₂(C₆F₅)H 10; ³¹P{¹H} NMR (d₆-benzene): δ 71.6 (t, *J*_{PF} 9.5 Hz). ¹H NMR (d₆-benzene): δ -15.16 (tqnt, *J*_{HF} 11.0 Hz, *J*_{HP} 21.9 Hz, Ru-*H*), 0.56 (t, *J*_{HH} 8.2 Hz, 12 H, 4 x CH₃), 1.07 (t, *J*_{HH} 8.7 Hz, 12 H, 4 x CH₃), 1.32 (br m, 8 H, 4 x PCH₂CH₃), 1.59 (br m, 8 H, 4 x PCH₂CH₃), 1.65 (m, 4 H, 4 x PCHH), 2.31 (m, 4 H, 4 x PCHH). ¹⁹F NMR (d₆-benzene): δ -92.8 (m, 2 F, *ortho* C₆F₅), δ -162.5 (m, 2 F, *meta* C₆F₅), δ -163.7 (t, *J*_{FF} = 20.3 Hz, 1 F, *para* C₆F₅). IR (Nujol): 1899 cm⁻¹ ν (Ru-H). 10 was obtained virtually free of any 11 by adding 10 equivalents of Et₃N prior to the introduction of C₆F₆. The solvent was removed and the yellow solid used for elemental analysis. Found (calculated); %C 45.4 (45.8) %H 7.88 (7.25).

trans-Ru(depe)₂(FHF)H, 11; ³¹P{¹H} NMR (d₆-benzene): δ 67.7 (s). ¹H NMR (d₆-benzene): δ -25.76 (tqnt, *J*_{HF} 31.2 Hz, *J*_{HP} 19.7 Hz, 1 H, Ru-*H*), 0.81 (t, *J*_{HH} 7.0 Hz, 12 H, 4 x CH₃), 1.10 (t, *J*_{HH} 10.0 Hz, 12 H, 4 x CH₃), 1.25 (br m, 8 H, 4 x PCH₂CH₃), 1.62 (br m, 8 H, 4 x PCH₂CH₃), 1.70 (m, 4 H, 4 x PCHH), 2.27 (m, 4 H, 4 x PCHH), 14.45 (t, *J*_{FH} 144.9 Hz, 1 H, F-*H*-F). ¹⁹F NMR (d₆-benzene): δ -429.9 (br m, F-*H*-F). IR (cm⁻¹) (Nujol) 2433, 1881 ν (HF₂). Elemental analysis unobtainable due to rapid decomposition in air.

ii) *cis*-Ru(depe)₂H₂ (2) and PFD; 0.010 g (0.019 mmol) of 2 was added to a J.Youngs resealable NMR tube, dissolved in d₆-benzene and 4.9 μL (0.019 mmol) of PFD was

added. After 69 h at 85 °C the solution had changed from colourless to yellow and $^{31}\text{P}\{^1\text{H}\}$ NMR spectroscopy showed only the presence of **11**. The PFD was only partially converted to new unidentified fluoroorganic products, the same as seen for the reaction of **1** and PFD. ^{19}F NMR (d_6 -benzene): Unidentified fluoroorganic products seen at δ -104.6 (br), -104.9 (br), -105.3 (br), -107.1 (br), -107.8 (br), -108.3 (br), -128.3 (br), -130.1 (br), -131.2 (br), -135.1 (sh), -135.4 (br), -136.3 (br).

iii) **cis-Ru(depe)₂H₂ (2) and PFD (10:1)**; 0.050 g (0.097 mmol) of **2** was added to a J.Youngs NMR tube and dissolved in d_6 -benzene. 2.5 μL (0.010 mmol) of PFD was added to the solution and the NMR tube heated at 85 °C for 69 h. The solution turned yellow and $^{31}\text{P}\{^1\text{H}\}$ and ^1H NMR showed presence of **2** and **11** in a ratio ~ 5.7:1. ^{19}F NMR: No remaining PFD. Unidentified fluoroorganic products as detailed in 1:1 reaction.

iv) **cis-Ru(depe)₂H₂ (2) and PFPPHA**; 0.010 g (0.019 mmol) of **2** was added to a J.Youngs resealable NMR tube, dissolved in d_6 -benzene and 6.2 μL (0.019 mmol) of PFPPHA was added. After 250 h at 85 °C the solution had turned from colourless to yellow and **2** had been completely converted to **11**. ^{19}F NMR: Unidentified fluoroorganic products seen in similar regions as for **1**/PFD reaction but obscured by resonances of PFPPHA.

v) **cis-Ru(depe)₂H₂ (2) and PF1MD**; 0.010 g (0.019 mmol) of **2** was added to a J.Youngs resealable NMR tube, dissolved in d_6 -benzene and 5.1 μL (0.019 mmol) of PF1MD was added. After 85 h at 85 °C the solution turned from colourless to yellow and **2** was completely converted to **11**. ^{19}F NMR (d_6 -benzene): Unidentified fluoroorganic products at δ -69.6 (m), -69.7 (m), -70.0 (m), -110.9 (br), -113.0 (br), -122.7 (br), -126.0 (br), -131.2 (br), -135.7 (sh), -141.2 (br), -142.5 (br).

vi) *cis*-Ru(depe)₂H₂ (**2**) and other perfluoroalkanes; The 1:1 reactions of **2**/PFMCH and **2**/PF2MP were prepared similar to the other perfluoroalkanes above. In both cases, no reaction was seen by ³¹P{¹H} NMR spectroscopy after heating at 85 °C for three weeks

vii) *cis*-Ru(depe)₂H₂ (**2**) and PFD plus 30 equivalents of pyridine; 0.010 g (0.019 mmol) of **2** was added to a J.Youngs resealable NMR tube, dissolved in d₆-benzene and 48 μL (0.58 mmol) of dry pyridine added, followed by 4.9 μL (0.019 mmol) of PFD. Heating at 85 °C for 150 h resulted in a colour change (colourless to yellow) and complete conversion of **2** to two new ruthenium phosphine species according to ³¹P{¹H} NMR spectroscopy. The products in a 5:1 ratio were a ruthenium hydride species (³¹P{¹H} NMR (d₆-benzene): δ 65.5 (s), ¹H NMR (d₆-benzene): δ -20.72 (qnt, *J*_{HP} 19.9 Hz)) and a non hydridic species (³¹P{¹H} NMR (d₆-benzene): δ 62.1 (s). ¹⁹F NMR (d₆-benzene) PFD and unidentified fluoroorganic products as seen in **2** and PFD (1:1) reaction present. Also δ -134.4 (s) which may be representative of a fluoride.

ix) *cis*-Ru(depe)₂H₂ (**2**) and PFD in a 1:1 pyridine/C₆D₆ solution; 0.010 g (0.019 mmol) of **2** was added to a J.Youngs resealable NMR tube, dissolved in a 1:1 mixture of d₆-benzene and dry pyridine and 4.9 μL (0.019 mmol) of PFD added. After 16 h at 85 °C, the solution had changed from colourless to yellow and **2** was completely converted to the same two new ruthenium phosphine species as seen in the **2**/PFD/30 x pyridine reaction. This time the non hydridic product was found in a 3:1 ratio with the ruthenium hydride.

x) *cis*-Ru(depe)₂H₂ (**2**) and PFD plus 30 equivalents Et₃N; 0.010 g (0.019 mmol) of **2** was added to a J.Youngs resealable NMR tube, dissolved in d₆-benzene and 80 μL (0.58 mmol) of dry Et₃N added, followed by 4.9 μL (0.019 mmol) of PFD. After 19 h at 85 °C, the colourless solution slowly turned yellow and NMR spectra showed the

ruthenium hydride species as seen in the reactions in pyridine. After 61 h at 85 °C, **2** had been completely converted to a 10:1 ratio of **11** and the new ruthenium hydride species. ^{19}F NMR (d_6 -benzene) PFD and unidentified fluoroorganic products as seen in **2** and PFD (1:1) reaction present.

5.3.3 Reactions of *cis*-Ru(dmpm) $_2$ H $_2$ (**3**) with perfluorocarbons

i) *cis*-Ru(dmpm) $_2$ H $_2$ (**3**) and hexafluorobenzene; 0.010 g (0.027 mmol) of **3** was added to a J. Youngs resealable NMR tube, dissolved in d_6 -benzene and excess C_6F_6 was condensed into the tube. An immediate reaction occurred upon thawing the solution as shown by a colour change from colourless to yellow. NMR spectroscopy showed that **3** had been completely converted to *trans*-Ru(dmpm) $_2$ (C_6F_5)H, **12**. On standing at room temperature for 3 days small colourless crystals were formed and isolated by filtration, 13 mg (89.2 %). $^{31}\text{P}\{^1\text{H}\}$ NMR (d_6 -benzene): δ -21.5 (t, J_{PF} 20.0 Hz). ^1H NMR (d_6 -benzene): δ -9.32 (br m, 1H, Ru-H), 1.03 (s, 6 H, PCH_3), 1.29 (s, 6 H, PCH_3), 2.52 (m, 2 H, PCHH), 2.73 (m, 2 H, PCHH). ^{19}F NMR (d_6 -benzene): δ -99.7 (m, 2 F, *ortho* C_6F_5), δ -164.9 (m, 2 F, *meta* C_6F_5), δ -165.7 (t, J_{FF} = 20.3 Hz, 1 F, *para* C_6F_5). IR (Nujol): 1815 cm^{-1} v (Ru-H). Elemental analysis, found (calculated) %C 37.1 (35.5), %H 6.08 (5.40).

ii) *cis*-Ru(dmpm) $_2$ H $_2$ (**3**) and pentafluorobenzene; 0.010 g (0.027 mmol) of **3** was added to a J. Youngs resealable NMR tube, dissolved in d_6 -benzene and an excess of $\text{C}_6\text{F}_5\text{H}$ was condensed into the tube. After 2 h at room temperature, the solution turning from colourless to pale yellow. NMR spectroscopy showed that **3** had been completely converted to *trans*-Ru(dmpm) $_2$ (*p*- $\text{C}_6\text{F}_4\text{H}$)H, **13**. $^{31}\text{P}\{^1\text{H}\}$ NMR (d_6 -benzene): δ -21.1 (t, J_{PF} 19.3 Hz, 4 P). ^1H NMR (d_6 -benzene): δ -9.15 (br m, 1H, Ru-H), 1.05 (s, 6 H, PCH_3),

1.35 (s, 6 H, PCH_3), 2.54 (m, 2 H, PCHH), 2.85 (m, 2 H, PCHH), 6.68 (tt, J_{HF} 6.8 Hz, J_{HF} 9.2 Hz, 1 H, $-\text{C}_6\text{F}_4\text{H}$). ^{19}F NMR (d_6 -benzene): δ -101.7 (m, 2 F, *ortho*), δ -143.0 (m, 2 F, *meta*).

iii) ***cis*-Ru(dmpm) $_2$ H $_2$ (3) and PFD**; 0.010 g (0.027 mmol) of **3** was added to a J. Youngs resealable NMR tube, dissolved in d_6 -benzene and 6.7 μL (0.027 mmol) of PFD added. After 20 h at 85 $^\circ\text{C}$, the solution turned from colourless to pale yellow. $^{31}\text{P}\{^1\text{H}\}$ NMR spectroscopy showed complete depletion of **3** and the formation of a substantial number of new products. $^{31}\text{P}\{^1\text{H}\}$ NMR (d_6 -benzene): Broad resonances at δ 9.8, 7.3, 4.1, 2.1, -9.2, -10.5, -26.5, -27.5, -30.4, -38.2, -40.7. ^1H NMR (d_6 -benzene): Broad multiplet hydride resonances at δ -8.24, -12.13, -16.19, -18.92, -21.64. ^{19}F NMR (d_6 -benzene): Mostly PFD present, also weak multiplet resonances at δ -81.6, -111.5, -112.5, -121.9, -135.7, -136.1.

5.3.4 Reactions of *cis*-Ru(dcpe) $_2$ H $_2$ (4), *cis*-Ru(dppe) $_2$ H $_2$ (5) and *cis*-Ru(PMe $_3$) $_4$ H $_2$ (6) with perfluorocarbons

NMR tube scale reactions of dihydrides **4**, **5** and **6** with both hexafluorobenzene or PFD gave no reactions by $^{31}\text{P}\{^1\text{H}\}$ NMR spectroscopy, even after heating at 85 $^\circ\text{C}$ for five weeks.

5.4 Fluorination reactions using ruthenium bifluoride hydride complexes

5.4.1 Fluorinations with *trans*-Ru(dmpe) $_2$ (FHF)H (8)

i) ***trans*-Ru(dmpe) $_2$ (FHF)H (8) and CH $_3\text{C}(\text{O})\text{Cl}$** ; *trans*-Ru(dmpe) $_2$ (FHF)H, **8**, was generated *in situ* in an NMR tube by reaction of **1** and PFD. Removal of the volatiles

gave **8** (0.011 g, 0.025 mmol), which was then dissolved in d_6 -benzene. 3.5 μ l (0.050 mmol) of $\text{CH}_3\text{C}(\text{O})\text{Cl}$ was added. After 10 mins at room temperature the solution had turned from pale to dark yellow with the formation of $\text{CH}_3\text{C}(\text{O})\text{F}$ as observed by ^{19}F NMR spectroscopy. ^{19}F NMR (d_6 -benzene): δ 51.5 (q, $^3J_{\text{FH}}$ 7.3 Hz, $\text{CH}_3\text{C}(\text{O})\text{F}$).

$^{31}\text{P}\{^1\text{H}\}$ NMR spectroscopy showed that **8** had been converted to *cis*- $\text{Ru}(\text{dmpe})_2\text{Cl}_2$, by comparison with the literature⁷, and a product proposed to be *trans*- $\text{Ru}(\text{dmpe})_2\text{HCl}$ in a 5:1 ratio. $^{31}\text{P}\{^1\text{H}\}$ NMR (d_6 -benzene): *cis*- $\text{Ru}(\text{dmpe})_2\text{Cl}_2$, AA'BB', δ 49.3 (t, J_{PP} 23.2 Hz), 40.1 (t, J_{PP} 23.2 Hz); *trans*- $\text{Ru}(\text{dmpe})_2\text{HCl}$, δ 44.5 (s). ^1H NMR (d_6 -benzene): *trans*- $\text{Ru}(\text{dmpe})_2\text{HCl}$, δ -20.71 (qnt, $^2J_{\text{HP}}$ 23.7 Hz, Ru-H).

ii) ***trans*- $\text{Ru}(\text{dmpe})_2(\text{FHF})\text{H}$ (**8**) and CH_3I** ; 3.1 μ l (0.050 mmol) of CH_3I was added to a d_6 -benzene solution of **8** (0.011 mg, 0.025 mmol) in a resealable NMR tube, After 2 h at room temperature, the solution had turned from pale yellow to orange. ^{19}F and ^1H NMR spectroscopy showed the formation of CH_3F . ^{19}F NMR (d_6 -benzene): δ -266.7 (q, $^2J_{\text{FH}}$ 46.5 Hz, CH_3F). ^1H NMR: δ 3.64 (d, $^2J_{\text{HF}}$ 46.5 Hz, CH_3F). *trans*- $\text{Ru}(\text{dmpe})_2\text{I}_2$ and *trans*- $\text{Ru}(\text{dmpe})_2\text{HI}$ ⁸ were observed in the $^{31}\text{P}\{^1\text{H}\}$ NMR spectrum in a 3:1 ratio, while two other minor products were seen in trace amounts. $^{31}\text{P}\{^1\text{H}\}$ NMR (d_6 -benzene): *trans*- $\text{Ru}(\text{dmpe})_2\text{I}_2$, δ 27.3 (s); *trans*- $\text{Ru}(\text{dmpe})_2\text{HI}$, δ 38.7 (s); Minor products, δ 40.1 (d, J 19.1 Hz), 45.4 (t, J 17.8 Hz). ^1H NMR (d_6 -benzene): *trans*- $\text{Ru}(\text{dmpe})_2\text{HI}$, δ -18.39 (qnt, $^2J_{\text{HP}}$ 21.5 Hz, Ru-H);.

iii) ***trans*- $\text{Ru}(\text{dmpe})_2(\text{FHF})\text{H}$ (**8**) and Cp_2TiCl_2** ; To a resealable NMR tube containing a d_6 -benzene solution of **8** (0.011 g, 0.025 mmol), Cp_2TiCl_2 0.006 mg (0.024 mmol) was added. The NMR tube was warmed slightly to dissolve the titanium complex. After 2 h at room temperature, the red solution turned yellow and a yellow precipitate was formed. The yellow precipitate was isolated by filtration (~ 3 mg) and dissolved in d_8 -thf. ^1H and ^{19}F NMR spectra showed the precipitate contained Cp_2TiClF and Cp_2TiF_2 in

a 1:4 ratio. ^1H NMR (d_8 -thf): δ 6.32 (br s, 10 H, $(\text{C}_5\text{H}_5)_2\text{TiF}_2$), 6.40 (br s, 10 H, $(\text{C}_5\text{H}_5)_2\text{TiClF}$), peak ratio 4:1. ^{19}F NMR (d_8 -thf): δ 85.73 (br s, 2 F, Cp_2TiF_2), 138.35 (br s, 1 F, Cp_2TiClF), peak ratio 8:1. The supernatant d_6 -benzene was found to contain *cis*- $\text{Ru}(\text{dmpe})_2\text{Cl}_2$ and *trans*- $\text{Ru}(\text{dmpe})_2\text{HCl}$ as seen in the reaction of **8** and $\text{CH}_3\text{C}(\text{O})\text{Cl}$.

5.4.2 Fluorinations with *trans*- $\text{Ru}(\text{depe})_2(\text{FHF})\text{H}$ (**11**)

i) *trans*- $\text{Ru}(\text{depe})_2(\text{FHF})\text{H}$ (**11**) and $\text{CH}_3\text{C}(\text{O})\text{Cl}$; *trans*- $\text{Ru}(\text{depe})_2(\text{FHF})\text{H}$, **11**, was generated *in situ* in an NMR tube by reaction of **2** and PFD. Removal of the volatiles gave **11** (0.010 g, 0.018 mmol), which was then dissolved in d_6 -benzene. 2.5 μl (0.036 mmol) of $\text{CH}_3\text{C}(\text{O})\text{Cl}$ was then added. After 3 h at room temperature the solution had turned from pale yellow to dark yellow. ^{19}F NMR spectroscopy showed the formation of $\text{CH}_3\text{C}(\text{O})\text{F}$. ^{19}F NMR (d_6 -benzene): δ 51.5 (q, $^3J_{\text{FH}}$ 7.3 Hz, $\text{CH}_3\text{C}(\text{O})\text{F}$). The $^{31}\text{P}\{^1\text{H}\}$ and ^1H NMR spectra indicated that **11** had been converted to *cis*- $\text{Ru}(\text{depe})_2\text{Cl}_2$, by comparison with literature data⁴, and a product believed to be *trans*- $\text{Ru}(\text{depe})_2\text{HCl}$, in a 6:1 ratio. $^{31}\text{P}\{^1\text{H}\}$ NMR (d_6 -benzene): *cis*- $\text{Ru}(\text{depe})_2\text{Cl}_2$, AA'BB', δ 59.6 (t, J_{PP} 22.2 Hz), 48.1 (t, J_{PP} 22.2 Hz); *trans*- $\text{Ru}(\text{depe})_2\text{HCl}$, δ 65.6 (s). ^1H NMR (d_6 -benzene): *trans*- $\text{Ru}(\text{depe})_2\text{HCl}$, δ -20.67 (qnt, $^2J_{\text{HP}}$ 19.3 Hz, Ru-H).

ii) *trans*- $\text{Ru}(\text{depe})_2(\text{FHF})\text{H}$ (**11**) and CH_3I ; 2.2 μl (0.036 mmol) of CH_3I was added to a d_6 -benzene solution of **11** (0.010 g, 0.018 mmol). After 24 h at room temperature the solution had turned from pale yellow to dark orange. ^1H and ^{19}F NMR spectroscopy showed the formation of CH_3F . ^1H NMR (d_6 -benzene) δ 3.64 (d, $^2J_{\text{HF}}$ 46.5 Hz, CH_3F). ^{19}F NMR (d_6 -benzene): δ -266.7 (q, $^2J_{\text{FH}}$ 46.5 Hz, CH_3F). $^{31}\text{P}\{^1\text{H}\}$ NMR spectroscopy displayed two new products believed to be *cis*- $\text{Ru}(\text{depe})_2\text{I}_2$ and *trans*- $\text{Ru}(\text{depe})_2\text{HI}$ in a 5:1 ratio. $^{31}\text{P}\{^1\text{H}\}$ NMR (d_6 -benzene): *cis*- $\text{Ru}(\text{depe})_2\text{I}_2$, AA'BB', δ 67.1 (t, J_{PP} 22.5 Hz),

47.7 (t, J_{PP} 22.5 Hz); *trans*-Ru(depe)₂HI, δ 38.7 (s). ¹H NMR (d₆-benzene): *trans*-Ru(depe)₂HI, δ -18.56 (br m, Ru-H).

5.5 Reaction of ruthenium dihydride complexes with perfluoroalkenes

5.5.1 Reaction of *cis*-Ru(dmpe)₂H₂ (1) with perfluoroalkenes

i) *cis*-Ru(dmpe)₂H₂ (1) and PF2M2P; 0.010 g (0.025 mmol) of 1 was added to a J.Youngs NMR tube, dissolved in d₆-benzene and 4.6 μ L (0.025 mmol) of PF2M2P was added. An immediate reaction occurred and the solution turned from colourless to yellow with ³¹P{¹H} NMR spectroscopy showing the formation of *trans*-Ru(dmpe)₂(FHF)H, 8, and *cis*-Ru(dmpe)₂(F..HF)F, 14, in a 1:4 ratio.

cis-Ru(dmpe)₂(F..HF)F, 14; ³¹P{¹H} NMR (d₆-benzene): AABB'XX', δ_A 42.2 (apparent quintet), δ_B 56.8 (m). ¹H NMR (d₆-benzene): δ 0.67 (br d, 6 H, 2 x CH₃), 0.98 (s, 6 H, 2 x CH₃), 1.17 (v. br m, 12 H, 4 x CH₃), 1.24 (br d, 4 H, 4 x PCHH), 1.62 (br s, 4 H, 4 x PCHH) (32 H, dmpe H), δ 14.2 (br d, J_{HF} 344.0 Hz, 1 H, RuF...HF). ¹⁹F NMR (d₆-benzene): δ -175.2 (d, J_{FH} 344.0 Hz, 1 F, RuF...HF), δ -343 (br m, 1 F, RuF...HF), δ -362 (br m, 1 F, RuF).

Due to the complexity of the ¹⁹F NMR spectrum, the fluoroorganic products detected by GC and GC-MS. The reaction was rerun in d₈-toluene and dodecane which yielded exactly the same products as in d₆-benzene. The volatiles products were condensed off and five products were found in the GC (DB-1 non-chiral column). GC-MS analysis found one product with m/z 282 (A (CF₃)₂C=CHCF₂CF₃) and four products m/z 246 (B, *trans*-FHC=C(CF₃)CH₂CF₂CF₃; C, *cis*-FHC=C(CF₃)CH₂CF₂CF₃; D, *trans*-(CF₃)₂CHCH=CHCF₃; E, *cis*-(CF₃)₂CHCH=CHCF₃). B and C were detected in

the ^1H NMR (d_6 -benzene): B δ 8.83 (d, 73.8 Hz, 1 H, =CFH), 3.81 (t, 17.8 Hz, 2H, CH_2); C δ 6.62 (d, 75.7 Hz, 1 H, =CFH) 2.17 (t, 17.1 Hz, 2 H, CH_2).

ii) ***cis*-Ru(dmpe) $_2$ H $_2$ (1) and PF2M2P (1:2);** 0.010 g (0.025 mmol) of **1** was added to a J.Youngs NMR tube, dissolved in d_6 -benzene and 9.2 μL (0.050 mmol) of PF2M2P was added. An immediate reaction occurred and the solution turned from colourless to yellow giving *cis*-Ru(dmpe) $_2$ (F..HF)F, **14**, as the major inorganic product. ^{19}F NMR showed PF2M2P remaining and fluoroorganic products seen in original **1**/PFP reaction.

iii) **Preparation of crystals of (14) by reaction of *cis*-Ru(dmpe) $_2$ H $_2$ (1) and PF2M2P plus 10 equivalents of Et $_3$ N;** 0.040 g (0.100 mmol) of **1** was added to a J.Youngs NMR tube, dissolved in d_6 -benzene, 140 μL (1.00 mmol) of Et $_3$ N added, followed by 18.4 μL (0.100 mmol) of PF2M2P. An immediate reaction occurred, the solution turning from colourless to yellow. By the $^{31}\text{P}\{^1\text{H}\}$ NMR spectrum the solution contained *cis*-Ru(dmpe) $_2$ (F..HF)F, **14**, as the only inorganic product. On standing at room temperature for 2 days yellow needle like crystals were formed and isolated by filtration (0.032 g, 70 %). IR (Nujol): 2452, 1915 cm^{-1} $\nu(\text{HF}_2)$ Elemental analysis fitted Ru(dmpe) $_2$ F $_2$, probably due to loss of HF in the furnace. Found (calculated) %C 32.5 (32.8), %H 7.28 (7.34).

iv) **Preparation of *cis*-Ru(dmpe) $_2$ F $_2$ by the reaction of *cis*-Ru(dmpe) $_2$ H $_2$ (1) and PF2M2P;** In a glovebox, 0.010 g (0.025 mmol) of **1** was added to a rigorously dried sample vial, dissolved in d_8 -thf and 4.6 μL (0.025 mmol) of PF2M2P was added. An immediate reaction occurred and the solution turned from colourless to yellow. The vial was left in the glovebox with the lid slightly open. After a week the solution had evaporated to leave an off white residue. $^{31}\text{P}\{^1\text{H}\}$ NMR (d_6 -benzene): δ 42.2 (apparent quintet), 56.8 (m), same as **14**. ^{19}F NMR (d_6 -benzene): -357 (br m). No peaks for HF. Elemental analysis, found (required) %C 33.0 (32.8), %H 7.19 (7.34).

v) **cis-Ru(dmpe)₂H₂ (1) and PFP**; 0.010 g (0.025 mmol) of **1** was added to a J.Youngs NMR tube and dissolved in d₆-benzene. The tube was degassed and 1 atm of PFP (~2 equivalents) was introduced. The tube was shaken leading to an immediate reaction as judged by the colour change from colourless to yellow. NMR spectroscopy showed formation of **14** as the only inorganic product. PFP was converted to a 4:1:3 ratio of *trans*-CF₃CF=CFH, *cis*-CF₃CF=CFH, and CF₃CF=CH₂.

***trans*-CF₃CF=CFH**; ¹⁹F NMR (d₆-benzene): δ -69.5 (dd, *J*_{FF} 11.9 Hz, *J*_{FF} 20.6 Hz, 3 F, CF₃), -163.5 (ddq, *J*_{FF} 20.6 Hz, *J*_{FF} 134.3 Hz, *J*_{FH} 68.2 Hz, 1 F, =CFH), -181.8 (ddq, *J*_{FF} 11.9 Hz, *J*_{FF} 134.3 Hz, *J*_{FH} 4.1 Hz, 1 F, =CF(CF₃)). ¹H NMR (d₆-benzene): δ 8.45 (dd, *J*_{HF} 4.1 Hz, *J*_{HF} 68.2 Hz, 1 H, =CFH).

***cis*-CF₃CF=CFH**; ¹⁹F NMR (d₆-benzene): δ -72.2 (dd, *J*_{FF} 14.5 Hz, *J*_{FF} 5.7 Hz, 3 F, CF₃), -152.9 (ddq, *J*_{FF} 5.7 Hz, *J*_{FF} 9.8 Hz, *J*_{FH} 66.1 Hz, 1 F, =CFH), -161.3 (ddq, *J*_{FF} 14.5 Hz, *J*_{FF} 9.8 Hz, *J*_{FH} 16.7 Hz, 1 F, =CF(CF₃)). ¹H NMR (d₆-benzene): δ 7.44 (dd, *J*_{HF} 16.7 Hz, *J*_{HF} 66.1 Hz, 1 H, =CFH).

CF₃CF=CH₂; ¹⁹F NMR (d₆-benzene): δ -73.9 (d, *J*_{FF} 10.3 Hz, 3 F, CF₃), -125.1 (ddq, *J*_{FF} 10.3 Hz, *J*_{FH} 43.4 Hz, *J*_{FH} 15.5 Hz, 1 F, =CF(CF₃)). ¹H NMR (d₆-benzene): δ 4.52 (dd, *J*_{HF} 15.5 Hz, *J*_{HH} 5.0 Hz, 1 H, =CHH), 4.47 (ddq, *J*_{FH} 1.6 Hz, *J*_{FH} 15.5 Hz, *J*_{HH} 5.0 Hz, 1 H, =CHH).

vi) **cis-Ru(dmpe)₂H₂ (1) and PFP (~10:1)**; 0.020 g (0.050 mmol) of **1** was added to a J.Youngs NMR tube and dissolved in d₆-benzene. The tube was degassed and ~ 100 mm Hg pressure of PFP was introduced (~ 10:1 **1**/PFP). The tube was shaken and the solution turned from colourless to pale yellow. NMR spectroscopy showed that only a small amount of **1** was converted to **14**. Bifluoride hydride **8** was also formed in a lesser amount. Fluoroorganic products were the same as found in the original **1**/PFP reaction.

Repeated degassing of the tube and addition of more of PFP led to complete reaction of **1** to give **8** and **14** in a 1:3 ratio.

vii) *cis*-Ru(dmpe)₂H₂ (1**) and PFP plus 5 equivalents of 9,10-dihydroanthracene;**
0.010 g (0.025 mmol) of **1** and 0.022 g (0.128 mmol) of 9,10-dihydroanthracene (DHA) were added to a J. Youngs NMR tube and dissolved in d₆-benzene. The tube was degassed and 1 atm of PFP (~2 equivalents) was introduced. The tube was shaken and an immediate reaction occurred, the solution turning from colourless to yellow. NMR spectroscopy showed the inorganic products to be **8** and **14** in a 1:3 ratio. The fluoroorganic products were no different to those formed in the absence of DHA.

5.5.2 Reaction of Ru(dcpe)₂H₂ (**4**) with perfluoroalkenes

i) Ru(dcpe)₂H₂ (4**) and PF2M2P;** 0.010 g (0.011 mmol) of **4** was added to a J. Youngs resealable NMR tube, dissolved in d₆-benzene and 1.9 µL (0.011 mmol) of PF2M2P was added. After 24 h at room temperature the colourless solution had turned orange and small orange needle like crystals of [Ru(dcpe)₂H][(CF₃)₂C=C(O)CF₂CF₃].2C₆H₆, **15**, were formed, yield 4 mg (27 %). The ³¹P{¹H} NMR spectroscopy showed no new products in the benzene solution so the reaction was repeated in d₈-thf. Now the solution stayed homogeneous and the ³¹P{¹H} NMR spectrum displayed a 5:1 ratio of **4** to **15**.
[Ru(dcpe)₂H][(CF₃)₂C=C(O)CF₂CF₃], **15**, ³¹P{¹H} NMR (d₈-thf): δ 73.4 (s). ¹H NMR (d₈-thf): δ -31.78 (qnt, J_{HP} 19.2 Hz, 1 H, Ru-H), -0.6 (v br, C-H..Ru), 1.27 (br m, 44 H, PC₆H₁₁), 1.83 (br m, 44 H, PC₆H₁₁), 1.96 (br m, 8H, PCHH), 2.24 (br m, 8H, PCHH).
¹⁹F NMR (d₈-thf): δ -45.5 (tq, J_{FF} 10.7 Hz, J_{FF} 19.6 Hz, 3F, CF₃ (*trans* to C₂F₅)), δ -51.3 (q, J_{FF} 10.7 Hz, 3F, CF₃ (*cis* to C₂F₅)), δ -77.8 (s, 3F, -CF₂CF₃) and δ -113.6 (q,

J_{FF} 19.6 Hz, 2F, $-\text{CF}_2\text{CF}_3$). IR (Nujol) 2041 cm^{-1} (Ru-H) FABMS m/z 947

$[\text{Ru}(\text{dcpe})_2\text{H}]^+$. Elemental analysis, found (calculated): %C 56.1 (56.0), %H 8.12 (7.86).

ii) $\text{Ru}(\text{dcpe})_2\text{H}_2$ (4) and PF2M2P under rigorously dry conditions; 0.010 g (0.011 mmol) of **4** was added to a flame dried J. Youngs resealable NMR tube, dissolved in d_8 -thf and 1.9 μL (0.011 mmol) of PF2M2P was added. After 24 h at room temperature, solution became pale orange. NMR spectroscopy showed **4** and **15** in a 10:1 ratio.

iii) $^{31}\text{P}\{^1\text{H}\}$ time course experiments of $\text{Ru}(\text{dcpe})_2\text{H}_2$ (4) and PF2M2P;

Experiment X; 0.010 g (0.011 mmol) of **4** was added to a J. Youngs resealable NMR tube and dissolved in d_8 -thf. 1.9 μL (0.011 mmol) of PF2M2P was added followed by 1.9 μL (0.110 mmol) degassed water. A second equivalent of PF2M2P (1.9 μL , 0.011 mmol) was added after 12 h.

Experiment Y; 0.010 g (0.011 mmol) of **4** was added to a J. Youngs resealable NMR tube and dissolved in d_8 -thf. 1.9 μL (0.011 mmol) of PF2M2P but no water.

iv) $\text{Ru}(\text{dcpe})_2\text{H}_2$ (4) and PF2M2P in the presence of 10 equivalents of degassed water; 0.010 g (0.011 mmol) of **4** was added to a J. Youngs resealable NMR tube and dissolved in d_6 -benzene. 1.9 μL (0.011 mmol) of PF2M2P was added followed by 1.9 μL (0.011 mmol) degassed water. After 3 h the solution became orange and crystals of **15** started to form. After standing for 24 h at room temperature 12 mg (93 %) of orange crystals of **15** were obtained.

v) $\text{Ru}(\text{dcpe})_2\text{H}_2$ (4) and PFP; 0.010 g (0.011 mmol) of **4** was added to a J. Youngs resealable NMR tube and dissolved in d_8 -thf. The NMR tube was degassed and 1 atm of PFP introduced. After 24 h at room temperature the colourless solution turned orange.

$^{31}\text{P}\{^1\text{H}\}$ NMR showed **4** and **15** in a ratio of 6:1. Addition of 1.9 μL (0.011 mmol) degassed water to the NMR tube resulted in almost complete conversion of **4** to **15**.

5.6 Cyclic Voltammetry

Dihydrides were prepared as in section 5.2. All measurements were carried out in an oxygen and moisture free glovebox to protect the dihydride from decomposition. In each case a small amount (~ 2 mg) was added to a thf solution containing 0.2 M $[\text{Bu}_4\text{N}][\text{BF}_4]$ as an electrolyte. Firstly measurements were carried out using a silver wire electrode and a vitreous carbon electrode (area = 0.0707 cm^2), and then the measurements referenced using a SCE (standard calomel electrode). Scan rate in all cases was 50 mV/s.

References

1. $\text{RuCl}_2(\text{PPh}_3)_3$; Holman, R.; Stephenson, T. A.; Wilkinson, G. *Inorg. Synth.*, **1970**, *12*, 237. $[\text{Ru}(\text{COD})\text{Cl}_2]_2$; Albers, M. O.; Ashworth, T. V.; Oosthuizen, E.; Singleton, E. *Inorg. Synth.*, **1989**, *26*, 68. $\text{Ru}(\text{DMSO})_4\text{Cl}_2$; Chaudret, B.; Commenges, G.; Poilblanc, R. *J. Chem. Soc., Dalton Trans.*, **1984**, 1635.
2. Hartwig, J. F.; Andersen, R. A.; Bergman, R. G. *Organometallics*, **1991**, *10*, 1710.
3. Nolan, S. P.; Belderrain, T. R.; Grubbs, R. H. *Organometallics*, **1997**, *16*, 5569.
4. Bautista, M. T.; Cappellani, E. P.; Drouin, S. D.; Morris, R. H.; Schweitzer, C. T.; Sella, A.; Zubkowski, J. *J. Am. Chem. Soc.*, **1991**, *113*, 4876.
5. Mainz, V. V.; Andersen, R. A. *Organometallics*, **1984**, *3*, 675.
6. Hartwig, J. F.; Andersen, R. A.; Bergman, R. G. *J. Am. Chem. Soc.*, **1991**, *113*, 6492.
7. Clark, S. F.; Petersen, J. D. *Inorg. Chem.*, **1983**, *22*, 620.
8. Kaplan, A. W.; Bergman, R. G.; *Organometallics*, **1998**, *17*, 5072.